UNIVERSITY OF CALIFORNIA, SAN DIEGO

Synthesis, Properties, and Asymmetric Catalysis of Chiral Cyclophanes and Their Metal Complexes

A dissertation submitted in partial satisfaction of the

requirements for the degree Doctor of Philosophy

in

Chemistry

by

So-Young Amy Choi

Committee in charge:

Professor Yitzhak Tor, Chair
Professor William Allison
Professor Gustaf Arrhenius
Professor Joseph O'Connor
Professor Charles L. Perrin
Professor Jay S. Siegel

2006

The dissertation of So-Young Amy Choi is approved, and it is acceptable in quality and form for publication on microfilm:

_____

_____

_____

_____

_____

_____

Chair

University of California, San Diego

2006

DEDICATION

This thesis work is dedicated in loving memory of my father In Kwon Choi, and to my family, especially my mother and mother-in-law, who have sacrificed so much and took care of Brendon and Haley so that I could finish this work. My husband Erik for his love, support and faith in me throughout this journey. Thank you!

TABLE OF CONTENTS

LIST OF SCHEMES

LIST OF FIGURES

LIST OF EQUATIONS

LIST OF TABLES

ABBREVIATIONS

BHT: 2,6-di-*tert*-butyl-4-methylphenyl

BINAP: 2,2'-bis(diphenylphosphino)-1,1'-binaphthyl

bu: butyl

bpy: 2,2'-bipyridine

$(imidH)_2dap$: 2,6-bis[1-((2-imidazol-4-ylethyl)imino)ethyl]pyridine

DFT: density functional theory

diars: *o*-phenylenebisdimethylarsine, *o*-$C_6H_4(AsMe_2)_2$

dmg: the anion of dimethylglyoxime ($dmgH_2$)

dmp: 2,9-dimethyl-1,10-phenanthroline

dnpp: 2,9-dineopentyl-1,10-phananthroline

EtOAc: ethyl acetate

Me: methyl

NBS: N-bromosuccinimide

NCS: N-chlorosuccinimide

phen: 1,10-phenanthroline

py: pyridine

tbp: trigonal bi-pyramidal

TES: tetraethylsilane

TMS: tetramethylsilane

triflate (OTf): trifluoromethanesulfonate

ACKNOWLEDGMENTS

So many people have helped me during my thesis work. It would have been impossible for me to get to this point without their encouragements, guidance and sacrifices. I would like to first thank Professor Jay S. Siegel for his inspiration, encouragement, teaching and for supporting me through many hard times during my studies. Especially, I would like to thank him for his faith in my ability to go through with this project. Augusto Fuchicelo, Petra Blom, Dr. Maurizio Benaglia, Dr. Craig R. Roberts, Dr. Richard Haldimann, Dr. Valentina Molteni, Dr. Gunther Grube, Dr. Jon C. Loren, Dr. Eric Elliot, Dr. Michael DeClue, Dr. Robert van Mullekom, Dr. Carissa Jones, Professor Kim Baldridge, Dr. Melissa Shults, Tim Barder, Jeremy Klosterman and other past Siegel members for sharing their chemical knowledge, inspiration, generosity and friendship.

Professor Yitzhak Tor, Professor Charles Perrin, Professor Joseph O'Connor, Professor William Allison, Professor Gustaf Arrhenius, Professor Murray Goodman, Professor Emmanuel Theodorakis, Professor Nathaniel Finney, Professor Susan Taylor, Professor Seth Cohen and their group members for sharing their instruments and expertise. Dr. Peter Gantzel and Dr. Anthony Linden for their help with X-ray crystallography. From Boston College, Professor Lawrence Scott, Professor John Boylan, Professor Mary Roberts and their students, especially Vicky Tsefrikas, for all their help.

Helen Choi, Dr. Kwang Woong Won, Dr. Alvina Won, Mrs. Maria Lee, Bernadeane Carr, Professor Betsy Komives, Julie and Andre de Rosier, Theresa Cha, Marianna Yang, Dr. Jesse Moore, Dr. Jesse Mello, and Dr. Albert Fang for their love, support and friendship.

CURRICULUM VITAE

Education:

University of California, San Diego, CA:
Ph.D. in Chemistry, 2006

University of California, San Diego, CA:
M.S. in Chemistry, 2000

Occidental College, Los Angeles, CA:
B.A. in Chemistry, 1998

Research Experience:

University of California, San Diego, CA:
Doctoral Research: Professor Jay S. Siegel 09/98 – 08/2003

Thesis Title: The Synthesis, Properties, and Asymmetric Catalysis of Chiral Cyclophanes and Their Metal Complexes

Occidental College, Los Angeles, CA:
Undergraduate Research: Professor Donald R. Deardorff 01/96 – 08/98

A Two-Step Procedure for the Conversion of α,β-Unsaturated Aldehydes into γ-Azido-α,β-Unsaturated Nitriles

Publications:

"Synthesis, X-Ray Structures, and Circular Dichroism of Helical Cyclophanes", So-Young Amy Choi, Craig Woods, Augusto Fuchicelo, Petra Blom, Anthony Linden, and Jay S. Siegel, *manuscript in preparation*.

"Metal Complexes of Helical Cyclophanes and Enantioselective Allylic Oxidation Using the Cu(I)-Complex of the Cyclophane.", So-Young Amy Choi, Anthony Linden, and Jay S. Siegel, *manuscript in preparation*.

"A Two-Step Procedure for the Conversion of α,β-Unsaturated Aldehydes into γ-Azido-α,β-Unsaturated Nitriles", Donald R. Deardorff, Cullen M. Taniguchi, Sanaz A. Tafti, Henry Y. Kim, So Young Choi, Katherine J. Donewy, and Thanh V. Nguyen, *J. Org. Chem.* 2001, *66*, 7191-7194.

Presentations:

"Synthesis of Metal-Binding Helical Cyclophanes", So-Young Amy Choi and Jay S. Siegel, poster presented at the *8th Annual Maria Goeppert-Mayer **20**isciplinary Symposium*; University of California San Diego, La Jolla, CA, March 1, 2003.

"Ag(I) & Cu(I) Complexations of Helical Cyclophanes", **"**, So-Young Amy Choi and Jay S. Siegel, poster presented at the *7th Annual Maria Goeppert-Mayer **20**isciplinary Symposium*; University of California San Diego, La Jolla, CA, March 2, 2002.

"Synthesis of Helical Cyclophanes", So-Young Amy Choi and Jay S. Siegel, poster presented at the *10th International Symposium on Novel Aromatics*: University of California San Diego, La Jolla, CA, August 4-8, 2001.

"Synthesis of Helical Cyclophanes", So-Young Amy Choi and Jay S. Siegel, poster presented at the *Gordon Research Conference on Physical Organic Chemistry*: Holderness School, Plymouth, NH, July 1-6, 2001.

"A Two-Step Procedure for the Conversion of α,β-Unsaturated Aldehydes into γ-Azido-α,β-Unsaturated Nitriles", So Young Choi, Henry Y. Kim, and Donald R. Deardorff, oral presentation at *American Chemical Society Southern California Conference on Undergraduate Research*: California State University Los Angeles, Los Angeles, CA, November, 1997

ABSTRACT OF THE DISSERTATION

Synthesis, Properties, and Asymmetric Catalysis of Chiral Cyclophanes and Their Metal Complexes

by

So-Young Amy Choi

Doctor of Philosophy in Chemistry

University of California, San Diego, 2006

Professor Yitzhak Tor, Chair

This dissertation has been devoted to the syntheses and studies of novel chiral, helical cyclophanes and their corresponding metal complexes. The subsequent part of the project involves the use of the copper complex of the chiral cyclophane **1** as an asymmetric catalyst in enantioselective organic transformation reactions.

There are three chapters in this thesis. Chapter 1 describes the synthesis of chiral cyclophanes and their metal complexes. Racemic spirobiindanol (±)-**6** was initially synthesized and resolved using literature methods. Metal-binding ligands were synthesized from each enantiomer, and Williamson ether synthetic method was used to obtain desired helical cyclophanes **1**-**5**. Metal ions, such as silver(I), copper(I),

mercury(II), zinc(II), and palladium(II), were used to form metal complexes of these cyclophanes.

Chapter 2 discusses structures and properties of both cyclophanes and their metal complexes using spectral data from NMR, MS, UV, CD and X-ray crystallography. Lastly, Chapter 3 describes the use of a copper complex of the cyclophane **1** as an asymmetric catalyst for cyclopropanation of styrene with diazoester and for allylic oxidation of cycloalkenes, otherwise known as the Kharash-Sosnovsky reaction. The cyclopropanation reaction favored the formation of *trans*-phenylcyclopropane carboxylate in ~ 20 % ee (68-87 % yield), and the allylic oxidation reactions produced the (*R*)-allylic carboxylate with ~16 % ee (< 80 % yield).

CHAPTER 1. SYNTHESIS OF CHIRAL CYCLOPHANES AND THEIR METAL COMPLEXES

1.1 Introduction

Cyclophanes are macrocycles with two or more aromatic rings incorporated into a larger ring system.[1,2] Initially, cyclophanes were designed and synthesized for the study of molecular strain on benzene rings.[2] However, recent researches in small, sterically congested cyclophanes have been growing rapidly due to their relevance in macrocyclic and supramolecular chemistry.[3-8] Although the binding features of cyclophanes with neutral guests[9-14] and small cationic metals have been widely recognized, their potential use in organometallic catalysis is not well studied.[15] Herein I report syntheses of novel helical cyclophanes **1**—**5** that can host cationic-metals in their chiral cavity. This property makes them ideal candidates for the asymmetric organometallic catalyst in enantioselective transformations.

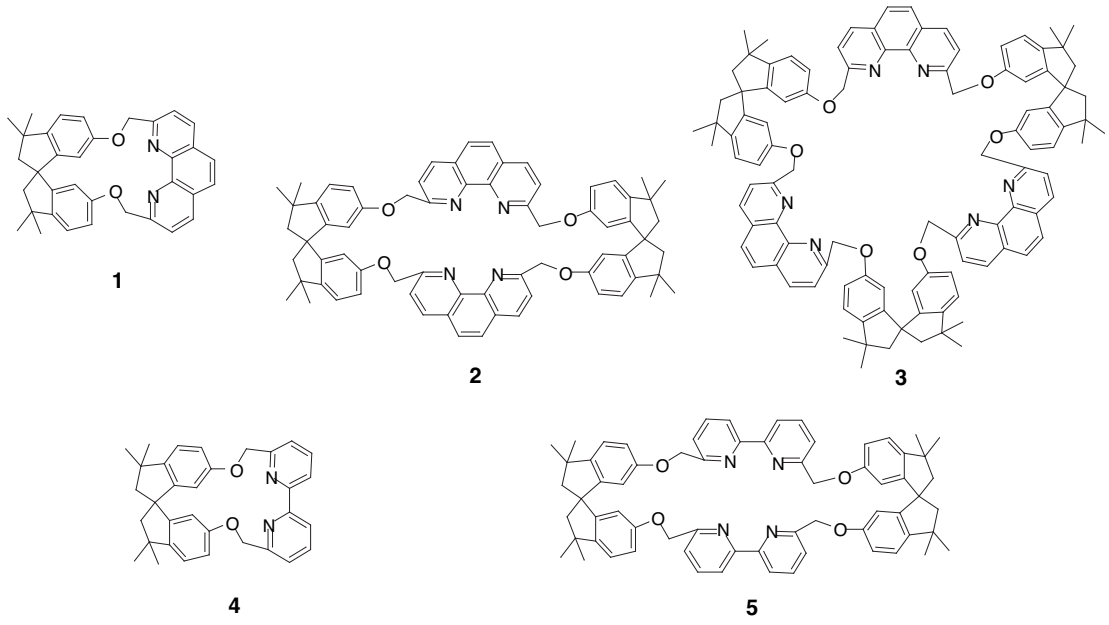

Figure 1.1 Cyclophanes **1** – **5**

1.1.1 Cyclophanes

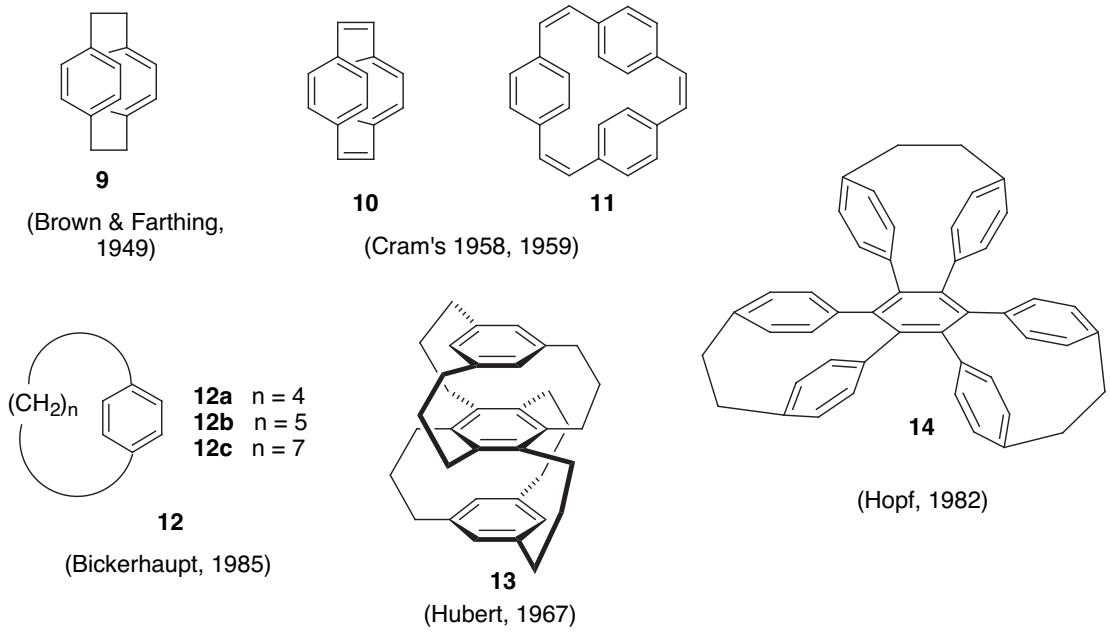

Figure 1.2 Structurally intriguing cyclophanes.

Cyclophane chemistry was born in 1949 when Brown and Farthing isolated [2.2]paracyclophane **9** from the thermolysis of *p*-xylene.[16] Cram reported the first designed synthesis of **9** in 1951[17] and his group cultivated the field of cyclophanes in the 1950's and 1960's.[2] His cyclophanes, such as **10** and **11** were mainly used to study the molecular strain on benzene rings, but their studies led others to create many different structurally interesting cyclophanes,[18-23] such as **12**--**14** (Figure 1.2).

Cram eventually synthesized helically chiral cyclophane **15** and its acyclic analogue **16** from phenanthroline and binapthol[24] units (Figure 1.3). The macrocycle **15** is built with only aromatic atoms, and it possesses a chiral system, D_2 symmetry, whose six aromatic residues describe an enforced helical structure. Nitrogen atoms from the two phenanthroline units are in nearly tetrahedral arrangement, which makes

it possible for them to bind small cationic metal ions, such as Li^+, Na^+, K^+, and Cu^+. Actually, the racemic mixture of **15** was isolated as a Cu^+ salt after the Ullman coupling reaction.[25] The *meso*-isomer of **15** was not found, probably because there were too many structural constraints for the two phenanthroline subunits to ligate the same metal ion at the same time. As expected, the entropic advantage of **15** over **16** causes increase in binding energy, having the difference of *ca.* 8.5 kcal/mol.

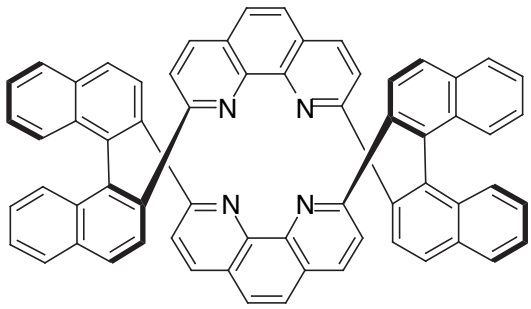

15

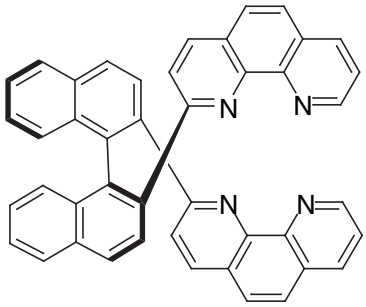

16

Figure 1.3 Cram's strongly binding, helically chiral ligand system.

1.1.2 Synthesis and Resolution of Spirobiindanol

1.1.2.1 Synthesis of Spirobiindanol

Spirobiindanol **6**, otherwise known as (±)-3,3,3',3'-tetramethyl-1,1'-spirobi(indan)-6,6'-diol, is chiral. With its rigid C_2-symmetric construction and quaternary carbon center, it would make an ideal chiral scaffold.[26.27] For instance, structurally similar [1,1'binapthalene]-2,2'-diol BINOL[28.29] **17** is one of the most widely used chiral auxiliaries; however, spirobiindanol was not used for this purpose until the last decade. Unlike BINOL, whose distance between hydroxy groups is only ~4.1.Å, the two hydroxy groups of spirobiindanol are farther apart (~7.4 Å), which

prevents chelation with a single metal center. A more prevalent usage of **6** was as an intermediate for polycarbonates[30-32] for optical instrumentations,[33] resins[34.35] with photosensitive properties, and antioxidants.[36.37] It is known to provide excellent transparency, heat resistance, and low birefringence.

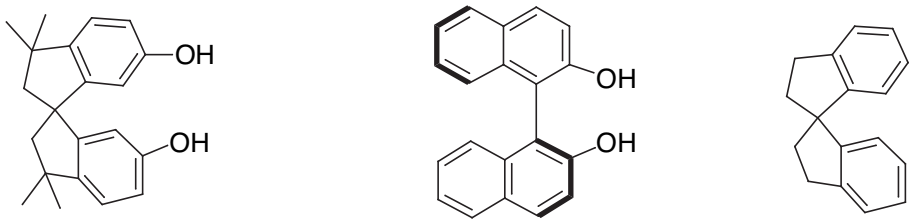

6 **17** **18**

Figure 1.4 Spirobiindanol **6**, BINOL **17**, and 1,1'-spirobiindane **18**.

Several different synthetic schemes for making spirobiindanol were known in the literature. Von Braun[38] first observed the production of **6** by treating bisphenol A--2,2-di-*p*-hydroxyphenylpropane--with HCl, even though he mistakenly assigned the structure to be **19**. He reported the liberation of phenol during the reaction, and he suggested the transient formation of **20**, which dimerized to form **19**. About 30 years later, Curtis[39] not only increased the yield of spirobiindanol by replacing HCl with HBr, he correctly elucidated the structure of spirobiindanol. He also used the structure of **6** to reveal the carbon analogue, 1,1'-spirobiindane[40] **18**, which had been incorrectly assigned as indenoindene structure **21a**--**b** by Hoffmann[41] and Barnes[42] (Figure 1.5). To further support his assertion, Curtis[40] used Barnes and Beitchman's 3,3,3'3',6,6'-hexamethyl-1,1'-spirobi-indane[42] to form spirobiindanol in four synthetic steps.

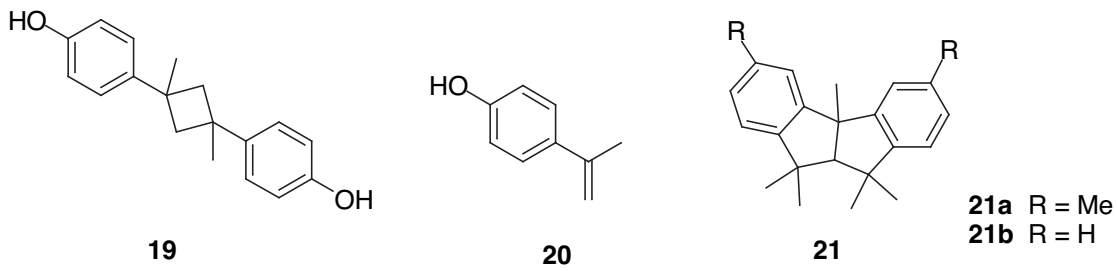

Figure 1.5 Incorrect assignments of spirobiindanol intermediates.

Silvio[43] et al employed commercially available alkylaryl bisphenol in the presence of a dry heterogeneous acid catalysts, such as Dowex MSC-1H—which is a strong acid cation exchange resin composed of sulfonated styrene divinylbenzene copolymer in bead—in toluene at reflux. Advantages of this method are convenient removal process of acid and higher yield of the product compared to other previously known methods.

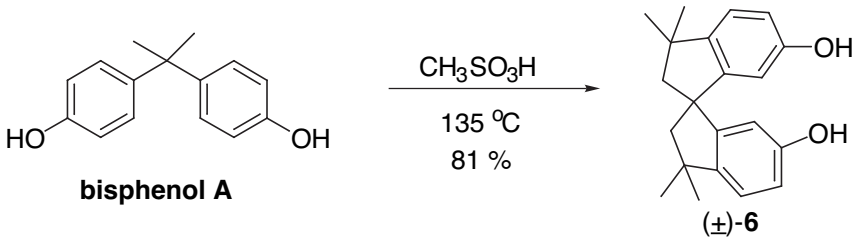

Scheme 1.1 Faler's synthesis of racemic spirobiindanol.

The easiest and most economical method of making spirobiindanol was developed by Faler[44] (Scheme 1.1). Commercially available bisphenol A and a catalytic amount of methanesulfonic acid were heated at 135 °C. Three equiv. of bisphenol A make one equiv. of (±)-**6** in 81 % yield. Faler's method is superior to all other methods because of the following: a) It produces products of high purity; b) It uses only catalytic amount of acid, reducing waste and simplifying work-up process;

therefore, it is the most economical and convenient way; c) The product yield is the highest among all the reported methods.

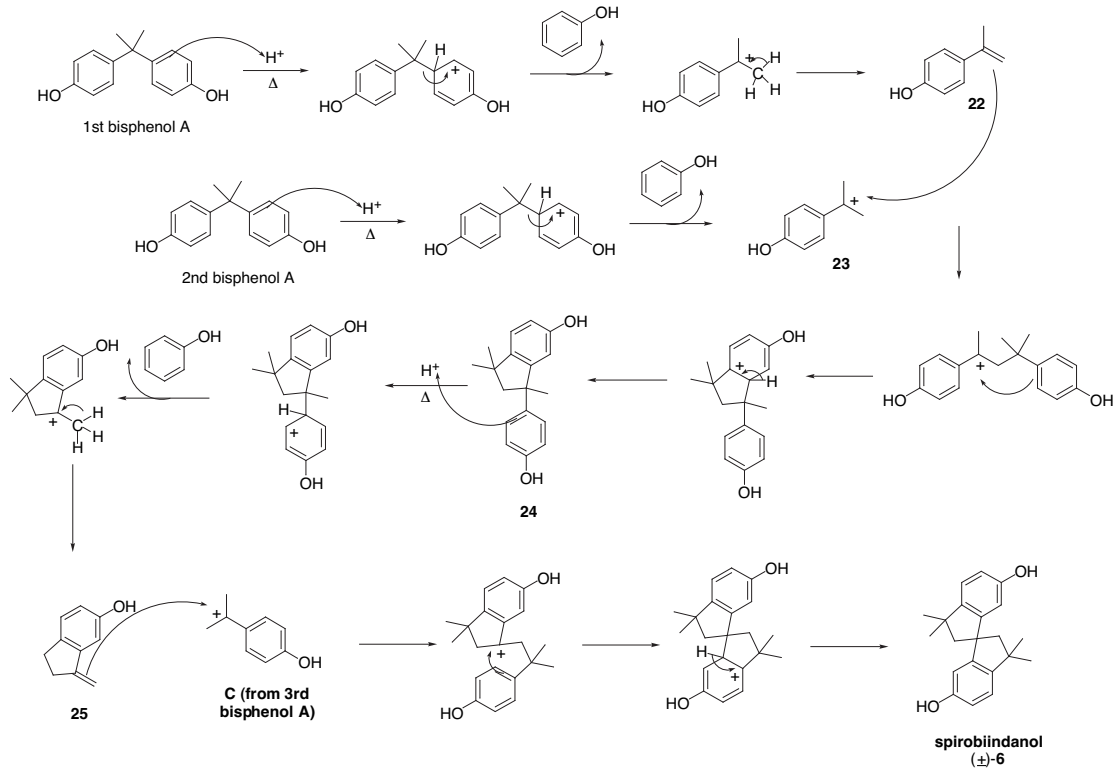

Scheme 1.2 Mechanisms for the synthesis of (±)-**6** from bisphenol A.

Looking at (Scheme 1.1) it is not clear how bisphenol A could convert to spirobiindanol. Isolated intermediate structures from the Faler's synthesis[44.45] of spirobiindanol elucidate the possible mechanistic steps [Scheme 1.2]. In proposed mechanisms, three equivalents of bisphenol A are needed to synthesize one equivalent of **6**. Under the hot, acidic reaction condition, the first bisphenol A cracks, producing phenol and isopropenylphenol, **22**. The cationic intermediate **23** is formed from the second bisphenol A. These two intermediates, **22** and **23**, dimerize to form 1-(4-hydroxyphenyl)-1,3,3-trimethyl)-6-indanol **24**. After the release of another equivalent

of phenol, **25** is formed. Barclay and Chapman[46] also reported the formation of similar exocyclic indene in the mechanistic study of 1,1'-spirobiindanes. Another cationic version of the isopropenylphenol **23**, which is derived from the third equivalent of bisphenol, reacts with **25** to form the desired spirobiindanol. A quick work up in water gets rid of phenol, and another reflux in dichloromethane, followed by filtration, yielded the pure final product (±)-**6**.

1.1.2.2 Resolution of Spirobiindanol

The axial chirality is exhibited in molecules such as allenes, alkylidene cycloalkenes, spirans, biaryls, and adamantoids. Spirobiindanol **6** is an axially chiral molecule. The chirality of four groups, labeled as **abcd**, arranged out-of-plane in pairs about an axis is represented in stretched tetrahedron models **26** and **27** (Figure 1.6). Fewer differences in groups involved along the asymmetric axis are required than are necessary for chirality around a center.[47] For example, the four groups, **a—d**, do not have to be different; as long as **a** and **b** are different, and **c** and **d** are different. It is sufficient that **a** and **b** are different, even if **a** and **a'** are the same, and **b** and **b'** are the same, as in the case of spirobiindanol **6**. The configuration of spirobiindanol is determined according to the specifications established by Cahn, Ingold, and Prelog.[47.48] Among external points, **a—d**, the group that falls near the end of axis are given precedence over groups at the far end, as represented in **28** and **29** (Figure 1.6). Following the rules, the configurations of spirobiindanol can be decided.

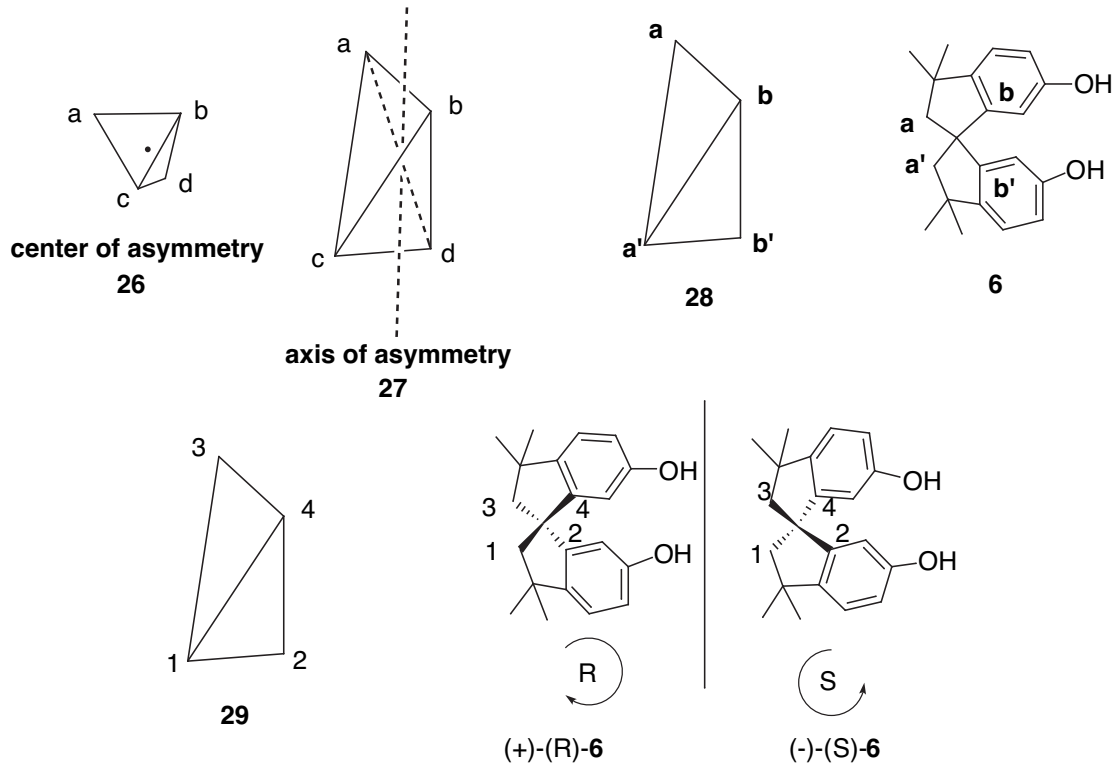

Figure 1.6 Configuration of axially chiral spirobiindanol **6**.

The first enantiomerically pure spirobiindanol was obtained by Hagishita's group[49] in five steps after the resolution of its corresponding diacid (±)-**30** by fractional crystallization of the (-)-dibrucine salt (-)-**31** (Scheme 1.3). The resolved (-)-**31** was hydrolyzed with HCl to form optically pure (-)-**30**, which was converted to di-acylchloride (-)-**32**, then diazide (-)-**33** through Curtius reaction. Subsequent transformation to optically active diamino derivative (-)-**34**, followed by diazotization and acylation produced diacetoxy derivative**,** (-)-**35**. Finally, base-catalyzed hydrolysis of (-)-**35** afforded the desired optically active diol, (-)-**6**.

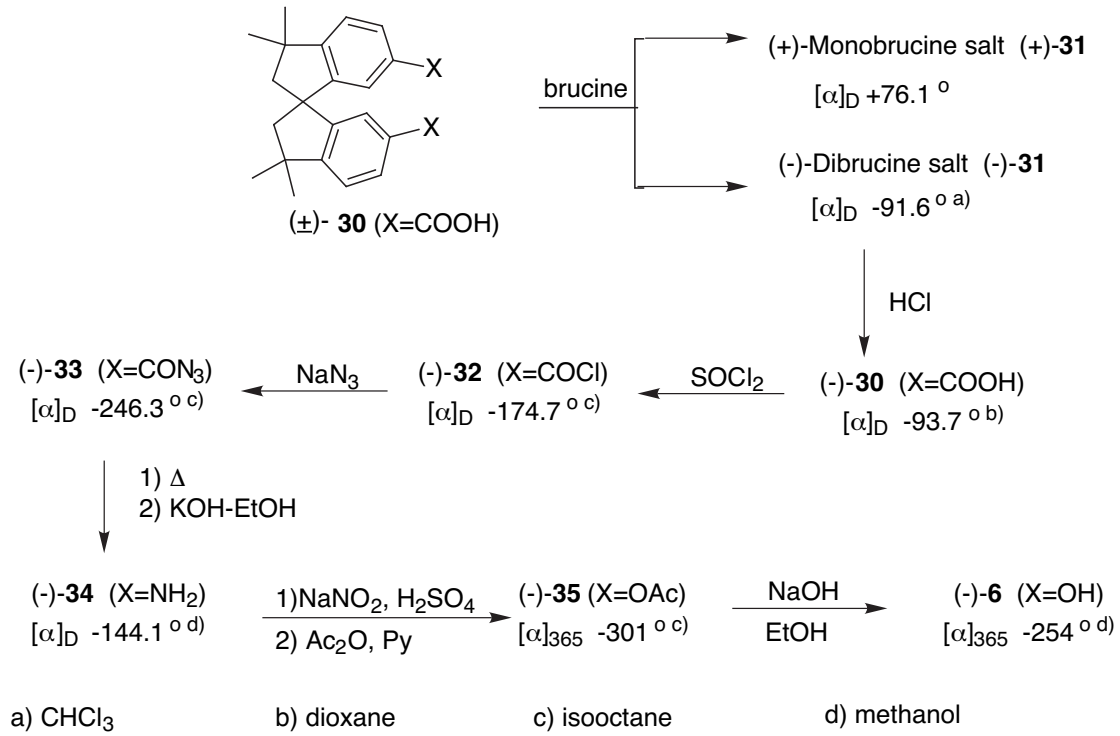

Scheme 1.3 Hagishita's resolution of spirobiindanol.

An improved resolution method of spirobiindanol was reported by Kazlauskas[50-52] (Scheme 1.4). In his paper, cholesterol esterase CE[53.54] from bovine pancreas was used for the resolution of both BINOL and spirobiindanol**.** Before the resolution, the racemic diol (±)-**6** was first converted into a diester. Specifically, dihexanoate ester (±)-**36** provided the best result for asymmetric hydrolysis of spirobiindanol. The enzyme selectively hydrolyzed the dihexanoate ester made from (*R)*-(+)-**6**, and the diester (*S*)-**36** was separated and hydrolyzed under basic condition. Both enantiomers were obtained in > 50 % theoretical yield with > 95 % enantiomeric purity after recrystallization from pet ether-ether.

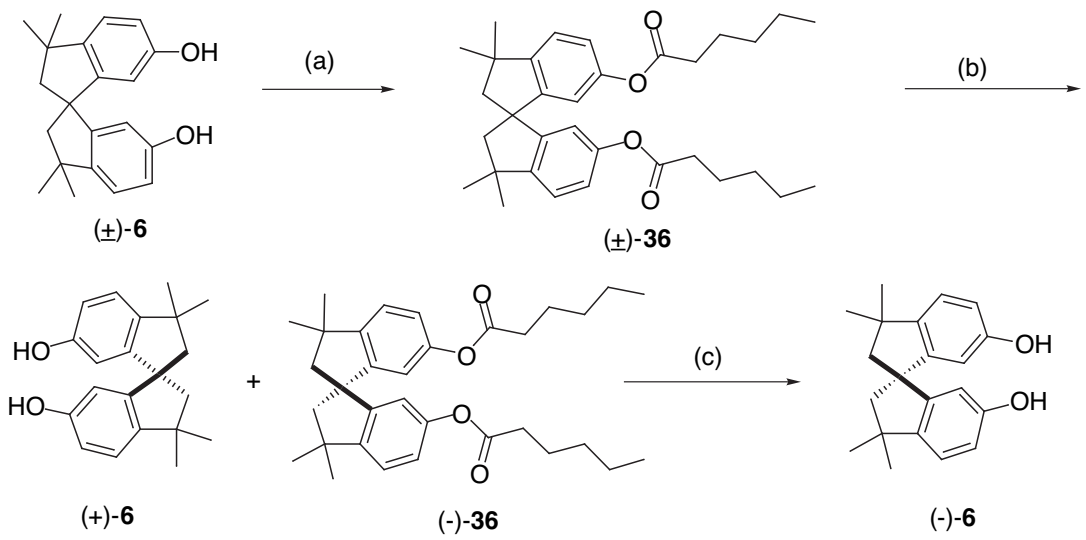

(a) hexanoylchloride, THF, Et_3N (b) cholesterol esterase, phosphate buffer pH~7.1, benzamidine, sodium taurocholate, trypsin inhibitor, Et_2O (c) KOH, Et_2O, EtOH

Scheme 1.4 Kazlauskas' resolution of (±)-**6** using cholesterol esterase.

Other spirobiindane analogues were resolved using different chiral reagents. For example, Hagishita also followed the scheme of Baker and Besly[55] to resolve (±)-6,6'-dihydroxy-3,3,5,3',3',5'-hexamethyl-bis-1,1'-spiroindane **37** using (+)-phenethyl-isocyanate.[56] Other chiral resolving agents, such as (+)-camphorsulfonic acid chloride, (-)-methoxyacetic acid chloride and (+)-α-phenchocomphorone-1-isocyanate all failed to provide enantiomerically enriched products. Consiglio succeeded in resolving spirobiindane bisphosphonates[57] **38** by direct HPLC resolution using Chiralpak AD column.

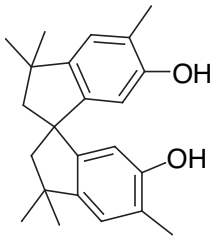

37

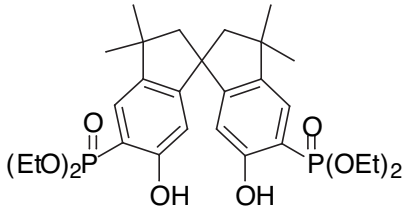

38

Figure 1.7 Spirobiindane analogues **37** and **38**.

It is known that another chiral spirobiindane derivative, (±)-1,1'-spirobiindane-7,7'-diol[58]—SPINOL—was first resolved by esterification with L-menthyl chloroformate, and NEt_3, but the better method is the inclusion crystallization with *N*-benzylcinchonidium chloride in toluene.[59] The enantioselectivity from the initial separation was upto 96 % ee with 93 % yield for (*R*)-(+)-SPINOL and 90 % ee with 88 % yield for (*S*)-(-)-SPINOL.

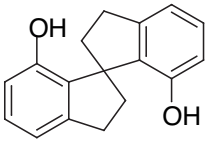

SPINOL

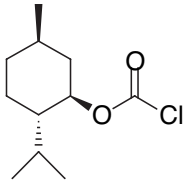

L-menthyl chloroformate

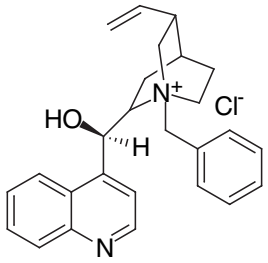

N-benzylcinchonidium chloride

Figure 1.8 Compounds used in the resolution of SPINOL.

1.1.3 Syntheses of Phenanthroline and Bipyridine Derivatives

1.1.3.1 Introduction

Nitrogen-containing heterocycles, such as bipyridine (bpy) and phenanthroline (phen), are widely used as ligands in supramolecular chemistry,[60-65] conformationally constrained peptides,[66-70] in sensors and receptors,[71-73] in polymer chemistry,[74-77] studies of redox electrocatalysis.[78] Metal-binding ability of 1,10-phenanthroline, phen, has been used in a wide range of analytical reagents and probes as well as herbicides.[79] Some natural compounds containing the phenanthroline moiety have been isolated and several of them have shown anti-cancer properties.[80]

Halomethyl derivatives of bipyridine and phenanthroline are especially useful because they can be used as precursors to many other analogues. Unfortunately, synthesis and purification of derivatives are difficult, and there is still a lot of room for improvement. Only a few known methods of synthesizing bishalomethylbipyridine and its phenanthroline analogues are known.[81-85] Several well-known synthetic methodologies to obtain the halomethyl phen and bpy derivatives will be discussed in the section.

1.1.3.2 Phenanthroline Derivatives

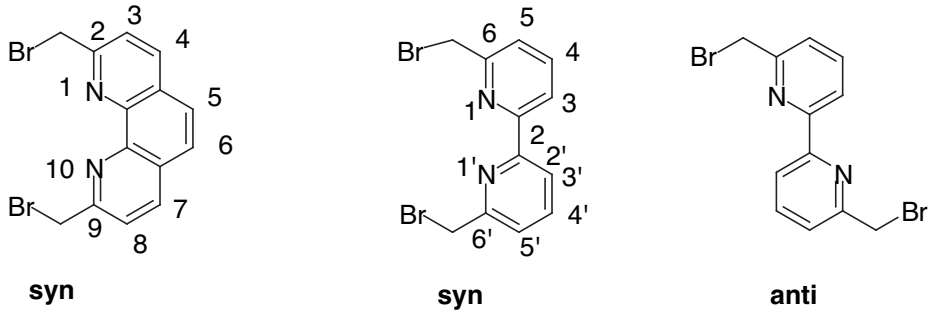

Figure 1.9 Conformation of nitrogen atoms in phen and bpy.

Due to their structural differences, there are distinctive advantages for phen over bpy.[86] Unlike bpy, which favors *anti*-conformation of two nitrogen atoms, phen has more rigid structure imposed by the central ring B, which fixes two nitrogen atoms in *syn* position all the time (Figure 1.9). This entropic advantage allows 1,10-phenanthroline to form complexes with metal ions more rapidly, as shown in the formation of cooperative complexes with lanthanide ions.[87] Other advantages include its ability to either intercalate or groove-bind to DNA or RNA strands,[88-92] and also it can be used as a triplet-state photosensitizer in complexes with lanthanides, such as europium.[93]

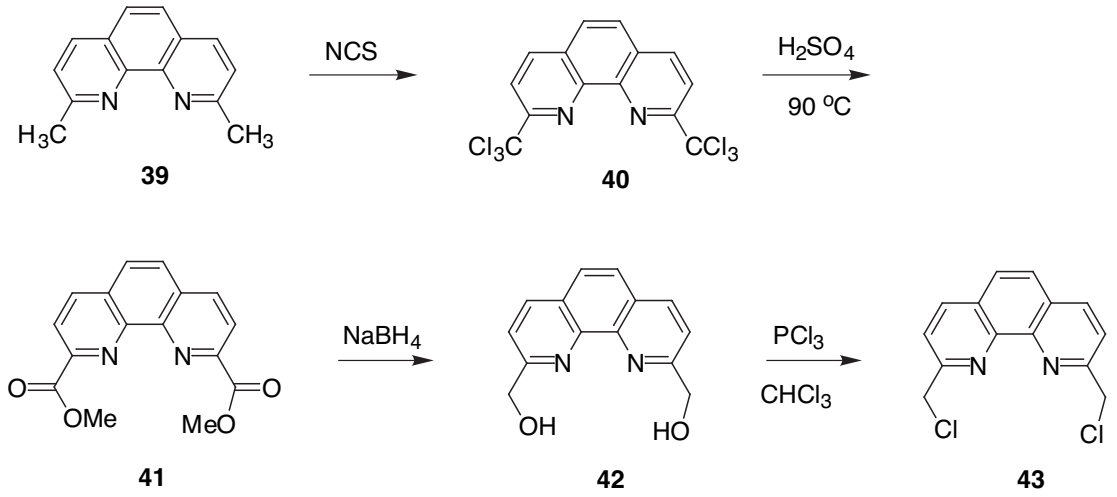

Scheme 1.5 Synthesis of 2,9,-bis(chloromethyl)-1,10-phenanthroline.

The synthesis of 2,9-bis(chloromethyl)-1,10-phenanthroline **43** starts from commercially available 2,9-dimethyl-1,10-phenanthroline (dmp) **39**, also known as neocuproine[94] (Scheme 1.5). Chandler[82] reported that direct chlorination of its methyl groups using NCS was not possible. For instance, unlike the bipyridyl derivative, **39** experienced enhanced reactivity under photochlorination condition,

resulting in the formation of the hexachloro derivative and a mixture of other chlorinated isomers. When 6 equivalents of NCS were added, trichloromethyl intermediate **40** was produced in quantitative yield.[95] Newkome[81] and coworkers treated **40** with concentrated sulfuric acid and methanol to obtain the diester **41**.[96] Reduction of **41** with $NaBH_4$ afforded the biscarbinol **42**[97], which was followed by chlorination with PCl_3. According to Newkome, when $SOCl_2$ was used, an unknown sulfur-containing compound was isolated.[81]

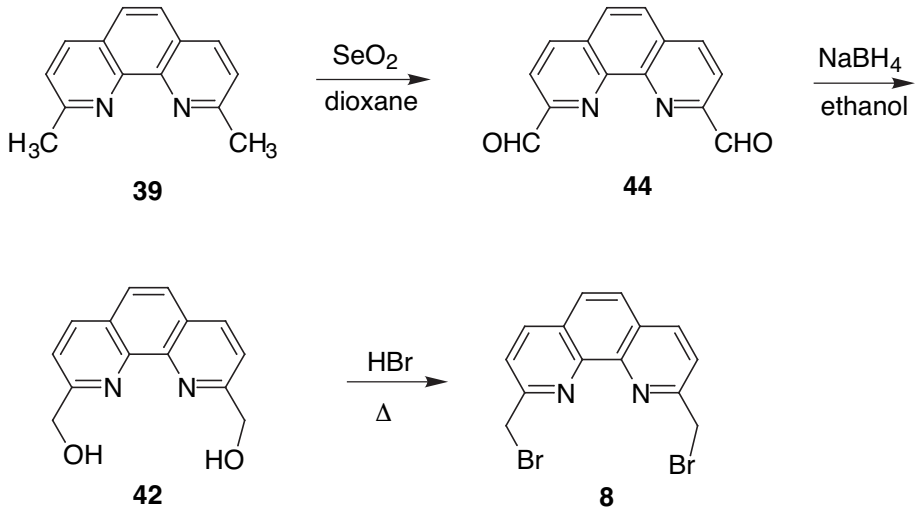

Scheme 1.6 Chandler's synthesis of **8**.

Chandler[82.95] and coworkers avoided the photohalogenation methodology all together to synthesize 2,9-bis(bromomethyl)-1,10-phenanthroline **8** (Scheme 1.6). Commercially available dmp was oxidized by selenium dioxide[98] to afford the dialdehyde **44**,[99.100] even though an earlier report[101] on the reaction scheme claimed to produce an unsymmetrical compound, which had one aldehyde and one carboxylic group as the product. The dialdehyde **44** was reduced by $NaBH_4$ to produce **42**, which was treated with refluxing HBr to afford the desired product **8**.

Various reaction conditions were tried to convert dmp **39** directly into **8** without any success. For example, the reaction with two moles of bromine in carbon tetrachloride produced a compound assigned as the hydrobromide perbromide of dmp. NMR data indicated no replacement of hydrogen by bromide. Some other groups have claimed that they were successful in converting **39** directly into **8** by photobromination[102] or acid-catalyzed bromination;[103] however, my personal experience with these procedures in lab were not successful.

1.1.3.3 Bipyridine Derivatives

Although bipyridine ligands have a wide application in chemistry, synthesis and purification of many desirable bipy ligands have been challenging.[104] Many groups have come forth with different synthetic schemes to produce substituted bipyridine derivatives. For example, 6,6'-difunctionalized bipyridine analogues were synthesized from 6,6'-dibromo-2,2'-bipyridine **47** via lithium-bromide exchange reaction, followed by addition of *N,N*-dimethylformamide to produce dialdehyde **48**.[105-108] Quantitative reduction of **48** by $NaBH_4$ yielded the diol **49**, which was converted to the bis(chloromethyl) derivative **45** upon treatment with purified[109] $SOCl_2$. [NOTE: *One must be very careful when handling all of these halomethyl derivatives since they are extremely irritating to the skin and mucous membranes*[110]]. However, this reaction scheme was plagued by the arduous large-scale lithiation procedure, which was potentially hazardous.

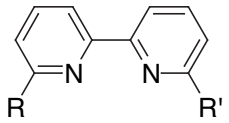

45. R = R' = CH_2Cl **49**. R = R' = CH_2OH
7. R = R' = CH_2Br **50.** R = R' = CH_3
46. R = CH_2Cl; R' = H **51**. 2N->O R = R' = CH_3
47. R = R' = Br **52.** R = R' = CH_2OAc
48. R = R' = CHO **53.** R = R' = $CHCl_2$

Figure 1.10 6,6'-bifunctionalized 2,2'-bipyridine derivatives.

Several other groups focused their efforts in improving the reaction conditions for the synthesis of 6,6'-dimethyl-2,2'-bipyridine **50**. Kauffman's nucleophilic alkylation of methyllithium to 2,2'-bipyridine afforded **50** in 40 % yield.[111] Direct coupling of 6-amino-2-picoline via either the Gomber-Bachmann or Gattermann reaction failed to produce the desired compound **50**.[112] On the other hand, the related 6-bromo-2-picoline, which could be synthesized from the corresponding amine, produced dimethylbipyridine in >50 % yield upon treatment with palladium on charcoal under phase-transfer condition.[113] Stoichiometric amount of Raney-nickel could be used to convert 6-bromo-2-picoline into **50** in 87 % yield.[114]

Direct chlorination of **50** with Cl_2 gas, excess anhydrous sodium carbonate, and a trace of water in CCl_4 failed to provide **45**, even though the identical conditions afforded 2-(chloromethyl)pyridine from 2-picoline.[115] Instead, a more roundabout way was employed to synthesize **45**. First, **50** was treated with excess peracetic acid to afford bis-*N*-oxide **51**,[116.117] which could be converted into diester **52** by refluxing it in redistilled acetic anhydride.[118] Transesterification of **52** with anhydrous potassium

carbonate in ethanol afforded a quantitative yield of diol **49**. Thionyl chloride was used to convert **49** to **45**.[119]

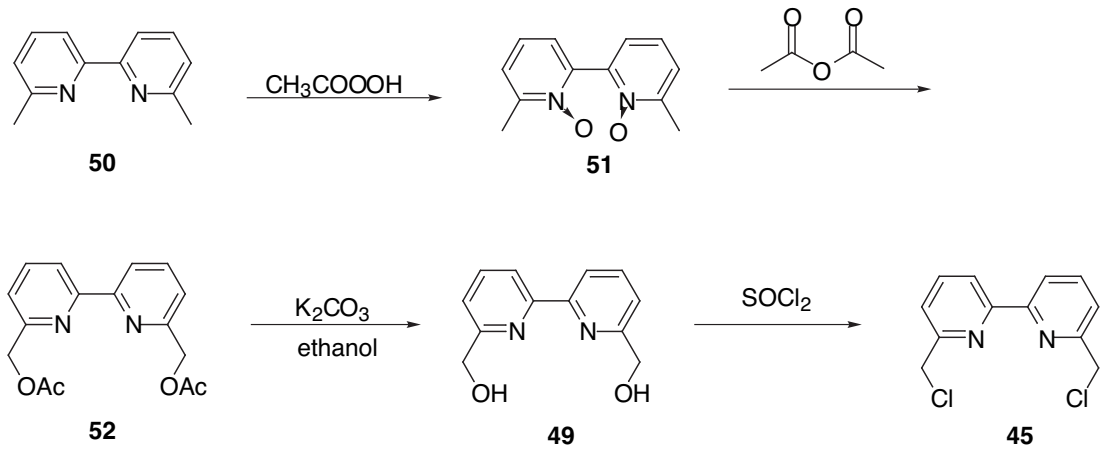

Scheme 1.7 Synthesis of 6,6'-bis(chloromethyl)-2,2'-bipyridine **45**.

Newkome's photochlorination[120] of **50** with *N*-chlorosuccinimide (NCS) provides an easier way to obtain **45** (>65 % yield), along with some unreacted **50** and *sym*-tetrachloride **53**. In the same paper, Newkome reported that the photobromination of **50** with *N*-bromosuccinimide (NBS) in diverse conditions[121] produced only complex brominated products in low yield. Nonetheless, other groups[76.83.122.123] were successful in using NBS with either benzoylperoxide or 2,2'-azobis(2-methylpropionitrile) in CCl_4 to brominate **50**, producing **7**, in 25 % - 59 % yield in gram scales.

Fraser[104.124] and the group reported much improved synthetic methods for both the synthesis of methyl 2,2'-bipyridine ligands **54** and bishalomethyl bipyridine ligands. First, the Negishi cross-coupling reaction between arylzinc and aryl triflate **56** in the presence of a catalytic amount of Pd was used to synthesize methyl 2,2'-bipyridine **55** in 93 % yield. Although it was not possible to trap transient formation

of bpy(CH_2Li) anion with electrophiles to form bishalomethyl bipyridine,[125] Fraser successfully trapped the dianion with TMSCl to generate 4,4'-[bis(trimethlysilyl)methyl]-2,2'-bpy **57** in ~ 99 % yield. The TMS group could then be removed by a dry F^- source in the presence of either BrF_2CCF_2Br or Cl_3CCCl_3 to produce bromide **59** in 97 % yield or chloride **60** in 94 % yield.

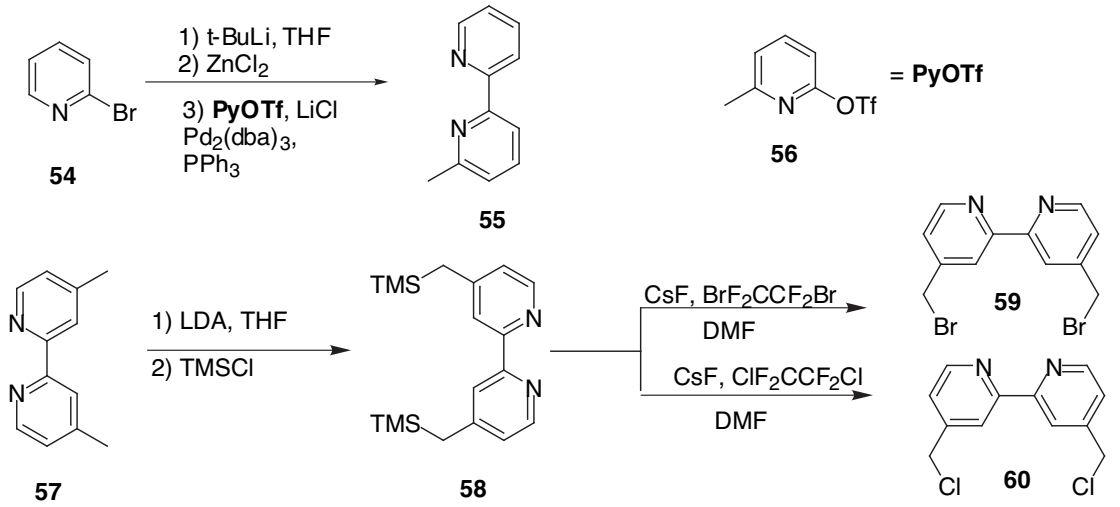

Scheme 1.8 Fraser's synthesis of **59**.

1.1.4 Metal Complexes of Nitrogen-Containing Ligands

The coordination chemistry of nitrogen heterocycles, such as bpy and phen, has been studied extensively and exploited in formation of supramolecular structures,[60.126-128] such as helicates,[62.129] catenates,[130.131] knots,[132.133] molecular grids,[134] and rotaxanes.[128.135.136] Especially, they are known to form stable tetrahedral complexes with Cu^I and Ag^I ions[133.137] and octahedral complexes with Ru^{II} ions.[138.139]

1.1.5 Related Work

A new set of chiral macrocycles using widely known chiral auxiliaries,[140-142] such as **61**-**64**, and bpy and phen ligands were synthesized by Benaglia and coworkers.[143] A simple condensation reaction between **61** and **7** afforded **67** in low yield (<10 %). A revised reaction condition with cesium carbonate in refluxing acetonitrile afforded the desired cyclophanes in total yield of 71 % with 1:1 ratio of **67** (36 %) and a dimeric compound **68** (35 %). Unlike bipyridine-based macrocycles, phen-based systems afforded only monomeric compounds **69** and **70**, although they were produced in higher yields—55 % for **69** and 53 % for **70**.

To study the effects of connecting units between the chiral template and the ligand unit, cyclophanes **71**-**72** were synthesized. Dicarboxylic acid **61** was first converted into acid chloride by treatment of oxalyl chloride, then it was reacted with either **65**[82] or **66**[133] to afford macrocycles **71** (21 % yield) and **72** (45 % yield). Cu(I) complexes of theses macrocycles were tried as possible chiral catalysts for asymmetric cyclopropanation reaction of cyclic alkenes.

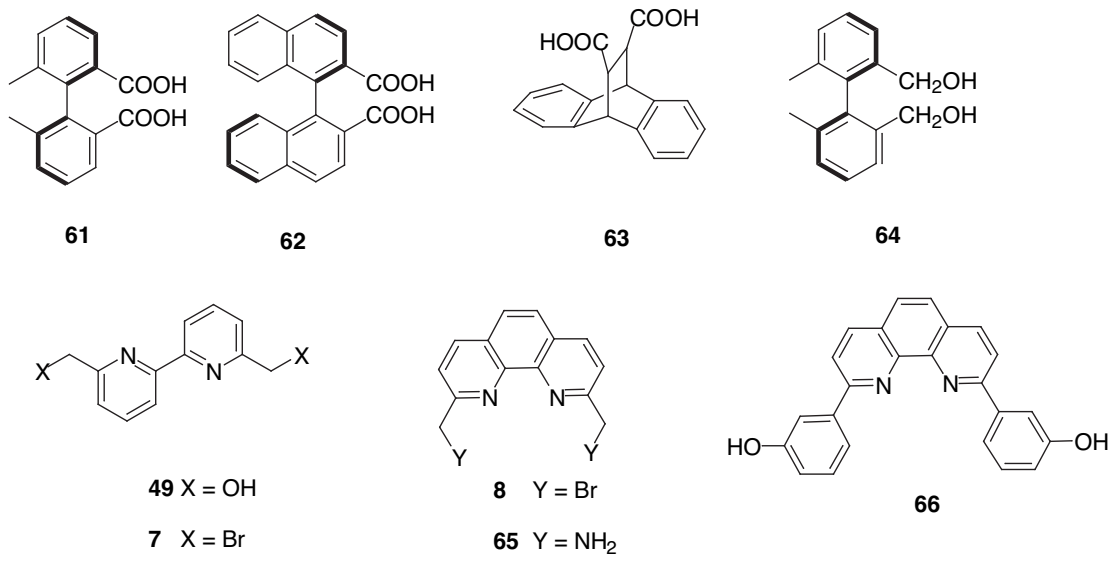

Figure 1.11 Chiral templates and metal-binding units of Benaglia's cyclophanes.

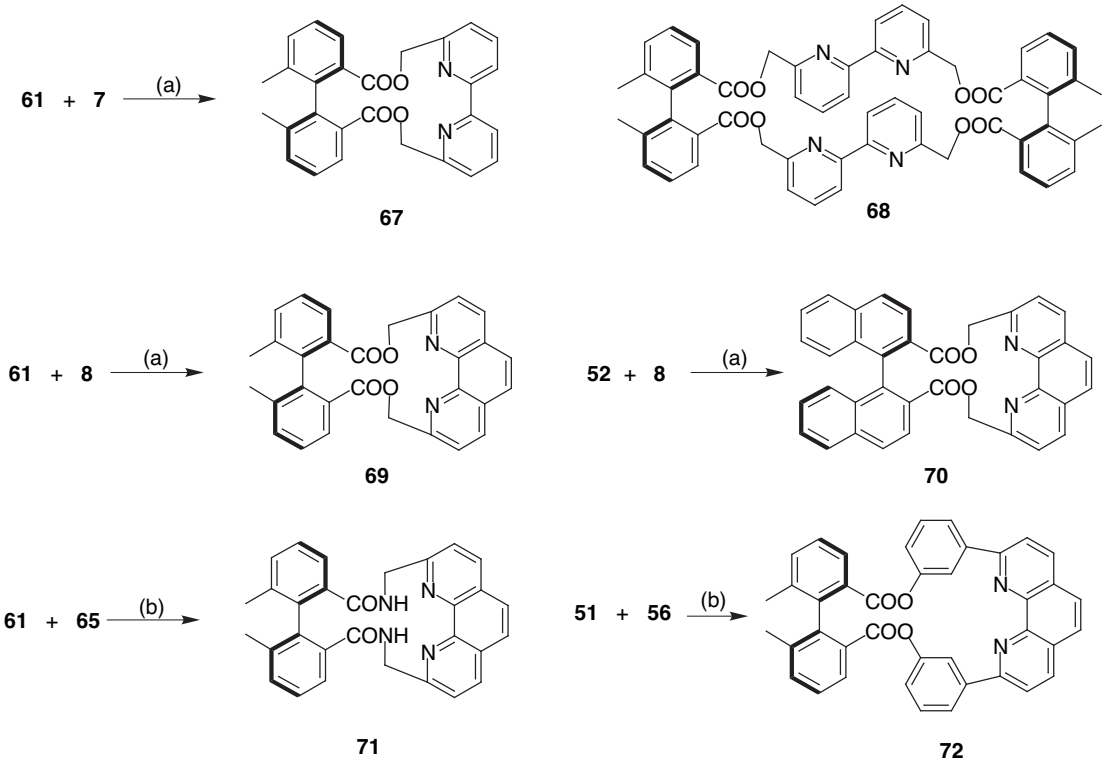

Scheme 1.9 Synthesis of cyclophanes **67**--**72**. (a) Cs_2CO_3 (7 eq), CH_3CN, 48 h, 60 °C. (b) 1) $(COCl)_2$ 2) binding unit **7** or **8**, TEA,

Finocchiaro[57.144.145] and his group have synthesized various chiral host molecules, such as **73a-b** and **74,** by condensing spirobiindane bisphosphonate moiety **38** with appropriate aromatic linkers (Figure 1.12). The Williamson procedure was used to produce these macrocycles in high yield ($\geq$ 70 %), and only [1 + 1] cyclization products were recovered. The cavity size of the C_1- symmetric chiral host[57] **73a** was not big enough to host small organic solvents, such as cyclohexene. However, the X-ray crystal structure of **73a** showed enclathration of the two molecules of cyclohexene in the lattice. After careful monodealkylation of the bisphosphonic acid tetraalkyl esters of **73a**, a new host[146] **73b** was obtained. The macrocycle **73b** has a potential to be used as a NMR chiral shift reagent for biologically relevant amino acids, because it binds enantioselectively to arginine and lysine. The macrocycle **73a** was also resolved using conventional HPLC methods, and the CD spectra of both enantiomers were taken. X-ray crystal structure of the cyclophane **74,** which has a bigger cavity size, showed one cyclohexane molecule inside the host cavity.

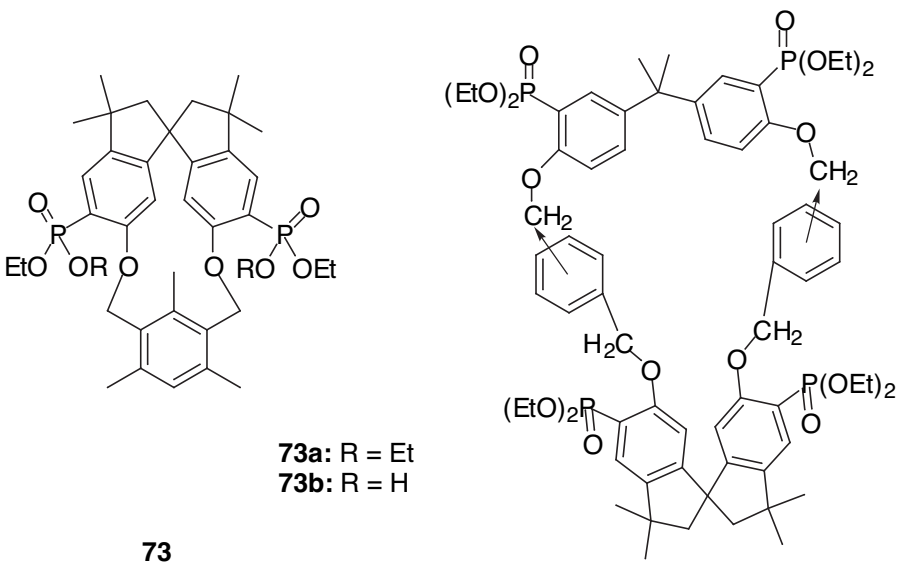

Figure 1.12 Consiglio's macrocycles derived from spirobiindane phosphonates **73** and **74**.

Frank[147] and the group synthesized nitronyl nitroxide biradicals, 6,6'-(4,4,5,5-tetramethylimidazolidine-3-oxide-1-oxyl)-3,3,3',3'-tetramethyl-1,1'-spirobisindane **75**, from functionalization of spirobiindanol followed by Ullmann condensation and oxidation (Figure 1.13). The X-ray crystallographic data of **75** indicates that dihedral angles between the nitronyl nitroxide moiety and the aromatic group is 28 ° with intramolecular through space radical-radical distances of 8.25 and 10.11 Å. There is an evidence for spiroconjugation as an exchange pathway.

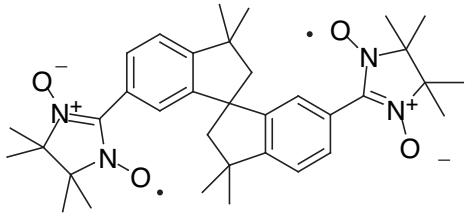

75

Figure 1.13 Frank's biradicals **75**.

Siegel group also used (*R*)-**6**, along with (*R*)-biphenyl **77** as their chiral templates in the enantioselective synthesis of copper(I) bpy based helicates.[64.148] Bipyridine strands were synthesized from 6,6'-dimethyl-2,2'-bipyridine **50** by photobromination, followed by repeated sequences of hydrolysis and/or Williamson etherification steps. The "remote asymmetric induction"[140] from the templates to the helicates was over a distance of 20 Å in the case of ligands containing three bipyridine units **76**.

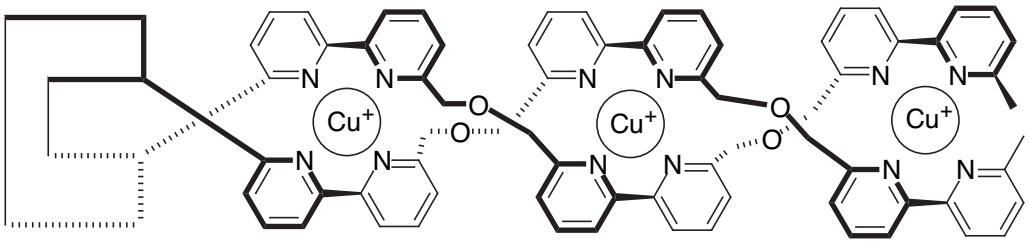

76

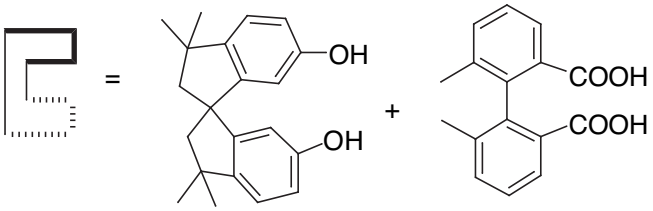

6 **77**

Figure 1.14 Siegel Group's Cu(I) complexed helicates **76**.

1.2 Results and Discussion

1.2.1 Synthesis and Resolution of Spirobiindanol

Spirobiindanol **6** was synthesized according to the method developed by Faler[44]--as shown in (Scheme 1.1). Racemic mixture of **6** was obtained in 81 % yield. An attempt was made to resolve **6** with (+)-phenethylisocyanate without any success.[149] Ultimately, the resolution was possible with a modified method from the report by Kazlauskas[50-52] (Scheme 1.4). A racemic mixture of (±)-**6** was first converted into a bishexanoate ester **36** after the treatment with excess hexanoylchloride, dry triethylamine, and anhydrous THF. The purified diester (±)-**36** was stirred in a mixture of bovine pancreas acetone powder, phosphate buffer, benzamidine, sodium taurocholate, trypsin inhibitor, and ether. The resulting enantiomerically enriched (+)-**6** was further purified by fractional recrystallization in petroleum ether and ethyl ether. Clear, needle-like crystals were obtained through recrystallization in hexanes, with enantiomeric excess < 99 %. The unreacted diester made from (*S*)-enantiomer was hydrolyzed under basic condition, followed by fractional recrystallization from petroleum ether and ethyl ether to obtain (-)-**6**.

The pure form of bovine cholesterol esterase (CE) was expensive, so a more economical source, bovine pancreas acetone powder (purchased from Sigma), was used instead. Pancreas acetone powder is basically a defattened powder of bovine pancreas; therefore, along with the desired enzyme, the powder also contains other digestive enzymes, such as trypsin, which breaks down CE. Addition of trypsin inhibitor prolonged the lifetime of cholesterol esterase during the reaction. Sodium

taurocholate, a bile salt, was added to activate the CE. The pH of the buffer was maintained around 7.1±0.05 by continuous pH monitoring and periodic addition of 1M KOH solutions. Benzamidine and sodium taurocholate assisted the formation of emulsion and created the optimal condition for cholesterol esterase activity. The formation of emulsion was necessary in order to allow CE in aqueous buffer to hydrolyze diester **36** in organic layer. The emulsified reaction mixture became very thick, so a mechanical stirrer was needed to provide constant stirring. Unlike the Kazlauskas' report, the enantioselective hydrolysis reaction was completed within 2 days with lower initial ee of (*R*)-**6**. Although it was possible to run multi-gram scale reactions, the enantioselectivity of alcohols varied from reaction to reaction. It was not possible to find a reaction condition that would provide consistent enantioselectivity even after many attempts.

1.2.2 Synthesis of 2,9-Bisbromomethyl-1,10-phenanthroline

Phenanthroline-based ligands were synthesized by a known method developed by Chandler[82] (Scheme 1.6). Commercially available dmp 39 was oxidized by SeO_2 in dioxane with 4 % water. The resulting yellow dicarbaldehyde 44 was reduced in the presence of $NaBH_4$ in ethanol. The crude diol 42 was brominatewith concentrated HBr.[103] Until the final step, all the intermediate compounds were used without purification. The final compound, 8, was purified by column chromatography (overall yield 23 %) and stored in the absence of light for up to 6 months at room temperature.

1.2.3 Synthesis of 6,6'-Bisbromomethyl-2,2'-bipyridine

Bipyridine ligand **7** was synthesized starting from the commercially available 2-amino-6-picoline [Scheme 1.10]. 2-Bromo-6-picoline was converted from the corresponding amine through diazotization followed by bromination.[83.150] Originally, 6,6'-dimethyl-2,2'-bipyridine, **50**, was synthesized by homolyptic coupling of two 2-bromo-6-picoline molecules through palladium(II)-mediated cross coupling reaction.[151] The reaction produced the desired **50** in over 90 % yield in a small scale. However, in a larger scale, the product yield decreased to 65 % due to the difficulty of removing a large amount of Bu_4NBr during the work-up. The second method using Loren's[152] modified Negishi-cross coupling reaction[104.124.152]. 2-Bromo-6-picoline was treated with BuLi, followed by $ZnCl_2$ to form *in situ* 2-methylpyridyl-ZnCl intermediate. The reaction with tetrakistriphenylphosphine palladium (0), along with one equivalent of 2-bromo-6-picoline, afforded **50** in 62 %. In spite of a slightly lower yield, this was the method of choice because it was possible to run the reaction in multi-gram scale, and pure products were obtained without column chromatography.

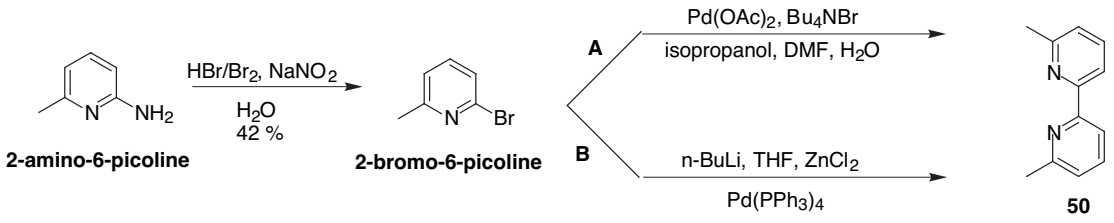

Scheme 1.10 Synthesis of **50**.

Scheme A

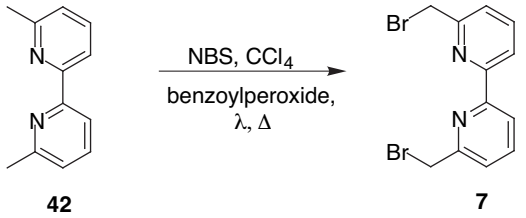

42 **7**

Scheme B

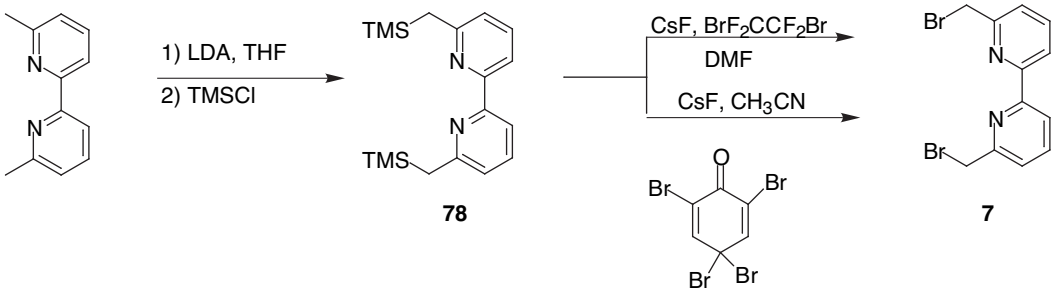

78 **7**

79

Scheme 1.11 Synthesis of **7**.

Photobromination[153] of **50** with *N*-bromosuccinimide in CCl_4 afforded **7**, along with other mono-brominated and poly-brominated bipyridine ligands. Numerous column chromatographies yielded enough ligand for cyclophane synthesis. An alternative method was using Fraser's[104.124] system of trapping the lithiated methyl groups with TMS-Cl, followed by quenching the intermediate **78** with a brominating reagent--dibromotetrafluoroethane**.** Unfortunately, the production of dibromotetrafluoroethane in US was prohibited due to a stricter environmental regulation, so it was not feasible to pursue this synthetic method further. Another possible brominating reagent, such as 2,4,4,6-tetrabromo-2,4-cyclohexadienone **79**, in place of BrF_2CCF_2Br, was tried with a limited success (23 % yield) (Scheme 1.11).

1.2.4 Synthesis of Chiral Cyclophanes

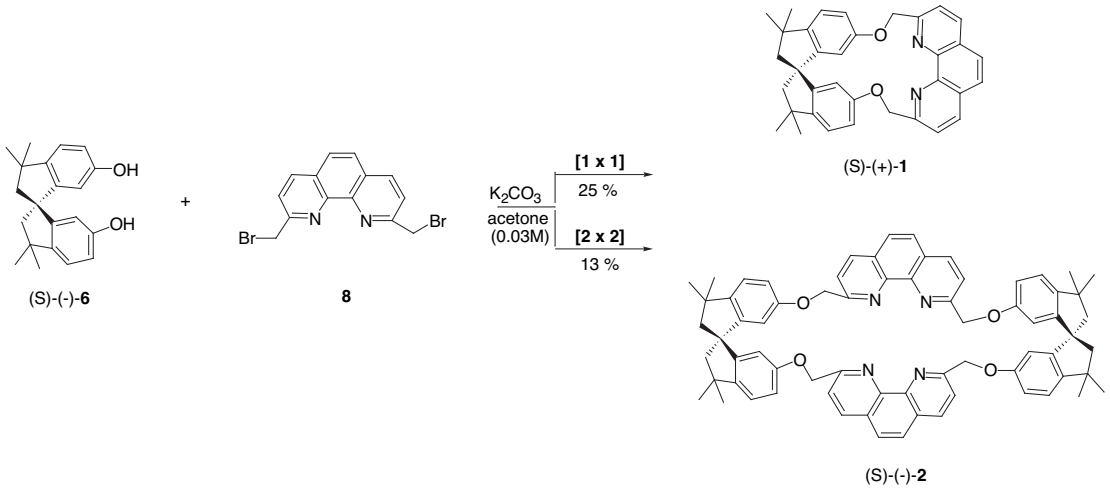

Scheme 1.12 Synthesis of **1** and **2** with (*S*)-(-)-**6**.

Table 1.1 Product Distributions of Phenanthroline-based Chiral Cyclophanes.

[**6** + **8** in acetone]	% **1**	% **2**	% **3**
0.03 M	25 %	13 %	Not detected
0.007 M	68 %	Trace	Not detected
0.007 M[a)]	42 %	6 %	1 %

a) In gram scale

The Corey-Pauling-Koltun (CPK) atomic models indicate that when one equivalent of bidentate ligand, phen or bpy, is covalently linked to a spirobiindanol, very sterically congested cyclophanes will be formed. Small cavities of these cyclophanes will be able to host only one small metal ion inside. Also, in such a strained geometric environment, aromatic groups in the molecule will in a close proximity to each other. In an effort to synthesize chiral [1+1] cyclophanes, other bigger compounds, [2+2] and [3+3] cyclophanes, were also isolated. Theses bigger cyclophanes are interesting because their bigger cavities can host more guest molecules, and their more flexible molecular frame can allow structural distortions.

The [2+2] cyclophanes are also of interest because nitrogen atoms in either phen or bpy ligands are predisposed to coordinate a metal ion in tetrahedral geometry.

Enantiomerically enriched chiral cyclophanes were synthesized by Williamson ether synthesis using either acetone or acetonitrile[57] as a solvent, and K_2CO_3 as a base with resolved *R* or *S* spirobiindanol with **8**. In the first condition (0.03 M solution), two different types of cyclophanes, **1** and **2**, were isolated as shown in (Scheme 1.12). Total yield of cyclophanes was 38 % with **1** being produced twice as much as **2**. In a more diluted condition (0.007 M solution), the compound **1** was obtained in 68 % yield, while [2+2] cyclized cyclophane **2** yield was minimized to a trace amount. When the reaction was run in gram scale at 0.007 M, cyclophanes, **1** (42 % yield) and **2** (6 % yield) were obtained, along with a miniscule amount of the [3+3] cyclized product **3** (1 % yield). It was not possible to drive the reaction to form cyclophane **2** selectively by increasing the concentration of the reaction condition. For example, in 0.6 M condition, only starting materials and insoluble oligomers were isolated.

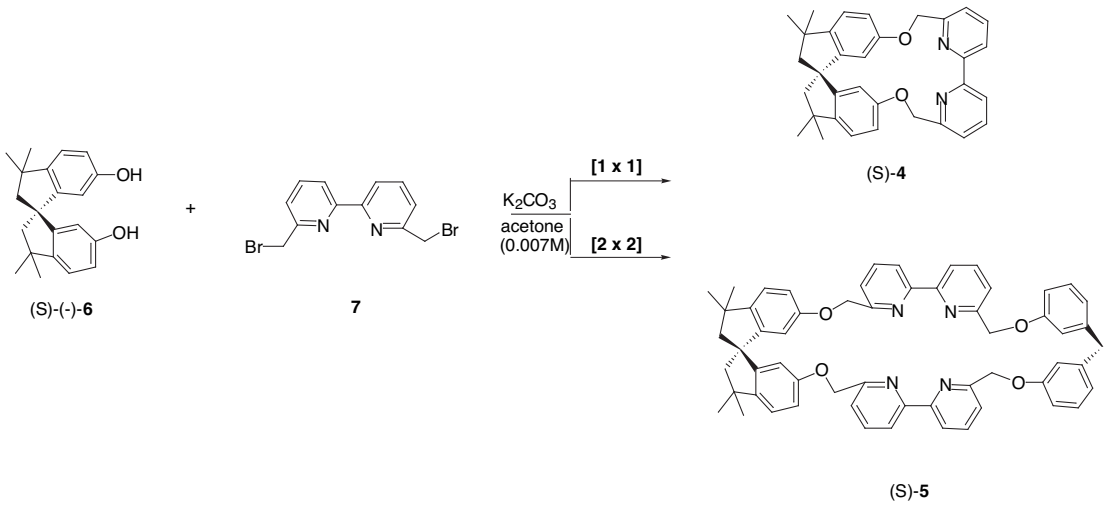

Scheme 1.13 Synthesis of **4** and **5** with (*S*)-(-)-**6**.

Table 1.2 Product Distributions of Bipyridine-based Chiral Cyclophanes.

[**6** + **7** in acetonitrile]	**% 4**	**% 5**	**Insoluble**
0.007 M	13 %	16 %	34 %

The Williamson ether synthetic method was used to synthesize bipyridine-based cyclophanes **4** and **5** (Scheme 1.13). Each *S* and *R*-enriched spirobiindanol was reacted with **7** in either acetonitrile or acetone with potassium carbonate under reflux. Unlike the phenanthroline-based cyclophane system, both monomeric cyclophane **4** and the dimeric cyclophane **5** were produced in almost 1:1 ratio. A reaction run in a mixture of solvents--ethanol, THF, and benzene--produced only the monomeric cyclophane **4**.[154] The "template" effect of benzene in the solvent system is known to improve the formation of [1×1] macrocycle without undergoing high dilution conditions. Ultimately, this condition was not pursed further because the yield from this reaction (14 %) was not much better results from other simpler reaction conditions. Bipyridine-based cyclophanes took longer to form—upto 6 days--compared to 24 h for phenanthroline-based cyclophanes. A set of inseparable

oligomers that could not be purified nor characterized actually made up the majority, 34 %, of isolated products.

More phen-based cyclophanes were synthesized than bpy-based cyclophanes because of their difference in flexibility of the structures. Because of the rigid carbon backbone at 5,6-positions in phen, the two bromomethyl substituents are fixed in *syn* position. The more flexible structure of the bipyridine allows both *syn* and *anti* conformations. Due to the electron rich nitrogen, the *anti*-conformation is more stable; therefore, it is dominant at room temperature.[155] For example, the ^{1}H NMR of **7** indicates that the 3-pyridyl hydrogen is shifted downfield (8.39 ppm) by the increased diamagnetic anisotropy because it is right next to the orthogonal nitrogen electrons of the adjacent pyridine ring.[155] However, when the bpy is incorporated into the conformationally rigid structure of **4**, the *syn* conformation is imposed, as shown in the dramatic upfield shift of H3 proton (Δ .90 ppm).[81] As the ring size gets bigger, as in the case of **5**, the 3-pyridyl proton shifts downfield (8.15 ppm), suggestive of an *anti* conformation.[156.157] Thus, the conformational flexibility of bpy means it takes longer for it to form the desired cyclophanes, and also longer oligomers or cyclophanes with bigger ring sizes can be formed more easily with bpy. Notably, Benaglia[143] was able to make both monomeric **67** and dimeric **68** cyclophanes with bpy ligands, but phen-based ligands produced only monomeric compounds **69** and **70** in higher yields.

1.2.5 Metal Complexes of Chiral Cyclophanes

Cyclophanes **1**–**4** were shown to host many different metal ions—such as Cu(I), Ag(I), Pd(II), Zn(II), and Hg(II) ions. Chiral cyclophanes were used to form complexes with Ag(I) and Cu(I) salts, and their chiroptical properties were studied by CD (will be addressed in Ch.2). More available cyclophane, *rac*-**1**, was used to make complexes with the last three metal ions.

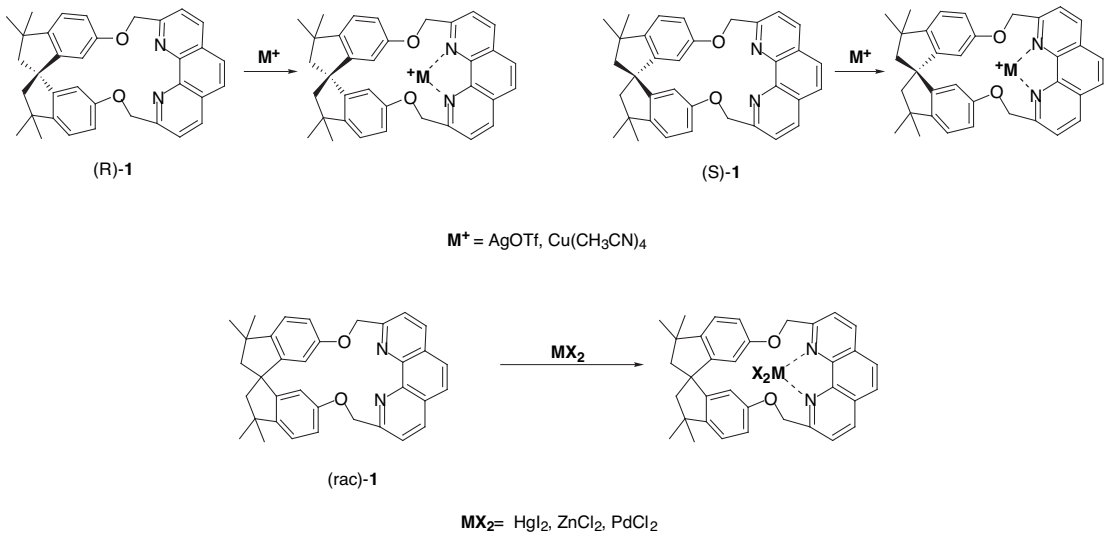

Scheme 1.14 Syntheses of metal complexes using **1**.

Table 1.3 Product yield of metal complexes made from cyclophane **1**.

Metal Complex	Ag(I) **80**	Cu(I) **81**	Hg(II) **82**	Pd(II) **83**	Zn(II) **84**
% Yield	68 %	28 %	44 %	95 %	47 %

The Ag^{I} complex **80** was formed by stirring a 1:1 ratio of silver(I) trifluoromethanesulfonate $Ag(CF_3SO_3)$ and the cyclophane **1** together in degassed acetonitrile under Ar in the absence of light. The Cu^{I} complex **81** followed the same reaction condition with a 1:1 ratio of tetrakis(acetonitrile)copper(I) hexafluorophosphate $[Cu(CH_3CN)_4](PF_6)$[158] and **1**. The progress of the reaction was

followed by TLC, and indicated by the color changes of the reaction solution—clear to slight yellow for silver and clear to light-orange for copper complex.

Crude ^{1}H NMR spectra of **80** and **81** show that desired complexes were formed quantitatively. Isolated yields were about 62 % for the silver(I) complex **80** and 28 % for the copper(I) complex **81** (problematic work-up process). Both metal salts and the metal complexes were readily soluble in acetonitrile, but the host molecule **1** was only slightly soluble in acetonitrile. Therefore, both the dissolution of all solids and disappearance of the starting material on TLC indicate the completion of complexation reaction. Clear crystals of [Ag(**1**)](OTf) **80** suitable for X-ray crystallography were grown in acetonitrile / ether system. These crystals were easily reduced, so it was important to keep them out of light under argon. Dark-yellow crystals of [Cu(**1**)](PF_6) **81** were obtained by diethyl diffusion into an acetonitrile solution of the complex. These crystals were easily oxidized to copper(II) salt, so they had to be kept away from oxygen.

Metal complexes of the racemic cyclophane **1** with Hg^{II}, Zn^{II} and Pd^{II} did not form easily under the reaction conditions used for silver(I) and copper(I) complexes. Therefore, other synthetic routes needed to be utilized. The mercury(II) complex **82** was prepared by reacting a slight excess of red HgI_2 dissolved in methanol with **1** in dichloromethane. The reaction mixture was refluxed for an hour to obtain the final product (44 % yield). Clear, yellow crystals suitable for X-ray crystallography were obtained from CH_2Cl_2/hexanes mixture. The palladium(II) complex **83** was obtained by refluxing a slight excess of $PdCl_2$ with the cyclophane in a mixture of

dichloromethane, acetonitrile, and methanol solution overnight (95 % yield). Excess palladium salt was removed by filtration to obtain the bright yellow solids. The zinc(II) complex **84** was formed by reacting a slight excess of anhydrous $ZnCl_2$ with **1** in dichloromethane (47 % yield). The white suspension was stirred overnight, followed by filtration to remove excess zinc salt.

Because there was not enough bipyridine-based cyclophanes, only silver(I) and copper(I) metal complexes were formed (Scheme 1.15). The cyclophane **4** was stirred in degassed acetonitrile under argon, and a slight excess of either Ag(OTf) or $[Cu(CH_3CN)_4](PF_6)$ was added. The reaction mixture was stirred until all the solids were dissolved. After purification, slightly gray silver(I) complex **87** (89 % yield) and orange copper(I) complex **88** (88 % yield) were obtained. Extensive efforts were put into getting X-ray quality single crystal; however, it was not possible to obtain one.

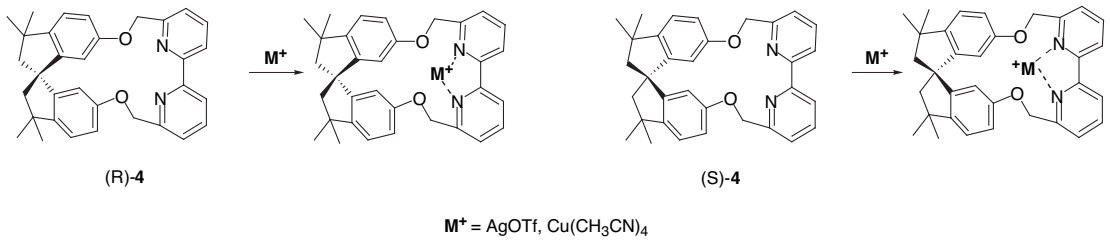

Scheme 1.15 Syntheses of metal complexes using **4**.

Only two metal ions, Ag^I and Cu^I, were used to prepare metal complexes for the larger cyclophanes--**2** and **5**. Either Ag(OTf) or $[Cu(CH_3CN_4)](PF_6)$ was dissolved in degassed acetonitrile and reacted with the appropriate cyclophane at room temperature. Metal complex formation was very rapid, forming a slightly yellow solution for silver(I) and dark-orange for copper(I). The progress of the reaction could

be followed visually because host molecules were only slightly soluble in acetonitrile, but both the metal salt and metal complexes were readily soluble. The excess acetonitrile was removed under reduced pressure. The crude product was taken up in dichloromethane and purified by a short column chromatography through celite. Removal of the solvent left slightly yellow solids for silver(I) complex and dark-orange solids for copper(I) complex. In spite of numerous attempts at crystallization, only X-ray quality crystals from the copper complex of **2** were obtained from slow diffusion of benzene vapor into the complex dissolved in dichloromethane.

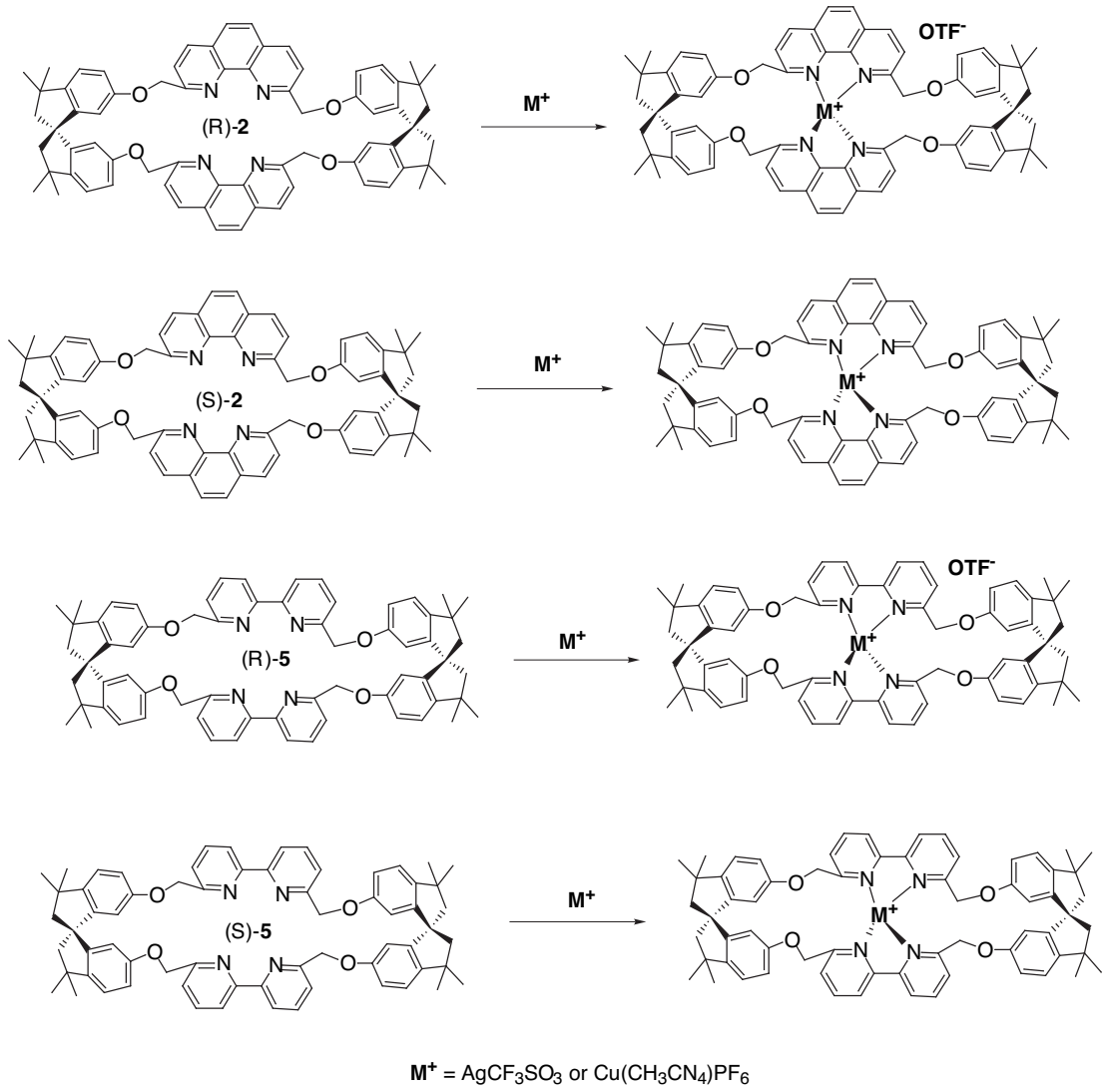

Scheme 1.16 Syntheses of metal complexes using macrocycles **2** and **5**.

Table 1.4 Product Yields of Metal Complexes **85**—**86** and **89**—**90**

Metal Complex	% Yield	Metal Complex	% Yield
[Ag(**2**)]OTf (**85**)	96 %	[Ag(**5**)]OTf (**89**)	78 %
[Cu(**2**)]PF_6 (**86**)	84 %	[Cu(**5**)]PF_6 (**90**)	92 %

1.3 Conclusion

Initially, a new synthetic scheme was designed to form a novel type of [1+1] helically chiral cyclophanes **1** and **4** from resolved spirobiindanol and metal-binding ligands with phen and bpy backbone. More structurally interesting cyclophanes **2** and **5**, which are predisposed to form tetrahedral coordination with a small metal ion, were also synthesized from reactions mentioned above. A trace of the bigger [3+3] cyclophane **3** was also isolated. Metal complexes of chiral cyclophanes **1—2** and **3--4** with silver(I) and copper(I) were synthesized, which will make it possible to study their chiroptical properties by CD (will be discussed in Ch.2). Generality of the cyclophane as a host was investigated when a racemic mixture of the cyclophane **1** was used to make additional metal complexes with mercury(II), palladium(II) and zinc(II).

A known resolution procedure[51] of spirobiindanol was modified by using a more economical source, pancreas acetone powder, instead of a pure cholesterol esterase. The duration of the process was shortened from 6 d to 48 h with less efficient enantioselectivity.

1.4 Experimental

General Data. Varian Mercury 300 MHz, 400 MHz Model L 600 Pulsed Gradient Driver spectrometer and a Varian 500 MHz Unity spectrometer were used for ^{1}H and ^{13}C NMR. Chemical shifts (δ) are reported in parts per million (ppm). Multiplicities are given as follows: s (singlet), d (doublet), t (triplet), q (quartet), dd (doublet of doublets), and m (multiplet). Coupling constants were given in hertz. ^{1}H NMR spectra were referenced to tetramethylsilane (TMS) at 0.00 ppm. In the following solvents, ^{1}H NMR shifts were measured relative to residual protiated solvents: CD_2Cl_2, δ 5.32; CD_3CN, δ 1.94. ^{13}C NMR shifts were relative to solvent resonance: $CDCl_3$, δ 77.0; CD_2Cl_2 δ 53.2; CD_3CN δ 118.3.

Mass spectra (MS) were taken at high-resolution mass spectrometry facilities at University of California at Riverside, University of California at San Diego, and University of Zurich in either MALDI or EI mode as indicated for each compound. IR spectra (cm^{-1}) were recorded on Perkin-Elmer 1420 Ratio Recording Infrared Spectrophotometer in KBr pellets. Ultraviolet spectra (UV) were obtained on Perkin-Elmer UV/Vis/NIR Spectrometer Lambda 19. Melting points were taken in an open capillary with a Melt-temp and were uncorrected. High-pressure liquid chromatographic (HPLC) analyses were carried out on a Hewlett-Packard Series 1100 HPLC system equipped with a diode array UV detector. UV detection was performed at 250 nm, and Chiracel OD column was used for the measurement of enantiomeric excess. X-ray crystallography was performed at University of Zurich under the

direction of Dr. Anthony Linden and at University of California, San Diego, by Dr. Peter Gantzel.

Optical rotations were determined at the sodium D line on a Perkin Elmer model 241 polarimeter and Jasco P-1010 polarimeter in Professor M. Goodman lab and Professor Emanuel Theodorakis lab, respectively, at the University of California, San Diego. All values were reported as follows: specific rotation is determined using the following formula:

$$[\alpha]_{\lambda}^{t} = \alpha / lc$$

Equation 1

[*a*] = specific rotation, *t* = temperature in degrees Celsius, λ = wavelength of incident light (the sodium D lamp is indicated by "D", λ = 589 nm, the yellow emission line of hot sodium vapor), *a* = observed optical rotation in degrees, *l* = length of sample container in decimeters (its value was 1 or 10 cm), *c* = concentration in grams per milliliter of solution. Circular dichroism measurements were conducted Aviv Circular Dichroism Spectrometer Model 202 in Professor Susan Taylor lab at the University of California, San Diego. The spectra were recorded θ in milidegrees, which were converted to molar absorptivity, Δε, by using the equation, $\Delta\varepsilon = \theta / (32982cl)$. The unit is the difference in molar absorptivity for oppositely polarized light in $M^{-1}cm^{-1}$, *c* is the concentration of the sample in moles per L, and *l* is the path length through the cell in cm.

Chromatography. Silica gel (230-425 mesh) for flash column chromatography was purchased from Aldrich/Fisher Scientific Company. Brockman type II neutral alumina was purchased from Acros Chemical Company. The commercially available alumina was deactivated by addition of 4 % water (w/w). Celite from Acros was used to filter excessive metal salts. Radial Chromatography, using Harrison Chromatotron was used with silica plate. Thin layer chromatography (TLC) was performed on alumina backed silica gel 60 F_{254} plates from Aldrich and alumina backed aluminum oxide 60 F_{254} neutral**.**

Materials. Anhydrous tetrahydrofuran (THF) was prepared by distilling it in sodium and benzophenone. Methylene chloride, toluene, and acetonitrile were dried by stirring and distilling over CaH_2. Anhydrous ether from Aldrich was used for the resolution of spirobiindanol to reduce the amount of side product formation. Petroleum ether was dried by fractional distillation in CaH_2. Bisphenol A and neocuproine hydrate were purchased from Aldrich, and bovine pancreas acetone powder, trypsin inhibitor from soybean, and sodium taurocholate from ox bile were obtained from Sigma. Anhydrous $ZnCl_2$, Ag(OTf), and $[Cu(CH_3CN)_4](PF_6)$ were kept in a dry box. Ag(OTf) was stored away from direct light. $PdCl_2$ and red HgI_2 were obtained from Sigma/Aldrich and used without further purification. Palladium catalyst and n-butyllithium were stored in a freezer. Other commercially available reagents were purchased from Sigma/Aldrich and used without further purification. All solvents were degassed under Ar prior to use and all reactions were run under Ar.

All glassware, syringe needles and cannula were oven dried. Hamilton syringes were dried in dry box under high vacuum.

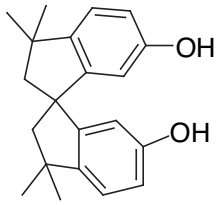

(±)-3,3,3',3'-Tetramethyl-1,1'-spirobi(indan)-6,6'-diol (Spirobiindanol) (6)

Racemic (±)-3,3,3',3'-tetramethyl-1,1'-spirobi(indan)-6,6'-diol, commonly known as spirobiindanol, **6**, was prepared by a method developed by Faler[45]. A 500 mL round-bottomed flask, equipped with a reflux condenser, was charged with bisphenol A (150.20 g, 0.66 mol) and a catalytic amount of methanesulfonic acid (5.06 mL, 0.078 mol). The reaction mixture was heated at 130 °C for 3 h. The hot, liquefied brown mixture was poured into a 200 mL of stirring water in a 500 mL Erlenmeyer flask at room temperature. The light-pink solid was separated by filtration, rinsed with chilled water to get rid of excess methanesulfonic acid and the side product, phenol. The crude product was added into a round-bottomed flask with CH_2Cl_2 (250 mL) and the white suspension was refluxed for 2 h. The resulting white solids were cooled, filtered through Büchner funnel, rinsed with chilled CH_2Cl_2, and air-dried. (81 % yield). (Recrystallized from pet ether-ether) mp 185-186 °C [Lit[40] 214 °C recrystallized from benzene-light petroleum] ^{1}H NMR (400 MHz, $CDCl_3$) δ 7.02 (d, 2H, *J* = 8.0 Hz), 6.70 (dd, 2H, *J* = 8.0, 2.4 Hz), 6.25 (d, 2H, *J* = 2.8 Hz), 4.48 (s, 2H), 2.33 (d, 2H, *J* = 13.2 Hz), 2.23 (d, 2H, *J* = 13.2 Hz), 1.36 (s, 6H), 1.31 (s, 6H); ^{13}C NMR (125 MHz, $CDCl_3$) δ 154.8, 152.0, 144.5, 122.5, 114.3, 110.6, 59.5, 57.5,

43.0, 31.9, 30.5; IR (KBr) ν = 3360 (br), 3120, 3000, 1630, 1500, 1260 cm^{-1}; HRMS-EI^+ *m / z*: $[M]^+$ calcd for $C_{21}H_{24}O_2$, 308.1776; found 308.1779 (26%); UV (CH_3OH) λ_{max}: 284 nm.

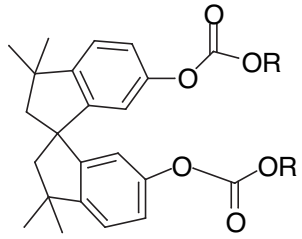

R = $(CH_2)_5CH_3$

(±)-3,3,3',3'-Tetramethyl-1,1'-spirobi(indan)-6,6'-dihexanoate (36)

An oven-dried round-bottomed flask, equipped with Teflon-coated stir bar, (±)-**6** (41 g, 0.13 mol) was charged under argon. Anhydrous THF (400 mL) was added, and the stirring, clear solution was chilled under ice-water bath. Anhydrous triethylamine (50 mL, 0.36 mol) was slowly added into the reaction flask. After the ice-water bath was removed, the THF solution was refluxed overnight under argon. The crude product was cooled to the room temperature, and wet ether (200 mL) was added to quench the reaction. The organic phase was washed with 1 M $NaHCO_3$ solution, 100 mL of water (x3), 20 mL of saturated NaCl solution, and dried over $MgSO_4$. The solvent was removed via rotary evaporator. Column chromatography in SiO_2 with CH_2Cl_2 yielded (±)-**36**. (64 g, 81% yield), ^1H NMR (400 MHz, $CDCl_3$) δ 7.14 (d, 2H, *J* = 8.0 Hz), 6.93 (dd, 2H, *J* = 8.4, 2.0 Hz), 6.50 (d, 2H, *J* = 2.0 Hz), 2.47 (t, 4H, *J* = 7.6 Hz), 2.36 (d, 2H, *J* = 13.2 Hz), 2.26 (d, 2H, *J* = 12.8 Hz), 1.7 (m, 4H), 1.38 (s, 6H), 1.35 (m, 8H), 1.33 (s, 6H), 0.90 (t, 6H, *J* = 6.4 Hz); ^{13}C NMR (75 MHz,

$CDCl_3$) δ 172.2, 151.3, 150.0, 149.3, 122.4, 120.4, 117.0, 59.4, 57.6, 43.2, 34.4, 31.7, 31.3, 30.3, 24.7, 22.4, 14.0. All the values agree with the known reference[51].

(*S*)-(-)-3,3,3',3'-Tetramethyl-1,1'-spirobi(indan)-6,6'-diol

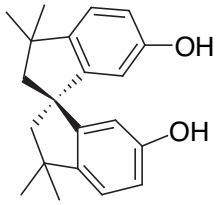

((*S*)-(-)-**6**)

(*R*)-(+)-3,3,3',3'-Tetramethyl-1,1'-spirobi(indan)-6,6'-diol

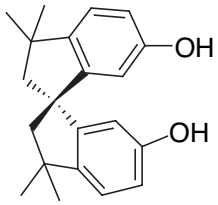

((*R*)-(+)**6**)

The resolution of (±)-**6** was accomplished by a method developed by Kazlauskas[51] using cholesterol esterase. Into a 1-L round-bottomed flask with a mechanical stirrer, dihexanoate (±)-**36** (10 g, 19.8 mmol) was added, followed by sodium taurocholate monohydrate (150 g, 0.28 mmol), benzamidine (402 mg), trypsin inhibitor (63 mg) and distilled diethyl ether (200 mL). The aqueous buffer (200 mL of 0.1 M potassium phosphate, pH = 7.5) and bovine acetone powder (40 g), which contains cholesterol esterase, were added respectively. The emulsified mixture was stirred at room temperature for 24 h. The pH of the aqueous phase was maintained around 7.1 by frequent addition of aqueous NaOH (1N) solution.

At the end of the reaction, the tan suspension was poured into a 2-L separatory funnel through cheesecloth and 200 mL of EtOH was added. The aqueous layer was allowed to settle for 8 h. The ether layer was separated and the aqueous layer was extracted with ether several times. The emulsion was broken by adding a large amount of $MgSO_4$. The combined ether layer was washed with water (3x), brine, and dried over $MgSO_4$. After the solvent was removed under reduced pressure, the ester and the alcohol were separated by a short column chromatography using SiO_2 and elution with CH_2Cl_2 and ether. The CH_2Cl_2 layer eluted (*S*)-enantiomer enriched ester, and the ether layer washed out the (*R*)-enantiomer enriched alcohol. The resulting (*R*)-**6** was furthered purified by triturating it in hexanes to remove impurities and recrystallization in petroleum ether and ether to increase its enantiomeric excess (> 95% ee.). $[\alpha]^{25}_D$ = +37.4° (c = 0.10 in CH_3OH) [lit.[50] +35.3 ° (c = 0.35 CH_3OH)]; CD (CH_3OH), 208 nm (Δε +147), 229 nm (Δε -8), 286 nm (Δε +3). The unhydrolyzed ester (*S*)-**28** was dissolved in diethyl ether (10 mL), NaOH (10 mL, 50 % wt.) and ethanol (10 mL). The resulting white gel was allowed to sit overnight. Additional ether (30 mL) was added, and the crude product was neutralized by a slow addition of concentrated HCl under ice-water bath. The organic layer was washed with water and brine, and dried over $MgSO_4$. A crude mixture of (*S*)-**6** (1.94g, 64% yield) was recrystallized in petroleum ether and ether to increase its enantiomeric excess (> 95 % ee.). $[\alpha]^{25}_D$ = -33.82° (c = 0.68 in CH_3OH) [lit.[51] –34.1 ° (c = 0.35 CH_3OH)]; CD (CH_3OH), 208 nm (Δε -156), 230 nm (Δε +8), 290 nm (Δε -5.5). Clear X-ray quality crystals of each enantiomer were obtained by recrystallization in hexanes.

General procedures for the synthesis of phenanthroline-based cyclophanes 1-3. In a 250 mL round-bottomed flask, **6** (0.849 g, 2.9 mmol) and K_2CO_3 (1.2 g, 8.7 mmol) were charged, followed by **8** (1 g, 2.73 mmol) and acetone (95 mL, 0.03 M). [NOTE: *Product yield and distribution were not affected by the reagent grade of the solvent*] The reaction mixture was refluxed for 21 h, and the solvent was removed under reduced pressure. A crude yellow residue was taken up in CH_2Cl_2 and insoluble solids were filtered. The organic layer was washed with water (3x), dried over $MgSO_4$, and concentrated under reduced pressure. Column chromatography in 4%-water-deactivated alumina with CH_2Cl_2 produced **1** and **2**.

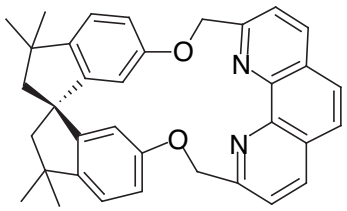

(1×1)-(*S*)-(+)-Cyclophane ((*S*)-**(-)-1**) (350 mg, 25 % yield); $[\alpha]^{25}_D$ = +183.6° (c = 0.0048 in $CHCl_3$); mp dark reddish-yellow (178 °C) melted 220-223 °C; ^{1}H NMR ($CDCl_3$: CD_3NO_2, 400 MHz) δ 8.33 (d, 2H, *J* = 8 Hz), 7.83 (s, 2H), 7.76 (d, 2H, *J* = 8 Hz), 7.02 (d, 2H, *J* = 8.4 Hz), 6.98 (d, 2H, *J* = 2 Hz), 6.77 (dd, 2H, *J* = 8.4, 2 Hz), 5.57 (d, 2H, *J* = 12.8 Hz), 5.34 (d, 2H, *J* = 12.8 Hz), 2.41 (d, 2H, *J* = 12.8 Hz), 2.21 (d, 2H, *J* = 12.8 Hz), 1.34 (s, 6H), 1.32 (s, 6H); (CD_3CN, 500 MHz) δ 8.34 (d, 2H, *J* = 7.5 Hz), 7.84 (s, 2H), 7.75 (d, 2H, *J* = 8 Hz), 7.02 (d, 2H, *J* = 8.5 Hz), 6.99 (d, 2H, *J* = 2 Hz), 6.71 (dd, 2H, *J* = 8, 2.5 Hz), 5.33 (d, 2H, *J* = 13.5 Hz), 5.29 (d, 2H, *J* = 13 Hz), 2.39 (d, 2H, *J* = 12.5 Hz), 2.18 (d, 2H, *J* = 13.5 Hz),1.31 (s, 6H), 1.30 (s, 6H); ^{1}H NMR (CD_2Cl_2, 400 MHz) δ 8.27 (d, 2H, *J* =

8.4 Hz), 7.79 (s, 2H), 7.71 (d, 2H, *J* = 8 Hz), 7.05 (d, 2H, *J* = 2 Hz), 7.03 (d, 2H, *J* = 8.4 Hz), 6.77 (dd, 2H, *J* = 8, 2 Hz), 5.65 (d, 2H, *J* = 12.8 Hz), 5.29 (d, 2H, *J* = 13.2 Hz), 2.40 (d, 2H, *J* = 12.8 Hz), 2.20 (d, 2H, *J* = 12.8 Hz), 1.34 (s, 6H), 1.34 (s, 6H); ^{13}C NMR ($CDCl_3$: CD_3NO_2, 125 MHz) δ 158.5, 156.9, 151.1, 145.1, 136.5, 127.8, 126.0, 122.5, 121.8, 111.3, 72.8, 59.0, 57.5, 42.3, 30.9, 29.6; (CD_3CN, 100 MHz) δ 159.8, 158.3, 155.4, 152.2, 146.1, 137.7, 129.0, 127.2, 123.8, 123.0, 111.8, 73.4, 59.9, 58.7, 43.4, 31.8, 30.4; IR (KBr) ν = 2920, 2830, 2340, 1660, 1590, 1470 cm^{-1}; HRMS-EI$^+$ *m/z* [M$^+$] calcd for $C_{35}H_{32}N_2O_2$ 512.2464; found 512.2463; UV (CH_3CN), λ_{max} 231 nm (ε 82000), 269 nm (ε 41000); CD (CH_3CN), 210 nm (Δε -44.5), 230 nm (Δε +47.5), 238 nm (Δε +59), 265 nm (Δε -4.6), 286 nm (Δε +26).

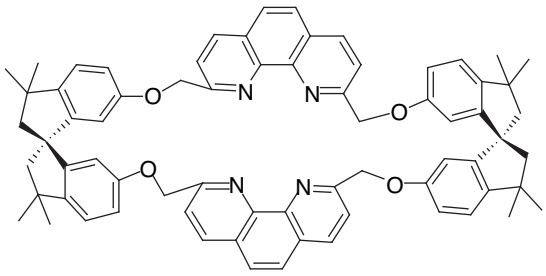

(2×2)-(*S*)-(-)-Cyclophane ((*S*)-(+)-**2**)

(180 mg, 13 % yield); $[\alpha]^{25}_D$ = -26.5° (c = 0.0047 in $CHCl_3$); mp 230-231 °C; ^{1}H NMR ($CDCl_3$:CD_3NO_2, 400 MHz) δ 8.35 (d, 4H, *J* = 8.4 Hz), 7.93 (d, 4H, *J* = 8.4 Hz), 7.78 (s, 4H), 7.18 (d, 4H, *J* = 8.4 Hz), 6.96 (dd, 4H, *J* = 84, 2.4 Hz), 6.54 (d, 4H, *J* = 2 Hz), 5.42(s, 8H), 2.45 (d, 4H, *J* = 12.8 Hz), 2.31 (d, 4H, *J* = 13.2 Hz), 1.43 (s, 12H), 1.38 (s, 12H); ^{1}H NMR ($CDCl_3$, 400 MHz) δ 8.21 (d, 4H, *J* = 8 Hz), 7.93 (d, 4H, *J* = 8.4 Hz), 7.66 (s, 4H), 7.15 (d, 4H, *J* = 8.4 Hz), 6.94 (dd, 4H, *J* = 8, 2 Hz), 6.57 (d, 4H, *J* = 2.4 Hz), 5.49 (d, 4H, *J* = 14 Hz), 5.44 (d, 4H, *J* = 14 Hz), 2.43 (d, 4H, *J* = 12.8 Hz), 2.35 (d, 4H, *J* = 12.8 Hz), 1.45 (s, 12H), 1.39 (s, 12H); ^{1}H NMR (CD_3CN, 400 MHz) δ

8.34 (d, 4H, *J* = 8.0 Hz), 7.74 (s, 4H), 7.72 (d, 4H, *J* = 8.4 Hz), 7.07 (d, 4H, *J* = 8.4 Hz), 6.88 (dd, 4H, *J* = 8.4, 2.8 Hz), 6.29(d, 4H, *J* = 2.4 Hz), 5.27 (d, 4H, *J* = 13.2 Hz), 5.21 (d, 4H, *J* = 13.2 Hz), 2.27 (d, 4H, *J* = 12.8 Hz), 2.03 (d, 4H, *J* = 13.2 Hz), 1.23 (s, 12H), 1.13 (s, 12H)); ^{1}H NMR (CD_2Cl_2, 400 MHz) δ 8.26 (d, 4H, *J* = 8.4 Hz), 7.90 (d, 4H, *J* = 8 Hz), 7.68 (s, 4H), 7.16 (d, 4H, *J* = 8.4 Hz), 6.96 (dd, 4H, *J* = 8.4, 2.8 Hz), 6.57 (d, 4H, *J* = 2 Hz), 5.35 (s, 8H), 2.43 (d, 4H, *J* = 13.2 Hz), 2.31 (d, 4H, *J* = 12.8 Hz), 1.43 (s, 12H), 1.37 (s, 12H); ^{13}C NMR ($CDCl_3$: CD_3NO_2, 125 MHz) δ 157.7, 157.5, 151.7, 144.6, 144.3, 136.6, 127.7, 125.7, 122.1, 120.2, 113.6, 109.5, 71.3, 59.0, 57.3, 42.6, 31.1, 29.6; ^{13}C NMR ($CDCl_3$, 100 MHz) δ 158.2, 158.1, 152.0, 144.8, 144.7, 136.6, 127.8, 125.9, 122.4, 120.3, 113.8, 110.1, 71.7, 59.5, 57.7, 43.1, 31.0, 30.5 ; IR (KBr) ν = 2920, 2830, 2330, 1580, 1470, 1450 cm^{-1}; HRMS-FAB *m/z* [M$^+$] calcd for $C_{70}H_{64}N_4O_4$ 1025.5006; found 1025.4967 (100%); UV (CH_3CN) λ_{max} = 229 (ε 43000), 271 (ε 25000), 320 (ε1200); CD (CH_3CN), 212 nm (Δε -60), 229 (Δε +5.5), 237 (Δε -7), 267 (Δε +16).

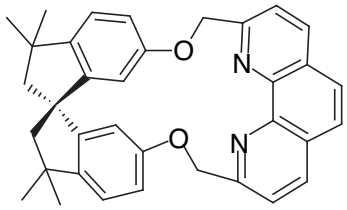

(1×1)-(*R*)-(-)-Cyclophane ((*R*)-(-)-**1**)

(523 mg, 42 % yield). $[\alpha]^{25}_{D}$ = -154.2° (c = 0.0016 in $CHCl_3$); CD (CH_3CN), 210 nm (Δε +65), 230 nm (Δε -52.6), 238 nm (Δε -57), 265 nm (Δε +3.7), 286 nm (Δε -22).

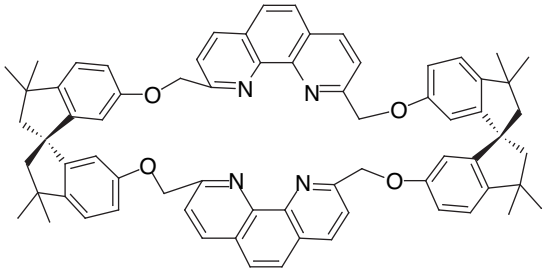

(2×2)-(*R*)-(+)-Cyclophane ((*R*)-(+)-2)

Purified by Chromatotron on a silica-coated plate with CH_2Cl_2 (50 mg, 6 % yield). CD (CH_3CN), 212 nm (Δε +51), 225 nm (Δε -6), 237 nm (Δε +21), 264 nm (Δε -14).

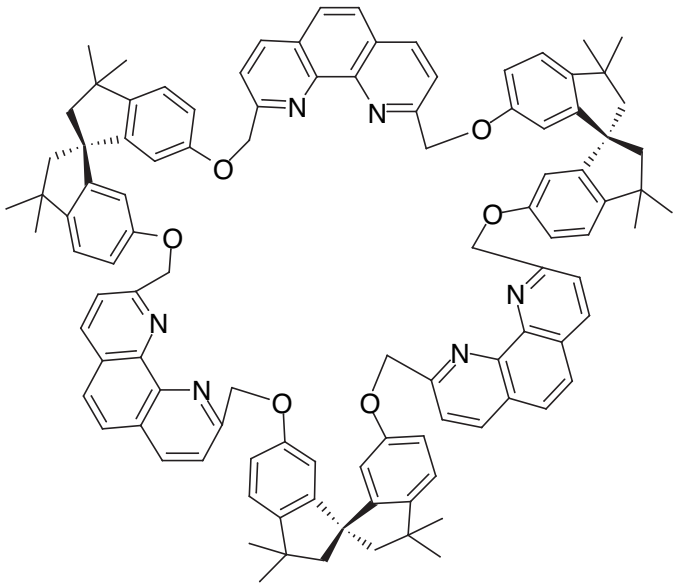

(3x3)-Cyclophane (3)

Purified by Chromatotron on a silica-coated plate with 1 % methanol-CH_2Cl_2 (8 mg, 1 % yield). ^{1}H NMR ($CDCl_3$, 400 MHz) δ 8.20 (d, 4H, *J* = 8.4 Hz), 7.88 (d 4H, *J* = 8.4 Hz), 7.62 (s, 4H), 7.09 (d, 4H, *J* = 8 Hz), 6.89 (dd, 4H, *J* = 8.4, 2.4 Hz), 6.47 (d, 4H, *J* = 2 Hz), 5.46 (s, 8H), 2.36 (d, 4H, *J* = 13.2 Hz), 2.27 (d, 4H, *J* = 13.2 Hz), 1.39 (s, 12H), 1.34 (s, 12H); ^{13}C NMR ($CDCl_3$, 100 MHz) δ 158.3, 157.8, 151.9, 144.8, 136.7, 127.8, 125.9, 122.5, 120.4, 113.8, 110.0, 71.2, 59.6, 43.0, 31.9, 30.5; HRMS-FAB *m/z* [M^+] calcd for $C_{105}H_{96}N_6O_6Na^+$ 1559.7289; found 1559.7270 (100%).

6,6'-dimethyl-2,2'-bipyridine (50) 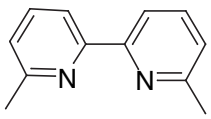

An oven-dried three-neck 1-L round-bottomed flask and magnetic stirbar, equipped with rubber septum, were cooled to room temperature under argon. Half equivalent of 2-bromo-6-picoline (2.5 g, 0.015 mol) and anhydrous THF (500 mL) were added to the reaction flask under argon. The stirring solution was chilled to –78 °C under dry ice-acetone bath. *n*-BuLi (6 mL, 2.4 M in hexanes) was injected very slowly. The lithiated reaction mixture turned orange initially, then it gradually turned brown. The reaction was stirred for 10 min at –78 °C. In another oven-dried 2-neck 250-mL round-bottomed flask, anhydrous $ZnCl_2$ (2 g, 0.015 mol) was stirred in 50 mL of anhydrous THF. The $ZnCl_2$ solution was cannulated into the lithiated mixture slowly. The stirring clear yellow solution was warmed up to the room temperature. Into the third oven-dried round-bottomed flask, the second half equivalent of 6-bromo-2-picoline (2.5 g, 0.015 mol) and $Pd(PPh_3)_4$ (168 mg, 1 mol %) were added into 180 mL of anhydrous THF. The third solution was cannulated into the 1 L flask containing the zinc complexed picoline. The reaction was refluxed overnight and was cooled to room temperature the next day. The solution was concentrated to half of its original volume, and it was chilled in a freezer for 2-3 h. The resulting white precipitate was collected by filtering it through a Büchner funnel. The filtered solid was stirred in a bi-phase mixture of basic EDTA (~pH 9) and chloroform for 1/2 h. The product **50** was extracted with chloroform, dried over $MgSO_4$, filtered through a

fluted filter paper, and concentrated under reduced pressure. (1.66 g, 62% yield). All physical data is in the references[104.124.152].

6,6'-Bis(bromomethyl)-2,2'-bipyridine (7) 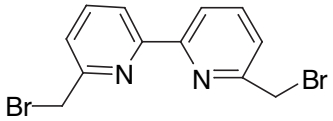

N-bromosuccinimide, CCl_4, **50** and benzoylperoxide were combined into a round-bottomed flask. The stirring suspension was refluxed in the presence of incandescent light for 2-3 h. Column chromatography in 4 %-water deactivated alumina with CH_2Cl_2 or recrystallization in CCl_4 afforded the pure product. All physical data matches with known literature.[159]

Alternate Synthetic Route.[104] Into a round-bottomed flask containing **78** (280 mg, 0.85 mmol) [synthesized by using Fraser's method][104], anhydrous CH_3CN (8 mL) was charged. Upon addition of 2,4,4,6-tetrabromo-2,4-cyclohexadienone **79** (873 mg, 2.13 mmol) into the stirring suspension, the reaction mixture became orange. Anhydrous CsF (324 mg, 2.13 mmol) was added and the resulting green suspension was stirred overnight under Ar. H_2O and EtOAc were added to quench the reaction. The organic layer was washed with brine, dried over $MgSO_4$, filtered and concentrated under reduced pressure. The crude product was first purified by column chromatography on 4 %-H_2O deactivated alumina, and further purified by recrystallization from CCl_4 (60 mg, 23 % yield).

Procedures for the synthesis of bipyridine-based cyclophanes 4-5

(1×1)-(*S*)-Cyclophane ((*S*)-4)

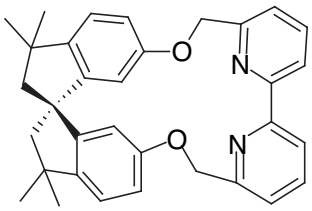

(*S*)-(-)-**6** (54 mg, 0.18 mmol) and **7** (60 mg, 0.18 mmol) were charged into an oven-dried flask, equipped with stirring bar. Anhydrous benzene (2 mL) was added, followed by anhydrous EtOH (13 mL). Anhydrous potassium *t*-butoxide (43 mg, 0.39 mmol) was charged, followed by THF (13 mL). The reaction was refluxed for 48 h. The solvent was removed via rotary evaporator, and the crude mixture was taken up in CH_2Cl_2 for work up. The organic layer was washed with saturated $NaHCO_3$ (3×), water (1×), dried over Na_2SO_4, filtered and concentrated. The crude mixture was purified via radial chromatography (silica gel- CH_2Cl_2, followed by 1 % methanolic CH_2Cl_2). White solid 12 mg (14 % yield), ^{1}H NMR ($CDCl_3$, 400 MHz) δ 7.74 (t, 2H, *J* = 7.6 Hz), 7.50 (d, 2H, *J* = 7.6 Hz), 7.40 (d, 2H, *J* = 7.6 Hz), 6.97 (d, 2H, *J* = 9.2 Hz), 6.78 (dd, 2H, *J* = 8.8, 2.4 Hz), 6.78 (d, 2H, *J* = 2.4 Hz), 5.38 (d, 2H, *J* = 13.2 Hz), 5.21(d, 2H, *J* = 13.2 Hz), 2.31 (d, 2H, *J* = 13.2 Hz), 2.17 (d, 2H, *J* = 13.2 Hz), 1.30 (s, 6H), 1.30 (s, 6H); ^{1}H NMR (1:1-$CDCl_3$: CD_3NO_2, 400 MHz) δ 7.84 (t, 2H, *J* = 8 Hz), 7.56 (d, 2H, *J* = 7.6 Hz), 7.46 (d, 2H, *J* = 8.4 Hz), 7.02 (d, 2H, *J* = 8.4 Hz), 6.82 (d, 2H, *J* = 2.4 Hz), 6.76 (dd, 2H, *J* = 8, 2.8 Hz), 5.36 (d, 2H, *J* = 13.6 Hz), 5.17 (d, 2H, *J* = 13.2 Hz), 2.39 (d, 2H, *J* = 12.8 Hz), 2.20 (d, 2H, *J* = 12.8 Hz), 1.33 (s, 12H); ^{1}H NMR (CD_3CN, 400 MHz) δ 7.82 (t, 2H, *J* = 7.6 Hz), 7.51 (d, 2H, *J* = 8 Hz), 7.43 (dd,

2H, *J* = 8, 0.8 Hz), 7.03 (d, 2H, *J* = 8 Hz), 6.73 (dd, 2H, *J* = 8, 2.8 Hz), 6.71 (d, 2H, *J* = 2.4 Hz), 5.34 (d, 2H, *J* = 13.6 Hz), 5.14 (d, 2H, *J* = 13.6 Hz), 2.35 (d, 2H, *J* = 13.2 Hz), 2.15 (d, 2H, *J* = 12.8 Hz), 1.33 (s, 6H), 1.29 (s, 6H); ^{13}C NMR ($CDCl_3$, 100 MHz, δ) 158.4, 157.6, 157.2, 151.3, 145.3, 136.8, 122.3, 122.0, 121.5, 116.6, 112.2, 72.2, 59.7, 58.0, 42.8, 31.8, 30.6; ^{13}C NMR (1:1-$CDCl_3$: CD_3NO_2, 100 MHz) δ 158.1, 157.1, 156.8, 150.9, 144.8, 136.8, 122.1, 121.8, 121.6, 116.0, 110.2, 70.7, 59.0, 57.7, 42.2, 30.9, 29.6; HRMS-FAB *m/z* [M^+] calcd for 489.2542 for $C_{33}H_{33}N_2O_2$; found 489.2565; mp 120-121 °C; UV (CH_3CN) λ_{max} = 221 (ε 700), 282 (ε 315); CD (CH_3CN), 217 nm (Δε -4), 253 nm (Δε +3.2), 291 nm (Δε +4.4), 300 nm (Δε -1.5).**(2×2)-(*S*)-Cyclophane** ((*S*)-**5**)

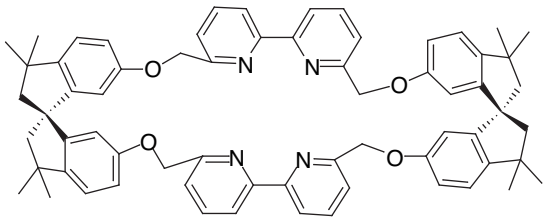

Into an oven-dried flask, (*S*)-(-)-spirobiindanol (135 mg, 0.44 mmol), K_2CO_3 (303 mg, 2.19 mmol), and 32-mL of freshly distilled CH_3CN were charged under argon. The suspension was brought to reflux. 6,6'-bis(bromomethyl)-2,2'-bipyridine **7** (180 mg, 0.53 mmol) dissolved in 25-mL of CH_3CN was dripped into the basic suspension over 15 min. The reaction was refluxed for three days. The suspension was cooled to room temperature and the solvent was removed under reduced pressure. The white residue was taken up in CH_2Cl_2 (10 mL), and excess K_2CO_3 was filtered off. The filtered organic layer was washed with an aqueous NaOH (1N, 10 mL x3) and water (10 mL x3). The organic phase was dried over $MgSO_4$, filtered and

concentrated under reduced pressure. The crude material was purified by column chromatography (4 %-water alumina, CH_2Cl_2). White solid (9 mg, 6 %), ^{1}H NMR ($CDCl_3$, 400 MHz) δ 8.15 (d, 2H, *J* = 7.6 Hz), 7.72 (t, 2H, *J* = 7.6 Hz), 7.34 (d, 2H, *J* = 7.2 Hz), 6.89 (d, 2H, *J* = 8.4 Hz), 6.71 (dd, 2H, *J* = 8.4, 2.4 Hz), 6.17 (d, 2H, *J* = 2.4 Hz), 5.14 (d, 2H, *J* = 14.4 Hz), 5.02 (d, 2H, *J* = 14.4 Hz), 2.60 (d, 2H, *J* = 13.2 Hz), 2.21 (d, 2H, *J* = 13.2 Hz), 1.36 (s, 6H), 1.29 (s, 6H); ^{1}H NMR (CD_2Cl_2, 400 MHz) δ 8.20 (d, 4H, *J* = 7.6 Hz), 7.74 (t, 4H, *J* = 7.6 Hz), 7.32 (d, 4H, *J* = 7.6 Hz), 6.87 (d, 4H, *J* = 8.4 Hz), 6.68 (dd, 4H, *J* = 8.4, 1.6 Hz), 6.14 (d, 4H, *J* = 2 Hz), 5.16 (d, 4H, *J* = 14.4 Hz), 5.05 (d, 4H, *J* = 14.4 Hz), 2.31 (d, 4H, *J* = 13.2 Hz), 2.20 (d, 4H, *J* = 13.2 Hz), 1.36 (s, 12H), 1.28 (s, 12H); ^{13}C NMR ($CDCl_3$, 100 MHz) δ 157.4, 156.9, 154.7, 151.7, 144.3, 137.2, 122.1, 120.8, 119.4, 114.5, 109.5, 70.6, 59.4, 57.6, 43.0, 31.9, 30.5; HRMS-MALDI *m/z* [M^+] calcd for 977.5000 for $C_{66}H_{64}N_4O_4$; found 977.4987; mp 198-201 °C; UV(CH_3CN) λ_{max} = 223 (ε 1600), 245 (ε 580), 284 (ε 1200), 290 (ε 1300), 304 (ε 610); CD (CH_3CN), 219 nm (Δε -19.5), 273 nm (Δε -15.3), 306 nm (Δε -11.3).

(1×1)-(*R*)-Cyclophane ((*R*)-4)

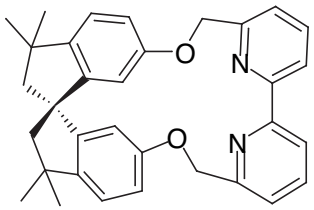

White solid 51mg (41% yield). CD (CH_3CN), 215 nm (Δε +9), 254 nm (Δε -3), 292 nm (Δε -3.8), 300 nm (Δε +0.8).

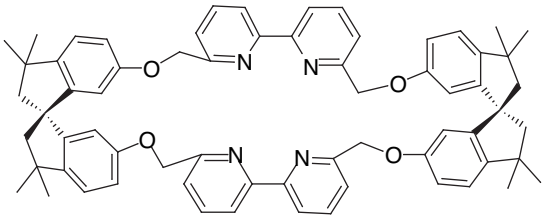

(2×2)-(*R*)-Cyclophane ((*R*)-**5**)

6,6'-bis(bromomethyl)-2,2'-bipyridine **7** (133 mg, 0.39 mmol) and freshly distilled CH_3CN (21 mL) were charged into an oven-dried flask under argon. The subsequent suspension was brought to reflux. The pre-formed suspension of K_2CO_3 (224 mg, 1.62 mmol) and (*R*)-(+)-**6** (100 mg, 0.324 mmol) was dripped into the basic suspension very slowly. The reaction was refluxed for 24 h. The suspension was cooled to room temperature and the solvent was removed under reduced pressure. The white residue was taken up in CH_2Cl_2 (10 mL), and excess K_2CO_3 was filtered off. The filtered organic layer was washed with an aqueous NaOH (1N, 10 mL x3) and water (10 mL x3). The organic phase was dried over $MgSO_4$, filtered and the concentrated under reduced pressure. The crude material was purified by radial chromatography using silica plate and CH_2Cl_2 as the eluent. White solids (*R*)-**4** (14.1 mg, 10 %) and (*R*)-**5** (23.6 mg, 15%). For (*R*)-**5**, CD (CH_3CN), 215 nm (Δε +79), 275 nm (Δε +13), 307 nm (Δε +8).

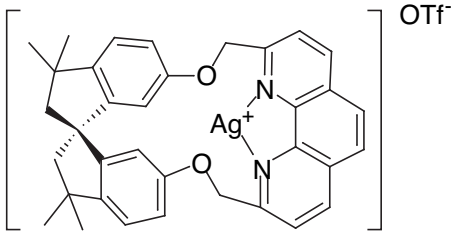

[Ag(*S*)-(**1**)](OTf) ((*S*)-**80**)

Into an oven-dried 10 mL round-bottomed flask, Ag(OTf) (35 mg, 0.14 mmol) was dissolved into 2 mL of freshly distilled CH_3CN. The clear silver solution was

cannulated into the stirring suspension of (*S*)-(-)-**1** (50 mg, 0.1 mmol) in 1 mL of distilled CH_3CN. The white suspension was stirred for 30 min in the absence of light. The reaction was monitored by TLC, and the clear solution indicated the completion of the reaction. [The cyclophane was not readily soluble in CH_3CN, but the silver complex of the cyclophane was very soluble in the same solvent system.] The clear, slightly yellow solution was filtered through celite in a glass pipette. Chilled anhydrous ether was added to complete the precipitation, and the ethereal suspension was further cooled to increase the precipitation formation. The white precipitates were filtered through a Hirsch funnel, and rinsed with minimal amount of chilled ether. White, light-sensitive solids **80** (41 mg, 55 %) were obtained. X-ray quality clear, needle-like crystals were grown from CH_3CN / Et_2O. ^{1}H NMR ($CDCl_3$:CD_3NO_2, 400 MHz) δ 8.63 (d, 2H, *J* = 8.4 Hz), 8.05 (d, 2H, *J* = 7.2 Hz), 8.04 (s, 2H), 7.32 (d, 2H, *J* = 2.4 Hz), 7.20 (d, 2H, *J* = 8.4 Hz), 6.87 (dd, 2H, *J* = 8.4, 2.4 Hz), 5.73 (d, 2H, *J* = 13.6 Hz), 5.44 (d, 2H, *J* = 13.6 Hz), 2.44 (d, 2H, *J* = 12.4 Hz), 2.40 (d, 2H, *J* = 14.8 Hz), 1.44 (s, 6H), 1.33 (s, 6H); ^{1}H NMR (CD_3CN, 500 MHz) δ 8.62 (d, 2H, *J* = 8.5 Hz), 8.04 (d, 2H, *J* = 8.5 Hz), 8.04 (s, 2H), 7.08 (d, 2H, *J* = 8 Hz), 6.80 (dd, 2H, *J* = 10.5, 2 Hz),6.79 (s, 2H), 5.54 (d, 2H, *J* = 13.5 Hz), 5.45 (d, 2H, *J* = 14 Hz), 2.33 (d, 2H, *J* = 12.5 Hz), 2.16 (d, 2H, *J* = 13 Hz), 1.28 (s, 6H), 1.25 (s, 6H); ^{13}C NMR ($CDCl_3$: CD_3NO_2, 125 MHz) δ 159.4, 156.8(2), 156.8(1), 155.7, 146.2, 141.1, 139.4, 128.8, 126.8, 124.8, 124.7, 118.1, 102.9, 73.4, 58.6, 57.4, 43.0, 31.2, 29.0; ^{13}C NMR (CD_3CN, 125 MHz) δ 159.7, 158.2, 153.9, 147.9, 140.4, 129.5, 127.8, 126.2, 125.8, 124.2, 119.1, 113.1, 76.1, 59.8, 58.3, 43.8, 32.0, 30.1; HRMS-FAB *m*/*z* calcd

619.1515 for $C_{35}H_{32}N_2O_2Ag^+$; found 619.1490 (99 %), 621 (100 %); UV (CH_3CN) λ_{max}: 231 (ε 4500), 273 (ε 2900); CD (CH_3CN), 213 nm (Δε -10.7), 238 nm (Δε +32), 271 nm (Δε -7.5), 286 nm (Δε +8.7).

[Ag(*R*)-(1)](OTf) ((*R*)-**80**)

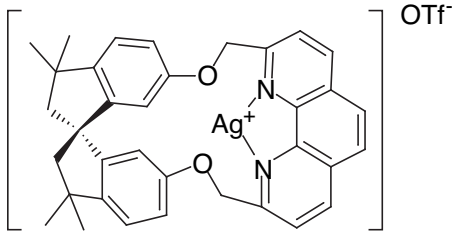

(white solids, 51 mg, 68 % yield). CD (CH_3CN) 212 nm (Δε +18), 238 nm (Δε -36), 271 nm (Δε +9), 288 nm (Δε -8.6).

[Cu(*S*)-(1)](PF_6) ((*S*)-**81**)

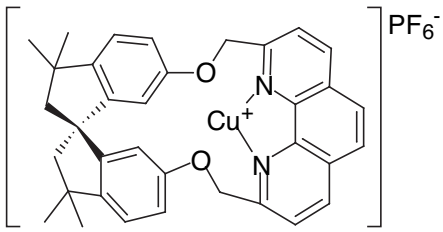

A stirring solution of tetrakis(acetonitrile)copper(I) hexafluorophosphate $[Cu(CH_3CN)_4](PF_6)$ (35 mg, 0.094 mmol) in 2mL of CH_3CN was cannulated into a suspension of the (*R*)-**1** (50 mg, 0.098 mmol) in CH_3CN (1 mL) under argon. The combined reaction mixture was stirred overnight under argon, and it was monitored by TLC (silica gel, 3:1-CH_2Cl_2:EtOAc). [NOTE: The complexation occurs very rapidly. It does not need to be stirred overnight]. The dark yellow solution was filtered through celite in a glass pipette. The filtrate was concentrated under reduced pressure and anhydrous ether was added to precipitate the yellow solid. The yellow solid was

filtered, washed successively with the following chilled solutions: Et_2O: CH_2Cl_2-9:1, Et_2O:CH_3CN-95:5, Et_2O. The product was dried under high vacuum for 1 h. (*S*)-**81** (20 mg, light yellow solid, 28 % yield) [NOTE: This copper(I) salt is very air-sensitive. Exposure to the atmosphere can oxidize it to copper(II) complex very easily. An NMR tube with screw-cap was used during NMR analysis]. ^{1}H NMR (CD_3CN, 500 MHz) δ 8.62 (d, 2H, *J* = 8.5 Hz), 8.08 (d, 2H, *J* = 8.5 Hz), 8.02 (s, 2H), 7.05 (d, 2H, *J* = 8.8 Hz), 6.82 (dd, 2H, *J* = 7, 3 Hz), 6.69 (s, 2H), 5.66 (d, 2H, *J* = 13 Hz), 5.43 (d, 2H, *J* = 13 Hz), 2.29 (d, 2H, *J* = 12.5 Hz), 2.09 (d, 2H, *J* = 13 Hz), 1.24 (s, 6H), 1.23 (s, 3 6H); ^{13}C NMR (CD_3CN, 100 MHz) δ 159.2, 157.9, 152.7, 148.1, 143.3, 140.5, 129.2, 127.6, 126.7, 124.0, 120.3, 115.4, 76.3, 60.1, 58.4, 43.6, 31.9, 30.3; HRMS-FAB *m/z* calcd 575.1760 for $C_{35}H_{32}N_2O_2Cu^+$; found 575.1761 (100 %); UV(CH_3CN) λ_{max}: 229 (ε 1700) , 271 (ε 800). CD (CH_3CN) 241 nm (Δε +9.6), 262 nm (Δε -16), 286 nm (Δε +40), 310 nm (Δε -36).

[Cu(*R*)-(1)](PF$_6$) ((*R*)-**81**)

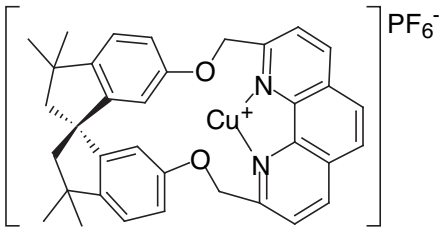

(18 mg of light yellow solid, 26 %) FABMS *m/z* [M^+] calcd 575.1760 for $C_{35}H_{32}N_2O_2Cu^+$; found 575.1761 (100 %); CD (CH_3CN) 240 nm (Δε -23.6), 267 nm (Δε +17), 285 nm (Δε -44), 309 nm (Δε +27). X-ray quality crystals were grown from CH_3CN / Et_2O. (clear light-yellow crystals)

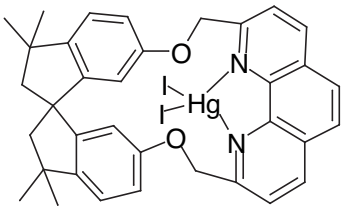

[Hg(±)-(1)I_2] ((±)-82)

The racemic cyclophane (±)-**1** (25 mg, 0.05 mmol) was added into a solution of CH_2Cl_2:MeOH-4 mL:1 mL. The red HgI_2 (31 mg, 0.07 mmol) was dissolved into degassed methanol (15 mL). The clear mercury(II) solution was cannulated into the stirring cyclophane mixture. The reaction was refluxed for 1 h (the solution became clear). Upon cooling it down to room temperature, the solution became slightly yellow. Excess solvent was removed under reduced pressure. The crude product was purified by recrystallization in CH_3CN. (25 mg, yellow crystals, 44 % yield). Crystals of the mercuric complex (±)-**82** suitable for the X-ray analysis was obtained from CH_2Cl_2/hexanes. (clear, yellow crystals) ^{1}H NMR (CD_2Cl_2, 400 MHz) δ 8.54 (d, 2H, *J* = 8.4 Hz), 7.96 (d, 2H, *J* = 8 Hz), 7.96 (s, 2H,), 6.93 (d, 2H, *J* = 8.0 Hz), 6.83 (s, 2H), 6.73 (d, 2H, *J* = 8.0 Hz), 5.79 (d, 2H, *J* = 13.2 Hz), 5.55 (d, 2H, *J* = 13.2 Hz), 2.27 (d, 2H, *J* = 12.8 Hz), 2.05 (d, 2H, *J* = 12.8 Hz), 1.25 (s, 6H), 1.22 (s, 6H); ^{13}C NMR (CD_2Cl_2, 100 MHz) δ 158.2, 152.3, 147.6, 142.1, 139.6, 129.6, 127.3, 125.4, 122.9, 118.9, 115.6, 74.0, 59.7, 58.1, 43.2, 31.8, 30.4; ESI *m/z* calcd 841.12 for $C_{35}H_{32}N_2O_2HgI^+$; found 840.15; UV($CHCl_3$) λ_{max}: 274 (ε 17000), 443 (ε 55).

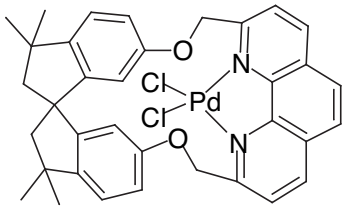

[Pd(±)-(1)Cl_2] ((±)-83)

Into a stirring solution of the racemic cyclophane (±)-**1** (5 mg, 0.01 mmol) in 1 mL of CH_2Cl_2, $PdCl_2$ (2.4 mg, 0.014 mmol) and 1 mL of methanol were added. Palladium(II) salt did not look very soluble in either solvent, so additional 1 mL of CH_3CN was injected. The light-brown solution was refluxed overnight. The solvent was removed under reduced pressure. (±)-**83** (7 mg, dark orange solids, 95 % yield) ^{1}H NMR (CD_2Cl_2, 400 MHz) δ 8.55 (d, 1H, *J* = 8.4 Hz), 8.50 (d, 1H, *J* = 8.4 Hz), 8.03 (d, 1H, *J* = 8.4 Hz), 7.94 (s, 2H), 7.91 (d, 1H, *J* = 8.4 Hz), 7.33 (d, 1H, *J* = 8.4 Hz), 7.17 (dd, 1H, *J* = 8.4, 2.8 Hz), 7.09 (d, 1H, *J* = 2 Hz), 6.70 (d, 1H, *J* = 8 Hz), 6.47 (d, 1H, *J* = 14.4 Hz), 6.44 (dd, 1H, *J* = 8, 2.4 Hz), 6.36 (d, 1H, *J* = 15.2 Hz), 5.85 (d, 1H, *J* = 2.4 Hz), 5.54 (d, 1H, *J* = 12.8 Hz), 5.43 (d, 1H, *J* = 15.2 Hz), 2.36 (d, 1H, *J* = 13.2 Hz), 2.23 (d, 1H, *J* = 14.4 Hz), 2.22 (d, 1H, *J* = 13.2 Hz), 1.88 (d, 1H, *J* = 13.2 Hz), 1.53 (s, 3H), 1.33 (s, 3H), 1.21 (s, 3H), 1.02 (s, 3H); ^{13}C NMR (CD_2Cl_2, 125 MHz) δ 165.5, 160.7, 156.2, 152.9, 148.7, 148.3, 146.2, 140.1, 139.2, 127.2, 127.0, 126.7, 123.8, 122.5, 119.7, 116.6, 115.9, 111.7, 78.0, 70.4, 59.5, 59.4, 59.0, 57.9, 43.3, 42.7, 32.0, 31.3, 30.2, 29.9, 29.7; ESI *m/z* calcd 654.12 for $C_{35}H_{32}N_2O_2PdCl^+$; found 654.52; UV($CHCl_3$) λ_{max}: 281 (ε 72000).

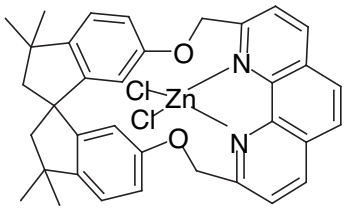

[Zn-(±)-(1)Cl_2] ((±)-**84**)

Into an oven-dried round-bottomed flask, the racemic cyclophane (±)-**1** (50 mg, 0.1 mmol) was dissolved in 1 mL of dry CH_2Cl_2. Anhydrous $ZnCl_2$ (2.4 mg, 0.014 mmol) was added, and the solution was stirred overnight. Next day, the white suspension was filtered through cotton to remove insoluble solids, and the filtrated was concentrated under reduced pressure. The crude product was recrystallized from ether-CH_2Cl_2 solvent system. (30 mg, opaque white solids, 47 % yield) ^{1}H NMR (CD_2Cl_2, 500 MHz) δ 8.70 (d, 1H, *J* = 8.5 Hz), 8.63 (d, 1H, *J* = 8 Hz), 8.21 (d, 1H, *J* = 8.5 Hz), 8.10 (d, 1H, *J* = 8.5 Hz), 8.07 (d, 1H, *J* = 8.5 Hz), 8.04 (d, 1H, *J* = 9 Hz), 7.58 (d, 1H, *J* = 2 Hz), 7.24 (d, 1H, *J* = 8 Hz), 7.13 (dd, 1H, *J* = 8, 2 Hz), 6.62 (d, 1H, *J* = 8.5 Hz), 6.41 (dd, 1H, *J* = 8.5, 2 Hz), 6.13 (d, 1H, *J* = 13.5 Hz), 5.80 (d, 1H, *J* =12.5 Hz), 5.55 (d, 1H, *J* = 13.5 Hz), 5.47 (d, 1H, *J* = 12 Hz), 2.28 (d, 1H, *J* = 12.5 Hz), 2.15 (d, 1H, *J* = 13.5 Hz), 2.09 (d, 1H, *J* = 13 Hz), 1.83 (d, 1H, *J* = 13 Hz), 1.44 (s, 3H), 1.29 (s, 3H), 1.14 (s, 3H), 0.95 (s, 3H); ^{13}C NMR (CD_2Cl_2, 125 MHz) δ 160.2, 159.5, 158.8, 153.1, 150.9, 149.8, 146.9, 141.8, 140.9, 139.4, 129.2, 129.1, 127.5, 127.4, 126.9, 126.7, 125.8, 124.3, 122.3, 121.6, 118.8, 117.4, 115.4, 77.2, 71.1, 64.5, 60.4, 59.8, 58.3, 43.2, 42.7, 31.9, 31.4, 30.9, 30.0; HRMS-FAB *m/z* calcd 611.1444 for $C_{35}H_{32}N_2O_2ZnCl^+$; found 611.1433 (94 %), 613 (100 %); UV($CHCl_3$) λ_{max} : 278 (ε 23000).

[Ag(*S*)-(2)](OTf) ((*S*)-**85**)

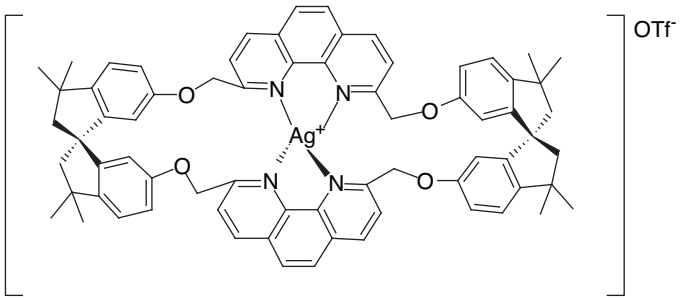

(*S*)-(-)-**2** (4 mg, 3.9 μmol) was dissolved into a NMR tube containing $CDCl_3$(0.5 mL) and CD_3NO_2 (0.5 mL). Silver triflate (1 mg, 3.9 μmol) was added, and the NMR tube was heated until the solution became clear yellow. (Quantitative yield on NMR) ^{1}H NMR ($CDCl_3$: CD_3NO_2, 400 MHz) δ 8.65 (d, 4H, *J* = 8.0 Hz), 8.11 (d, 4H, *J* = 8.0 Hz), 8.11 (s, 4H), 6.45 (d, 4H, *J* = 8.4 Hz), 6.04 (dd, 4H, *J* = 8.4, 2.4 Hz), 5.40 (d, 4H, *J* = 2 Hz), 5.37 (d, 4H, *J* = 14.4 Hz), 4.86 (d, 4H, *J* = 14.0 Hz), 2.13 (d, 4H, *J* = 13.2 Hz), 1.78 (d, 4H, *J* = 12.8 Hz), 1.14 (s, 12H), 0.91(s, 12H); ^{13}C NMR ($CDCl_3$: CD_3NO_2, 125 MHz) δ 158.0, 151.4, 145.1, 141.4, 138.9, 128.4, 126.5, 122.9, 121.4, 115.8, 110.5, 75.4, 57.7, 56.6, 42.4, 30.3, 29.1; ESI *m/z* 1133.5; UV (CH_3CN) λ_{max}: 229 (ε 82000), 275 (ε 59000); CD (CH_3CN) 211 nm (Δε -16), 238 nm (Δε -4.8), 278 nm (Δε +16).

[Ag(*R*)-(2)](OTf) ((*R*)-**85**)

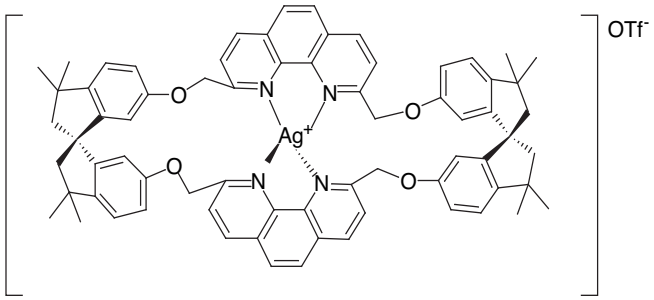

In an oven-dried vial equipped with a stirring bar and a rubber septum, (*R*)-(+)-**2** (11.4 mg, 0.01 mmol) was dissolved into CH_3CN (1 mL). Silver triflate (2.7 mg, 0.01 mmol) was added and the suspension was stirred under argon until it became clear yellow. The solution was filtered through celite and the complex was concentrated under reduced pressure (13.6 mg, light-yellow solids, 96 %). ^{1}H NMR (CD_2Cl_2, 500 MHz) δ 8.57 (d, 4H, *J* = 8.5 Hz), 8.07 (d, 4H, *J* = 7.5 Hz), 8.1 (s, 4H), 6.43 (d, 4H, *J* = 8.5Hz), 6.05 (dd, 4H, *J* = 8.5, 2.5 Hz), 5.36 (d, 4H, *J* = 2.5 Hz), 5.32 (d, 4H, *J* = 14.5 Hz), 4.81 (d, 4H, *J* = 14 Hz), 2.12 (d, 4H, *J* = 13 Hz), 1.77 (d, 4H, *J* = 13 Hz), 1.14 (s, 12H), 0.90 (s, 12H); ^{13}C NMR (CD_2Cl_2, 125 MHz) δ 159.1, 152.4, 146.4, 142.4, 139.8, 129.3, 127.5, 123.8, 122.4, 116.8, 111.4, 76.4, 58.6, 57.4, 43.2, 31.1, 30.1; CD (CH_3CN) 213 nm (Δε +20), 238 nm (Δε +6), 279 nm (Δε -22).

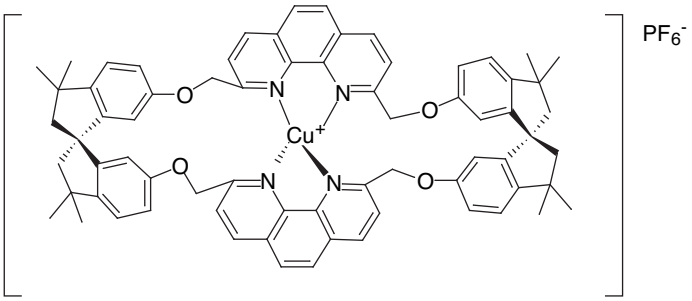

[Cu(*S*)-(2)](PF$_6$) ((*S*)-**86**)

Into a stirring suspension of (*S*)-(-)-**2** (12 mg, 0.012 mmol) in distilled CH_3CN (1 mL), $[Cu(CH_3CN)_4](PF_6)$ (4 mg, 0.012 mmol) was added. The suspension was stirred until all the solids went into solution. The dark yellow solution was filtered through celite in a glass pipette. The filtrate was concentrated under reduced pressure. The product was dried under high vacuum for 1 h. (12 mg, dark-orange solids, 83% yield). X-ray quality crystals of (*S*)-**86** were grown from benzene vapor diffusion into dichloromethane solution of the complex (dark-orange crystals). ^{1}H NMR (CD_2Cl_2, 400 MHz) δ 8.64 (d, 4H, *J* = 8 Hz), 8.18 (d, 4H, *J* = 8.4 Hz), 8.11 (s, 4H), 6.75 (d, 4H, *J* = 8.4 Hz), 6.47 (dd, 4H, *J* = 8, 2 Hz), 5.69 (d, 4H, *J* = 2.4 Hz), 5.04 (d, 4H, *J* = 16.4 Hz), 4.38 (d, 4H, *J* = 16 Hz), 2.26 (d, 4H, *J* = 12.8 Hz), 1.89 (d, 4H, *J* = 12.8 Hz), 1.26 (s, 12H), 1.08 (s, 12H); ^{13}C NMR (CD_2Cl_2, 100 MHz) δ 159.8, 158.7, 152.1, 147.8, 142.8, 138.8, 129.2, 127.1, 123.1, 122.8, 118.5, 112.6, 76.7, 58.3, 57.8, 43.2, 31.1, 30.6; HRMS-FAB$^+$ *m/z* calcd 1087.4224 for $C_{70}H_{64}N_4O_4Cu^+$; found 1087.4184; UV(CH_3CN) λ_{max}: 227 (21000), 277 (14000), 440 (1300); CD (CH_3CN) 234 nm (Δε -22.5), 244 nm (Δε +19.4), 284 nm (Δε +33.5).

[Cu(*R*)-(2)](PF$_6$) ((*R*)-**86**)

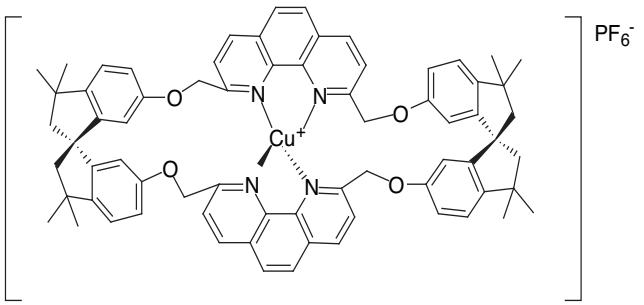

(9.6 mg, dark orange solids, 84 % yield) ^{1}H NMR (CD_3CN, 400 MHz) δ 8.68 (d, 4H, *J* = 8.4 Hz), 8.13 (s, 4H), 8.11 (d, 4H, *J* = 8.4 Hz), 6.70 (d, 4H, *J* = 8.0 Hz), 6.35 (dd, 4H, *J* = 8.4, 2.8 Hz), 5.64 (d, 4H, *J* = 2.8 Hz), 5.07 (d, 4H, *J* = 16 Hz), 4.35 (d, 4H, *J* = 15.6 Hz), 2.22 (d, 4H, *J* = 12.8 Hz), 1.79 (d, 4H, *J* = 12.8 Hz), 1.19 (s, 12H), 1.04 (s, 12H); ^{13}C NMR (CD_3CN, 125 MHz) δ 160.8, 159.7, 153.1, 148.0, 143.7, 139.5, 130.0, 127.9, 124.3, 123.5, 118.5, 113.5, 77.3, 58.8, 58.2, 43.7, 31.3, 30.3; CD (CH_3CN) 234 nm (Δε +8), 244 nm (Δε -2.5), 284 nm (Δε -5.5).

[Ag(*S*)-(4)](OTf) ((*S*)-**87**)

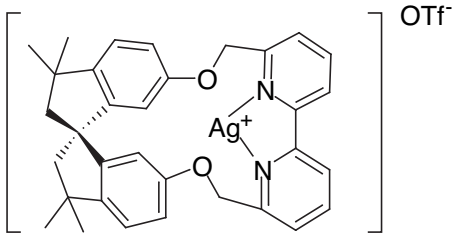

Into an oven-dried round-bottomed flask, (*S*)-**4** (10 mg, 0.02 mmol) was dissolved in CH_3CN. The stirring suspension was degassed for 5 min. Ag(OTf) (7 mg, 0.027 mmol) was added into the flask and the reaction was stirred until all the solids went into the solution. The complex was filtered through celite and concentrated under reduced pressure. (9.1 mg, slightly gray solids, 85 % yield) ^{1}H

NMR (CD_2Cl_2, 400 MHz) δ 8.03 (t, 2H, *J* = 8 Hz), 8.03 (d, 2H, *J* = 7.2 Hz), 7.68 (d, 2H, *J* = 6.8 Hz), 7.17 (d, 2H, *J* = 8.4 Hz), 7.10 (d, 2H, *J* = 2 Hz), 6.88 (dd, 2H, *J* = 8.4, 2.4 Hz), 5.34 (d, 2H, *J* = 13.6 Hz), 5.14 (d, 2H, *J* = 13.6 Hz), 2.36 (d, 2H, *J* = 13.2 Hz), 2.31 (d, 2H, *J* = 13.2 Hz), 1.41 (s, 6H), 1.30 (s, 6H); ^{1}H NMR (CD_3CN, 400 MHz) δ 8.03 (t, 2H, *J* = 8 Hz), 8.03 (d, 2H, *J* = 7.2 Hz), 7.68 (d, 2H, *J* = 6.8 Hz), 7.17 (d, 2H, *J* = 8.4 Hz), 7.10 (d, 2H, *J* = 2 Hz), 6.88 (dd, 2H, *J* = 8.4, 2.4 Hz), 5.34 (d, 2H, *J* = 13.6 Hz), 5.14 (d, 2H, *J* = 13.6 Hz), 2.36 (d, 2H, *J* = 13.2 Hz), 2.31 (d, 2H, *J* = 13.2 Hz), 1.41 (s, 6H), 1.30 (s, 6H); ^{13}C NMR (CD_3CN, 100 MHz) δ 159.8, 158.3, 153.9, 152.2, 147.7, 141.1, 126.7, 124.2, 123.4, 118.7, 118.1, 113.1, 75.7, 59.7, 58.2, 43.9, 31.9, 30.2; HRMS-FAB$^+$ *m/z* calcd 595.1515 for $C_{33}H_{33}N_2O_2Ag^+$; found 595.1513; UV (CH_3CN) λ_{max} = 286 (ε 11000); CD (CH_3CN) 216 nm (Δε -7.6), 227 nm (Δε -8), 257 nm (Δε +2.3), 282 nm (Δε -1.3), 293 nm (Δε +2).

[Ag(*R*)-(4)](OTf) ((*R*)-**87**)

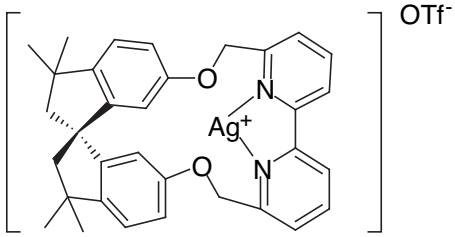

(10 mg, 93 % yield) ^{1}H NMR (1:1-$CDCl_3$: CD_3NO_2, 400 MHz) δ 8.22 (d, 2H, *J* = 8 Hz), 8.14 (t, 2H, *J* = 8 Hz), 7.77 (dd, 2H, *J* = 7.6, 0.8 Hz), 7.31 (d, 2H, *J* = 2.4 Hz), 7.21 (d, 2H, *J* = 8.4 Hz), 6.86 (dd, 2H, *J* = 8.4, 2.8 Hz), 5.57 (d, 2H, *J* = 13.6 Hz), 5.22(d, 2H, *J* = 13.6 Hz), 2.44 (d, 2H, *J* = 18.4 Hz), 2.41 (d, 2H, *J* = 18 Hz), 1.46 (s, 6H), 1.33 (s, 6H); ^{13}C NMR (1:1-$CDCl_3$: CD_3NO_2, 100 MHz) δ 159.6, 157.0, 156.3, 146.0, 140.0, 125.6, 125.6, 125.0, 122.7, 122.7, 117.9, 72.1, 58.5, 57.4, 43.0, 31.2,

28.9; CD (CH_3CN) 227 nm ($\Delta\varepsilon$ +9), 258 nm ($\Delta\varepsilon$ -3.4), 279 nm ($\Delta\varepsilon$ +1.8), 294 nm ($\Delta\varepsilon$ -1.4).

[Cu(*S*)-(4)](PF$_6$) ((*S*)-**88**) 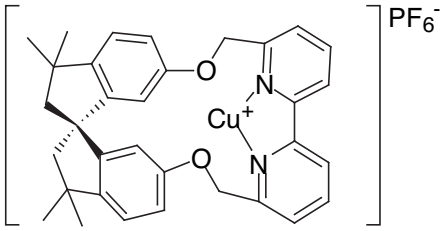

Into a stirring suspension of (*S*)-**4** (24 mg, 0.05mmol) in CH_3CN (1 mL), $[Cu(CH_3CN)_4](PF_6)$ (28mg, 0.07 mmol) in 2mL of CH_3CN was cannulated. The combined reaction mixture turned bright yellow, and it was stirred for 5 min under Ar. The solvent was removed under reduced pressure. The crude product was taken up in CH_2Cl_2 and was filtered through celite in a glass pipette. The filtrate was concentrated under reduced pressure. (29 mg, yellowish-orange solid, 83 % yield) ^{1}H NMR (CD_3CN, 400 MHz) δ 8.21 (dd, 2H, J = 8, 0.8 Hz), 8.15 (t, 2H, J = 7.6 Hz), 7.87 (dd, 2H, J = 8, 1.2 Hz), 7.09 (d, 2H, J = 8 Hz), 6.83 (dd, 2H, J = 8.4, 2.4 Hz), 6.54 (d, 2H, J = 2 Hz), 5.49 (d, 2H, J = 12.4 Hz), 5.26 (d, 2H, J = 12.8 Hz), 2.31 (d, 2H, J = 13.2 Hz), 2.09 (d, 2H, J = 13.2 Hz), 1.29 (s, 6H), 1.24 (s, 6H); ^{13}C NMR (CD_3CN, 100 MHz) δ 159.3, 158.0, 153.2, 152.6, 147.6, 141.0, 127.0, 123.8, 122.6, 119.6, 118.0, 114.6, 75.5, 60.1, 58.4, 43.6, 31.9, 30.4; ESI: *m/z* calcd 552.18 for $C_{33}H_{32}N_2O_2Cu^+$; found 551.18; UV(CH_3CN) λ_{max}: 281 (ε 9600).

[Cu(*R*)-(4)](PF$_6$) ((*R*)-**88**) 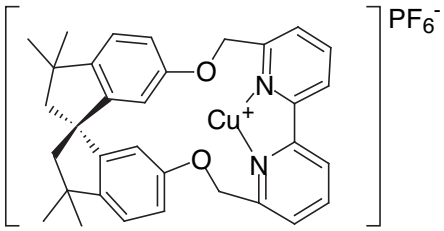

(26 mg, dark orange powder, 93 % yield)

[Ag(*S*)-(5)](OTf) ((*S*)-**89**) 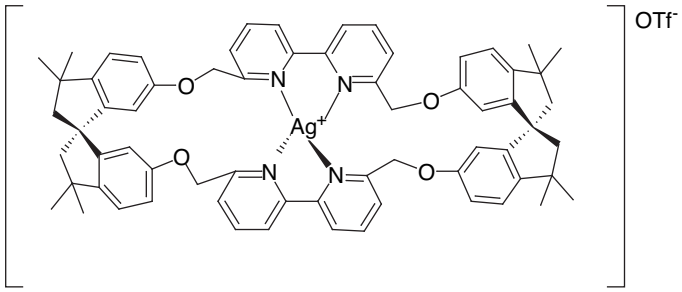

(*S*)-**5** (9 mg, 0.01 mmol) was dissolved into CH_3CN (1 mL). Silver triflate (1.3 mg, 0.01 mmol) was added and the solution was stirred for 15 min in the absence of light. The light-yellow solution was filtered through celite, concentrated in vacuo. (Quantitative yield on NMR) ^{1}H NMR (CD_2Cl_2, 500 MHz) δ 8.13 (d, 4H, *J* = 7.5 Hz), 8.12 (t, 4H, *J* = 7.5 Hz), 7.82 (d, 4H, *J* = 7 Hz), 6.75 (d, 4H, *J* = 8.5 Hz), 6.30 (d, 4H, *J* = 6.5 Hz), 5.61 (s, 4H), 5.05 (d, 4H, *J* = 13 Hz), 4.49 (d, 4H, *J* = 13.5 Hz), 2.22 (d, 4H, *J* = 13 Hz), 1.84 (d, 4H, *J* = 12.5 Hz), 1.24 (s, 12H), 1.08 (s, 12H); ^{1}H NMR ($CDCl_3$:CD_3NO_2, 500 MHz) δ 8.18 (d, 4H, *J* = 8 Hz), 8.16 (s, 4H), 7.83 (d, 4H, *J* = 6 Hz), 6.75 (d, 4H, *J* = 8.5 Hz), 6.29 (d, 4H, *J* = 8 Hz), 5.61 (s, 4H), 5.06 (d, 4H, *J* = 13.5 Hz), 4.49 (d, 4H, *J* = 13.5 Hz), 2.22 (d, 4H, *J* = 12.5 Hz), 1.85 (d, 4H, *J* = 12.5 Hz), 1.25 (s, 12H), 1.08 (s, 12H); ^{13}C NMR ($CDCl_3$:CD_3NO_2, 125 MHz) δ 158.5, 158.1, 151.8, 151.7, 145.9, 140.1, 124.4, 122.2, 115.7, 110.9, 74.9, 58.0, 56.9, 42.8, 30.6, 29.7; HRMS-MALDI *m*/*z* calcd 1083.3973 for $C_{66}H_{64}N_4O_4Ag^+$; found

1083.3980; UV (CH_3CN) λ_{max}: 290 (ε 12000); CD (CH_3CN) 216 nm (Δε -15.4), 271 nm (Δε -3.2), 295 nm (Δε -6.6), 302 (Δε -6.5), 311 (Δε -5.9).

[Ag(*R*)-(5)](OTf) ((*R*)-**89**)

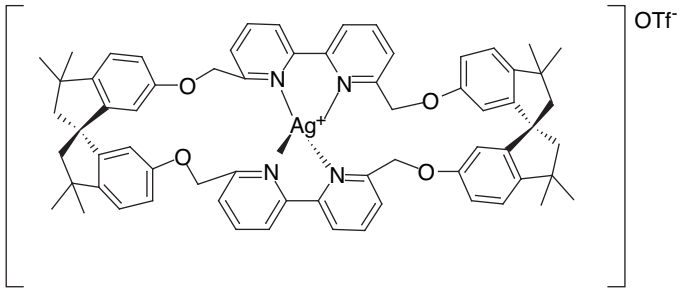

(11 mg, light-yellow solids, 78 %). ^{13}C NMR (CD_2Cl_2, 125 MHz) δ 159.2, 158.8, 152.5, 152.3, 146.7, 140.7, 125.0, 122.8, 122.5, 116.5, 111.6, 75.7, 58.7, 57.6, 43.4, 31.1, 30.3; CD (CH_3CN) 214 nm (Δε +25.1), 273 nm (Δε +1.7), 293 nm (Δε 6.7), 301 (Δε +6.2), 313 (Δε +5.7).

[Cu(*S*)-5](PF$_6$) ((*S*)-**90**)

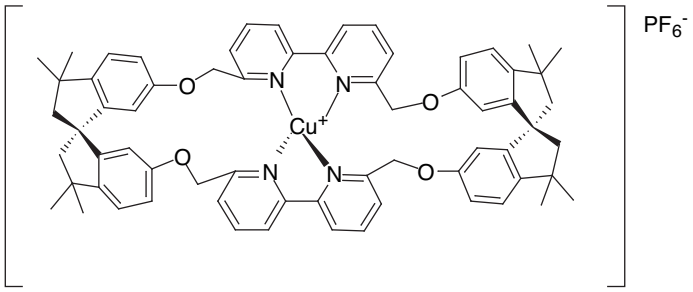

Into a vial, (*S*)-**5** (8 mg, 0.01 mmol) and distilled CH_3CN (1 mL) were loaded. $Cu(CH_3CN)_4PF_6$ (3.4 mg, 0.009 mmol) was added, and the orange solution was stirred for 15 min. The reaction mixture was concentrated under reduced pressure. The crude product was dissolved into CH_2Cl_2 and the solution was filtered through celite in a glass pipette. The filtrate was concentrated under reduced pressure. The product was dried under high vacuum for 1 h. (11 mg, dark-orange solids, 93 % yield). ^1H NMR (CD_2Cl_2, 500 MHz) δ 8.26 (d, 4H, *J* = 8.5 Hz), 8.16 (t, 4H, *J* = 8 Hz), 7.88 (d,

4H, *J* = 8 Hz), 6.92 (d, 4H, *J* = 8.5 Hz), 6.63 (dd, 4H, *J* = 8, 2.5 Hz), 5.77 (d, 4H, *J* = 2.5 H), 4.77 (d, 4H, *J* = 15.5 Hz), 4.17 (d, 4H, *J* = 15.5 Hz), 2.31 (d, 4H, *J* = 13 Hz), 1.88 (d, 4H, *J* = 13 Hz), 1.31 (s, 12H), 1.15 (s, 12H); ^{13}C NMR (CD_2Cl_2, 125 MHz) δ 160.2, 158.5, 152.4, 151.5, 148.2, 140.0, 124.2, 123.1, 121.7, 118.7, 112.8, 76.3, 58.4, 57.9, 43.3, 31.1, 30.4; HRMS-MALDI *m/z* calcd 1039.4218 for $C_{66}H_{64}N_4O_4Cu^+$; found 1039.4226; UV(CH_3CN) λ_{max}: 289 (ε 15000), 429 (ε 240); CD (CH_3CN) 212 nm (Δε -174).

[Cu(*R*)-(5)](PF$_6$) ((*R*)-**90**)

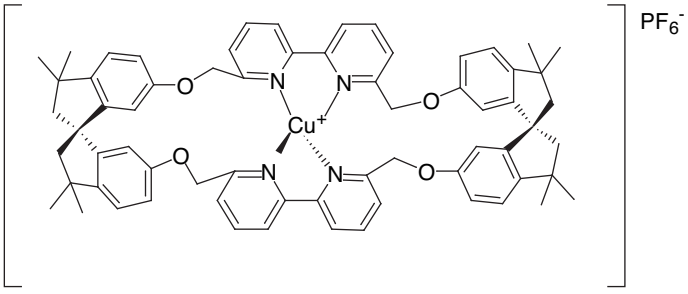

Into a small vial containing (*R*)-**5** (10 mg, .010 mmol), 1 mL of dry CH_2Cl_2 was charged and degassed for 5 min with stirring. [$Cu(CH_3CN)_4$](PF_6) (3.4 mg, 0.009 mmol) was added, then the suspension was stirred for 10 min until it became a clear-orange solution. The solution was filtered through celite. The filtrate was concentrated under reduced pressure. (9.8 mg, dark orange solids, 91 % yield); CD (CH_3CN) 213 nm (Δε +132).

CHAPTER 2. STRUCTURE AND PROPERTIES OF CHIRAL CYCLOPHANES AND THEIR METAL COMPLEXES

2.1 Introduction

Among many nitrogen-containing bidentate ligands, 1,10-phenanthroline[86.160] (phen) and 2,2'-bipyridine[79] (bpy) are well-known for the generality of their stable metal complexes. When these bidentate ligands are covalently linked to chiral spirobiindanol, chemistry becomes even more intriguing. Newly formed helical macrocycles give rise to unusual chiroptical and electronic properties. Syntheses of cyclophanes **1**—**5** and their metal complexes were described in the previous chapter. Their property and structural information, derived from NMR, MS, X-ray crystallography and circular dichroism (CD) spectroscopic data, will be analyzed and discussed in this chapter.

2.1.1 Optical and Chiroptical Spectroscopy

2.1.1.1 Ultraviolet Spectroscopy

When a molecule is exposed to UV (200-400 nm) or visible light (400-800 nm), it undergoes electronic changes, which involves the excitation of an electron from a bonding or non-bonding orbital to an antibonding molecular orbital. The part of the molecule that absorbs the UV light is called a chromophore, and UV peak at a particular wavelength, λ_{max}, measures the electronic excitation from the lower energy level to the higher energy level. UV light can elevate electrons from single bonds (σ-electrons), unsaturated bonds (π-electrons, the highest occupied molecular orbital, HOMO), or in non-bonded orbitals of heteroatoms attached to sp^2 carbons (n-electrons) to excited states (antibonding orbitals, σ^* and π^* such as the lowest unoccupied molecular orbital, LUMO). No $\sigma \rightarrow \sigma^*$ excitation is observed by UV

spectroscopy because it occurs below 200 nm. Mostly, $n \rightarrow \pi^*$ and $\pi \rightarrow \pi^*$ excitations are studied by the given technique.

An UV spectrum measures the variation of the absorption of photon energy as a percent absorbance (% A) or optical density versus wavelength in nm. The molar extinction coefficient, ε, measures the intensity of the absorbance peak at a λ_{max}. It is calculated by using the Beer-Lambert law:[161]

$$A = \log\left(\frac{I^o}{I}\right) = \varepsilon c l$$

Equation 2

$I°$ indicates the intensity of the incident light, I is the intensity of the transmitted light, c is the concentration in moles per liter, and l is the cell path length in centimeters, which is normally 1 cm.

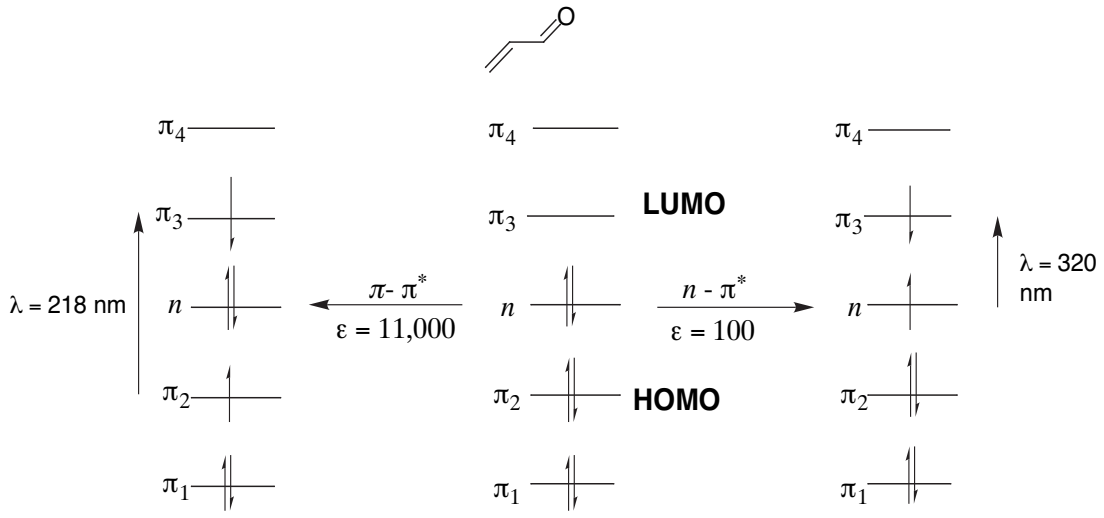

Figure 2.1 Molecular orbitals responsible for UV transitions.

In a conjugated system like 2-propenal, two types of electronic transitions, $\pi \rightarrow \pi^*$ and $n \rightarrow \pi^*$, are possible.[162] The molecular orbital diagram (Figure 2.1) shows

that the first transition from HOMO to LUMO, or $\pi \rightarrow \pi^*$, occurs at 218 nm with high intensity. The second transition comes from the interaction between carbonyl carbon and electrons from the non-bonding orbital of oxygen, $n \rightarrow \pi^*$. This particular transition is weaker than the first—only $\varepsilon = 100$. All UV absorptions are solvent-dependent and concentration dependent. It may be necessary to use more diluted sample to detect transitions with weaker intensity.

2.1.1.2 Optical Rotary Dispersion (ORD) and Circular Dichroism (CD)

Although the first resolution of a chiral metal complex into its enantiomers was achieved by Werner in 1911,[163] the optical rotation and circular dichroism studies of Cu^{II} and Cr^{III} complexes with tartrate and malate as ligands had already been reported by Cotton in the 1890.[164.165] Chiral molecules can rotate the plane of polarized light, and they are said to be optically active. The device that measures the optical activity is called a polarimeter. A pre-requisite for observing optical activity is the presence of an enantiomeric excess of a chiral species. Conventionally, chemists call the optical rotation α positive if the sample rotates the plane of polarized light in the clockwise direction, and the plus (+)-sign is assigned. The opposite rotation, counterclockwise direction, is given the negative sign (-). A pair of enantiomers rotates the plane of polarized light by equal amounts in opposite directions.[166]

The optical rotation depends on the concentration of sample, c (g/mL), and the length, l, of the sample container, which is normally 1 dm. The proportionality factor, or specific rotation $[\alpha]$, is the standard measure of optical activity, and it is measured

at a specific temperature, concentration and wavelength of light, usually at 589 nm of sodium D line.

$$[\alpha] = \frac{\alpha}{cl}$$

Equation 3

Chiral molecules not only rotate the plane of polarized light, but they also absorb it differently; that is $\varepsilon_L \neq \varepsilon_R$. The difference $\Delta\varepsilon \equiv \varepsilon_L - \varepsilon_R$ is known as circular dichroism. In other words, using the Beer-Lambert-Bouguer law, the difference of the absorbances can be recorded directly:

$$\Delta A = A_L - A_R = \log_{10}\left(\frac{I_0}{I_L}\right) - \log_{10}\left(\frac{I_0}{I_R}\right) = \log_{10}\left(\frac{I_R}{I_L}\right)$$

Equation 4

$$\Delta\varepsilon = \left(\frac{1}{cl}\right)\Delta A$$

Equation 5

Circular dichroism also results in another effect, "ellipticity". Initially I_{0L} and I_{0R} are equal to each other at $d = 0$. Upon leaving the cell, $I_L \neq I_R$, and when the corresponding sum vector for each pair of angles (γ, $-\gamma$) is constructed, the trip no longer oscillates along one line. Instead, the originally linear polarized light has become elliptically polarized. Mathematically, the angle ψ = arctan (b/a) is called, *ellipticity*. In theory, ellipticity may be measured directly on a machine; however, all commercially available machines measure the absorbance A, instead. These machines are occasionally calibrated inψ, using the equation 5.

$$\psi = 33\Delta A$$

Equation 6

The value of α increases as A/λ when moving from long to short wavelengths. Biot noticed that the absolute value of α rose more slowly when approaching much shorter wavelengths. He termed the former case "normal" and the second one "anomalous optical rotary dispersion" (ORD). Around the region of absorption, spectra look even more complicated because the anomalous sigmoidal curve appears superimposed to the regular ORD, or background rotation. For example, for an originally positive rotation at long wavelengths, two principal types of ORD are possible.

According to a rule set by Natanson and Bruhat, a positive CD or ellipticity is associated with a "positive anomalous ORD", and all three of these effects, (anomalous ORD, CD, and ellipticity) are called a "Cotton effect" (CE) in honor of Cotton. The interconversion between ORD curves and CD curves is feasible[167] using the very complicated Kronig-Kramers formalism;[168.169] however, it is rarely done. Rarely, it provides any additional information, and due to the molecular vibrations, it becomes even more difficult to extract useful information about a CD from ORD. In this thesis work, only CD data will be used to discuss structures of chiral cyclophanes and their metal complexes.

In a case where molecules with the same "chiral" parts have different number of repeating subunits, their rotation values can be normalized by multiplication with the relative molar mass M.. In turn, values become very large, so it was proposed that they be divided by 100. [NOTE: The division by 100 is introduced purely for

convenience unlike the specific rotation, $[\alpha] = \frac{100\alpha}{c_p l}$, where 100 is necessary to match g/ml (density for pure oils and liquids). A "molar rotation", $[M]$, is defined by:

$$[M] = [\Phi] = \frac{[\alpha]M}{100}$$

Equation 7

Finally, because ellipticity ψ is an angle like α, Moscowitz introduced the definition of specific ellipticity:

$$[\psi] = \frac{\psi}{\rho l} = \frac{100\psi}{cl}$$

Equation 8

and molar ellipticity:

$$[\Theta] = \frac{[\psi]M}{100}$$

Equation 9

Usually, very small values of ellipticity is obtained in liquid phase; therefore, one may use the approximation (Equation 6) to obtain the following:

$$[\Theta] = 3300\Delta\varepsilon$$

Equation 10

Finally, CD and ORD offer a large quantity of structural information of a molecule that can elucidate the absolute configuration of chiral molecules.[170] The task can be achieved in the following manners:

1. **Correlation method**: Spectra from similar compounds are compared, where the absolute configuration had been determined by Bijvoet's method.[171] This method is based on the assumption that small geometrical

and electronic changes would not affect the overall chiroptical properties. However, this method must be used with some care. For example, a series of similar spiro-compounds have been known to produce nearly mirror CD spectra.[172]

2. **Sector rules**: The signs of Cotton effects of transition bands are compared. These rules are available for ligand field transitions, such as Co^{III} metal complexes[173] of pseudo tetragonal class[174] and metal complexes with amino acids.[175.176] However, the method is known to be problematic and a number of exceptions are reported.[177]
3. **Comparing spectra to calculate models**: ORD and CD spectra are compared with models, such as exciton theory, semi empirical, or ab initio quantum mechanical methods.

2.1.1.3 Exciton Chirality Method

The exciton chirality method[178] is a simple and extremely versatile way of establishing absolute configurations and conformations of organic molecules in solution[179]. When two or more chromophores are present nearby in space of a chiral system, exciton coupling is observed. These chromophores can be identical or different, and they can be located within the same molecule or between different molecules as in the case of a ligand and its biopolymeric receptor. The exciton coupling occurs due to spatial interactions of the electronic transition moments of chromophores, resulting in the splitting of energy levels of the excited state, which can be observed by UV-vis and CD.

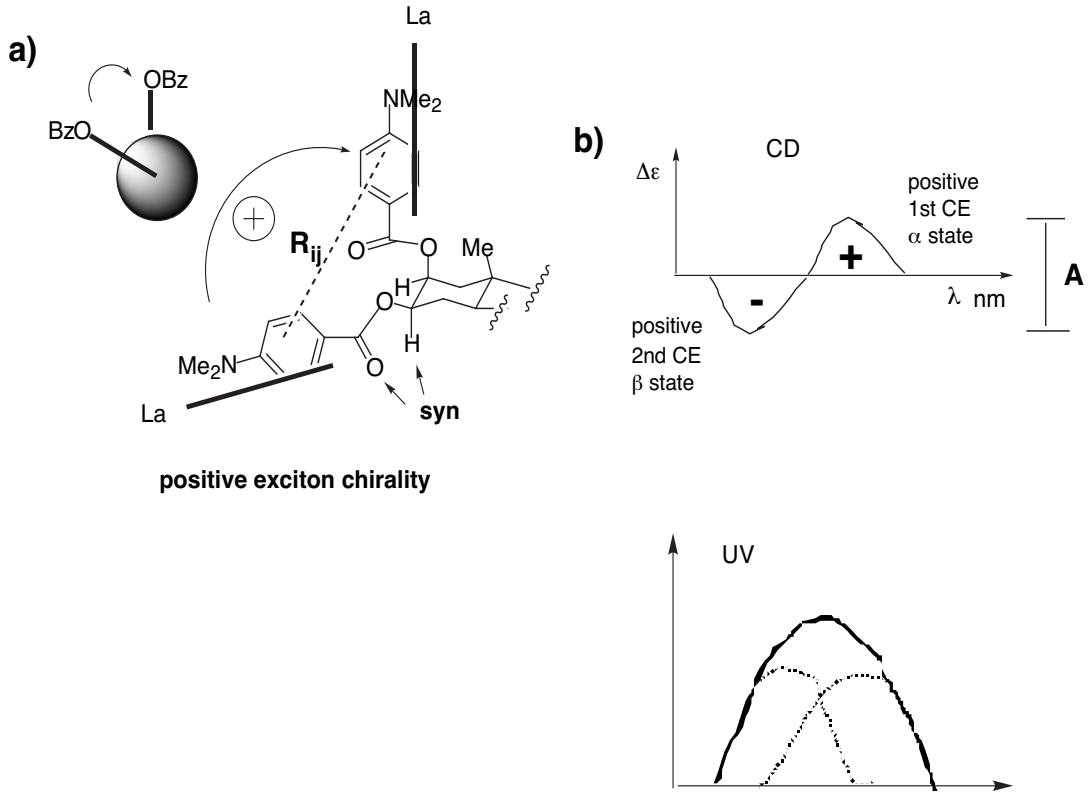

Figure 2.2 a) Exciton coupling of two identical chromophores (*I* and *j*) of steroidal 2,3-bis-*p*-dimethylaminobenzoate. b) Summation of CD and UV curves.

For example,[179] the coupling of identical chromophores is shown by *p*-substituted bisbenzoates of a vicinal cyclohexanediol—a steroidal 2,3-bisbenzoate. In order to determine the absolute configuration, the absolute sense of chirality between the C2-O and C3-O bonds must be determined. Figure 2.2(a) shows that two chromophores are twisted in clockwise fashion, defined as a positive chirality. There may be some rotations between two bonds; however, the X-ray crystal structure of the molecule indicates the bond to be locked in a rigid system, where the ester carbonyls are *syn* to the methane hydrogens of the cyclohaxane.[180] The interaction of two ^1L_a transition moments from each chromophore results in the splitting of the excited energy level into a red-shifted α and blue-shifted β. The coupling results in two

bisignate curves with opposite signs as positive and negative Cotton effects on the CD spectrum.

The CD spectrum shown in Figure 2.2(b) displays a positive CE first at longer wavelength and a negative second CE at higher wavelength, so the spectrum is defined as positive because its chirality of the transition moments is clockwise. The sum of the distance between the peak and trough of the split CD curve is called an *amplitude* or *A*. The value of *A* is either positive or negative depending of the sign of the first CE. CD absorptions and UV absorption occur near each other. In the case of the UV spectrum, the coupling gives rise to two spectra with positive sign (+), which add up to appear as a single absorption maximum with double intensity.

2.1.1.4 Circular Dichroism of Spirobiindanol

Harada[181.182] has successfully determined the absolute configuration of chiral spiroaromatic compounds using the CD exciton coupling method. A group of molecules from the chiral 9,9'spirobifluorene derivatives are similar to spirobiindanol because their optical activities originate from chromophores twisted at the quaternary carbon center (Figure 2.3). Prelog[183.184] and his group were the first to synthesize (-)-[6,6]-vespirene, (-)-**91** and they assigned its absolute configuration as *R* using the results from CD exciton coupling method. Their assignment was based on the interpretation that (*R*)-(-)-**91** exhibited negative first and positive second Cotton effects at 297 nm and 272 nm on CD around the region of 270 nm UV transition.

There are some problems with using (*R*)-(-)-**91** as the model system to study the absolute configuration of other spirobifluorene compounds. Besides the Cotton

effects used for the study, there were additional CD absorptions, such as Cotton effect of negative sign at 255 nm and the most intense negative Cotton effect at 320 nm. These complications indicate that the 9,9'-spirobifluorene may to too strained for a system to use exciton-coupling studies because normally, Cotton effects show up at the wavelength of strongest absorption.[178] In order to make sure that exciton-coupling method can be used to determine the absolute configuration of such a twisted and congested system, additional chiral spiroaromatic compounds, (*R*)-(+)-**92** and (*R*)-(+)-**93**, with naphthalene and anthracene chromophores, were studied.[181.185.186]

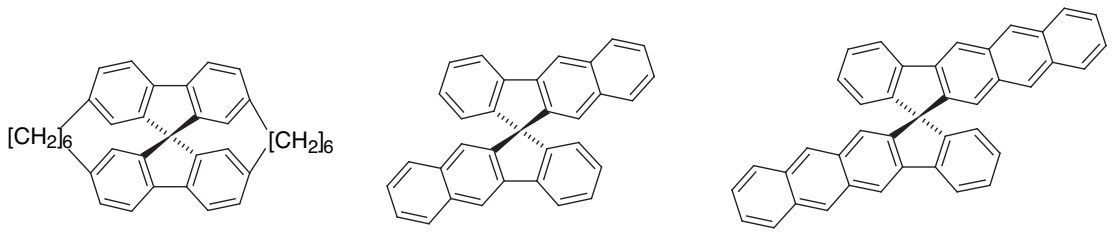

(R)-(-)-91
(R)-(-)-[6,6]-vespirene

(R)-(+)-**92**

(R)-(+)-**93**

Figure 2.3 Chiral spiroaromatic 9,9'-Spirobifluorene derivatives.

The UV spectrum of the bis(naphthalene) compound (*R*)-(+)-**92** shows strong long-axis polarized ^1B_b transition absorption (λ_{max} 251.5 nm, ε 86100). In the corresponding region, the CD spectrum shows strong Cotton effects of positive first and negative second signs: λ_{ext} 272.3 nm Δε +188.3 and λ_{ext} 252.0 nm, Δε -207.2; *A* = +395.5. All the results indicate that the long-axis polarized transition moment of two chromophores is in a clock-wise screw sense, or positive exciton coupling. With the positive value of amplitude *A*, this enantiomer of **92** was assigned (*R*) configuration. In a similar fashion, the UV spectrum of the bis(anthracene) compound (*R*)-(+)-**93**

shows an intense ^1B_b band (λ_{max} 288.6 nm, ε 152000). It also shows strong Cotton effects of positive first and negative second signs along the corresponding region: λ_{ext} 300.5 nm Δε +551.0 and λ_{ext} 278.5 nm, Δε -207.2 A = +560.7. The absolute configuration of (+)-**93** was assigned *R*.

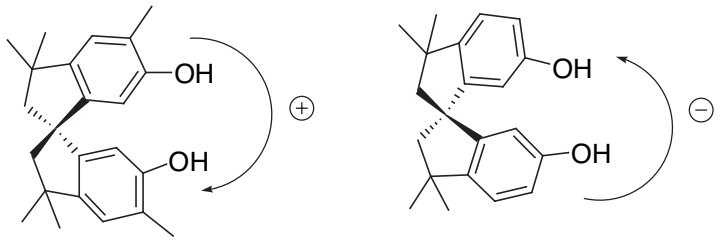

(R)-(+)-**94** (S)-(-)-**6**

Figure 2.4 Configurational assignments based on exciton coupling between two aromatic groups.

Table 2.1 UV and CD Spectra Spirobiindane Derivatives.

Compd	**Solv.**	**UV** α	$\lambda_{m\mu}$ P	(ε × **10²**) β	**CD** α	$\lambda_{m\mu}$ P	([θ] × **10³**) β
(+)-**94**	MeOH	286 (89.0)	223 (165)[i]	202.3 (667)	292 (+17.6) 274 (-1.65)	231 (-15.8) 223[i] (+14.6)	209 (+250)
(-)-**6**	MeOH	289 (62.4) 284 (65.8)	220[i] (165)		290 (-10.9) 284 (-8.05) 270 (+1.98)	236 (-1.98) 229 (+18.6)	209 (-289)

[i]: inflection

CD spectra of (+)-6,6'-dihydroxy-3,3,5,3',3',5'-hexamethyl-bis-1,1'-spiroindane (+)-**94** and (-)-spirobiindanol (-)-**6** in methanol were investigated by Hagishita[49.187.188] and his group in 1971 (Figure 2.4). In the given rigid chiral system, they wanted to study the exciton coupling, which originates from an interaction of transition dipoles of the same two aromatic chromophores. They synthesized and resolved a series of twisted spiroaromatic compounds. Since Hagishita reasoned that extra methyl groups in the first compound would only have a minimal perturbation effects on the phenol chromophores, two compounds, (+)-**94** and (-)-**6**, were picked

for the model system. As expected, two gave a set of very similar peaks for Cotton effects that turned out to be complementary (Table 2.1).

The spiro-compound (+)-**94** showed a positively signed Cotton effect at the longest wavelength: 292 ([θ] +17,600), and a negatively signed CE at 274 nm ([θ] –1,650). The clock-wise, or positive, chirality indicates that the molecule is a *R*-enantiomer. On the contrary, (-)-**6** showed a negatively signed Cotton effect at the longest wavelength: 290 ([θ] -10,900) and a positively signed CE at 270 nm ([θ] +1,980). The given data were categorized into three different types of wavelengths, α, *P*, and β from the longer wavelength according to the classification of Clar.[189]

Theoretical CD spectra of the spiroaromatic compounds with (*S*)-configuration show the positive Cotton effect at the longer wavelength and then negative Cotton effect at the shorter wavelength in the region of the α band. The result contradicts the findings from actual CD measurements. Other spiro-aromatic compounds listed on Hagishita's work also produced conflicting results from what was expected according to the exciton coupling theory. Unfortunately, the exciton coupling theory could not predict all the configurations of these compounds. At times, the exciton coupling is weak or there are more couplings occurring from the molecule than one of interest for assigning the configuration..

2.1.2 Metals Used in the Complex Formation

2.1.2.1 Palladium

Palladium belongs to the group 10 elements, which have the completed *d* shell. Most common oxidation states for palladium are II, d^8, and IV, d^6. Most of Pd^{II} complexes are square planar, being the type MX_2L_2 (X = monodentate anion; L = donor ligand) in *trans* or *cis* isomers. Other forms, ML^{2+}_4, ML_3X^+, MLX^-_3, and MX^{2-}_4 are possible too (Table 2.2). Palladium(II) generally shows low affinity for "hard" ligands, such as F^- or O^-, but prefers heavier halogens or ligands that can π bond.

Table 2.2 Oxidation State and Stereochemistry of Palladium[II].

Oxidation State	Coordination Number	Geometry	Examples
Pd^{II}, d^8	4[a]	Planar	$[PdCl_2]_n$, $[Pd(NH_3)_4]Cl_2$, $[Pd(CN)_4]^{2-}$
	5	*tbp*	$[Pd(diars)_2Cl]^+$
	6[a]	Octahedral	PdF_2 (rutile type), $Pd(diars)_2I_2$, $Pd(dmgH)_2$

[a] Most common states

2.1.2.2 Copper and Silver

Group 11 elements copper and silver have a single *s* electron outside the completed *d* shell. They have similar electronic structures and ionization potentials, with silver having a slightly bigger covalent radius than copper. Only oxidation state +1 of each metal ion will be discussed because that was the only one used to make complexes with chiral cyclophanes.

Copper(I) compounds are diamagnetic and have no *d-d* transition. Its complexes are usually colorless, unless there are charge transfer transitions (both LMCT and MLCT), in which case they appear as red or orange[190]. The copper(I)halide and other complexes are synthesized by following ways: a) direct

introduction of ligands to copper(I)halides or triflate; b) reduction of copper(II) complex; or c) reduction of copper(II) in the presence of, or by the ligand. The most common group of ligands for copper(I) complexes consists of unsaturated heteroaromatic compounds with empty π anti-bonding orbitals, such as phen, bpy, $(imidH)_2dap$, and $(py)_2dap$ (Table 2.3). Using the tetrahedral $[Cu(CH_3CN)_4]PF_6$ as a starting material, many tetrahedral L_4Cu^I and trigonal L_3Cu^I can be formed[191].

Table 2.3 Oxidation States and Stereochemistry of Copper[I].

Oxidation State	Coordination Number	Geometry	Examples
Cu^I, d^{10}	2	Linear	Cu_2O, KCuO, $CuCl_2^-$, $CuBr_2^-$
	3	Planar	$K[Cu(CN)_2]$, $[Cu(SPMe_3)_3]ClO_4$
	4[a]	Tetrahedral	CuI, $[Cu(CN)_4]^{3-}$, $[Cu(MeCN)_4]^+$
	4	Distorted planar	CuL[b]
	5	*sp*	[CuLCO][b]

[a] most common state. [b] L = a macrocyclic N_4 anionic ligand

The oxidation state +1 is very common for silver. The stereochemistry and examples of silver(I) compounds are shown in (Table 2.4). In general, silver ion readily forms complexes with nitrogen ligands, most notably with NH_3. In aqueous state, linear coordination is preferred, as $[H_3N—Ag—NH_3]^+$, but in non-aqueous conditions, tetrahedral complexes, such as $[Ag(py)_2]^+ClO_4$ can be obtained. Organosilver compounds are sensitive to light, air and moistures. Since the finding of silver (I) complexes with arenes by A.E. Hill,[192] there have been many different silver(I) complexes of planar and nonplanar arenas reported.[193.194] Interestingly, arene ligands are either η^1 or η^2- and not η^6- bonded, which is different from other transition metal arene complexes.

Table 2.4 Oxidation States and Stereochemistry of Silver[I].

Oxidation State	Coordination Number	Geometry	Examples
Ag^{I}, d^{10}	2[a]	Linear	$[Ag(CN)_2]^-$, $[Ag(NH_3)_2]^+$, AgSCN
	3	Trigonal	$[Ag(PCy_2Ph)_3]BF_4$
	4[a]	Tetrahedral	$[Ag(SCN)_4]^{3-}$, $[AgI(PR_3)]_4$, $[Ag(py)_4]^+$, $[Ag(PPh_3)_4]ClO_4$, $[Ag(NCMe)_4]^+$
	5	Distorted pentagonal plane	$[Ag(L)]^+$
	5	Pentagonal pyramidal	$[Ag(L)]_2^{2+}$
	6	Octahedral	AgF, AgCl, AgBr (NaCl structure)

[a] Most common states.

2.1.2.3 Zinc and Mercury

Elements Zn, Cd and Hg make up the group 12 metals.[195] Each has a filled $(n\text{-}1)d$ shell plus two *ns* electrons. The chemistry of zinc and cadmium are similar, but mercury chemistry is very different. For example, $ZnCl_2$ and $CdCl_2$ typically have ionic structures, but $HgCl_2$ crystals are composed of linear molecules. Zinc is not known to be toxic in any form, but cadmium and mercury are extremely toxic and must be handled with care.

The coordination numbers ranging from 2 to 8 are possible for all three metals. The geometry for the coordination 4 is tetrahedral, and some of the examples are $[Zn(CN)_4]^{2-}$, $ZnCl_2(s)$, ZnO, $[Cd(NH_3)_4]^{2+}$, $HgCl_2(OAsPh_3)_2$. Both zinc and cadmium have been used to form many complexes with amine ligands, ranging from NH_3 through other substituted diamines[196.197] to a variety of macrocycles.[198.199] Other nitrogen-containing heterocyclic molecules, such as pyridines an pyrazoles, are also good ligands for these metals.[200.201]

All four mercuric halides HgX_2 (X = F, Cl, Br, I) are known. Mercury(II) fluoride has the fluorite structure and is not volatile. $HgCl_2$ and $HgBr_2$ have linear molecular structures, but HgI_2 exits as layers of linked HgI_4 tetramer at room temperature and appears red. The yellow molecular form can be obtained when it is heated above 126 °C. Mercury(II) is considered a "soft" cation because it shows strong preference for halogens, such as Cl, Br, I, along with P, S, Se, and some nitrogen-containing ligands. It can have coordination numbers from 2-6, favoring the lower ones—especially for the linear 2-coordination.

2.2 Results and Discussion

2.2.1 Spirobiindanol

When an enantiomerically enriched sample of a C_2-symmetric molecule spirobiindanol **6** is dissolved a chlorinated solvent, protons corresponding to H_i, which are *ortho* to the phenolic OH, resonate as different peaks on ^1H NMR. The aggregation of enantiomers in a concentrated sample leads to transient diastereomeric interactions among enantiomeric spirobiindanol. This phenomenon is only observed in concentrated samples in aprotic chlorinated solvents, such as chloroform and dichloromethane. The separate resonance is not observed in protic solvent, such as methanol, or even an aprotic solvent, such as acetonitrile. The ability of the solvent to accept hydrogen bond seems to affect whether the diastereomeric interaction can be detected or not.

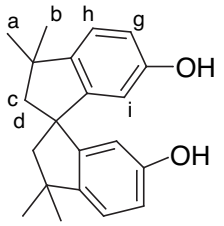

$$\delta_{obs}H_S = \chi_{SS}\,\delta H_{SS} + \chi_{RS}\,\delta H_{RS} \qquad \delta_{obs}H_R = \chi_{RR}\,\delta H_{RR} + \chi_{RS}\,\delta H_{RS}$$

Equation 11

Table 2.5 Spirobiindanol with different enantiomeric purity

Entry	Mixture	[*R*]	[*S*]	χ_{RR}	χ_{SS}	χ_{RS}
1	Racemate	50 %	50 %	25 %	25 %	50 %
2	Pure *R*	100 %	0 %	100 %	0 %	0 %
3	Pure *S*	0 %	100 %	0 %	100 %	0 %
4	Enantiomerically Enriched	20 %	80 %	4 %	64 %	32 %

Equation 11 and Table 2.5 show that the observed chemical shift, $\delta_{obs}H$, of each enantiomer, *R* and *S*, comes from the sum of two possible aggregates—enantiomeric aggregate (*SS* or *RR*) or diastereomeric aggregate (*RS* or *SR*). Therefore, the actually ppm value for each enantiomer is affected by the concentration, or mole ratio χ, of each aggregate. Values for $\delta_{obs}H_S$ and $\delta_{obs}H_R$ are identical for racemic or enantiomerically pure mixture (Table 2.5 entries 1--3). On the other hand, observed ppm values of two enantiomers would be different in a mixture with unequal concentration of *R* and *S* (Table 2.5 entry 4). The result is two peaks with separate ppm values and different integrated peak areas. By integrating areas for each peak, a relative value of enantiomeric excess can be estimated.

Circular dichroism of both enantiomers of **6** was taken in methanol in order to compare the data with the earlier work by Hagishita,[49.187.188] which had established the configuration of (-)-**6** to be *S*. As a result, spirobiindanol with the (+) optical rotation was determined to be *R*. Even though the absolute configuration of spirobiindanol had already been established, CD of cyclophanes would lead to the study effects of other polyaromatic chromophores and steric constraints from cyclization on the transition moment of the spirobiindanol.

CD spectra of **6** show the expected complementary Cotton effects at 230 nm and 208 nm (Table 2.6). The UV spectrum shows absorbance (λ_{max} 220 nm, ε 17000) as an inflection point. (*R)*-Spirobiindanol has a negative $\Delta\varepsilon$ -8 at λ_{ext} 229 nm and a positive $\Delta\varepsilon$, +147 at λ_{ext} 208 nm. (*S*)-Spirobiindanol has CE with opposite signs at the same wavelengths—λ_{ext} 230 nm, $\Delta\varepsilon$ +8 and λ_{ext} 208 nm, $\Delta\varepsilon$ -156. Consiglio's

spirobiindanol phosphonates[57] **38** show the similar CD split at nearby wavelength range (Δε +60 at λ_{ext} 215 nm and Δε -78 at λ_{ext} 205 nm), but their spectra were taken in ethanol and absolute configuration was not determined. On the other hand, Hagishita's CD spectra of the same spirobiindanol in methanol look very different. Especially, the α band region looks very different from the Hagishita's work, which is very unfortunate because he had used the Cotton effect trend in this region to establish the absolute configuration of spirobiindanol. The CD taken from this study shows only a small absorption at 280 nm in the α band region. There are smaller UV absorbances at 284 nm and 290 nm without distinctly measurable Cotton effect.

The most interesting region in the CD spectra is the *β* region, which is missing in Hagishita's work. The strongest Cotton effects were shown at the shortest wavelength, 208 nm. A positive Cotton effect is observed for the (*R*)-**6**, and the negative Cotton effect was shown for the (*S*)-**6**. Unfortunately, the Cotton effects in the *β* region could not be used to study other cyclophanes because less polar cyclophanes were not soluble in methanol. They were soluble only in acetonitrile and chloroform, whose observable wavelength does not go beyond 220 nm and 240 nm, respectively.

Table 2.6. CD and UV Spectra of Spirobiindanol

Compd	**Solv.**	**UV**	$\lambda_{m\mu}$ **(ε × 10²)**		**CD**	$\lambda_{m\mu}$ **(*Δε*)**	
		α	*P*	*β*	*α*	*P*	*β*
(+)-(*R*)-**6**	MeOH	290 (76.7) 284 (79.7)	222 (172.8)	------	286 [a] (+3)	230 (-7.2)	208 (+147)
(-)-(*S*)-**6**	MeOH				290 [a] (-5.5)	230 (+7.9)	208 (-156)

[a] Estimated value.

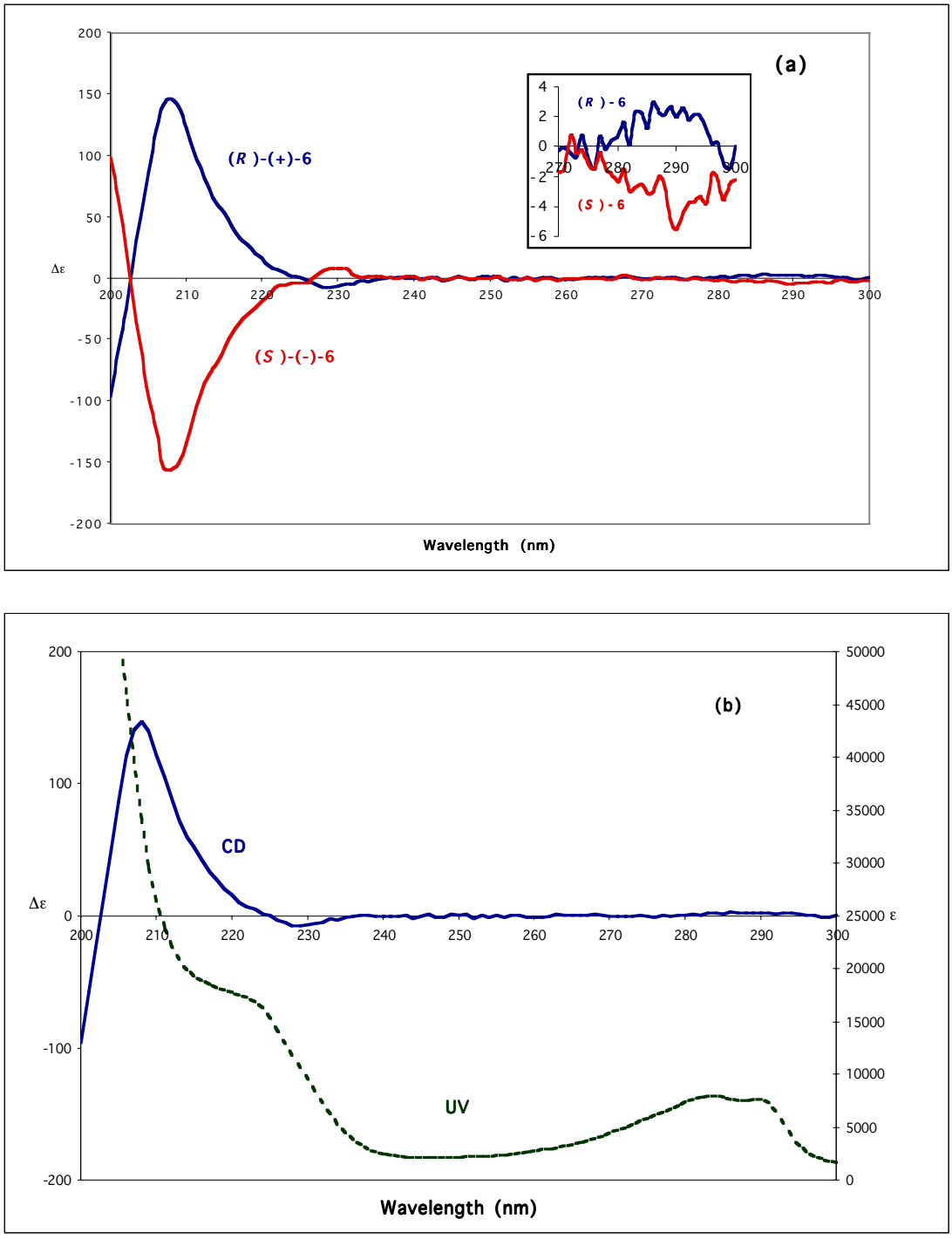

Figure 2.5 (a) CD spectra of (*R*)-**6** and (*S*)-**6** from 200 nm to 300 nm in methanol. Δε unit is $Lcm^{-1}mol^{-1}$ (b) CD and UV spectra of (*S*)-spiro in CH_3OH.

2.2.2 Chiral Cyclophanes

^{1}H NMR spectra of phenanthroline-incorporated cyclophanes, **1**--**3**, show distinctively different sets of peaks (Table 2.7). Protons H_a to $H_{c,}$ of the cyclophane **1** remain essentially unchanged from corresponding protons in spirobiindanol **6**. In cyclophanes **2** and **3**, the same series of protons are all shifted downfield. The proton H_d, which may be pointing toward the inside cavity of the host molecule, is shifted downfield by $\Delta\delta$ 0.1 ppm for cyclophanes **1** and **2**. On the other hand, the bigger cyclophane **3** show only a slight downfield shift. Only in a more rigid and sterically congested molecule **1**, diastereotopic protons from the bridging CH_2O--H_e and H_f--resonate as two separate peaks in AABB pattern in the ^{1}H NMR. The same methylene protons in bigger cyclophanes **2** and **3** resonate as a single peak, which probably is the result of signal averaging over several interchanging conformations in a flexible system.

Table 2.7 ^{1}H NMR Peak Assignments of **1**, **2**, and **3**

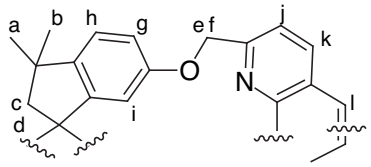

Comp	H_a	H_b	H_c	H_d	H_e	H_f	H_g	H_h	H_i	H_j	H_k	H_l
1[a]	1.32	1.34	2.21	2.41	5.34	5.57	6.77	6.98	7.02	7.76	8.33	7.83
2[a]	1.39	1.44	2.32	2.45	5.43	5.43	6.96	7.18	6.55	7.95	8.36	7.78
3[b]	1.34	1.39	2.27	2.36	5.46	5.46	6.89	7.09	6.47	7.88	8.20	7.62
6[b]	1.31	1.36	2.23	2.33	------	------	6.70	7.02	6.25	------	------	------
8[b]	------	------	------	------	5.00	5.00	------	------	------	7.93	8.31	7.83

[a)] ^{1}H NMR was taken in a mixed solvent system, 1:1-$CDCl_3$:CD_3NO_2, in 400 MHz NMR. All ppm values were referenced to TMS at 0 ppm. [b)] ^{1}H NMR was taken in $CDCl_3$ in 400 MHz NMR. All ppm values were referenced to TMS at 0 ppm.

The proton H_i on phenyl ring of **1** shifts downfield ($\Delta\delta$ = 0.8 ppm) compared to the corresponding proton in spirobiindanol **6**. All three protons (H_g-H_i) for **2** experienced some downfield shift, all less than $\Delta\delta$ 0.3 ppm. Electronic perturbation on aromatic rings of phenanthroline appears to be greater on geometrically congested compound **1** than **2**. Compared to 2,9-bis(bromomethyl)-1,10-phenanthroline **8**, H_j on **1** is shifted upfield ($\Delta\delta$ = 0.2 ppm), and H_l on **2** is also shifted upfield ($\Delta\delta$ = 0.5 ppm). Signals for protons from the biggest cyclophane, **3**, resonate between **1** and **2** under the magnetic field. Changes in NMR chemical shifts and splitting patterns indicate that both spirobiindanol and phenanthroline groups on the more rigid cyclophane **1** experience greater changes in their chemical and electronic environments than in more flexible macrocycles **2** and **3**.

Table 2.8 ^{1}H NMR Peak Assignments of **4** and **5**

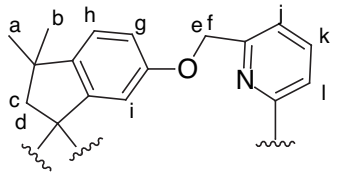

Comp	H_a	H_b	H_c	H_d	H_e	H_f	H_g	H_h	H_i	H_j	H_k	H_l
4	1.30	1.30	2.17	2.31	5.21	5.38	6.78	6.97	6.78	7.40	7.74	7.50
5	1.29	1.36	2.21	2.60	5.02	5.14	6.71	6.89	6.17	7.34	7.72	8.15
6	1.31	1.36	2.23	2.33	------	------	6.70	7.02	6.25	------	------	------
7	------	------	------	------	4.63	4.63	------	------	------	7.47	7.83	8.39

Bipyridine-based cyclophanes, **4** and **5**, also show distinctively different sets of peaks in ^{1}H NMR spectra (Table 2.8). Compared to phen-based cyclophane **1**, spirobiindanol units from both **4** and **5** seem to be less contorted, generally showing smaller changes in its chemical shifts from **6**. Protons H_e and H_f from the methylene bridges resonate differently for both **4** and **5**. The over all changes in ppm ($\Delta\delta$) for

cyclophanes **4** and **5** from their building units, **6** and **7**, are smaller than the observed Δδ for phen-based cyclophanes **1**--**3**.

The formation of **4** forces both nitrogen atoms from each pyridine units to be in the *syn* conformation, and the change is indicated by the upfield shift of H_l proton (Δδ = 0.90 ppm). In a more energetically stable *anti* conformation of bpy, the signature hydrogen H_l, or 3-pyridyl hydrogen, appears farther downfield (7.50 ppm), due to the proton, which is anisotropically deshielded by the nitrogen lone-pair electrons of the adjacent pyridine ring.[155] ^{1}H NMR spectra of both the bpy ligand **7** and a more relaxed macrocycle **5** show the proton $H_{l,}$ at lower field (8.39 ppm and 8.15 ppm, respectively), which suggests an *anti* conformation.[156.157] In summary, ^{1}H NMR spectra of **4** and **5** show that nitrogen units in **4** are in *syn* conformation due to the geometric constriction imposed by cyclization. The inherently more flexible bipyridine unit allows both cyclophanes to be less rigid than their phenanthroline counterparts.

The complete cyclization of cyclophanes products **1**—**5** are supported by the absence of a broad peak (3360 cm^{-1}) characteristic of O-H bond from spirobiindanol in IR. MS-spectra also show the absence of isotope distribution from Br, which also indicates the cyclic ether formation. Minimal fragmentation patterns indicate that these cyclophanes are very stable.

Optical rotations of two cyclophanes **1** and **2** from the same enantiomeric spirobiindanol produced opposite signs. For instance, the cyclophane **1** made from (*R*)-(+)-**6** gave a negative sign, but the cyclophane **2** produced a positive sign. The

reverse was true for the (*S*)-(-)-**6** derived cyclophanes. Signs in optical rotation of **2** correlates to the sign of the spirobiindanol, but **1** shows the opposite rotation sign.

2.2.2.1 CD and UV Spectra of Chiral Cyclophanes

Phenanthroline-based Cyclophanes 1 and 2

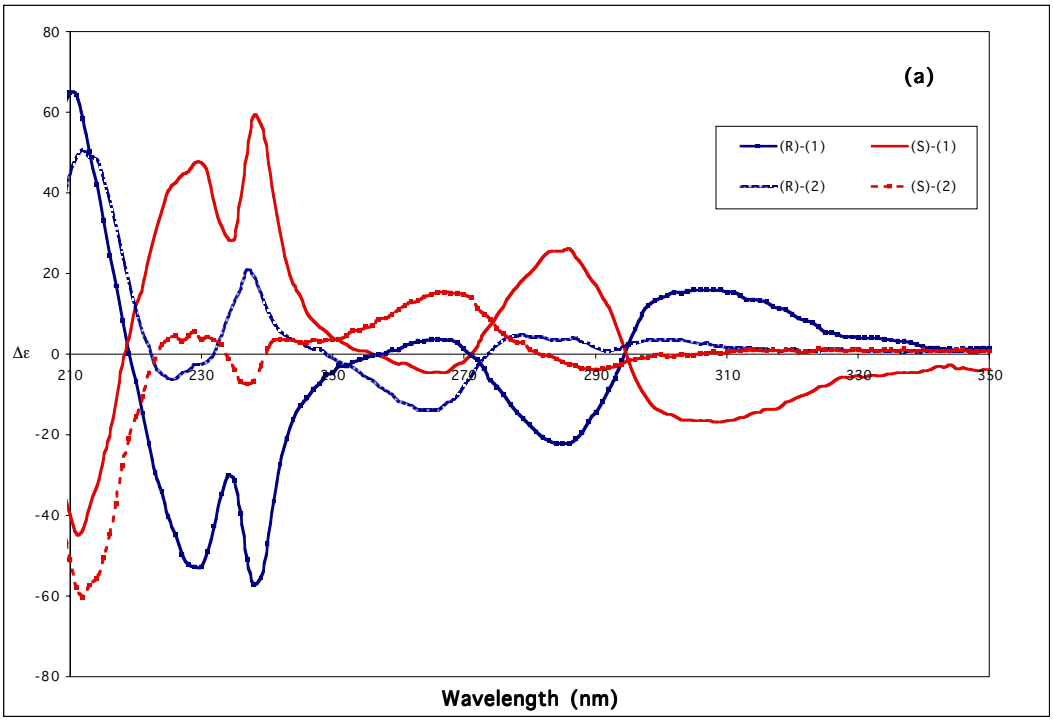

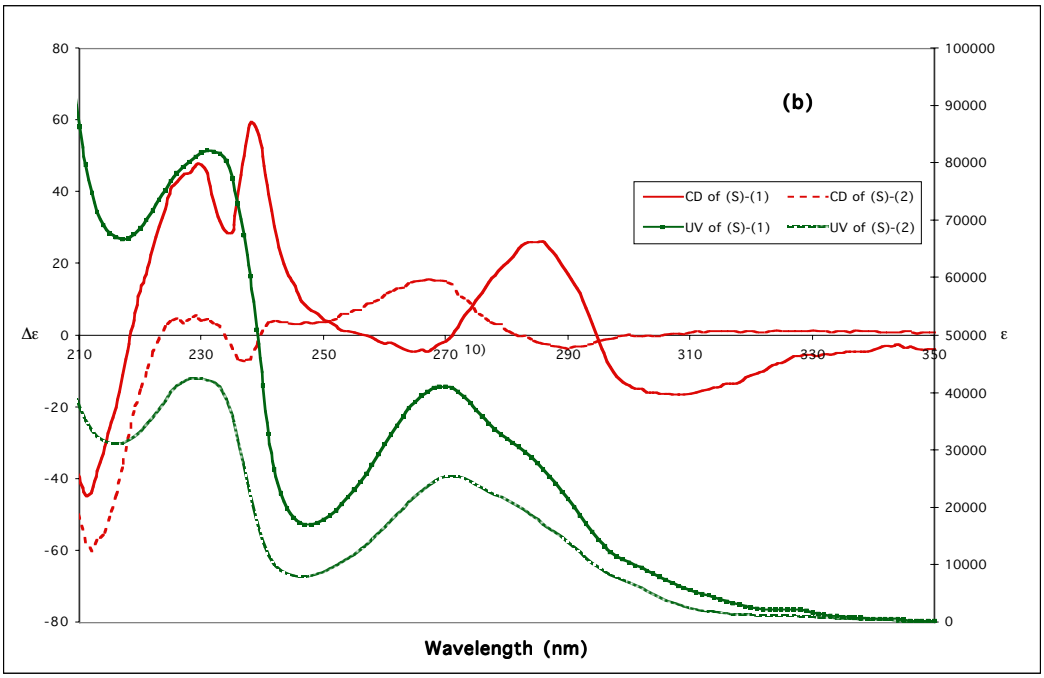

Figure 2.6 (a) CD spectra of **1** and **2**. Δε unit is L $cm^{-1}mol^{-1}$ (b) CD and UV spectra of (*S*)-**1** and (*S*)-**2** in CH_3CN.

Table 2.9 UV and CD Spectra of **1** and **2**

Compd	**Solv.**	**UV** α	$\lambda_{m\mu}$ ($\varepsilon \times 10^2$) P	β	**CD** α	$\lambda_{m\mu}$ ($\Delta\varepsilon$) P	β
(-)-(*R*)-**1**	CH_3CN	269 (41000)	231 (82000)	----	286 (-22) 265 (+3.7)	238 (-57) 230 (-53)	210 (+65)
(+)-(*S*)-**1**	CH_3CN				286 (+26) 265 (-4.6)	238 (+59) 230 (+47.5)	210 (-44.5)
(+)-(*R*)-**2**	CH_3CN	271 (25000) 320 (1200)	229 (43000)		264 [a] (-13.8)	237 (+21) 225 [a] (-5.8)	212 (+51)
(-)-(*S*)-**2**	CH_3CN				267 [a] (+15.5)	237 (-7) 229 [a] (+5.5)	212 (-60)

[a] Values are different

Circular dichroism of enantiomeric cyclophane pairs of **1** and **2** shows complementary Cotton effects. The assigned absolute configuration of each cyclophane was derived from the known configuration of the spirobiindanol **6**.[49] The complementary Cotton effects show up at λ_{ext} 286 nm, λ_{ext} 265 nm, λ_{ext} 238 nm, λ_{ext} 230 nm, and λ_{ext} 210 nm for the cyclophane **1** pair (Figure 2.6). The two Cotton effects at 238 nm and 230 nm are important because the UV spectrum shows a strong absorbance at 231 nm. However, this absorption does not appear at two opposite signs. Perhaps, an electronic interaction between phenyl chromophore of spirobiindanol and aromatic rings of phenanthroline gives rise to additional Cotton effects.

The cyclophane (*R*)-(-)-**1** derived from (*R)*-(+)-**6** has a negative Cotton effect first and positive Cotton effect second: λ_{ext} 286 $\Delta\varepsilon$ –22, λ_{ext} 265 $\Delta\varepsilon$ +3.7. The cyclophane (*S*)-(+)-**1**, which was made from (*S*)-(-)-**6**, has a positive Cotton effect first and negative Cotton effect second: λ_{ext} 286 $\Delta\varepsilon$ +26, λ_{ext} 265 $\Delta\varepsilon$ -4.6 (Table 2.9). The same trend was found in Hagishita's work[49] with (*S*)-(-)-spirobiindanol **6**. Different values in amplitude are caused by the difference in optical purity of the spirobiindanol

used in the synthesis of the cyclophane. A smaller UV absorption at 269 nm corresponds to Cotton effects at 286 nm and 265 nm. Because acetonitrile has absorption around 220 nm under UV light, it was not possible to detect the UV-absorption of the cyclophane in the β region. An additional pair of absorbances around 300 nm was observed; however, it lacked the characteristic bisigmoidal curve-shape Cotton effect and the corresponding UV absorbance around the region.

The Cotton effects from the more flexible dimeric cyclophane pair of **2** are not neatly complementary. The CD spectra of two enantiomeric cyclophanes show Cotton effects at slightly different wavelengths: 264 nm (267 nm for (*S*)-derivative), 237 nm, 225 nm (229 nm for (*S*)-derivative), and 212 nm. The absorption at 212 nm is substantially stronger than others: $\Delta\varepsilon$ +51 for (*R*)-**2** and $\Delta\varepsilon$ -60 for (*S*)-**2**. Unlike the smaller compound **1**, the Cotton effect at 286 nm is missing in the cyclophane **2** even though there seems to be absorption without the characteristic bisignate curve shape.

Unlike the UV and CD spectra of spirobiindanol, the UV absorbance at 290 nm is missing in cyclophane **1** and **2**. Also missing are absorbances at longer wavelengths, such as 276 nm, 330 nm, and 345 nm, which were found in 2,9-bisbromomethyl-1,10-phenanthroline. Unlike spirobiindanol, both enantiomers of the cyclophane **1** have strong absorptions at α region with two bisignate curves with opposite signs. Most likely, the conjugated system from phen chromophores contributes to the Cotton effects observed in the longer wavelength. UV absorbances of **2** appear at 270 nm and 232 nm, which have a slight bathochromic shift compared to the compound **1**.

Bipyridine-based Cyclophanes

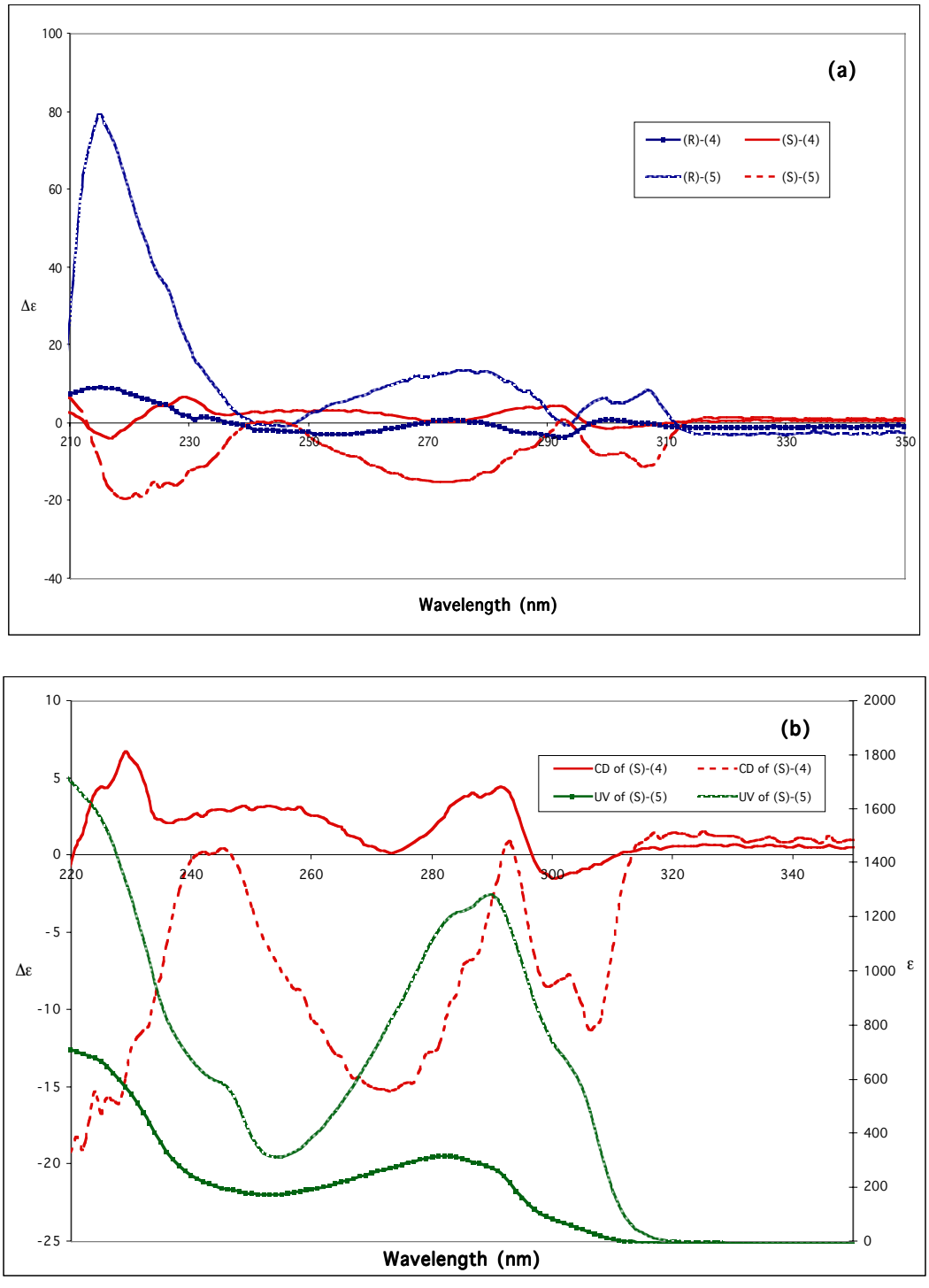

Figure 2.7 (a) CD spectra of **4** and **5** cyclophanes in CH_3CN. (b) CD and UV spectra of (*S*)-**4** and (*S*)-**5** cyclophanes in CH_3CN.

Table 2.10 UV and CD Spectra of **4** and **5**

Compd	**Solv.**	**UV** $\lambda_{m\mu}$ (ε)			**CD** $\lambda_{m\mu}$ ($\Delta\varepsilon$)		
		α	*P*	β	α	*P*	β
(*R*)-**4**	CH_3CN	282 (320)	221 (700)	----	300 (+0.8) 292 (-3.8) 254 (-3)	-----	215 (+9)
(*S*)-**4**	CH_3CN				300 (-1.5) 291 (+4.4) 253 (+3.2)	-----	217 (-4)
(*R*)-**5**	CH_3CN	304 (600) 290 (1300) 284 (1200)	245 (590) 223 (1600)		307 (+8) 275 (+13)	-----	215 (+79)
(*S*)-**5**	CH_3CN				306 (-11.3) 273 (-15.3)	-----	219 (-19.5)

Cotton effects from CD spectra of the monomeric compound **4** have the smallest values, and absorptions look inconsistent from 210 nm to 250 nm wavelength range(Figure 2.7). The cyclophane derived from (*S*)-**6** shows negative Cotton effect at the longest wavelength, then positive at the next: λ_{ext} 300 $\Delta\varepsilon$ –1.5, λ_{ext} 291 $\Delta\varepsilon$ +4.4. The cyclophane from (*R*)-**6** shows the complementary values: λ_{ext} 300 $\Delta\varepsilon$ +0.8, λ_{ext} 292 $\Delta\varepsilon$ -3.8 (Table 2.10). The trend is opposite of what was found with phenanthroline-based cyclophanes.

Dimeric cyclophanes (*R*)-**5** and (*S*)-**5** show better-defined CD spectra than their monomeric analogues. The observation is also contrary to what was found with phenanthroline-based cyclophanes. Interestingly, the cyclophane (*R*)-**5** has Cotton effects with only positive signs, and the opposite is true for (*S*)-**5**. Amplitude values of both cyclophanes are similar, except with the absorptions at the β-region: λ_{ext} 215 $\Delta\varepsilon$ +79 for (*R*)-**5** and λ_{ext} 219 $\Delta\varepsilon$ -19.5 for (*S*)-**5**. UV spectra of bipyridine-based cyclophanes, **4** and **5**, display unusually small extinction coefficient values.

2.2.2.2 X-Ray Crystal Structures of Phenanthroline-Based Cyclophanes

X-ray crystal structures of **1** and **2** were successfully solved. Unfortunately, it was not possible to obtain X-ray quality crystals of bpy-based cyclophanes. The structure of **1**--($C_{35}H_{32}N_2O_2$)--was solved and refined successfully from clear crystals of the cyclophane made from racemic spirobiindanol in acetonitrile by recrystallization. The structure belongs to monoclinic system and the space group is centrosymmetric, *C*2/*C*, with Z = 4, which means crystals are racemic (Figure 2.8). Bond lengths and bond angles of the compound fall within the normal range. In order to have an idea of the cavity dimension, the distance between two oxygen atoms O(1)--O(1') derived from spirobiindanol (7.1 Å) and the distance from either nitrogen molecules N(1) or N(1') to the quaternary carbon C(8) of the spirobiindanol (5.6 Å) were measured. The host molecule is big enough to contain a small metal ion, but not enough to encapsulate the solvent molecule, acetonitrile. The proton H(12) from CH_2O bridge faces toward the inside of the ring, but the geminal proton H(11) faces away from the ring. Cyclopentene rings from spirobiindanol are in an envelope conformation, and aromatic rings in the phenanthroline subunits appear to deviate slightly from being completely planar.

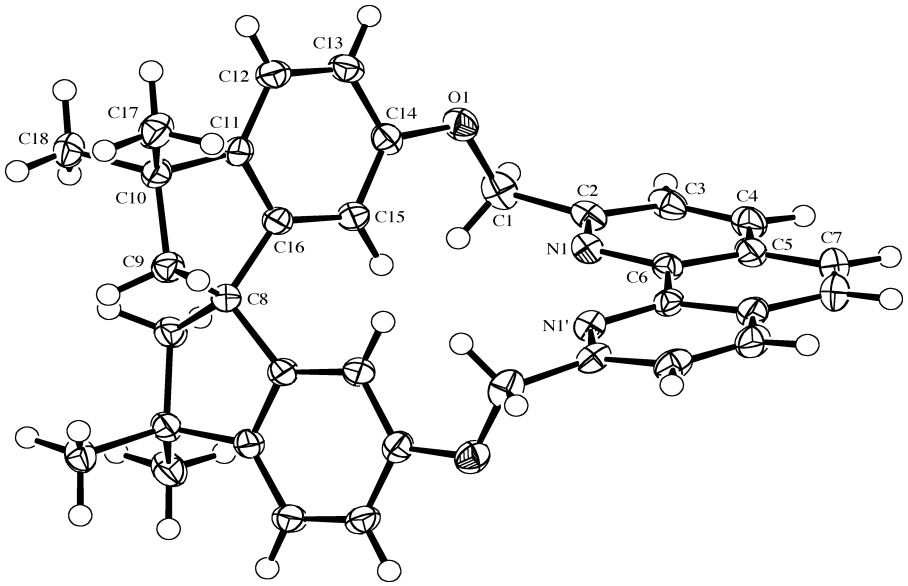

Figure 2.8 ORTEP[202] representation of **1** (50% probability ellipsoids; H-atoms given arbitrary displacement parameters for clarity).

The structure of the cyclophane **2**—($C_{70}H_{64}N_4O_4 \cdot 4CH_2Cl_2$)**--**was solved and refined successfully with no unusual features (Figure 2.9). These clear crystals were grown from dichloromethane through very slow evaporation. The crystals are enantiomerically pure and the absolute structure of **6** has been determined *S* [Flack's x = -0.02(5)]. The structure belongs to triclinic system, and the space group is *P*1 with Z = 1. The asymmetric unit contains one molecule of the macrocycle plus four molecules of dichloromethane. There is no disorder in the structure.

In its 'open' state, the inner cavity of **2** is rectangular, and the dimension is around 11 Å × 7 Å. There are four dichloromethane molecules placed above and below nitrogen atoms of phenanthroline with chlorides pointing away from electron-rich nitrogen. The dipole moments of four dichloromethane molecules are pointing away from each other (↑↓↑↓). The arrangement of dichloromethane molecules in the

cavity of the cyclophane indicates that it will be possible to host electrophilic metal ions inside. The internuclear distance between N(1)···N(3) from different phenanthroline units is 9.3 Å. Hydroxy groups of the spirobiindane are about 7 Å from each other. Spirobiindane-backbone of the cyclophane is more twisted in **2** than **1** because the torsional angle between C(52) to C(57) is –132.5 (3) ° for **2**; whereas, the torsional angle for the same carbons in **1** is 105.8 (1) ° (Figure 2.10).

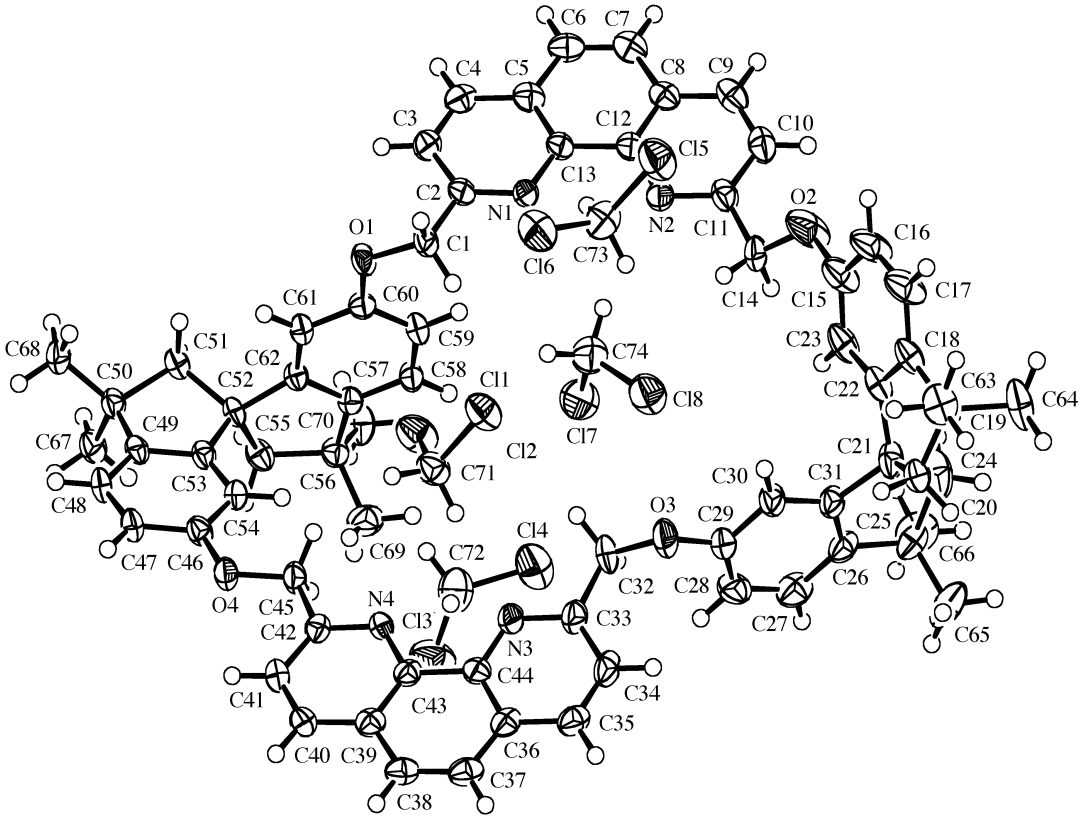

Figure 2.9 ORTEP[202] drawing of **2** with four CH_2Cl_2 molecules (50% probability ellipsoids; H-atoms given arbitrary displacement parameters for clarity).

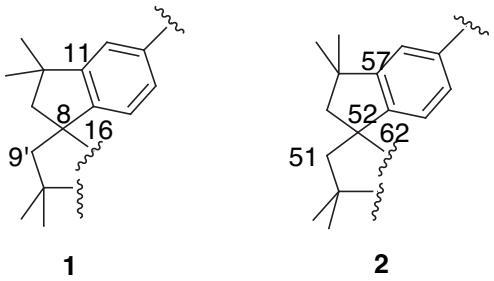

1 **2**

Figure 2.10 Torsional angles of spirobiindanol in macrocycles **1** and **2**

2.2.3 Metal Complexes of 1

The sterically congested cyclophane **1** turned out to be a very versatile host molecule. Five different metal ions, Ag(I), Cu(I), Hg(II), Pd(II), and Zn(II), could coordinate to phenanthroline subunit of the cyclophane. Cyclophanes made from previously resolved (*R*) and (*S*)-spirobiindanol subunits were used to synthesize enantiomeric pair of metal complexes with Ag(OTf) and $[Cu(CH_3CN)_4](PF_6)$. More easily available racemic cyclophane (*rac*)-**1** made from (*rac*)-spirobiindanol was used to make complexes with Hg(II), Pd(II), and Zn(II) ions.

^{1}H NMR spectra show that upon coordination to copper(I) and silver(I), the cationic metals draw electron density away from phenanthroline units, as indicated by downfield shifts of protons H_j--H_l (Figure 2.11, Table 2.11) . Comparatively speaking, protons from spirobiindanol unit are less affected by presence of either metal ion than protons on phenanthroline backbone. Spirobiindane backbone is probably too far from the metal coordination site to be influenced by a metal ion. The only noticeable change is felt by the upfield shift of H_i proton ($\Delta\delta$ 0.2 ppm for silver(I) complex **80** and $\Delta\delta$ 0.3 ppm for the copper(I) complex **81**). Methylene bridging protons, H_e and H_f, experience the effects of the metal differently, since one faces toward the inside of the cyclophane cavity and the other away from it. The proton facing toward the metal, namely H_f, is further shifted downfield than its geminal proton H_e.

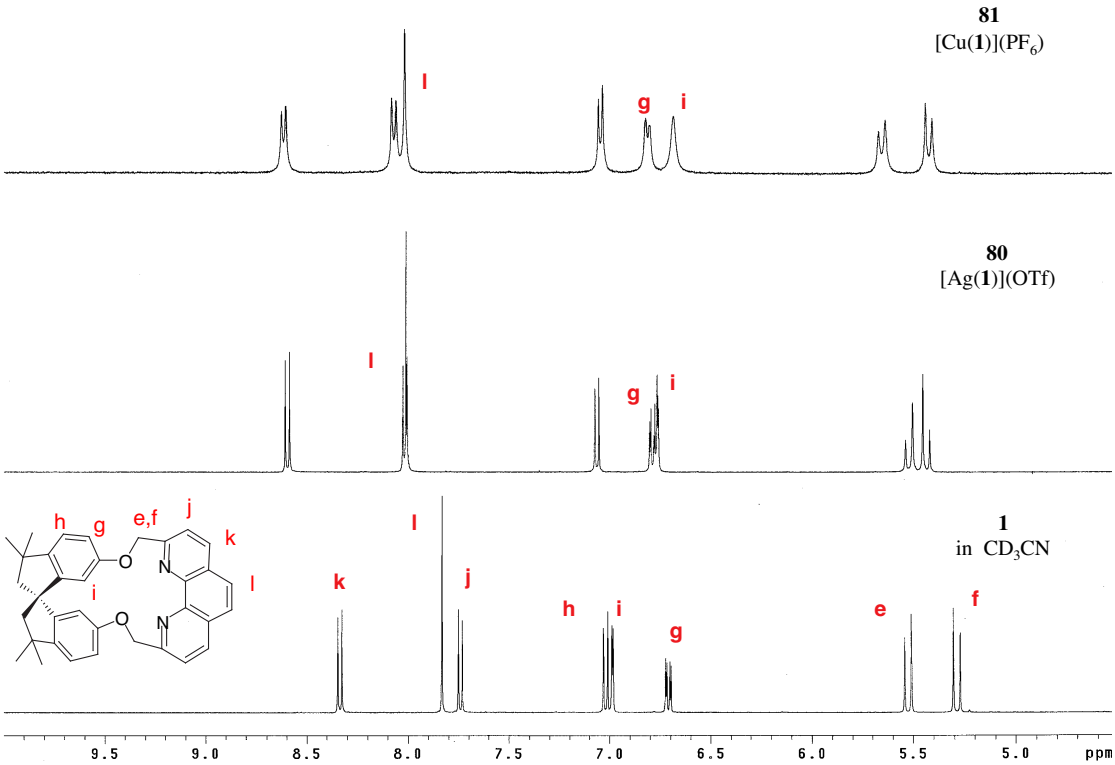

Figure 2.11 ^{1}H NMR Spectra of [Ag(**1**)](OTf) **80**, [Cu(**1**)](PF$_6$) **81**, and **1** in CD_3CN.

Table 2.11 Selected ^{1}H NMR Peak Assignments of **1** and its metal complexes with silver(I) and copper(I) ions.

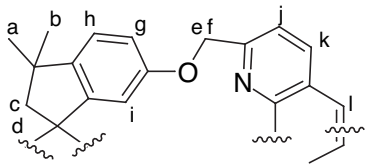

Compound	H_e	H_f	H_g	H_h	H_i	H_j	H_k	H_l
1	5.29	5.33	6.71	7.02	6.99	7.75	8.34	7.84
80	5.45	5.54	6.80	7.08	6.78	8.04	8.62	8.04
81	5.43	5.66	6.82	7.05	6.69	8.08	8.62	8.02

^{1}H NMR spectra were taken in CD_3CN in 400 MHz NMR. All ppm values were referenced to TMS at 0 ppm.

Next three metal ions, Hg^{II}, Pd^{II}, and Zn^{II} have different effects on **1**, compared to the previous d^{10} metals like Cu^{I} and Ag^{I} (Figure 2.12. Table 2.12). The Hg^{II} complexes **82** show upfield shift of all protons on the aromatic rings of spirobiindanol after the complexation occurs. All protons on phenanthroline group have been shifted

downfield by about 0.2 ppm. Signals for protons on aromatic rings of **6** and the methylene-bridging group have become less definite upon coordination.

Most notably, the C_2-symmetry of the cyclophane is destroyed upon coordination to Pd^{II} **83** and Zn^{II} **84** ions. All nuclei of these complexes are chemically and magnetically different, and this is confirmed by ^{1}H and ^{13}C NMR. Apparently, the deshielding cone of the metal ion affects half of the molecule, and the other half is more shielded. A five-coordinate *tbp* complex of platinum(II) containing two halogen ligands in axial positions, an alkene and a bidentate N-containing ligand, such as phen, is well known.[203.204] This type of complex is known to retain the symmetry of the phen in ^{1}H NMR spectra even down to –90 °C. Looking at the congested inner cavity of the cyclophane, it would not be possible for π-bond from the aromatic ring of **6** to coordinate to the palladium(II) metal center in the equatorial plane, along with two coplanar nitrogen atoms, while retaining two halogens in apical positions. It has been suggested that mono-dentate coordination to the metal center by one nitrogen from phen is possible.[203] However, it probably is not likely the cause of the asymmetry in the structure. Unfortunately, X-ray quality crystals could not be grown to confirm these speculations.

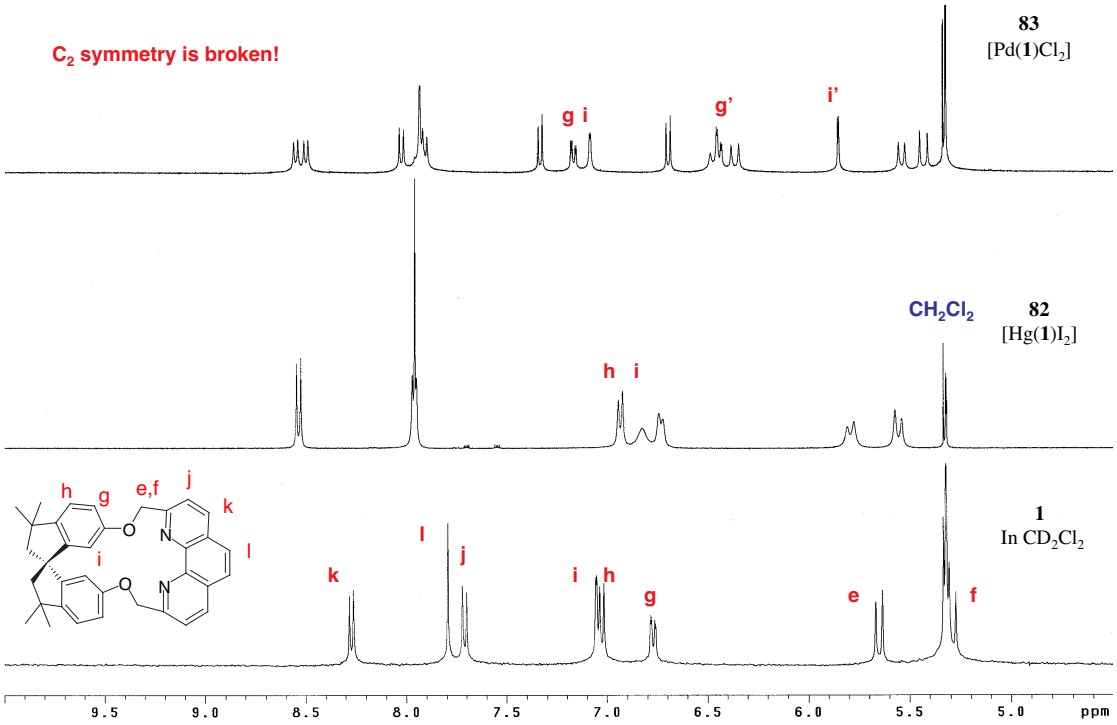

Figure 2.12 ^{1}H NMR Spectra of [Pd(**1**)Cl$_2$] **83**, [Hg(**1**)I$_2$] **82**, and **1** in CD_2Cl_2 in the lower field.

Table 2.12 Selected ^{1}H NMR Peak Assignments of **1** and its metal complexes with Hg(II), Pd(II), and Zn(II) ions.

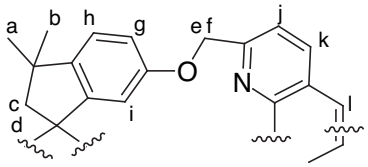

Compound	H_e	H_f	H_g	H_h	H_i	H_j	H_k	H_l
1	5.29	5.65	6.77	7.03	7.05	7.71	8.27	7.79
82 [Hg(**1**)I$_2$]	5.55	5.79	6.73	6.93	6.83	7.96	8.54	7.96
83 [Pd(**1**)Cl$_2$]	5.54 5.43	6.47 6.36	7.17 6.44	7.33 6.70	7.09 5.85	8.03 7.91	8.55 8.50	7.94 7.94
84 [Zn(**1**)Cl$_2$]	5.55 5.47	6.13 5.67	7.13 6.41	7.24 6.62	7.58 5.80	8.21 8.10	8.70 8.63	8.07 8.04

^{1}H NMR was taken in CD_2Cl_2, in 400 MHz NMR. All ppm values were referenced to dichloromethane at 5.32 ppm.

Isotope distributions shown in mass spectra of these metal complexes also support the coordination of metals to the phen-based cyclophane **1**. Both silver(I) complex—619 (100 %) and 621 (100 %)--and copper(I) complex--575 (100 %) and

577 (52 %)--display the expected isotope distributions. The last three complexes show up as +1 charged ions caused by the loss of one halogen.

2.2.3.1 CD and UV Spectra of 80 and 81

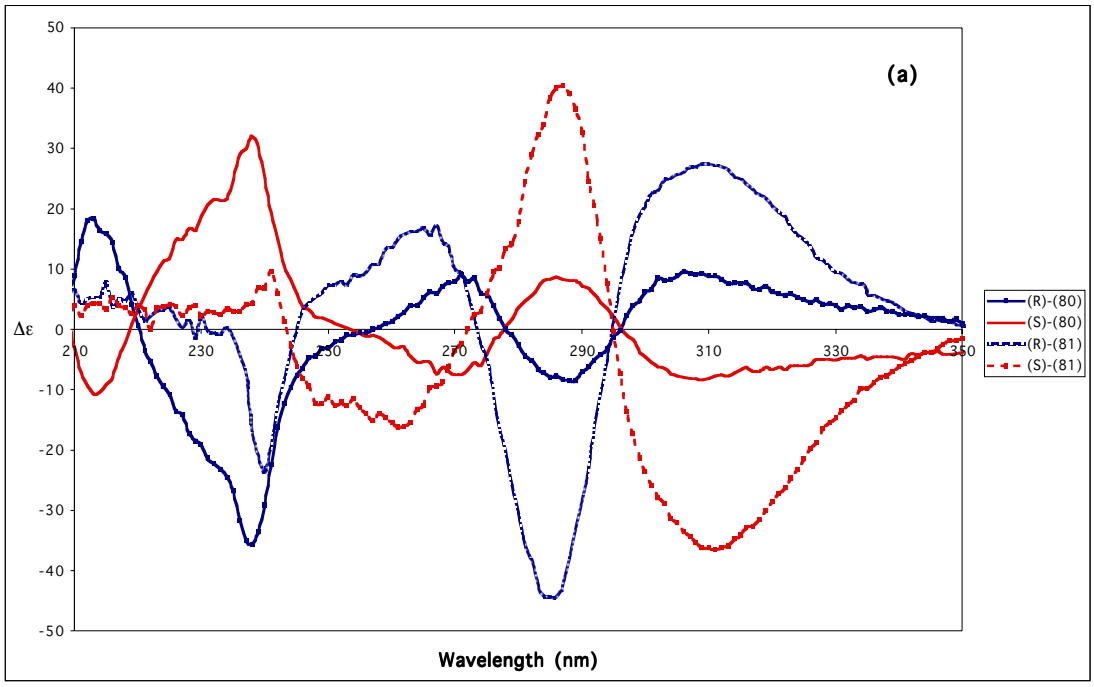

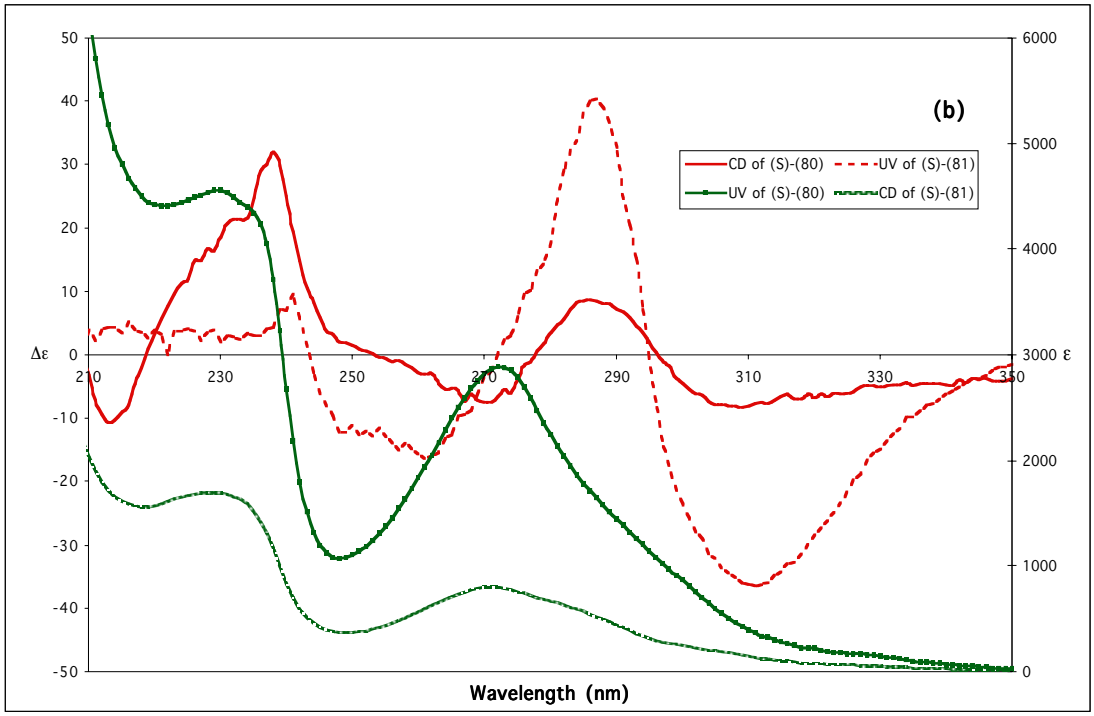

Figure 2.13 (a) CD spectra of [Ag(**1**)](OTf) **80** and [Cu(**1**)](PF_6) **81** in CH_3CN. (b) CD and UV of **80** and **81** in CH_3CN.

Table 2.13 CD and UV Spectra of **1** and Metal Complexes **80** and **81**.

Compd	**Solv.**	**UV** α	$\lambda_{m\mu}$ (ε) *P*	β	**CD** α	$\lambda_{m\mu}$ *P*	($\Delta\varepsilon$) β
(-)-(*R*)-**1**	CH_3CN	269 (41000)	231 (82000)	----	286 (-22) 265 (+3.7)	238 (-57) 230 (-53)	210 (+65)
(+)-(*S*)-**1**	CH_3CN				286 (+26) 265 (-4.6)	238 (+59) 230 (+47.5)	210 (-44.5)
(*R*)-**80**	CH_3CN	273 (2900)	231 (4500)		288 (-8.6) 271 (+9)	238 (-36)	212 (+18)
(*S*)-**80**	CH_3CN				286 (+8.7) 271 (-7.5)	238 (+32)	212 (-11)
(*R*)-**81**	CH_3CN	271 (798)	229 (1691)		309 (+27) 286 (-44) 267 (+17)	241 (-23.6)	
(*S*)-**81**	CH_3CN				309 (-36) 286 (+40) 262 (-16)	241 (+9.6)	

Metal-to-ligand-charge-transfer (MLCT) is observed at low energies if the metal is reducing and the ligand offers a low-lying empty orbital. Metal complexes of Rh^{II}, Pt^{II}, Ag^{I} and Cu^{I} ions coordinated to conjugated ligands, such as bpy and phen, are the type of complexes where MLCT is observed.[205] In this work, only Ag^{I} and Cu^{I} complexes were formed from enantiomerically enriched samples of the cyclophane **1**, and their chiroptical properties will be discussed in the section.

There are some noticeable changes when **1** complexes with Ag(OTf). Both UV and CD spectra show slight bathochromic shifts at the α band transition, and the Cotton effect at 230 nm is missing in the silver(I) complex **80**. An additional bathochromic shift is observed in the CD spectra at the β transition, too. The intensity of the peak at 271 nm is markedly increased compared to the host cyclophane **1**. Signs of the Cotton effects at the α region are identical to the ones observed in **1**. The complex derived from (*S*)-**1** has Cotton effect with a positive sign at the longer wavelength: λ_{ext} 286 Δε +8.7, and the negative sign at the next wavelength: λ_{ext} 271 Δε

-7.5. Complementary Cotton effect is observed from the silver complex made from (*R*)-**1**: λ_{ext} 286 Δε -8.6 and λ_{ext} 271 Δε -9 (Figure 2.13).

The copper complex **81** also shows changes in its absorbances compared to the host molecule **1**. There is a slight bathochromic shift in the α region and hypsochromic shift in the *p* region in the UV spectra. It should be noted that Cotton effect in the β region collapses, and there is an additional Cotton effect observed at 309 nm (Δε +27) for (*R*)-**81** and (Δε -36) for the (*S*)-**81**. CD absorptions have a blue shift in the α region, which makes their pattern of absorption similar to that of the host. The Cotton effect in the *p* region shows up in the longer wavelength, at 241 nm, with lesser intensity than either **80** or the host cyclophane. All UV and CD spectra are summarized in (Table 2.13).

A set of empirical trends can be established after analyzing CD spectra of **1** and its metal complexes **80** and **81**.

- The cyclophane and its metal complexes derived from (*R*)-spirobiindanol have Cotton effect with a negative sign around 286 nm and Cotton effect with a positive sign at the next lower wavelength in the α region. On the other hand, (*R*)-spirobiindanol has a small Cotton effect with a positive sign at 286 nm.
- The cyclophane and its metal complexes derived from (*S*)-spirobiindanol have Cotton effect with a positive sign around 286 nm and Cotton effect with a negative sign at the next lower wavelength in the α region. On the

other hand, (*S*)-spirobiindanol has a small Cotton effect with a negative sign at 286 nm.

2.2.3.2 X-Ray Crystal Structures of Metal Complexes Made from Phenanthroline-based Cyclophane 1

X-ray crystal structures of silver(I), copper(I), and mercury(II) complexes of cyclophane **1** were resolved successfully. Unfortunately, crystals from palladium(II) and zinc(II) ions complexes, which are more structurally interesting, could not be grown even after numerous attempts.

X-ray quality crystals of **80** $[Ag(C_{35}H_{32}N_2O_2)(CH_3CN)^+][CF_3SO_3^-]\cdot C_4H_{10}O$ were grown by diethyl ether diffusion into an acetonitrile solution of the complex. These clear, light-sensitive crystals were used to solve and refine the structure of the complex. The quality of the results is a little lower than normal. This may, in part, be due to the nature of the crystal. Visual inspection of the crystals showed that many are intergrown with very shallow angles of intersection. The crystal used for data collection was cut carefully from a larger fragment while trying to avoid intergrowth regions. Nonetheless, the crystal still appears to be suffering from intergrowth or twinning to some extent. Analysis of the collected diffraction images by generating synthetic precession images showed a second weak reflection lattice in the *h*0*l* layer, which was oriented diagonally such that every 6^{th} or 7^{th} line of reflections in the *l* direction were overlapping with those of the lattice used to derive the data. This overlap has led to small errors in some reflection intensities and will therefore be affecting the quality of the results. This may be part of the reason for significant peaks of residual electron density near the Ag-atoms, and also the distorted atomic displacement ellipsoids for some of the atoms of the cations.

The compound crystallizes in a polar space group *P*1 and the structure is triclinic system. The absolute structure has been determined (*S*) [Flack's x = 0.06(2)]. The asymmetric unit contains two Ag-complex cations, two disordered triflate anions, and probably two disordered diethyl ether molecules (Figure 2.14). The conformations of the two symmetry-independent cations are generally quite similar and almost superimposable, except for the region about one O-atom and its neighboring benzyl ring. A twist of approximately 160° about the C(1)–C(2) bond in cation A produces the conformation of cation B [serendipitously, the atoms have been numbered the other way around in cation B, so O(1) in cation A corresponds with O(42) in cation B]. This brings O(42) in cation B inside the Ag coordination sphere with Ag(2)–O(42) = 2.870(4). The corresponding distance in cation A is Ag(1)···O(1) = 4.367(5) Å. The other relevant distances are: Ag(1)···O(2) = 3.485(5) and Ag(2)···O(41) = 3.987(5) Å.

The coordination sphere of Ag also includes two nitrogens from phenanthroline and one nitrogen molecule from acetonitrile. For the complex with cation A, the sum of three bond angles around Ag with nitrogens is 350 °; therefore, the coordination of Ag is a distorted trigonal planar. The nitrogen from acetonitrile is bound to silver(I) metal center most tightly with shortest bond length as shown in Table 2.14. Ag--N distances (2.308(5) Å, 2.326(4) Å) between silver(I) and nitrogen from phenanthroline are similar to the normal range found in other structurally similar silver(I)-complexes.[206-208] The complex with cation B has additional oxygen O(42) in the coordination sphere of Ag; therefore, the geometry around Ag is a very distorted

tetrahedral. With silver metal ion occupying the cavity of the cyclophane, spirobiindane unit has been pinched down, which flattens the whole cyclophane structure. The distance between two hydroxy groups has been decreased to 6.37 Å from 7.11 Å of the host **1**. The torsional angle around the quaternary carbon C(20)--C(21)--C(31)--C(26) = 108.6(4) °; which is slightly more twisted than the uncomplexed host molecule **1** (torsional angle = 105.8 (1) °). The distance between nitrogen from phenanthroline to the quaternary carbon of **6** has increased to 6.03 Å from 5.56 Å of the host molecule.

The disorder of the ether molecules could not be modeled adequately although the backbone for one molecule could be distinguished. Therefore, the contribution of the ether molecules to the intensity data was removed by using the *SQUEEZE* routine of the *PLATON* program. Omission of the ether molecule leaves one cavity of 276 $Å^3$ per unit cell. The number of electrons contributing to each void in the structure was calculated by the *SQUEEZE* routine to be approximately 109 e. Allowing for two ether molecules per cavity yields 84 e and this was used in the subsequent calculation of the empirical formula, formula weight, density, linear absorption coefficient and *F*(000). Each symmetry-independent triflate anion is disordered over two orientations, which were modeled successfully.

Table 2.14 Selected Interatomic Distances (Å) and Angles (deg) for [Ag(**1**)](OTf) **80**.

Distance			
With Cation A		**With Cation B**	
Ag(1)–N(3)[a]	2.144(5)	Ag(2)–N(43)[a]	2.197(7)
Ag(1)–N(2)	2.308(5)	Ag(2)–N(42)	2.293(6)
Ag(1)–N(1)	2.326(4)	Ag(2)–N(41)	2.323(5)
		Ag(2)···O(42)	2.870(4)
Angles			
N(3)[a] –Ag(1)–N(2)	146.5(2)	N(43)[a]–Ag(2)–N(42)	155.2(2)
N(3)[a] –Ag(1)–N(1)	131.0(2)	N(43)[a]–Ag(2)–N(41)	131.5(2)
N(2)–Ag(1)–N(1)	73.3 (2)	N(42)–Ag(2)–N(41)	72.9(2)
		N(42)–Ag(2)–O(42)	64.2(2)

a) Nitrogen from acetonitrile.

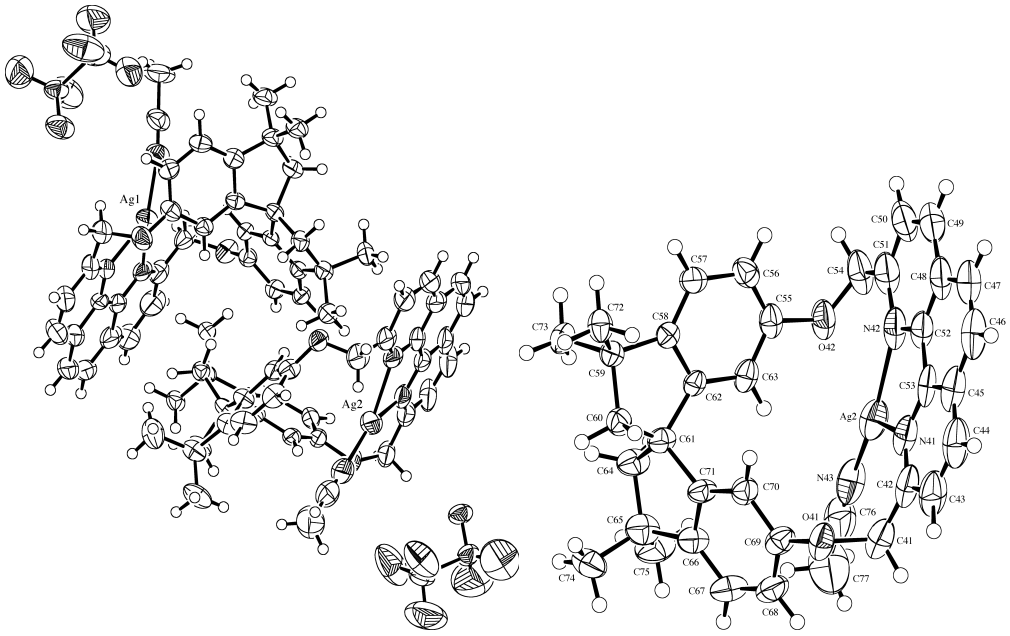

(a) (b)

Figure 2.14. (a) *ORTEP*[202] representation of **80** with both first and second Ag^+ ions and counter anions (50% probability ellipsoids; H-atoms given arbitrary displacement parameters for clarity). (b) *ORTEP*[202] representation of **80** with the second Ag^+ ion. (50% probability ellipsoids; H-atoms given arbitrary displacement parameters for clarity)

Another set of X-ray-crystallography data was obtained from the silver complex **80** made with racemic cyclophane **1**. This time, crystals were grown from 1:1-chloroform: nitromethane solvent system as clear solids. In the absence of more coordinating solvent, such as acetonitrile, the counter anion, triflate, is still within the coordination sphere of the silver(I) ion. The distance between Ag—O(12) is 2.29 Å, which is shorter than Ag—N distances (2.34 Å and 2.33 Å). One of the aromatic rings from **6** is also in close proximity to the metal cation. The intermolecular distances between Ag(1)···C(7) and Ag(1)···C(6) are 2.73 Å and 3.04 Å, respectively. Therefore, the olefin from the ring participates in η^2 coordination to the silver ion, making the geometry of Ag (I) coordination a pseudo-tetrahedral.

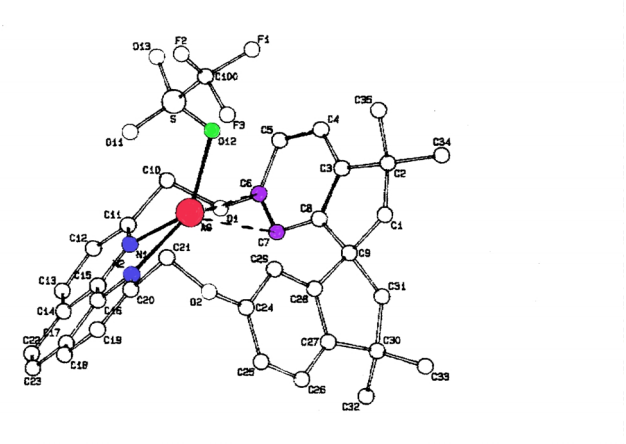

Figure 2.15 Additional ORTEP[202] of [Ag(*rac*)-(**1**)](OTf) **80**.

The structure of **81** $[Cu(C_{35}H_{32}N_2O_2)(CH_3CN)^+][PF_6^-]\cdot 0.5CH_3CN\cdot 0.5C_4H_{10}O$ was solved and refined successfully. The X-ray quality clear yellow crystals were prepared by diethyl ether diffusion into an acetonitrile solution of the complex. Both solvents are incorporated into the crystal lattice. The compound crystallizes in a polar space group *C*2 with Z = 4 and in monoclinic crystal system. The absolute structure has been determined (*R*) [Flack's x = -0.003(11)]. The asymmetric unit contains one three-coordinate Cu-complex cation, one PF_6^- anion, one site for an acetonitrile molecule that is approximately 50% occupied, and one half of a diethyl ether molecule which is highly disordered and sits across a two-fold axis (Figure 2.16).

The disorder of the ether molecule was so severe that it could not be modeled adequately. Therefore, the contribution of the ether molecules to the intensity data was removed by using the *SQUEEZE* routine of the *PLATON* program. This procedure made it unnecessary to include any ether atoms in the model and produced satisfactory refinement results for the structure of the remaining moieties, with R-factors similar to those obtained from attempts to model the ether molecule. Omission of the ether molecule leaves two cavities of 245 $Å^3$ per unit cell, which are located about two-fold axes. The number of electrons contributing to each void in the structure was calculated by the *SQUEEZE* routine to be approximately 53 e. Allowing for one ether molecule per cavity yields 43 e, which is a fair approximation and was used in the subsequent calculation of the empirical formula, formula weight, density, linear absorption coefficient and *F*(000). The atomic displacement parameters of the F

atoms of the PF_6^- anion are significantly elongated, as is often observed for this anion. No attempt has been made to define a disordered model for this anion.

The coordination of nitrogens around Cu is tighter than it was around the silver ion. The nitrogen from acetonitrile, N(3), forms the tightest bond with Cu. Notably, the distance between O(1)…O(2) of spirobiindane backbone was increased to 7.35 Å from 6.37 Å of **80**. The torsional angle around the quaternary carbon C(21) is 111.5 (3) °, which is bigger than both **1** and silver(I) complex **80**. The phenanthroline unit and spirobiindane unit were brought closer together (average distance between nitrogen to C(21) is 5.75 Å) than they were in **80**.

Interatomic distances between copper and nitrogen from phenanthroline range from 2.027 to 2.035 Å, which is slightly longer than the calculated Cu--N distances (1.942 to 1.966 Å) between copper and chiral bisoxazoline ligands studied by Fraile.[209] However, the Cu--N distances from the complex **81** are similar to the Cu--N distances (2.002 Å to 2.036 Å) of Zelewsky[210]'s pseudotetrahedral copper(II)-complexes with chiral pinene-[5,6]-bipyridine ligands. Compared to the widely used chiral auxiliary, such as bisoxazoline, the cyclophane **1** forms a bigger host pocket space for the copper and the guest to occupy. Nitrogen from acetonitrile interacts most closely with the copper ion with Cu--N distance of 1.848 Å. Essentially, acetonitrile may compete against other substrates for the coordination site on the copper ion, reducing its effectiveness as an asymmetric catalyst.

Table 2.15 Selected Interatomic Distances (Å) and Angles (deg) for [Cu(*R*)-(**1**)](PF$_6$) **81**.

Distances		**Angles**	
Cu–N(3)	1.848(3)	N(3)–Cu–N(2)	140.9(1)
Cu–N(2)	2.027(3)	N(3)–Cu–N(1)	135.6(1)
Cu–N(1)	2.035(3)	N(2)–Cu–N(1)	82.3(1)

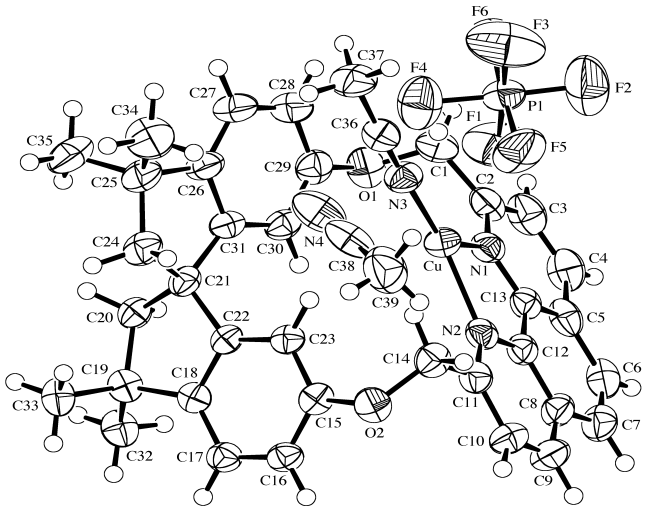

Figure 2.16 ORTEP[202] representation of **81** (50% probability ellipsoids; H-atoms given arbitrary displacement parameters for clarity).

Racemic crystals of **82** [$Hg(C_{35}H_{32}N_2O_2)I_2$] were obtained from hexanes vapor diffusion into the complex dissolved in dichloromethane. These clear, yellow crystals were used to solve and refine the structure of the molecule with no unusual features. The crystal system is triclinic and the space group is centrosymmetric *P*1 with Z = 2; therefore, the crystals are racemic. There are no solvent molecules incorporated in the crystal lattice. The unit cell contains cyclophane **1**, Hg(II) metal ion, and two iodide units (Figure 2.17). In general, mercury(II) is situated further way from the cyclophane than either **80** or **81**. Also, the metal interacts more closely with one of the nitrogens on phenanthroline than the other, as shown by the different Hg—N distances (Table 2.16). The cyclophane **1** is bent downward, making an upside down U-shape. Two iodides are sticking up like two rabbit ears above the plane of the cyclophane.

The mercury(II) complex has a pseudo-tetrahedral structure. Smaller halogens, such as chloro and bromo complexes have been shown to form centrosymmetric dinuclear molecules with two bridging halogen ligands.[211] Bigger radius of the iodo groups and sterically compact structure of the cyclophane allow complexation with one mercury atom. The Hg—I distances-- Hg--I(1) = 2.6263 (5) Å; Hg--I(2) = 2.6728 (6) Å--are shorter than what was found in molecular HgI_2, which is 2.78 Å. The distance is longer than 2.61 (2) Å found in Vezzosi's mercury(II) complex.[212] The distance between two hydroxy groups is 7.19 Å, and the average distance from nitrogen of phen to the quaternary carbon C(21) is about 5.9 Å. The dimension of the cyclophane is closer to the host molecule **1**.

The tetrahedral coordination around the mercury ion is very distorted. The bite angle is very small, 67.2 (2)°, and the angle between two iodo groups is unusually wide I(1)--Hg--I(2) = 131.92 (2) °. Two angles, N(1)–Hg–I(2) = 96.8(1) ° and N(2)–Hg–I(2) = 92.3(1) °, are closer to being perpendicular. Looking down from the longest bond Hg—I(2), the coordination around mercury(II) also resembles trigonal pyramidal geometry.

Table 2.16 Selected Interatomic Distances (Å) and Angles (deg) for [Hg(**1**)I_2] **82**.

Distances			
Hg–N(1)	2.451(5)	Hg–I(1)	2.626(5)
Hg–N(2)	2.541(5)	Hg–I(2)	2.673(6)
Angles			
N(1)–Hg–N(2)	67.2(2)	N(1)–Hg–I(2)	96.8(1)
N(1)–Hg–I(1)	123.0(1)	N(2)–Hg–I(2)	92.3(1)
N(2)–Hg–I(1)	125.7(1)	I(1)–Hg–I(2)	131.92(2)

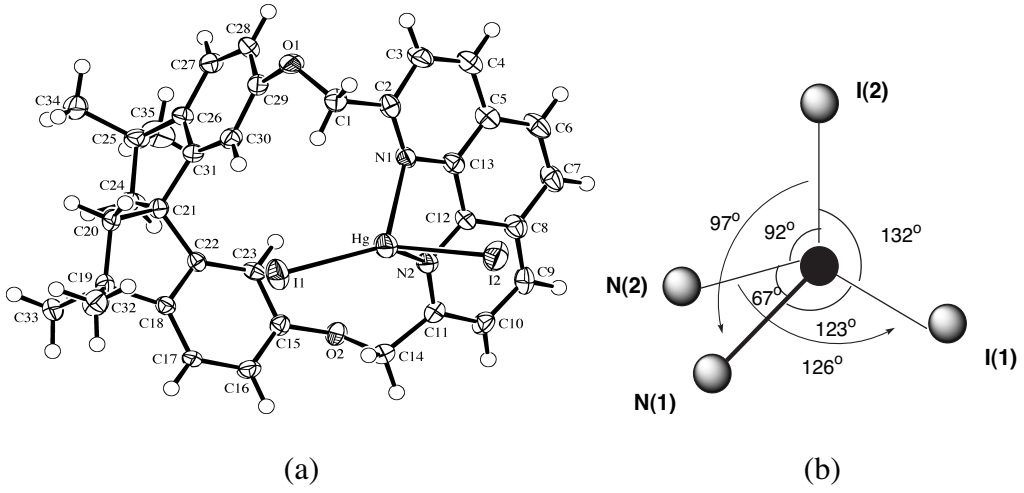

(a) (b)

Figure 2.17 (a) ORTEP[202] representation of **82** (50% probability ellipsoids; H-atoms given arbitrary displacement parameters for clarity). (b) Co-ordination polyhedron of Hg^{II}.

The cyclophane **1** is found to be a very versatile host molecule, which can coordinate many small metal ions. These metal complexes may be stabilized by

participation from solvent molecules, interactions with counter anions, or even the aromatic ring or bridging oxygen from the cyclophane itself. X-ray crystal structures of metal complexes suggest that even though the cyclophane is structurally rigid, the ether bridges between spirobiindanol and phenanthroline subunits allow some flexibility. Additionally, X-ray crystallographic study of metal complexes confirmed the absolute configuration of spirobiindanol, which had been determined by CD.

2.2.4 Metal Complexes of 2

Enantiomerically enriched chiral cyclophane **2** was used to make metal complexes **85**—**86** with Ag(OTf) and $[Cu(CH_3CN)_4](PF_6)$. The cyclophane should prevent two coordinating phenanthroline units from separation while they are complexed to a given cationic species in a distorted tetrahedral geometry.[213] Unlike Sauvage's catenates-30,[214] silver(I) complex of **2** was more reducible in the presence of light. The copper(I) complex was more readily oxidized to the copper(II) structures, as shown by the loss of defined peaks in NMR after being exposed to the air for a few days. Thus, the metal complexes of the cyclophane **2** behave more like the acyclic analogue of the catenate, which is the metal complexes of two equivalents of 2,9-di-*p*-anisyl-1,10-phenanthroline.

Many copper(I) complexes of either methyl or phenyl substituents at 2- and 9-positions on phen are known to undergo photo-induced metal-to-ligand charge transfer (MLCT)[215-217] and their excited states have lifetimes of ~70—250 ns in dichloromethane solution.[217-219] It was found recently that the pristine $[Cu(phen)_2]$ can be weakly luminescent in the solid state,[220] but the copper(I) complex of the **2** displayed no phosphorescence even though its phen has 2- and 9- substituents.

Chemical shift changes in NMR spectra of metal complexes show that coordinations to metal ions have major impacts on both chemical and structural environments of the cyclophane **2** (Table 2.17). Coordination to silver(I) or copper(I) ion causes protons at the CH_2—O bridge of the cyclophane to be separated and shifted upfield in different degrees. In the free ligand **2**, both protons H_e and H_f appear as a

singlet in dichloromethane due to accidental isochrony of the diastereotopic protons.[64] Complexations with metal ions force the cyclophane **2** to be locked in a more rigid conformation, which sets each geminal proton in very different chemical environments. The upfield shift[126] is especially pronounced in the proton H_e of [Cu(**2**)](PF_6) **86**, which was shifted by Δδ 1 ppm. The observation suggests that geminal protons, H_e and H_f, lie in the shielding region of the phenanthroline subunit of the cyclophane, which indicates that the whole cyclophane structure is helically twisted. The degree of changes in the corresponding protons of the silver(I) complex **73** is smaller, probably due to the larger radius of the silver ion, which would distort the structure of the cyclophane to lesser degree.

Protons H_g through H_i from the phenyl rings of the spirobiindanol unit on **85** are affected by the presence of the cationic metal in a larger degree. All three protons were shifted upfield in the range from Δδ 0.7 to Δδ 1.2 ppm. Similar upfield shift pattern is observed in **86**, but in smaller degree. Proton H_k of **86** is shielded upon complexation to the cationic metal. As expected, other protons on phenanthroline portion of the cyclophane are deshielded because their electron density is pulled away by the electron-deficient copper metal center. Lastly, isotope distributions from mass spectra also show the coordination of both silver(I) and copper(I) ion on the host molecule **2**.

Table 2.17 Selected ^{1}H NMR peak assignments of **2** and its metal complexes [Ag(**2**)](OTf) **85** and [Cu(**2**)](PF_6) **86**.

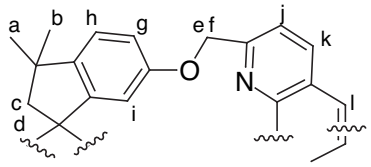

Compound	H_e	H_f	H_g	H_h	H_i	H_j	H_k	H_l
85	4.81	5.32	6.05	6.43	5.36	8.07	8.57	8.07
86	4.38	5.04	6.47	6.75	5.69	8.11	8.18	8.64
2	5.35	5.35	6.96	7.16	6.57	7.90	8.26	7.68

^{1}H NMR was taken in CD_2Cl_2, in 400 MHz NMR. All ppm values were referenced to dichloromethane at 5.32 ppm.

2.2.4.1 CD and UV Spectra of 85 and 86

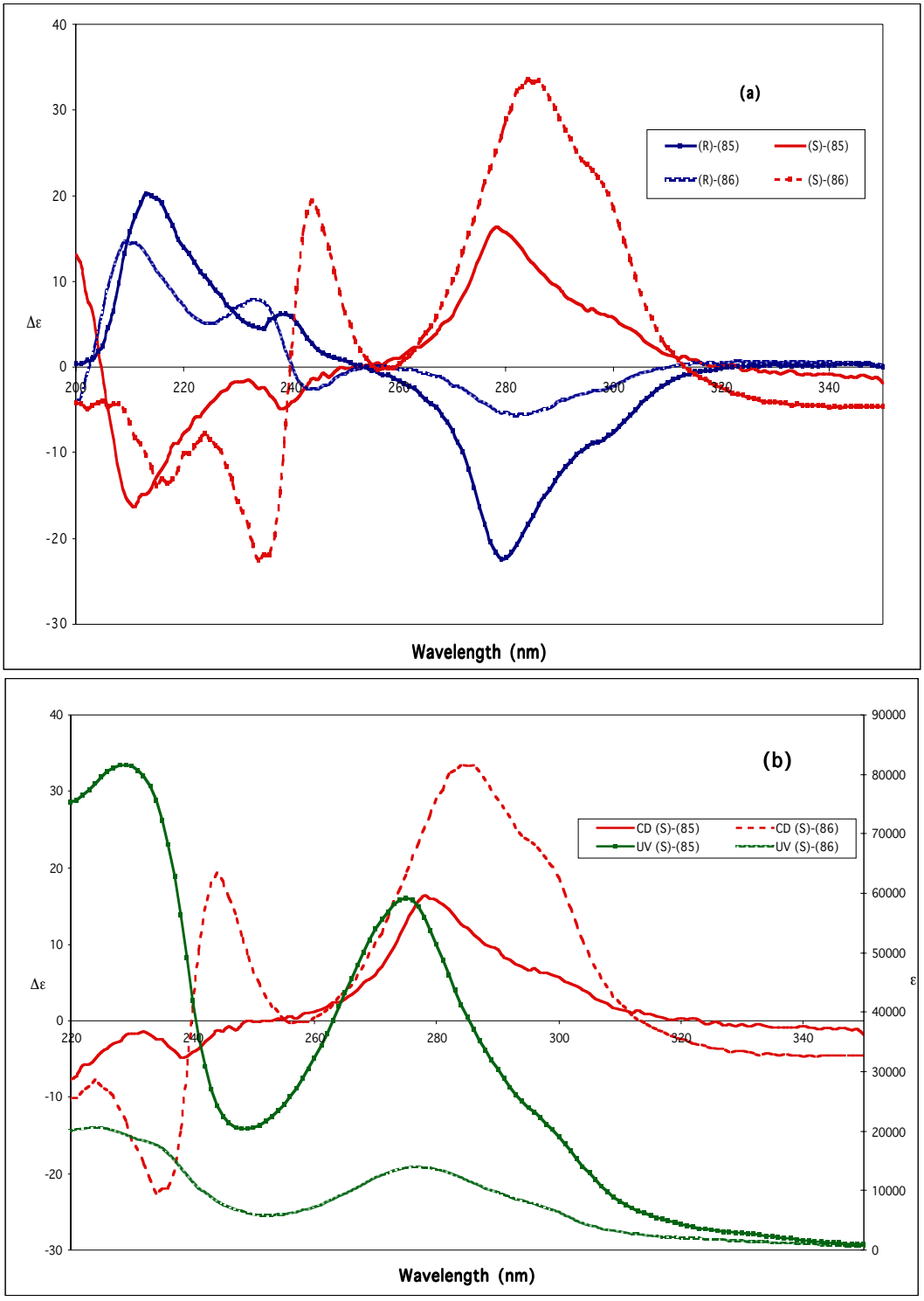

Figure 2.18 (a) CD spectra of [Ag(**2**)](OTf) **85** and [Cu(**2**)](PF_6) **86** in CH_3CN. (b) CD and UV spectra of (*S*)-**85** and (*S*)-**86** in CH_3CN.

Upon complexation with metals, such as Ag(OTf) and $[Cu(CH_3CN)_4](PF_6)$, once structurally flexible compound **2** takes a distinct shape, and CD spectra of **85** and **86** become better defined (Figure 2.18). The UV spectra of the silver(I) complex **85** show a red shift at α region and blue shift at *p* region. The CD spectra of **85** are marked by the disappearance of the Cotton effect around 225 nm. Instead, the amplitude of the Cotton effect at 278 nm is increased drastically (Δε +16 for (*S*)-**85**; Δε -22 for (*R*)-**85**). Other complementary Cotton effects appear at 238 nm (Δε -4.8 for (*S*)-**85**; Δε +6.2 for (*R*)-**85**) and 211 nm (Δε -16 for (*S*)-**85**; Δε +20 for (*R*)-**85**) (Table 2.18).

The copper(I) complex **86** displays similar changes as **85** in UV spectra, which are a bathochromic shift at α region and a hypsochromic shift at *p* (Table 2.18). In solution, $[Cu(dmp)_2]^+$ complex exhibits a CT absorption maximum at 457 nm. In a more bulky complex of dnnp, the absorption is blue shifted to 445 nm. In the complex **86**, the absorption appears in lower wavelength at 440 nm; however, no interesting Cotton effects were observed in CD around that region.

Over all, better-defined CD spectra were obtained for copper(I) complex **86** than the host molecule **2**. The major Cotton effect appears at 284 nm, which looks as prominent as the absorption at 278 nm for **85**. There is an additional Cotton effect at 244 nm, which was absent in the CD of silver(I) complex. Lastly, unlike **85** and the host molecule **2**, the absorption at the *β*-region is absent in the copper complex.

Table 2.18 CD and UV Spectra of **2** and Metal Complexes **85** and **86**.

Compd	**Solv.**	**UV** α	$\lambda_{m\mu}$ (ε) P	β	**CD** α	$\lambda_{m\mu}$ ($\Delta\varepsilon$) P	β
(*R*)-(+)-**2**	CH_3CN	271 (25000) 320 (1200)	229 (43000)		264 (-13.8)	237 (+21) 225 (-5.8)	212 (+51)
(*S*)-(-)-**2**	CH_3CN				267 (+15.5)	237 (-7) 229 (+5.5)	212 (-60)
(*R*)-**85**	CH_3CN	275 (59000)	229 (82000)		278 (-22)	238 (+6.2)	213 (+20)
(*S*)-**85**	CH_3CN				278 (+16)	238 (-4.8)	211 (-16)
(*R*)-**86**	CH_3CN	277 (14000) 440 (1000)	224 (21000)		284 (-5.5)	244 (-2.5) 234 (+8)	
(*S*)-**86**	CH_3CN				284 (+33.5)	244 (+19.4) 234 (-22.5)	

Another set of empirical trends can be established after analyzing CD spectra of **2** and its metal complexes.

- Cyclophanes derived from (*R*)-spirobiindanol: The longest wavelengths (264 nm – 284 nm) of the cyclophane and its metal complexes have Cotton effects with a negative sign in the α region. On the other hand, (*R*)-spirobiindanol has a small Cotton effect with a positive sign at 286 nm. The absorption around 230 nm in *P* region has Cotton effect with a positive sign.
- Cyclophanes derived from (*S*)-spirobiindanol: The longest wavelengths (264 nm – 284 nm) of the cyclophane and its metal complexes have Cotton effects with a positive in the α region. On the other hand, (*S*)-spirobiindanol has a small Cotton effect with a negative sign at 286 nm. The absorption around 230 nm in *P* region has Cotton effect with a negative sign.

- It is interesting to note that the copper complexation makes the Cotton effect at β region disappear for metal complexes made from both **1** and **2**.

2.2.4.2 X-Ray Crystal Structures of (*S*)-86

X-ray quality crystals of the silver complex **85** could not be obtained even after numerous attempts. However, dark-orange crystals of **86** $[Cu(C_{70}H_{64}N_4O_4)^+][PF_6^-]\cdot 2C_6H_6$ were prepared by benzene vapor diffusion into a dichloromethane solution of the copper complex. The compound crystallizes in a polar space group $P2_12_12_1$, with Z = 4, and in orthorhombic system. The absolute structure has been determined to be (*S*) [Flack's x = -0.016(10)]. The asymmetric unit contains one four-coordinate Cu-complex cation, one disordered PF_6^- anion, and two disordered benzene molecules (Figure 2.19). Two positions were defined for each F^- atom of the anion with the major orientation of the PF_6^- octahedron being present in approximately 78 % of the anions. Two orientations were defined for each of the two independent benzene molecules with occupancies of approximately 62 and 59 % for the major orientations of each molecule. The pseudo-tetrahedral coordination of the complex deviates from the idealized D_{2d} symmetry.[221,222]

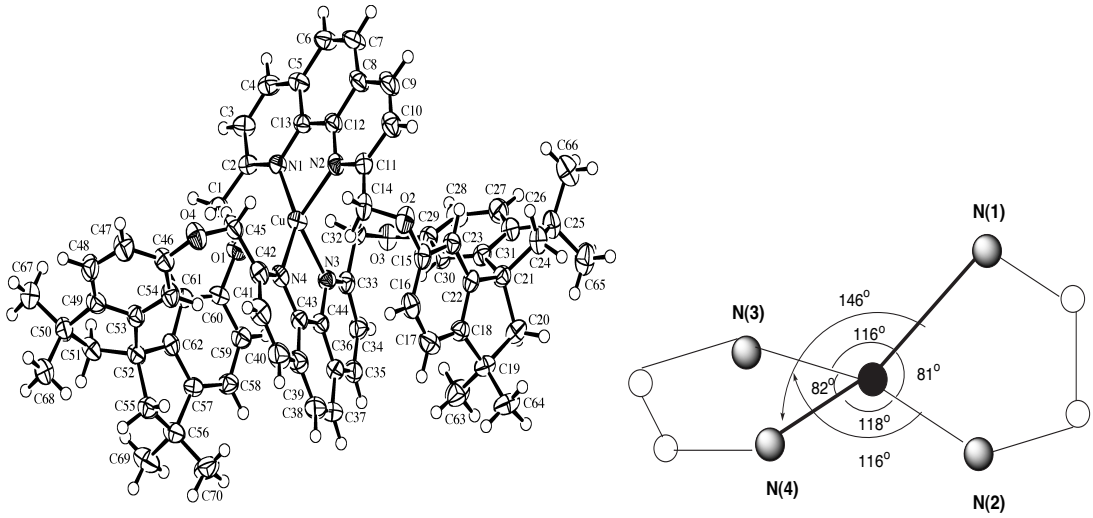

(a) (b)

Figure 2.19 (a) ORTEP[202] representation of (*S*)-**86** (50% probability ellipsoids; H-atoms given arbitrary displacement parameters for clarity) and (b) the co-ordination polyhedron of Cu^{I}.

Each orientation of the benzene molecules was refined as a rigid hexagon. Within the cation, atom O(1) lies 3.378(2) Å from the Cu-atom. Also one of spirobiindane backbones is more bent than the other because its two oxygen atoms are closer to each other (O(1)—O(4) 6.16 Å) than the distance between their complementary pair (O(2)—O(3) 6.91 Å). Benzene rings from **6** are also lying almost directly above aromatic rings of phenanthroline substituents. The interatomic distance between two aromatic groups can be as close as 3.45 Å and as far as 6.89 Å. It explains why protons from aromatic rings of **6** in the copper(I) complex **86** were shifted upfield in the ^{1}H NMR. These protons are shielded by the π-electron density from the ring current of the phenanthroline. Compared to the 'rectangular' shape of the host molecule **2**, the Cu(I) complex **86** has gone through a major structural distortion, becoming a helical molecule, surrounding the meal center.

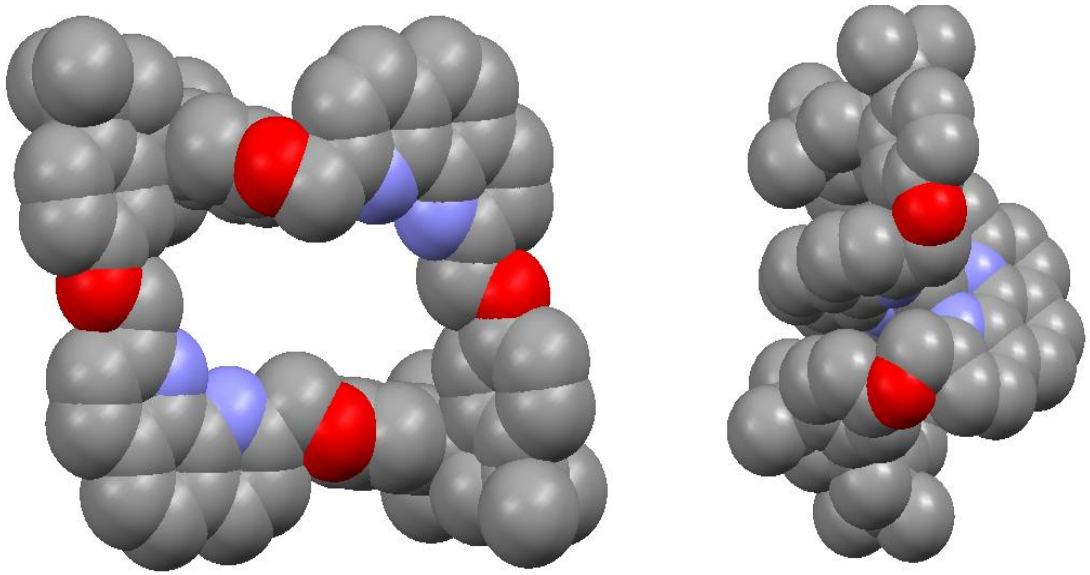

(a) **(b)**

Figure 2.20 a) Space-filled representation of the host cyclophane **2** (b) space-filled representation of **86**

The average chelate bite angle is 81.5 °, which is around a typical value for such phenanthroline complexes,[223-225] but other *trans* N—Cu—N angles range from 116 ° to 146 °, which deviate significantly from 90 ° of the idealized D_{2d} symmetry (Table 2.19). The apparent distortion around the copper(I) center is caused by phenanthroline units being covalently linked to bulky spirobiindanol units, which prevents two bidentate ligands from forming tighter coordination around the metal. However, the bulkiness of spirobiindanol also prevents other ligands from attaching to the metal center, in spite of the 'open' geometry around Cu^{I}. The Cu—N bond lengths range from 2.028 Å to 2.095 Å, which are close to values found in other tetrahedral copper(I) complexes of related ligands.[136.221.226.227]

Table 2.19 Selected Interatomic Distances (Å) and Angles (deg) for (*S*)-**86**.

Distances			
Cu–N(1)	2.028(3)	Cu–N(2)	2.095(3)
Cu–N(4)	2.029(3)	Cu–N(3)	2.093(3)
Angles			
N(1)–Cu–N(4)	145.6(1)	N(1)–Cu–N(3)	116.2(1)
N(1)–Cu–N(2)	81.4(1)	N(4)–Cu–N(3)	81.7(1)
N(4)–Cu–N(2)	118.4(1)	N(2)–Cu–N(3)	116.4(1)

Orientation angles, θ_x, θ_y, θ_z, of the (*S*)-**86** are 104.3 °, 100.1 °, and 99.2 °. It is noteworthy to point out that θ_x and θ_y are by far the largest ones reported[228]. The θ_z measurement indicates that the dihedral angle between the Cu—N(1)—N(2) and the Cu—N(4)—N(3) planes is not orthogonal. The coordination around the metal center has a very large rocking distortion, which should make the coordination closer to the trigonal bipyramidal geometry. However, no single Cu—N bond, which should move toward the axial position, is particularly longer than the other. Finally crystallographic data for metal complexes are summarized in Table 2.20.

Table 2.20 Crystallographic Data for metal complexes of cyclophanes.

	80	**81**	**82**	**86**
Empirical formula	$C_{42}H_{45}Ag$-$F_3N_3O_6S$	$C_{40}H_{41.5}Cu$-$F_6N_{3.5}O_{2.5}P$	$C_{35}H_{32}HgI_2N_2O_2$	$C_{82}H_{76}Cu$-$F_6N_4O_4P$
Crystal size (mm^3)	0.18 × 0.20 × 0.25	0.15 × 0.23 × 0.30	0.10 × 0.20 × 0.22	0.02 × 0.15 × 0.25
Crystal system	triclinic	monoclinic	triclinic	orthorhombic
Space group	$P1$ (#1)	$C2$ (#5)	$P\bar{1}$ (#2)	$P2_12_12_1$ (#19)
a (Å)	11.0040 (1)	24.2009 (7)	9.1738 (2)	14.1496 (2)
b (Å)	13.6737 (1)	11.3769 (4)	10.4862 (2)	17.9544 (3)
c (Å)	14.2536 (1)	14.4656 (5)	17.4758 (4)	27.6580 (5)
α (deg)	80.1155 (4)	90	89.3421 (7)	90
β (deg)	87.2178 (4)	95.645 (1)	84.2641 (7)	90
γ (deg)	66.8566 (4)	90	75.538 (1)	90
V ($Å^3$)	1942.38 (3)	3963.5 (2)	1619.57 (6)	7026.4 (2)
Z	2	4	2	4
D_X [g cm^{-3}]	1.513	1.374	1.983	1.314
$2\theta_{(max)}$ [deg]	55	50	55	50
Reflns collected	59044	27239	36884	65106
Unique reflns (R_{int})	17085 (0.050)	6936 (0.059)	7425 (0.086)	12335 (0.077)
Parameters refined; restraints	1077; 477	486; 1	384:0	1009; 510
$R(F)$ [$I>2\sigma(I)$ reflections],	0.0605,	0.0446	0.0447	0.0480
$wR(F^2)$	0.1778	0.1169	0.1158	0.1008
GOF	1.029	1.000	1.107	1.028

2.2.5 Metal Complexes of Bipy-based Cyclophanes

The silver(I) complex **87** and copper(I) complex **88** were synthesized from both enantiomers of **4**. Most protons in the ^{1}H NMR spectra show expected downfield shifts upon complexation with electropositive metal ions--copper(I) and silver(I). Protons in the bpy moiety of the [Cu(**4**)](PF$_6$) **88** are more deshielded than protons attached to the Ag^I-complex **87**, due to the tighter binding of the ligand to copper(I) caused by higher ligand field of Cu ion.[229] For instance, it is known that the formation constant for Ag(bpy)$^+$ is much lower than that for Cu(bpy)$_2^+$.[229.230] Just like phen-based cyclophanes **1**, the proton H$_i$ in Cu-complex is more shielded than the corresponding proton in the host molecule **4**. Data from mass spectra indicates the expected isotope distribution for each silver(I) and copper(I) complexes **87** and **88**.

Table 2.21 Selected ^{1}H NMR Peak Assignments of **4** and its metal complexes [Ag(**4**)](OTf) **87** and [Cu(**4**)](PF$_6$) **88**.

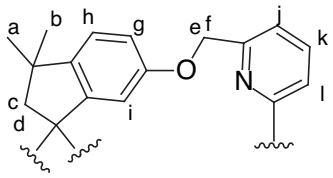

Compound	H$_e$	H$_f$	H$_g$	H$_h$	H$_i$	H$_j$	H$_k$	H$_l$
4[a]	5.14	5.34	6.73	7.03	6.71	7.43	7.82	7.51
87[b]	5.14	5.34	6.88	7.17	7.10	7.68	8.03	8.03
88[a]	5.26	5.49	6.83	7.09	6.54	7.87	8.15	8.21

a) ^{1}H NMR was taken in CD$_3$CN in 400 MHz NMR. All ppm values were referenced to TMS at 0 ppm.
b) ^{1}H NMR was taken in CD$_2$Cl$_2$, in 400 MHz NMR

Metal complexes of **5** behave very similar to metal complexes of phenanthroline-derived cyclophane **2**. Two bidentate bpy ligands are known to from a pseudotetrahedral coordination around copper(I) center.[126.221.231] Unfortunately, X-ray quality crystals of these complexes could not be obtained. However, X-ray crystal

structure from the analogous compound **86** is very helpful in understanding the physical data obtained from bpy-based cyclophane metal complexes **89** and **90**.

Table 2.22 Selected ^{1}H NMR Peak Assignments of **5** and its metal complexes [Ag(**5**)](OTf) **89** and [Cu(**5**)](PF_6) **90**.

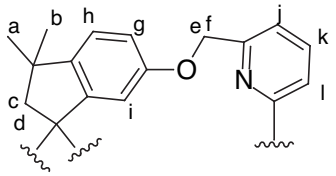

Compound	H_e	H_r	H_g	H_h	H_i	H_j	H_k	H_l
5[a]	5.05	5.16	6.68	6.87	6.14	7.32	7.74	8.20
89	4.49	5.05	6.30	6.75	5.61	7.82	8.11	8.13
90[b]	4.17	4.77	6.63	6.92	5.77	7.88	8.16	8.26

[a] ^{1}H NMR were taken in CD_2Cl_2, in 400 MHz NMR. All ppm values were referenced to dichloromethane at 5.32 ppm. [b] ^{1}H NMR were taken in CD_2Cl_2, in 500 MHz NMR. All ppm values were referenced to dichloromethane at 5.32 ppm

Coordination to copper(I) ion makes the cyclophane **5** more rigid and gives it a shaper peak signals on ^{1}H NMR. The geminal diastereotopic protons from methylene bridges, H_e and H_f, appear farther away ($\Delta\delta \sim 0.5$ ppm) from each other than they were in the free ligand. Both peaks are also shifted upfield ($\Delta\delta \sim 0.1—0.9$ ppm) (Table 2.22). The nearness of these protons to shielding cone of the heterocycles is the likely cause of the upfield shift and the greater manifestation of diasterotopism.[64] Protons from the bpy substituent, H_j--H_l, are deshielded due to their close proximity to electron-poor cationic metals, rather than because they are in *anti* conformation. Protons from the aromatic groups of the spirobiindanol unit, H_e through H_i, are shifted upfield. The observation suggests that the ring current from bpy unit influences phenyl rings in spirobiindanol. Lastly, mass spectra show the expected isotope distributions for all complexes.

2.2.5.1 CD and UV Spectra of 87 and 89

CD spectra of the silver(I) complexes 87 show complementary CE with lower amplitude values than were seen in phen-based cyclophanes. There is a problem with the observed absorptions. The (*R*)- and (*S*)-enantiomers show different CE around 210-230 nm range. There is a strong positive CE around 230 nm for (*R*)-87, but (*S*)-87 also has another CE around 210 nm, which is missing in the (*R*)-enantiomer. The copper(I) complexes showed inconsistent CD spectra, so they won't be discussed in the section.

Enantiomers of the silver(I) complex **89** shows CD absorptions at slightly different wavelengths. The overall shape of the CD absorptions shows that the enantiomeric pair has complementary Cotton effects. There is a strong CE absorption near 214 nm with $\Delta\varepsilon$ +25.1 for (*R*)-**89** and $\Delta\varepsilon$ -15.4 for (*S*)-**89**. The α-region has multiple splitting of CD absorptions, but no definite CE values could be determined. It is unfortunate because **89** has a strong UV absorption at 290 nm (ε 12336), so the α-region would have been the most likely area to look for an exciton coupling of chromophores.

CD spectra of the copper(I) complex **90** cannot be shown because inconsistent data was obtained. Many attempts to obtain copper(I) crystal of the bipyridine-based cyclophanes were futile. Katsuki[232] reported that the copper(I) complex of his chiral bipyridine ligand was not very stable.

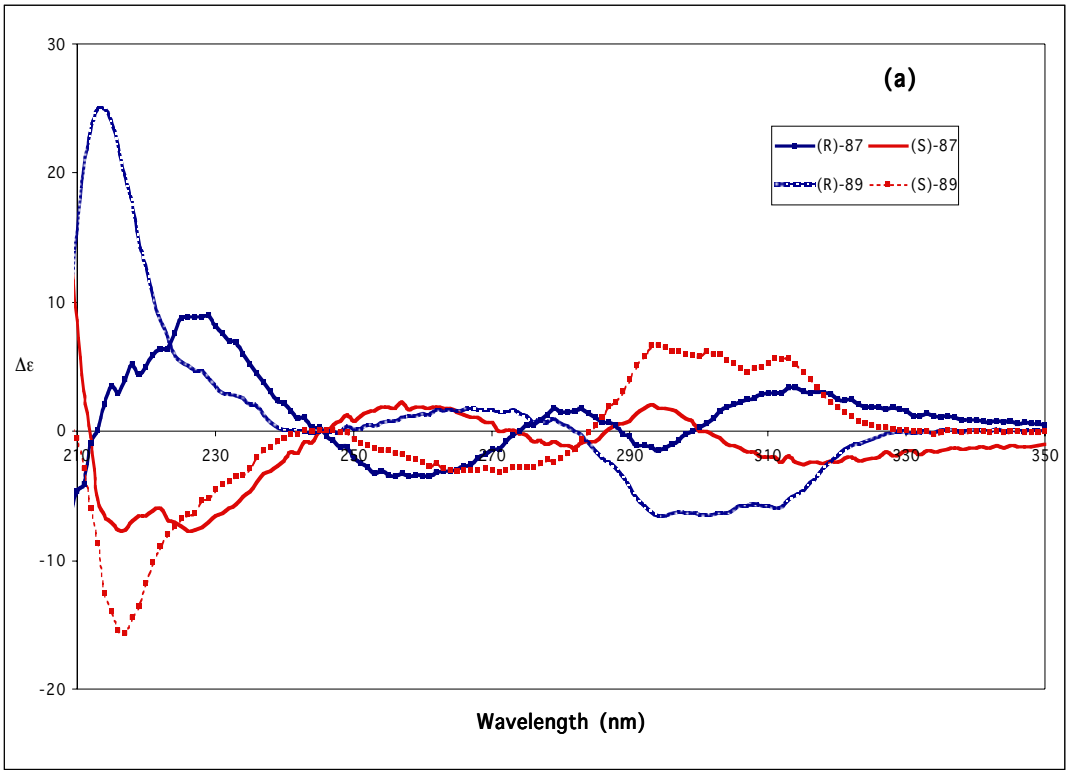

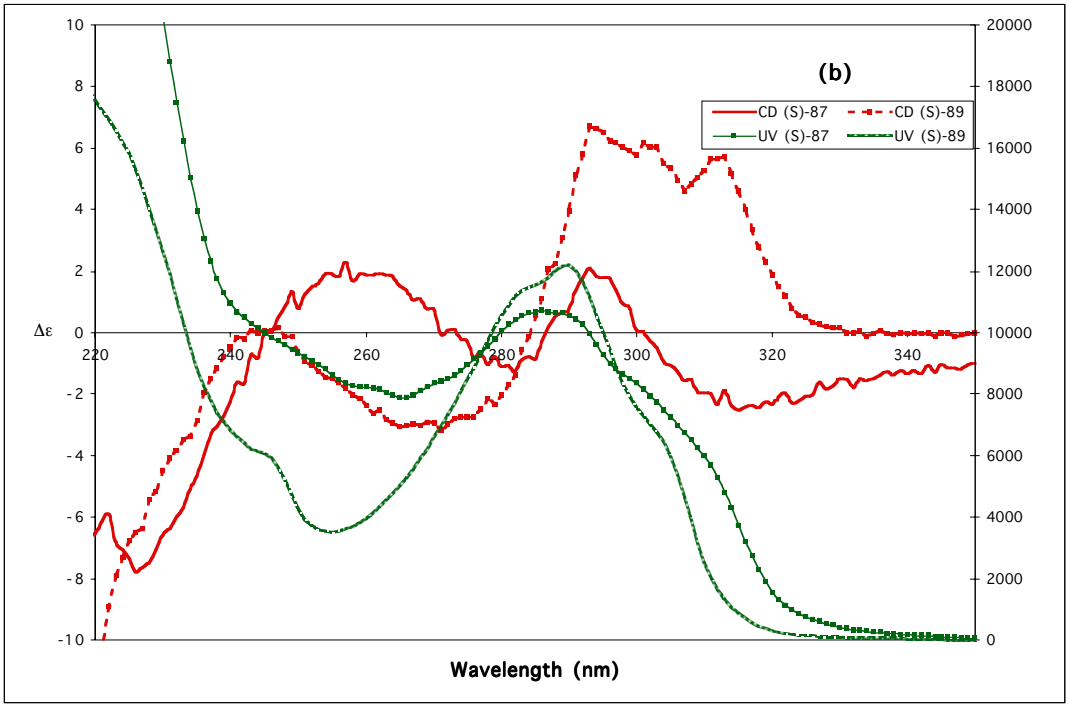

Figure 2.21 (a) CD spectra of [Ag(*S*)-(**4**)](OTf) **87** and [Ag(*S*)-(**5**)](OTf) **89** in CH_3CN. (b) CD and UV spectra of (*S*)-**87** and (*S*)-**89** in CH_3CN.

Table 2.23 CD and UV Spectra of Silver Complexes **87** and **89**

Compd	**Solv.**	**UV** $\lambda_{m\mu}$ (ε)			**CD** $\lambda_{m\mu}$ ($\Delta\varepsilon$)		
		α	*P*	β	α	*P*	β
(*R*)-**87**	CH_3CN	286 (11000)		----	294 (-1.4) 279 (+11.8) 258 (-3.4)	227 (+9)	215 (+9)
(*S*)-**87**	CH_3CN				293 (+2) 282 (-1.3) 257 (+2.3)	226 (-7.8)	216 (-7.6)
(*R*)-**89**	CH_3CN	290 (12000)			311 (-5.9) 302 (-6.5) 295 (-6.6) 273 (+1.7)	-----	214 (+25.1)
(*S*)-**89**	CH_3CN				313 (+5.7) 301 (6.2) 293 (6.7) 271 (-3.2)	-----	216 (-15.4)

2.3 Conclusion

Structure and properties of chiral cyclophanes **1** through **5** were studied by NMR, MS, CD and X-ray crystallography. NMR spectra of these cyclophanes have shown that monomeric cyclophanes **1** and **4** are sterically congested and very rigid. Bigger cyclophanes, **2**, **3**, and **5**, have more flexible structures, which allow more structural distortions. Circular Dichroism studies have shown that enantiomeric pairs of cyclophanes made from (*R*)- and (*S*)-spirobiindanol gave complementary Cotton effects.

X-ray crystal structures of metal complexes **80**--**82** of the cyclophane **1** show that the structurally rigid cyclophane will distort itself, even coordinating to a metal, in order to accommodate its guest metals. NMR spectra of metal complexes show that spirobiindane subunit may be too far from the metal coordinating site to transfer chiral information effectively to ligands attached to the metal. This may become problematic if the cyclophane **1** were to be used as an enantioselective catalyst. The X-ray structure of **86** showed two bidentate phen ligands coordinated to the copper metal center in a very distorted tetrahedral coordination. In spite of being very "open" in its coordination, steric bulkiness of spirobiindanol units stabilizes the copper(I) coordination vs. copper(II), which usually favors pentahedral or octahedral geometry around the metal center. The whole structure of the cyclophane becomes very helical and more defined upon coordination to metal centers.

2.4 X-Ray Crystallography Experimental

Definition of Terms

Function minimized: $\Sigma w(F_o^2 - F_c^2)^2$

Where $w = [\sigma^2(F_o^2) + (aP)^2 + bP]^{-1}$ and $P = (F_o^2 + 2F_c^2)/3$

$F_o^2 = S(C - RB)/Lp$

and $\sigma^2(F_o^2) = S^2(C + R^2B)/Lp^2$

S = Scan rate

C = Total integrated peak count

R = Ratio of scan time to background counting time

B = Total background count

Lp = Lorentz-polarization factor

R-factors: $R_{int} = \Sigma|<F_o^2> - F_o^2|/\Sigma F_o^2$ summed only over reflections for which more than one symmetry equivalent was measured.

$R(F) = \Sigma||F_o| - |F_c||/\Sigma|F_o|$ summed over all observed reflections.

$wR(F^2) = [\Sigma w(F_o^2 - F_c^2)^2/\Sigma w(F_o^2)^2]^{1/2}$ summed over all reflections.

Standard deviation of an observation of unit weight (goodness of fit):

$[\Sigma w(F_o^2 - F_c^2)^2/(N_o - N_v)]^{1/2}$

where N_o = number of observations; N_v = number of variables

Crystal Determination of 1. A crystal of $C_{35}H_{32}N_2O_2$, obtained from MeCN, was mounted on a glass fiber and used for a low-temperature X-ray structure determination. The unit cell constants and an orientation matrix for data collection were obtained from a least-squares refinement of the setting angles of 16875 reflections in the range $4° < 2\theta < 60°$. The mosaicity was 0.427 (1)°. A total of 350 frames were collected using ϕ and ω scans with κ offsets, 14 seconds exposure time and a rotation angle of 2.0° per frame, and a crystal-detector distance of 30.0 mm.

Data reduction was performed with *HKL Denzo* and *Scalepack*[233]. The intensities were corrected for Lorentz and polarization effects, and an absorption correction based on the multi-scan method[234] was applied. Standard reflection intensities were not monitored. The space group was determined from the systematic absences, packing considerations, a statistical analysis of intensity distribution, and the successful solution and refinement of the structure. Equivalent reflections were merged.

The structure was solved by direct methods using *SIR92*[235], which revealed the positions of all non-hydrogen atoms. The non-hydrogen atoms were refined anisotropically. All of the H-atoms were placed in geometrically calculated positions and refined using a riding model where each H-atom was assigned a fixed isotropic displacement parameter with a value equal to $1.2U_{eq}$ of its parent atom ($1.5U_{eq}$ for the methyl groups). Refinement of the structure was carried out on F^2 using full-matrix least-squares procedures, which minimized the function $\Sigma w(F_o^2 - F_c^2)^2$. The weighting scheme was based on counting statistics and included a factor to

downweight the intense reflections. Plots of $\Sigma w(F_o^2 - F_c^2)^2$ versus $F_c / F_c(\max)$ and resolution showed no unusual trends. A correction for secondary extinction was not applied.

Crystal Determination of 2. A crystal of $C_{70}H_{64}N_4O_4 \cdot 4CH_2Cl_2$, obtained from CH_2Cl_2, was mounted in oil on a glass fiber and used for a low-temperature X-ray structure determination. The unit cell constants and an orientation matrix for data collection were obtained from a least-squares refinement of the setting angles of 111337 reflections in the range $4° < 2\theta < 50°$. The mosaicity was 1.879 (2)°. A total of 500 frames were collected using ϕ and ω scans with κ offsets, 36 seconds exposure time and a rotation angle of 1.2° per frame, and a crystal-detector distance of 30.0 mm.

Data reduction was performed with *HKL Denzo* and *Scalepack* [233]. The intensities were corrected for Lorentz and polarization effects, and an absorption correction based on the multi-scan method[234] was applied. Standard reflection intensities were not monitored. The space group was determined from packing considerations, a statistical analysis of intensity distribution, and the successful solution and refinement of the structure. Equivalent reflections, other than Friedel pairs, were merged.

The structure was solved by direct methods using *SHELXS97* [235], which revealed the positions of all non-hydrogen atoms. The asymmetric unit contains one molecule of the macrocycle plus four molecules of dichloromethane. The non-

hydrogen atoms were refined anisotropically. All of the H-atoms were placed in geometrically calculated positions and refined using a riding model where each H-atom was assigned a fixed isotropic displacement parameter with a value equal to $1.2U_{eq}$ of its parent atom ($1.5U_{eq}$ for the methyl groups). Refinement of the structure was carried out on F^2 using full-matrix least-squares procedures, which minimized the function $\Sigma w(F_o^2 - F_c^2)^2$. The weighting scheme was based on counting statistics and included a factor to downweight the intense reflections. Plots of $\Sigma w(F_o^2 - F_c^2)^2$ versus $F_c / F_c(\max)$ and resolution showed no unusual trends. A correction for secondary extinction was applied. Refinement of the absolute structure parameter[236.237] yielded a value of -0.02(5), which confidently confirms that the refined coordinates represent the true enantiomorph.

Crystal Determination of 80. A crystal of $[Ag(C_{35}H_{32}N_2O_2)(CH_3CN)^+][CF_3SO_3^-]\cdot C_4H_{10}O$, obtained from MeCN / Et_2O, was mounted on a glass fiber and used for a low-temperature X-ray structure determination. All measurements were made on a *Nonius KappaCCD* area-detector diffractometer[2] using graphite-monochromated Mo $K\alpha$ radiation (λ = 0.71073 Å) and an Oxford Cryosystems Cryostream 700 cooler. The unit cell constants and an orientation matrix for data collection were obtained from a least-squares refinement of the setting angles of 98796 reflections in the range $4° < 2\theta < 55°$. The mosaicity was 0.634 (1)°. A total of 853 frames were collected using ϕ and ω scans with κ offsets, 50 seconds exposure

time and a rotation angle of 1.0° per frame, and a crystal-detector distance of 30.0 mm.

Data reduction was performed with *HKL Denzo* and *Scalepack* [233]. The intensities were corrected for Lorentz[238] and polarization effects, and an absorption correction based on the multi-scan method[234] was applied. Standard reflection intensities were not monitored. The space group was determined from packing considerations, a statistical analysis of intensity distribution, and the successful solution and refinement of the structure. Equivalent reflections, other than Friedel pairs, were merged.

The structure was solved by direct methods using *SIR92*[235], which revealed the positions of all non-hydrogen atoms. The asymmetric unit contains two cations, two disordered triflate anions, and probably two disordered diethyl ether molecules. The disorder of the ether molecules could not be modeled adequately, so the *SQUEEZE* routine[239] of the program *PLATON*[240] was employed. This procedure, which allows the disordered solvent molecules to be omitted entirely from the subsequent refinement model, gave satisfactory refinement results and there were no significant peaks of residual electron density to be found in the voids of the structure. The procedure leaves one cavity of 276 $Å^3$ per unit cell. The electron count in the disordered region was calculated to be 109 e per unit cell. Allowing for two ether molecules per cavity yields 84 e, and this estimate was used in the subsequent calculation of the empirical formula, formula weight, density, linear absorption coefficient and $F(000)$. Each symmetry-independent triflate anion is disordered over

two orientations. Two positions were defined for each atom of each anion. Refinement of constrained site occupation factors for the two orientations yielded values of 0.53(1) and 0.52(7) for the major conformations of anions 1 and 2, respectively. Extensive similarity restraints were applied to the chemically equivalent bond lengths and angles involving all disordered atoms from both anions. Furthermore, neighboring disordered atoms were restrained to have similar atomic displacement parameters and pseudo-isotropic restraints were applied to the disordered C- and O-atoms, which helped to maintain logical atomic displacement parameters for all of the disordered atoms.

The non-hydrogen atoms were refined anisotropically. All of the H-atoms were placed in geometrically calculated positions and refined using a riding model where each H-atom was assigned a fixed isotropic displacement parameter with a value equal to $1.2U_{eq}$ of its parent atom ($1.5U_{eq}$ for the methyl groups). Refinement of the structure was carried out on F^2 using full-matrix least-squares procedures, which minimized the function $\Sigma w(F_o^2 - F_c^2)^2$. The weighting scheme was based on counting statistics and included a factor to downweight the intense reflections. Plots of $\Sigma w(F_o^2 - F_c^2)^2$ versus $F_c / F_c(\max)$ and resolution showed no unusual trends. A correction for secondary extinction was applied. One reflection, whose intensity was considered to be an extreme outlier, was omitted from the final refinement. Refinement of the absolute structure parameter[236.237] yielded a value of 0.06(2), which confidently confirms that the refined coordinates, as listed in Table 2, represent the

true absolute structure. The two largest peaks of residual electron density are 2.01 and 1.48 e A^{-3} and lie within 1.0 Å of the Ag-atoms. The next largest peak is 0.78 e A^{-3}.

Neutral atom scattering factors for non-hydrogen atoms were taken from Maslen, Fox and O'Keefe[241], and the scattering factors for H-atoms were taken from Stewart, Davidson and Simpson[242]. Anomalous dispersion effects were included in F_c[243]; the values for f' and f'' were those of Creagh and McAuley[244]. The values of the mass attenuation coefficients are those of Creagh and Hubbel[245]. All calculations were performed using the *SHELXL97*[246] program

Crystal Determination of 81. A crystal of $[Cu(C_{35}H_{32}N_2O_2)(CH_3CN)^+][PF_6^-]\cdot 0.5CH_3CN\cdot 0.5C_4H_{10}O$, obtained from MeCN / Et_2O, was mounted on a glass fiber and used for a low-temperature X-ray structure determination. The unit cell constants and an orientation matrix for data collection were obtained from a least-squares refinement of the setting angles of 38895 reflections in the range $4° < 2\theta < 50°$. The mosaicity was 1.096 (2)°. A total of 207 frames were collected using ϕ and ω scans with κ offsets, 28 seconds exposure time and a rotation angle of 2.0° per frame, and a crystal-detector distance of 30.0 mm.

Data reduction was performed with *HKL Denzo* and *Scalepack* [233]. The intensities were corrected for Lorentz and polarization effects, and an absorption correction based on the multi-scan method[234] was applied. Standard reflection intensities were not monitored. The space group was determined from the systematic absences, packing considerations, a statistical analysis of intensity distribution, and the

successful solution and refinement of the structure. Equivalent reflections, other than Friedel pairs, were merged.

The structure was solved by direct methods using *SIR92*[235], which revealed the positions of all non-hydrogen atoms. . In addition to one cation and one anion, the asymmetric unit contains one partially occupied site for an acetonitrile molecule whose occupancy refined to 0.491(9), and one half of a diethyl ether molecule, which is highly disordered and sits across a two-fold axis. The disorder of the ether molecules could not be modeled adequately, so the *SQUEEZE* routine[239] of the program *PLATON*[240] was employed. This procedure, which allows the disordered solvent molecules to be omitted entirely from the subsequent refinement model, gave satisfactory refinement results and there were no significant peaks of residual electron density to be found in the voids of the structure. The procedure leaves two cavities of 245 $Å^3$ per unit cell, which are located about two-fold axes. The electron count in the disordered region was calculated to be 107 e per unit cell. Allowing for one ether molecule per cavity yields 43 e, and this estimate was used in the subsequent calculation of the empirical formula, formula weight, density, linear absorption coefficient and $F(000)$.

The non-hydrogen atoms were refined anisotropically. All of the H-atoms were placed in geometrically calculated positions and refined using a riding model where each H-atom was assigned a fixed isotropic displacement parameter with a value equal to $1.2U_{eq}$ of its parent atom ($1.5U_{eq}$ for the methyl groups). Refinement of the structure was carried out on F^2 using full-matrix least-squares procedures,

which minimized the function $\Sigma w(F_o^2 - F_c^2)^2$. The weighting scheme was based on counting statistics and included a factor to downweight the intense reflections. Plots of $\Sigma w(F_o^2 - F_c^2)^2$ versus $F_c / F_c(\max)$ and resolution showed no unusual trends. A correction for secondary extinction was applied. One reflection, whose intensity was considered to be an extreme outlier, was omitted from the final refinement. Refinement of the absolute structure parameter[236.237] yielded a value of -0.003(11), which confidently confirms that the refined coordinates represent the true absolute structure.

Crystal Determination of 82. A crystal of $[Hg(C_{35}H_{32}N_2O_2)I_2]$, obtained from CH_2Cl_2 / hexanes, was mounted on a glass fiber and used for a low-temperature X-ray structure determination. The unit cell constants and an orientation matrix for data collection were obtained from a least-squares refinement of the setting angles of 41892 reflections in the range $4° < 2\theta < 55°$. The mosaicity was 0.770 (2)°. A total of 361 frames were collected using ϕ and ω scans with κ offsets, 21 seconds exposure time and a rotation angle of 1.8° per frame, and a crystal-detector distance of 30.0 mm.

Data reduction was performed with *HKL Denzo* and *Scalepack* [233]. The intensities were corrected for Lorentz and polarization effects, and an absorption correction based on the multi-scan method[234] was applied. Standard reflection intensities were not monitored. The space group was determined from packing

considerations, a statistical analysis of intensity distribution, and the successful solution and refinement of the structure. Equivalent reflections were merged.

The structure was solved by direct methods using *SHELXS97* [246], which revealed positions of all non-hydrogen atoms. The non-hydrogen atoms were refined anisotropically. All of the H-atoms were placed in geometrically calculated positions and refined using a riding model where each H-atom was assigned a fixed isotropic displacement parameter with a value equal to $1.2U_{eq}$ of its parent atom ($1.5U_{eq}$ for the methyl groups). Refinement of the structure was carried out on F^2 using full-matrix least-squares procedures, which minimized the function $\Sigma w(F_o^2 - F_c^2)^2$. The weighting scheme was based on counting statistics and included a factor to downweight the intense reflections. Plots of $\Sigma w(F_o^2 - F_c^2)^2$ versus $F_c / F_c(\text{max})$ and resolution showed no unusual trends. A correction for secondary extinction was applied.

Crystal Determination of 86. A crystal of $[Cu(C_{70}H_{64}N_4O_4)^+][PF_6^-]\cdot 2C_6H_6$, obtained from CH_2Cl_2 / benzene, was mounted on a glass fiber and used for a low-temperature X-ray structure determination. The unit cell constants and an orientation matrix for data collection were obtained from a least-squares refinement of the setting angles of 279347 reflections in the range $4° < 2\theta < 50°$. The mosaicity was 1.214 (1)°. A total of 880 frames were collected using ϕ and ω scans with κ offsets, 120 seconds exposure time and a rotation angle of 0.6° per frame, and a crystal-detector distance of 41.5 mm.

Data reduction was performed with *HKL Denzo* and *Scalepack* [233]. The intensities were corrected for Lorentz and polarization effects, and an absorption correction based on the multi-scan method[234] was applied. Standard reflection intensities were not monitored. The space group was uniquely determined by the systematic absences. Equivalent reflections, other than Friedel pairs, were merged.

The structure was solved by direct methods using *SIR92* [235], which revealed the positions of all non-hydrogen atoms. The asymmetric unit contains one cation, one disordered anion, and two disordered benzene molecules. Two sets of F-atoms were defined for the anion and refinement of the site occupation factors led to an occupancy of 0.78(2) for the major orientation. Initially, the P–F and F···F distances were restrained tightly, so as to maintain octahedral geometry and uniform P–F bond lengths. This strategy kept the R-factor elevated, so all restraints were removed in the final refinement. The resultant geometry of the two disordered orientations of the anion is poorer with considerable variation in the lengths of the P–F bonds. However, the R-factor improved significantly, which also improves the precision of the geometric parameters of the cation. Two orientations were defined for each of the two independent benzene molecules and each orientation was refined as a rigid idealized hexagon. Refinement of the site occupation factors led to occupancies of 0.617(10) and 0.588(1) for the major orientations of each benzene molecule. The non-hydrogen atoms were refined anisotropically. All of the H-atoms were placed in geometrically calculated positions and refined using a riding model where each H-atom was assigned a fixed isotropic displacement parameter with a value equal to $1.2U_{eq}$ of its parent

atom ($1.5U_{eq}$ for the methyl groups). Refinement of the structure was carried out on F^2 using full-matrix least-squares procedures, which minimized the function $\Sigma w(F_o^2 - F_c^2)^2$. The weighting scheme was based on counting statistics and included a factor to downweight the intense reflections. Plots of $\Sigma w(F_o^2 - F_c^2)^2$ versus $F_c / F_c(\max)$ and resolution showed no unusual trends. A correction for secondary extinction was applied. Refinement of the absolute structure parameter[236.237] yielded a value of -0.016(10), which confidently confirms that the refined coordinates represent the true enantiomorph.

2.5 **X-Ray Crystal Structure Data**

Table 2.24 Crystal data and structure refinement for **6**

Identification code	amy31m	
Empirical formula	C25 H36 O4	
Formula weight	400.54	
Temperature	100(2) K	
Wavelength	0.71073 ≈	
Crystal system	Orthorhombic	
Space group	Fddd	
Unit cell dimensions	a = 13.8849(9) ≈	a= 90∞.
	b = 17.3756(12) ≈	b= 90∞.
	c = 38.946(3) ≈	g = 90∞.
Volume	9396.1(11) ≈^{3}	
Z	16	
Density (calculated)	1.133 Mg/m^3	
Absorption coefficient	0.075 mm^{-1}	
F(000)	3488	
Crystal size	0.60 x 0.60 x 0.60 mm^3	
Theta range for data collection	1.95 to 27.49∞.	
Index ranges	-16<=h<=17, -22<=k<=22, -45<=l<=50	
Reflections collected	12741	
Independent reflections	2657 [R(int) = 0.0188]	
Completeness to theta = 27.49∞	98.1 %	
Absorption correction	None	
Max. and min. transmission	0.9564 and 0.9564	
Refinement method	Full-matrix least-squares on F^2	
Data / restraints / parameters	2657 / 0 / 137	
Goodness-of-fit on F^2	1.046	
Final R indices [I>2sigma(I)]	R1 = 0.0458, wR2 = 0.1237	
R indices (all data)	R1 = 0.0507, wR2 = 0.1287	
Largest diff. peak and hole	0.434 and -0.224 e.≈$^{-3}$	

Table 2.25 Atomic coordinates (x 10^4) and equivalent isotropic displacement parameters (≈^{2}x 10^3) for **6**

	x	y	z	U(eq)
O(1)	2766(1)	1982(1)	1139(1)	30(1)
C(1)	2521(1)	4698(1)	-22(1)	23(1)
C(2)	2802(1)	3833(1)	-17(1)	22(1)
C(3)	3750	3750	195(1)	18(1)
C(4)	3769(1)	3021(1)	409(1)	18(1)
C(5)	3190(1)	2855(1)	690(1)	19(1)
C(6)	3315(1)	2153(1)	857(1)	21(1)
C(7)	4009(1)	1632(1)	745(1)	24(1)
C(8)	4582(1)	1807(1)	463(1)	24(1)
C(9)	4460(1)	2505(1)	294(1)	20(1)

Table 2.25 continued

C(10)	1434(1)	4821(1)	1(1)	34(1)
C(11)	2911(1)	5096(1)	-346(1)	33(1)
O(2)	1250	4482(1)	1250	34(1)
C(12)	542(1)	4929(1)	1081(1)	43(1)
C(13)	-245(1)	4419(1)	955(1)	46(1)
O(3)	1250	2884(1)	1250	64(1)

U(eq) is defined as one third of the trace of the orthogonalized U^{ij} tensor.

Table 2.26 Bond lengths [≈] and angles [∞] for **6**

O(1)-C(6)	1.3701(14)
C(1)-C(9)#1	1.5160(15)
C(1)-C(10)	1.5265(18)
C(1)-C(11)	1.5378(17)
C(1)-C(2)	1.5538(15)
C(2)-C(3)	1.5613(13)
C(3)-C(4)#1	1.5180(13)
C(3)-C(4)	1.5180(13
C(3)-C(2)#1	1.5613(13)
C(4)-C(5)	1.3879(15)
C(4)-C(9)	1.3877(15)
C(5)-C(6)	1.3939(15)
C(6)-C(7)	1.3927(16)
C(7)-C(8)	1.3887(16)
C(8)-C(9)	1.3909(15)
C(9)-C(1)#1	1.5160(15)
O(2)-C(12)#2	1.4159(16)
O(2)-C(12)	1.4159(16)
C(12)-C(13)	1.490(2)
C(9)#1-C(1)-C(10)	112.10(10)
C(9)#1-C(1)-C(11)	110.17(9)
C(10)-C(1)-C(11)	109.47(11)
C(9)#1-C(1)-C(2)	101.58(9)
C(10)-C(1)-C(2)	112.51(10)
C(11)-C(1)-C(2)	110.83(10)
C(1)-C(2)-C(3)	107.86(8)
C(4)#1-C(3)-C(4)	113.19(12)
C(4)#1-C(3)-C(2)	101.53(6)
C(4)-C(3)-C(2)	112.51(6)
C(4)#1-C(3)-C(2)#1	112.51(6)
C(4)-C(3)-C(2)#1	101.53(6)
C(2)-C(3)-C(2)#1	116.09(12)
C(5)-C(4)-C(9)	121.49(10)
C(5)-C(4)-C(3)	126.65(9)
C(9)-C(4)-C(3)	111.87(9)
C(4)-C(5)-C(6)	118.49(10)
O(1)-C(6)-C(7)	119.79(10)
O(1)-C(6)-C(5)	119.60(10)
C(7)-C(6)-C(5)	120.60(10)

Table 2.26 continued

C(8)-C(7)-C(6)	120.11(10)
C(7)-C(8)-C(9)	119.76(10)
C(4)-C(9)-C(8)	119.55(10)
C(4)-C(9)-C(1)#1	111.86(10)
C(8)-C(9)-C(1)#1	128.57(10)
C(12)#2-O(2)-C(12)	113.47(15)
O(2)-C(12)-C(13)	109.63(13)

Symmetry transformations used to generate equivalent atoms:
#1 -x+3/4,-y+3/4,z #2 -x+1/4,y,-z+1/4

Table 2.27 Anisotropic displacement parameters ($\approx^2$x 10^3) for **6**

	U^{11}	U^{22}	U^{33}	U^{23}	U^{13}	U^{12}
O(1)	40(1)	22(1)	27(1)	8(1)	8(1)	-2(1)
C(1)	28(1)	18(1)	24(1)	2(1)	-5(1)	-2(1)
C(2)	28(1)	18(1)	21(1)	1(1)	-5(1)	-4(1)
C(3)	23(1)	15(1)	17(1)	0	0	-3(1)
C(4)	23(1)	13(1)	18(1)	-1(1)	-3(1)	-3(1)
C(5)	23(1)	15(1)	20(1)	0(1)	0(1)	0(1)
C(6)	25(1)	18(1)	20(1)	1(1)	0(1)	-2(1)
C(7)	30(1)	15(1)	27(1)	3(1)	-1(1)	2(1)
C(8)	26(1)	17(1)	29(1)	-3(1)	1(1)	2(1)
C(9)	23(1)	17(1)	21(1)	-3(1)	1(1)	-3(1)
C(10)	29(1)	29(1)	44(1)	-3(1)	-10(1)	1(1)
C(11)	47(1)	26(1)	25(1)	8(1)	-9(1)	-7(1)
O(2)	34(1)	22(1)	45(1)	0	-4(1)	0
C(12)	43(1)	33(1)	52(1)	-2(1)	-6(1)	8(1)
C(13)	44(1)	38(1)	54(1)	-9(1)	-13(1)	9(1)
O(3)	106(2)	19(1)	67(1)	0	21(1)	0

The anisotropic displacement factor exponent takes the form: $-2p^2[\ h^2\ a^{*2}U^{11} + \ldots + 2\ h\ k\ a^*\ b^*\ U^{12}]$

Table 2.28 Crystallographic Data of **1**

Crystallized from		CH_2Cl_2
Empirical formula		$C_{74}H_{72}Cl_8N_4O_4$
Formula weight [g mol^{-1}]		1365.03
Crystal color, habit		colorless, prism
Crystal dimensions [mm]		0.18 × 0.25 × 0.40
Temperature [K]		160 (1)
Crystal system		triclinic
Space group		*P*1 (#1)
Z		1
Reflections for cell determination		111337
2θ range for cell determination [°]		4–50
Unit cell parameters	*a* [Å]	7.9560 (2)
	b [Å]	13.5072 (3)
	c [Å]	17.4228 (5)
	α [°]	112.171 (1)
	β [°]	91.016 (2)
	γ [°]	103.309 (2)
	V [$Å^3$]	1675.90 (8)
F(000)		712
D_x [g cm^{-3}]		1.352
μ(Mo *K*α) [mm^{-1}]		0.389
Scan type		ϕ and ω
$2\theta_{(max)}$ [°]		50
Transmission factors (min; max)		0.885; 0.938
Total reflections measured		32925
Symmetry independent reflections		11225
R_{int}		0.044
Reflections with $I > 2\sigma(I)$		9574
Reflections used in refinement		11225
Parameters refined; restraints		820; 3
Final *R(F)* [$I>2\sigma(I)$ reflections]		0.0536
wR(F^2) (all data)		0.1410
Weights:	$w = [\sigma^2(F_o^2) + (0.0734P)^2 + 0.8663P]^{-1}$	
where $P = (F_o^2 + 2F_c^2)/3$		
Goodness of fit		1.069
Secondary extinction coefficient		0.011 (2)
Final Δ_{max}/σ		0.001
$\Delta\rho$ (max; min) [e $Å^{-3}$]		0.31; -0.41
$\sigma(d_{(C-C)})$ [Å]		0.005–0.007

Table 2.29 Fractional atomic coordinates and equivalent isotropic displacement of **1**

ATOM	x	y	z	U_{eq}^*
O(1)	1.0126(3)	0.7785(2)	0.6806(2)	0.0379(6)
O(2)	0.4541(6)	0.6229(3)	0.1597(2)	0.077(1)
O(3)	0.2897(4)	0.1873(3)	0.2961(2)	0.0583(9)
O(4)	0.7756(4)	0.3821(2)	0.8428(2)	0.0360(6)

Table 2.29 continued

N(1)	0.8496(4)	0.8294(3)	0.5081(2)	0.0319(7)
N(2)	0.6398(4)	0.7851(3)	0.3636(2)	0.0365(8)
N(3)	0.3716(4)	0.1542(3)	0.4870(2)	0.0390(8)
N(4)	0.5270(4)	0.2098(3)	0.6442(2)	0.0317(7)
C(1)	0.9786(5)	0.7562(3)	0.5938(2)	0.0356(9)
C(2)	0.9470(5)	0.8536(3)	0.5785(2)	0.0326(8)
C(3)	1.0244(5)	0.9623(3)	0.6352(2)	0.0379(9)
C(4)	1.0026(5)	1.0474(3)	0.6168(2)	0.0385(9)
C(5)	0.9030(5)	1.0269(3)	0.5422(2)	0.0363(9)
C(6)	0.8794(6)	1.1145(4)	0.5190(3)	0.042(1)
C(7)	0.7861(6)	1.0926(4)	0.4482(3)	0.042(1)
C(8)	0.7053(5)	0.9805(3)	0.3916(2)	0.0351(9)
C(9)	0.6064(6)	0.9560(4)	0.3162(3)	0.043(1)
C(10)	0.5268(6)	0.8496(4)	0.2676(3)	0.044(1)
C(11)	0.5435(5)	0.7647(4)	0.2931(2)	0.0389(9)
C(12)	0.7207(5)	0.8922(3)	0.4123(2)	0.0322(8)
C(13)	0.8268(5)	0.9159(3)	0.4890(2)	0.0325(8)
C(14)	0.4470(6)	0.6471(4)	0.2446(2)	0.048(1)
C(15)	0.3800(8)	0.5147(4)	0.1046(3)	0.055(1)
C(16)	0.4535(8)	0.4823(4)	0.0289(3)	0.065(2)
C(17)	0.3879(7)	0.3777(4)	-0.0300(3)	0.060(1)
C(18)	0.2531(6)	0.3039(4)	-0.0160(2)	0.041(1)
C(19)	0.1573(6)	0.1871(4)	-0.0745(2)	0.0385(9)
C(20)	0.0592(6)	0.1441(4)	-0.0125(2)	0.044(1)
C(21)	0.0329(5)	0.2467(4)	0.0620(2)	0.043(1)
C(22)	0.1840(5)	0.3366(3)	0.0591(2)	0.0376(9)
C(23)	0.2482(7)	0.4430(4)	0.1204(2)	0.047(1)
C(24)	-0.1431(6)	0.2784(6)	0.0562(3)	0.067(2)
C(25)	-0.2582(5)	0.2415(4)	0.1183(3)	0.043(1)
C(26)	-0.1259(5)	0.2278(3)	0.1746(2)	0.0399(9)
C(27)	-0.1469(6)	0.2108(4)	0.2475(3)	0.052(1)
C(28)	-0.0102(6)	0.1968(4)	0.2897(3)	0.053(1)
C(29)	0.1466(6)	0.2000(4)	0.2587(3)	0.043(1)
C(30)	0.1717(6)	0.2164(4)	0.1847(3)	0.044(1)
C(31)	0.0338(5)	0.2300(4)	0.1431(2)	0.0398(9)
C(32)	0.3084(7)	0.2215(5)	0.3851(3)	0.062(1)
C(33)	0.2897(6)	0.1266(4)	0.4117(2)	0.045(1)
C(34)	0.1987(5)	0.0182(4)	0.3617(2)	0.047(1)
C(35)	0.2021(5)	-0.0650(4)	0.3867(3)	0.043(1)
C(36)	0.2951(5)	-0.0404(3)	0.4637(2)	0.0360(9)
C(37)	0.3200(5)	-0.1250(4)	0.4909(3)	0.042(1)
C(38)	0.4105(5)	-0.0975(3)	0.5643(3)	0.0396(9)
C(39)	0.4837(5)	0.0158(3)	0.6195(2)	0.0354(9)
C(40)	0.5745(5)	0.0479(3)	0.6989(2)	0.0362(9)
C(41)	0.6351(5)	0.1563(3)	0.7482(2)	0.0359(9)
C(42)	0.6095(5)	0.2357(3)	0.7193(2)	0.0318(8)
C(43)	0.4638(5)	0.1009(3)	0.5949(2)	0.0320(8)
C(44)	0.3741(5)	0.0723(3)	0.5133(2)	0.0332(8)
C(45)	0.6619(5)	0.3583(3)	0.7705(2)	0.0356(9)
C(46)	0.8245(5)	0.4920(3)	0.8968(2)	0.0330(8)

Table 2.29 continued

C(47)	0.9403(5)	0.5175(3)	0.9671(2)	0.0350(9)
C(48)	0.9941(5)	0.6237(3)	1.0252(2)	0.0356(9)
C(49)	0.9341(5)	0.7076(3)	1.0147(2)	0.0291(8)
C(50)	0.9726(5)	0.8309(3)	1.0715(2)	0.0337(8)
C(51)	0.9190(5)	0.8776(3)	1.0080(2)	0.0326(8)
C(52)	0.7731(5)	0.7841(3)	0.9430(2)	0.0289(8)
C(53)	0.8217(5)	0.6824(3)	0.9445(2)	0.0299(8)
C(54)	0.7670(5)	0.5750(3)	0.8845(2)	0.0314(8)
C(55)	0.5844(5)	0.7892(3)	0.9647(2)	0.0366(9)
C(56)	0.4695(5)	0.7723(3)	0.8852(2)	0.0335(8)
C(57)	0.6009(5)	0.7738(3)	0.8235(2)	0.0290(8)
C(58)	0.5687(5)	0.7669(3)	0.7426(2)	0.0324(8)
C(59)	0.7032(5)	0.7703(3)	0.6938(2)	0.0340(8)
C(60)	0.8708(5)	0.7793(3)	0.7259(2)	0.0306(8)
C(61)	0.9035(5)	0.7857(3)	0.8061(2)	0.0313(8)
C(62)	0.7675(5)	0.7845(3)	0.8548(2)	0.0287(8)
C(63)	0.2762(7)	0.1148(4)	-0.1197(3)	0.053(1)
C(64)	0.0311(8)	0.1900(4)	-0.1408(3)	0.062(1)
C(65)	-0.3916(7)	0.1334(4)	0.0759(4)	0.077(2)
C(66)	-0.3490(7)	0.3324(4)	0.1638(4)	0.064(1)
C(67)	0.8547(6)	0.8485(4)	1.1419(2)	0.0396(9)
C(68)	1.1611(5)	0.8826(4)	1.1089(2)	0.0411(9)
C(69)	0.3294(7)	0.6649(4)	0.8537(3)	0.056(1)
C(70)	0.3874(6)	0.8694(4)	0.8997(3)	0.045(1)
Cl(1)	0.7933(2)	0.3828(1)	0.46282(7)	0.0579(3)
Cl(2)	0.6966(2)	0.5072(1)	0.62334(8)	0.0635(3)
C(71)	0.7180(7)	0.3766(4)	0.5570(3)	0.048(1)
Cl(3)	0.1335(2)	0.3672(1)	0.73294(9)	0.0792(4)
Cl(4)	0.1734(2)	0.4128(2)	0.5850(1)	0.0969(6)
C(72)	0.2751(7)	0.3905(5)	0.6627(4)	0.067(1)
Cl(5)	0.9390(2)	0.6396(1)	0.23648(8)	0.0671(4)
Cl(6)	1.0377(2)	0.5621(1)	0.3596(1)	0.0761(4)
C(73)	0.8835(6)	0.6136(4)	0.3255(3)	0.053(1)
Cl(7)	0.3670(2)	0.6121(1)	0.51587(9)	0.0688(4)
Cl(8)	0.4350(2)	0.4648(1)	0.35499(8)	0.0653(4)
C(74)	0.5223(7)	0.5832(4)	0.4461(3)	0.062(1)

parameters ($Å^2$) with standard uncertainties in parentheses.

* U_{eq} is defined as one third of the trace of the orthogonalized U^{ij} tensor.

Table 2.30 Bond lengths (Å) with standard uncertainties in parentheses. of **1**

O(1) -C(60)	1.388(4)	C(27) -C(28)	1.390(7)
O(1) -C(1)	1.433(4)	C(28) -C(29)	1.366(6)
O(2) -C(15)	1.389(6)	C(29) -C(30)	1.399(6)
O(2) -C(14)	1.394(5)	C(30) -C(31)	1.388(6)
O(3) -C(29)	1.379(5)	C(32) -C(33)	1.497(7)
O(3) -C(32)	1.434(5)	C(33) -C(34)	1.397(7)
O(4) -C(46)	1.381(5)	C(34) -C(35)	1.354(7)
O(4) -C(45)	1.424(4)	C(35) -C(36)	1.406(6)

Table 2.30 continued

N(1) -C(2)	1.327(5)	C(36) -C(44)	1.416(6)
N(1) -C(13)	1.376(5)	C(36) -C(37)	1.441(6)
N(2) -C(11)	1.336(5)	C(37) -C(38)	1.334(6)
N(2) -C(12)	1.361(5)	C(38) -C(39)	1.437(6)
N(3) -C(33)	1.332(5)	C(39) -C(43)	1.409(6)
N(3) -C(44)	1.353(5)	C(39) -C(40)	1.411(6)
N(4) -C(42)	1.335(5)	C(40) -C(41)	1.351(6)
N(4) -C(43)	1.358(5)	C(41) -C(42)	1.396(6)
C(1) -C(2)	1.510(6)	C(42) -C(45)	1.505(5)
C(2) -C(3)	1.406(6)	C(43) -C(44)	1.449(5)
C(3) -C(4)	1.349(6)	C(46) -C(54)	1.387(5)
C(4) -C(5)	1.410(6)	C(46) -C(47)	1.402(5)
C(5) -C(13)	1.410(6)	C(47) -C(48)	1.368(6)
C(5) -C(6)	1.434(6)	C(48) -C(49)	1.395(6)
C(6) -C(7)	1.324(6)	C(49) -C(53)	1.385(5)
C(7) -C(8)	1.443(6)	C(49) -C(50)	1.535(5)
C(8) -C(12)	1.400(6)	C(50) -C(68)	1.516(6)
C(8) -C(9)	1.403(6)	C(50) -C(67)	1.537(5)
C(9) -C(10)	1.351(6)	C(50) -C(51)	1.562(5)
C(10) -C(11)	1.409(6)	C(51) -C(52)	1.557(5)
C(11) -C(14)	1.494(6)	C(52) -C(53)	1.519(5)
C(12) -C(13)	1.454(5)	C(52) -C(62)	1.539(5)
C(15) -C(23)	1.363(7)	C(52) -C(55)	1.565(5)
C(15) -C(16)	1.408(6)	C(53) -C(54)	1.390(5)
C(16) -C(17)	1.367(7)	C(55) -C(56)	1.558(5)
C(17) -C(18)	1.380(7)	C(56) -C(69)	1.510(6)
C(18) -C(22)	1.383(6)	C(56) -C(57)	1.515(5)
C(18) -C(19)	1.520(6)	C(56) -C(70)	1.537(6)
C(19) -C(63)	1.530(6)	C(57) -C(62)	1.379(5)
C(19) -C(64)	1.535(6)	C(57) -C(58)	1.393(5)
C(19) -C(20)	1.552(6)	C(58) -C(59)	1.381(5)
C(20) -C(21)	1.561(6)	C(59) -C(60)	1.398(5)
C(21) -C(31)	1.512(5)	C(60) -C(61)	1.383(5)
C(21) -C(22)	1.516(6)	C(61) -C(62)	1.388(5)
C(21) -C(24)	1.568(6)	Cl(1) -C(71)	1.782(4)
C(22) -C(23)	1.397(6)	Cl(2) -C(71)	1.755(4)
C(24) -C(25)	1.577(7)	Cl(3) -C(72)	1.744(6)
C(25) -C(65)	1.499(6)	Cl(4) -C(72)	1.720(6)
C(25) -C(26)	1.515(6)	Cl(5) -C(73)	1.757(5)
C(25) -C(66)	1.534(6)	Cl(6) -C(73)	1.738(5)
C(26) -C(27)	1.380(6)	Cl(7) -C(74)	1.754(6)
C(26) -C(31)	1.392(6)	Cl(8) -C(74)	1.758(5)

Table 2.31 Bond angles (°) with standard uncertainties in parentheses of **1**

C(60) -O(1) -C(1)	116.9(3)	C(30) -C(31) -C(21)	127.0(4)
C(15) -O(2) -C(14)	117.3(4)	C(26) -C(31) -C(21)	112.4(4)
C(29) -O(3) -C(32)	118.4(4)	O(3) -C(32) -C(33)	112.9(4)
C(46) -O(4) -C(45)	115.0(3)	N(3) -C(33) -C(34)	122.6(4)

Table 2.31 continued

C(2) -N(1) -C(13)	117.8(3)	N(3) -C(33) -C(32)	113.8(4)
C(11) -N(2) -C(12)	118.1(3)	C(34) -C(33) -C(32)	123.5(4)
C(33) -N(3) -C(44)	118.0(4)	C(35) -C(34) -C(33)	120.0(4)
C(42) -N(4) -C(43)	117.8(3)	C(34) -C(35) -C(36)	119.2(4)
O(1) -C(1) -C(2)	113.2(3)	C(35) -C(36) -C(44)	117.4(4)
N(1) -C(2) -C(3)	123.6(4)	C(35) -C(36) -C(37)	122.6(4)
N(1) -C(2) -C(1)	115.9(3)	C(44) -C(36) -C(37)	119.9(4)
C(3) -C(2) -C(1)	120.5(3)	C(38) -C(37) -C(36)	120.4(4)
C(4) -C(3) -C(2)	118.9(4)	C(37) -C(38) -C(39)	121.9(4)
C(3) -C(4) -C(5)	120.2(4)	C(43) -C(39) -C(40)	117.1(4)
C(13) -C(5) -C(4)	117.8(4)	C(43) -C(39) -C(38)	119.4(4)
C(13) -C(5) -C(6)	119.9(4)	C(40) -C(39) -C(38)	123.4(4)
C(4) -C(5) -C(6)	122.2(4)	C(41) -C(40) -C(39)	119.9(4)
C(7) -C(6) -C(5)	120.8(4)	C(40) -C(41) -C(42)	119.5(4)
C(6) -C(7) -C(8)	121.5(4)	N(4) -C(42) -C(41)	123.0(3)
C(12) -C(8) -C(9)	118.0(4)	N(4) -C(42) -C(45)	112.9(3)
C(12) -C(8) -C(7)	119.9(4)	C(41) -C(42) -C(45)	124.1(3)
C(9) -C(8) -C(7)	122.1(4)	N(4) -C(43) -C(39)	122.7(3)
C(10) -C(9) -C(8)	119.4(4)	N(4) -C(43) -C(44)	118.1(3)
C(9) -C(10) -C(11)	119.8(4)	C(39) -C(43) -C(44)	119.2(3)
N(2) -C(11) -C(10)	122.2(4)	N(3) -C(44) -C(36)	122.5(4)
N(2) -C(11) -C(14)	116.3(4)	N(3) -C(44) -C(43)	118.6(3)
C(10) -C(11) -C(14)	121.5(4)	C(36) -C(44) -C(43)	118.9(3)
N(2) -C(12) -C(8)	122.5(4)	O(4) -C(45) -C(42)	110.2(3)
N(2) -C(12) -C(13)	118.8(3)	O(4) -C(46) -C(54)	124.1(3)
C(8) -C(12) -C(13)	118.7(3)	O(4) -C(46) -C(47)	115.8(3)
N(1) -C(13) -C(5)	121.7(3)	C(54) -C(46) -C(47)	120.1(3)
N(1) -C(13) -C(12)	119.2(3)	C(48) -C(47) -C(46)	120.3(3)
C(5) -C(13) -C(12)	119.1(3)	C(47) -C(48) -C(49)	120.2(3)
O(2) -C(14) -C(11)	109.0(4)	C(53) -C(49) -C(48)	119.3(3)
C(23) -C(15) -O(2)	124.5(4)	C(53) -C(49) -C(50)	111.1(3)
C(23) -C(15) -C(16)	121.1(4)	C(48) -C(49) -C(50)	129.5(3)
O(2) -C(15) -C(16)	114.4(4)	C(68) -C(50) -C(49)	113.9(3)
C(17) -C(16) -C(15)	118.9(5)	C(68) -C(50) -C(67)	109.5(3)
C(16) -C(17) -C(18)	121.2(4)	C(49) -C(50) -C(67)	110.2(3)
C(17) -C(18) -C(22)	119.2(4)	C(68) -C(50) -C(51)	112.3(3)
C(17) -C(18) -C(19)	129.1(4)	C(49) -C(50) -C(51)	100.0(3)
C(22) -C(18) -C(19)	111.7(4)	C(67) -C(50) -C(51)	110.7(3)
C(18) -C(19) -C(63)	114.3(4)	C(52) -C(51) -C(50)	106.9(3)
C(18) -C(19) -C(64)	110.5(4)	C(53) -C(52) -C(62)	111.7(3)
C(63) -C(19) -C(64)	107.9(4)	C(53) -C(52) -C(51)	100.6(3)
C(18) -C(19) -C(20)	100.9(3)	C(62) -C(52) -C(51)	115.0(3)
C(63) -C(19) -C(20)	111.6(4)	C(53) -C(52) -C(55)	113.6(3)
C(64) -C(19) -C(20)	111.7(4)	C(62) -C(52) -C(55)	102.3(3)
C(19) -C(20) -C(21)	107.3(3)	C(51) -C(52) -C(55)	114.1(3)
C(31) -C(21) -C(22)	114.7(3)	C(49) -C(53) -C(54)	121.2(3)
C(31) -C(21) -C(20)	112.0(4)	C(49) -C(53) -C(52)	111.9(3)
C(22) -C(21) -C(20)	100.8(3)	C(54) -C(53) -C(52)	126.9(3)
C(31) -C(21) -C(24)	102.8(3)	C(46) -C(54) -C(53)	118.8(3)
C(22) -C(21) -C(24)	110.4(4)	C(56) -C(55) -C(52)	109.3(3)

Table 2.31 continued

C(20) -C(21) -C(24)	116.7(4)	C(69) -C(56) -C(57)	111.7(3)
C(18) -C(22) -C(23)	120.9(4)	C(69) -C(56) -C(70)	109.8(4)
C(18) -C(22) -C(21)	111.8(4)	C(57) -C(56) -C(70)	108.2(3)
C(23) -C(22) -C(21)	127.2(4)	C(69) -C(56) -C(55)	112.6(3)
C(15) -C(23) -C(22)	118.7(4)	C(57) -C(56) -C(55)	102.6(3)
C(21) -C(24) -C(25)	106.9(4)	C(70) -C(56) -C(55)	111.7(3)
C(65) -C(25) -C(26)	109.1(4)	C(62) -C(57) -C(58)	119.7(3)
C(65) -C(25) -C(66)	109.6(4)	C(62) -C(57) -C(56)	113.5(3)
C(26) -C(25) -C(66)	113.8(4)	C(58) -C(57) -C(56)	126.8(3)
C(65) -C(25) -C(24)	113.4(5)	C(59) -C(58) -C(57)	120.0(3)
C(26) -C(25) -C(24)	102.7(3)	C(58) -C(59) -C(60)	119.6(3)
C(66) -C(25) -C(24)	108.3(4)	C(61) -C(60) -O(1)	115.5(3)
C(27) -C(26) -C(31)	119.4(4)	C(61) -C(60) -C(59)	120.7(3)
C(27) -C(26) -C(25)	128.9(4)	O(1) -C(60) -C(59)	123.8(3)
C(31) -C(26) -C(25)	111.6(4)	C(60) -C(61) -C(62)	119.0(3)
C(26) -C(27) -C(28)	120.6(4)	C(57) -C(62) -C(61)	121.0(3)
C(29) -C(28) -C(27)	119.6(4)	C(57) -C(62) -C(52)	111.5(3)
C(28) -C(29) -O(3)	123.8(4)	C(61) -C(62) -C(52)	127.3(3)
C(28) -C(29) -C(30)	121.1(4)	Cl(2) -C(71) -Cl(1)	109.7(2)
O(3) -C(29) -C(30)	115.1(4)	Cl(4) -C(72) -Cl(3)	112.1(3)
C(31) -C(30) -C(29)	118.7(4)	Cl(6) -C(73) -Cl(5)	111.3(3)
C(30) -C(31) -C(26)	120.6(4)	Cl(7) -C(74) -Cl(8)	111.7(3)

Table 2.32 Torsion angles (°) with standard uncertainties in parentheses of **1**

C(60) -O(1) -C(1) -C(2)	76.3(4)	C(29) -O(3) -C(32) -C(33)	112.5(5)
C(13) -N(1) -C(2) -C(3)	1.4(5)	C(44) -N(3) -C(33) -C(34)	3.9(6)
C(13) -N(1) -C(2) -C(1)	-175.9(3)	C(44) -N(3) -C(33) -C(32)	-174.6(4)
O(1) -C(1) -C(2) -N(1)	-153.7(3)	O(3) -C(32) -C(33) -N(3)	154.5(4)
O(1) -C(1) -C(2) -C(3)	28.9(5)	O(3) -C(32) -C(33) -C(34)	-24.0(7)
N(1) -C(2) -C(3) -C(4)	-1.5(6)	N(3) -C(33) -C(34) -C(35)	-4.9(7)
C(1) -C(2) -C(3) -C(4)	175.8(4)	C(32) -C(33) -C(34) -C(35)	173.4(5)
C(2) -C(3) -C(4) -C(5)	0.3(6)	C(33) -C(34) -C(35) -C(36)	1.2(6)
C(3) -C(4) -C(5) -C(13)	0.8(5)	C(34) -C(35) -C(36) -C(44)	3.0(6)
C(3) -C(4) -C(5) -C(6)	-178.5(4)	C(34) -C(35) -C(36) -C(37)	-173.5(4)
C(13) -C(5) -C(6) -C(7)	0.3(6)	C(35) -C(36) -C(37) -C(38)	179.5(4)
C(4) -C(5) -C(6) -C(7)	179.5(4)	C(44) -C(36) -C(37) -C(38)	3.1(6)
C(5) -C(6) -C(7) -C(8)	-0.3(6)	C(36) -C(37) -C(38) -C(39)	1.0(6)
C(6) -C(7) -C(8) -C(12)	1.9(6)	C(37) -C(38) -C(39) -C(43)	-1.7(6)
C(6) -C(7) -C(8) -C(9)	-179.8(4)	C(37) -C(38) -C(39) -C(40)	177.6(4)
C(12) -C(8) -C(9) -C(10)	1.6(6)	C(43) -C(39) -C(40) -C(41)	1.2(6)
C(7) -C(8) -C(9) -C(10)	-176.8(4)	C(38) -C(39) -C(40) -C(41)	-178.0(4)
C(8) -C(9) -C(10) -C(11)	0.1(6)	C(39) -C(40) -C(41) -C(42)	-1.0(6)
C(12) -N(2) -C(11) -C(10)	1.3(6)	C(43) -N(4) -C(42) -C(41)	0.9(5)
C(12) -N(2) -C(11) -C(14)	-175.8(3)	C(43) -N(4) -C(42) -C(45)	-175.8(3)
C(9) -C(10) -C(11) -N(2)	-1.7(6)	C(40) -C(41) -C(42) -N(4)	0.0(6)
C(9) -C(10) -C(11) -C(14)	175.3(4)	C(40) -C(41) -C(42) -C(45)	176.3(4)
C(11) -N(2) -C(12) -C(8)	0.5(5)	C(42) -N(4) -C(43) -C(39)	-0.7(5)
C(11) -N(2) -C(12) -C(13)	-179.7(3)	C(42) -N(4) -C(43) -C(44)	180.0(3)

Table 2.32 continued

C(9)	-C(8)	-C(12)	-N(2)	-1.9(5)	C(40)	-C(39)	-C(43)	-N(4)	-0.3(5)
C(7)	-C(8)	-C(12)	-N(2)	176.4(3)	C(38)	-C(39)	-C(43)	-N(4)	178.9(3)
C(9)	-C(8)	-C(12)	-C(13)	178.3(3)	C(40)	-C(39)	-C(43)	-C(44)	179.0(3)
C(7)	-C(8)	-C(12)	-C(13)	-3.3(5)	C(38)	-C(39)	-C(43)	-C(44)	-1.8(5)
C(2)	-N(1)	-C(13)	-C(5)	-0.3(5)	C(33)	-N(3)	-C(44)	-C(36)	0.7(5)
C(2)	-N(1)	-C(13)	-C(12)	-180.0(3)	C(33)	-N(3)	-C(44)	-C(43)	179.5(4)
C(4)	-C(5)	-C(13)	-N(1)	-0.8(5)	C(35)	-C(36)	-C(44)	-N(3)	-4.1(5)
C(6)	-C(5)	-C(13)	-N(1)	178.5(3)	C(37)	-C(36)	-C(44)	-N(3)	172.5(3)
C(4)	-C(5)	-C(13)	-C(12)	178.9(3)	C(35)	-C(36)	-C(44)	-C(43)	177.0(3)
C(6)	-C(5)	-C(13)	-C(12)	-1.8(5)	C(37)	-C(36)	-C(44)	-C(43)	-6.4(5)
N(2)	-C(12)	-C(13)	-N(1)	3.3(5)	N(4)	-C(43)	-C(44)	-N(3)	6.1(5)
C(8)	-C(12)	-C(13)	-N(1)	-176.9(3)	C(39)	-C(43)	-C(44)	-N(3)	-173.2(3)
N(2)	-C(12)	-C(13)	-C(5)	-176.5(3)	N(4)	-C(43)	-C(44)	-C(36)	-175.0(3)
C(8)	-C(12)	-C(13)	-C(5)	3.3(5)	C(39)	-C(43)	-C(44)	-C(36)	5.7(5)
C(15)	-O(2)	-C(14)	-C(11)	176.2(4)	C(46)	-O(4)	-C(45)	-C(42)	-176.6(3)
N(2)	-C(11)	-C(14)	-O(2)	-140.3(4)	N(4)	-C(42)	-C(45)	-O(4)	-169.5(3)
C(10)	-C(11)	-C(14)	-O(2)	42.5(6)	C(41)	-C(42)	-C(45)	-O(4)	13.9(5)
C(14)	-O(2)	-C(15)	-C(23)	26.5(7)	C(45)	-O(4)	-C(46)	-C(54)	1.3(5)
C(14)	-O(2)	-C(15)	-C(16)	-152.9(5)	C(45)	-O(4)	-C(46)	-C(47)	-178.3(3)
C(23)	-C(15)	-C(16)	-C(17)	1.4(9)	O(4)	-C(46)	-C(47)	-C(48)	-178.8(3)
O(2)	-C(15)	-C(16)	-C(17)	-179.2(5)	C(54)	-C(46)	-C(47)	-C(48)	1.6(6)
C(15)	-C(16)	-C(17)	-C(18)	-0.6(9)	C(46)	-C(47)	-C(48)	-C(49)	-0.1(6)
C(16)	-C(17)	-C(18)	-C(22)	-0.2(8)	C(47)	-C(48)	-C(49)	-C(53)	-0.9(6)
C(16)	-C(17)	-C(18)	-C(19)	176.8(5)	C(47)	-C(48)	-C(49)	-C(50)	178.6(4)
C(17)	-C(18)	-C(19)	-C(63)	46.5(6)	C(53)	-C(49)	-C(50)	-C(68)	-139.2(3)
C(22)	-C(18)	-C(19)	-C(63)	-136.4(4)	C(48)	-C(49)	-C(50)	-C(68)	41.2(5)
C(17)	-C(18)	-C(19)	-C(64)	-75.5(6)	C(53)	-C(49)	-C(50)	-C(67)	97.2(4)
C(22)	-C(18)	-C(19)	-C(64)	101.7(4)	C(48)	-C(49)	-C(50)	-C(67)	-82.3(5)
C(17)	-C(18)	-C(19)	-C(20)	166.3(5)	C(53)	-C(49)	-C(50)	-C(51)	-19.3(4)
C(22)	-C(18)	-C(19)	-C(20)	-16.5(4)	C(48)	-C(49)	-C(50)	-C(51)	161.1(4)
C(18)	-C(19)	-C(20)	-C(21)	26.2(4)	C(68)	-C(50)	-C(51)	-C(52)	150.8(3)
C(63)	-C(19)	-C(20)	-C(21)	147.9(4)	C(49)	-C(50)	-C(51)	-C(52)	29.7(4)
C(64)	-C(19)	-C(20)	-C(21)	-91.2(4)	C(67)	-C(50)	-C(51)	-C(52)	-86.5(4)
C(19)	-C(20)	-C(21)	-C(31)	-148.5(3)	C(50)	-C(51)	-C(52)	-C(53)	-29.1(3)
C(19)	-C(20)	-C(21)	-C(22)	-26.1(4)	C(50)	-C(51)	-C(52)	-C(62)	-149.2(3)
C(19)	-C(20)	-C(21)	-C(24)	93.5(5)	C(50)	-C(51)	-C(52)	-C(55)	93.0(4)
C(17)	-C(18)	-C(22)	-C(23)	0.3(6)	C(48)	-C(49)	-C(53)	-C(54)	0.4(5)
C(19)	-C(18)	-C(22)	-C(23)	-177.2(4)	C(50)	-C(49)	-C(53)	-C(54)	-179.3(3)
C(17)	-C(18)	-C(22)	-C(21)	177.7(4)	C(48)	-C(49)	-C(53)	-C(52)	-178.9(3)
C(19)	-C(18)	-C(22)	-C(21)	0.3(5)	C(50)	-C(49)	-C(53)	-C(52)	1.4(4)
C(31)	-C(21)	-C(22)	-C(18)	136.6(4)	C(62)	-C(52)	-C(53)	-C(49)	139.7(3)
C(20)	-C(21)	-C(22)	-C(18)	16.1(4)	C(51)	-C(52)	-C(53)	-C(49)	17.2(4)
C(24)	-C(21)	-C(22)	-C(18)	-107.9(4)	C(55)	-C(52)	-C(53)	-C(49)	-105.2(4)
C(31)	-C(21)	-C(22)	-C(23)	-46.2(6)	C(62)	-C(52)	-C(53)	-C(54)	-39.6(5)
C(20)	-C(21)	-C(22)	-C(23)	-166.7(4)	C(51)	-C(52)	-C(53)	-C(54)	-162.0(4)
C(24)	-C(21)	-C(22)	-C(23)	69.4(5)	C(55)	-C(52)	-C(53)	-C(54)	75.6(5)
O(2)	-C(15)	-C(23)	-C(22)	179.3(4)	O(4)	-C(46)	-C(54)	-C(53)	178.3(3)
C(16)	-C(15)	-C(23)	-C(22)	-1.4(7)	C(47)	-C(46)	-C(54)	-C(53)	-2.2(6)
C(18)	-C(22)	-C(23)	-C(15)	0.6(6)	C(49)	-C(53)	-C(54)	-C(46)	1.2(5)
C(21)	-C(22)	-C(23)	-C(15)	-176.5(4)	C(52)	-C(53)	-C(54)	-C(46)	-179.6(3)

Table 2.32 continued

C(31) -C(21) -C(24) -C(25)	-17.6(5)	C(53) -C(52) -C(55) -C(56)	-111.1(3)
C(22) -C(21) -C(24) -C(25)	-140.4(4)	C(62) -C(52) -C(55) -C(56)	9.5(4)
C(20) -C(21) -C(24) -C(25)	105.3(4)	C(51) -C(52) -C(55) -C(56)	134.3(3)
C(21) -C(24) -C(25) -C(65)	-99.5(5)	C(52) -C(55) -C(56) -C(69)	112.7(4)
C(21) -C(24) -C(25) -C(26)	18.0(5)	C(52) -C(55) -C(56) -C(57)	-7.5(4)
C(21) -C(24) -C(25) -C(66)	138.7(4)	C(52) -C(55) -C(56) -C(70)	-123.1(3)
C(65) -C(25) -C(26) -C(27)	-69.0(6)	C(69) -C(56) -C(57) -C(62)	-118.6(4)
C(66) -C(25) -C(26) -C(27)	53.6(6)	C(70) -C(56) -C(57) -C(62)	120.4(4)
C(24) -C(25) -C(26) -C(27)	170.4(5)	C(55) -C(56) -C(57) -C(62)	2.3(4)
C(65) -C(25) -C(26) -C(31)	108.7(5)	C(69) -C(56) -C(57) -C(58)	62.2(5)
C(66) -C(25) -C(26) -C(31)	-128.6(4)	C(70) -C(56) -C(57) -C(58)	-58.7(5)
C(24) -C(25) -C(26) -C(31)	-11.8(5)	C(55) -C(56) -C(57) -C(58)	-176.9(4)
C(31) -C(26) -C(27) -C(28)	0.4(7)	C(62) -C(57) -C(58) -C(59)	0.3(5)
C(25) -C(26) -C(27) -C(28)	178.1(4)	C(56) -C(57) -C(58) -C(59)	179.4(4)
C(26) -C(27) -C(28) -C(29)	0.1(7)	C(57) -C(58) -C(59) -C(60)	0.8(6)
C(27) -C(28) -C(29) -O(3)	179.8(4)	C(1) -O(1) -C(60) -C(61)	171.4(3)
C(27) -C(28) -C(29) -C(30)	-0.5(7)	C(1) -O(1) -C(60) -C(59)	-6.4(5)
C(32) -O(3) -C(29) -C(28)	-29.3(6)	C(58) -C(59) -C(60) -C(61)	-0.6(6)
C(32) -O(3) -C(29) -C(30)	151.0(4)	C(58) -C(59) -C(60) -O(1)	177.1(4)
C(28) -C(29) -C(30) -C(31)	0.3(7)	O(1) -C(60) -C(61) -C(62)	-178.7(3)
O(3) -C(29) -C(30) -C(31)	-180.0(4)	C(59) -C(60) -C(61) -C(62)	-0.8(5)
C(29) -C(30) -C(31) -C(26)	0.3(7)	C(58) -C(57) -C(62) -C(61)	-1.7(5)
C(29) -C(30) -C(31) -C(21)	-178.9(4)	C(56) -C(57) -C(62) -C(61)	179.0(3)
C(27) -C(26) -C(31) -C(30)	-0.6(6)	C(58) -C(57) -C(62) -C(52)	-176.8(3)
C(25) -C(26) -C(31) -C(30)	-178.6(4)	C(56) -C(57) -C(62) -C(52)	4.0(4)
C(27) -C(26) -C(31) -C(21)	178.7(4)	C(60) -C(61) -C(62) -C(57)	2.0(5)
C(25) -C(26) -C(31) -C(21)	0.7(5)	C(60) -C(61) -C(62) -C(52)	176.2(3)
C(22) -C(21) -C(31) -C(30)	-50.0(6)	C(53) -C(52) -C(62) -C(57)	113.7(3)
C(20) -C(21) -C(31) -C(30)	64.1(6)	C(51) -C(52) -C(62) -C(57)	-132.5(3)
C(24) -C(21) -C(31) -C(30)	-169.9(5)	C(55) -C(52) -C(62) -C(57)	-8.2(4)
C(22) -C(21) -C(31) -C(26)	130.7(4)	C(53) -C(52) -C(62) -C(61)	-61.0(5)
C(20) -C(21) -C(31) -C(26)	-115.1(4)	C(51) -C(52) -C(62) -C(61)	52.8(5)
C(24) -C(21) -C(31) -C(26)	10.8(5)	C(55) -C(52) -C(62) -C(61)	177.1(4)

Table 2.33 Crystallographic Data of **2**

Crystallized from		MeCN
Empirical formula		$C_{35}H_{32}N_2O_2$
Formula weight [g mol^{-1}]		512.65
Crystal color, habit		colorless, prism
Crystal dimensions [mm]		0.27 × 0.27 × 0.30
Temperature [K]		160 (1)
Crystal system		monoclinic
Space group		*C*2/*c* (#15)
Z		4
Reflections for cell determination		16875
2θ range for cell determination [°]		4–60
Unit cell parameters	*a* [Å]	15.7613 (2)
	b [Å]	17.9189 (3)
	c [Å]	9.3255 (1)
	α [°]	90
	β [°]	99.4639 (8)
	γ [°]	90
	V [Å^3]	2597.91 (6)
F(000)		1088
D_x [g cm^{-3}]		1.311
μ(Mo *K*α) [mm^{-1}]		0.0810
Scan type		ϕ and ω
2$\theta_{(max)}$ [°]		60
Transmission factors (min; max)		0.732; 0.803
Total reflections measured		34048
Symmetry independent reflections		3799
R_{int}		0.052
Reflections with $I > 2\sigma(I)$		2815
Reflections used in refinement		3799
Parameters refined		179
Final *R(F)* [$I>2\sigma(I)$ reflections]		0.0466
wR(F^2) (all data)		0.1336
Weights:		$w = [\sigma^2(F_o^2) + (0.0706P)^2 + 0.7699P]^{-1}$
where $P = (F_o^2 + 2F_c^2)/3$		
Goodness of fit		1.063
Final Δ_{max}/σ		0.001
$\Delta\rho$ (max; min) [e Å^{-3}]		0.24; -0.25
$\sigma(d_{(C-C)})$ [Å]		0.001–0.003

Table 2.34 Fractional atomic coordinates and equivalent isotropic displacement of **2**

ATOM	x	y	z	U_{eq}*
O(1)	0.21646(5)	0.36712(5)	0.43363(9)	0.0322(2)
N(1)	0.06716(6)	0.46835(5)	0.36804(9)	0.0232(2)
C(1)	0.16852(8)	0.39741(7)	0.5385(1)	0.0304(3)
C(2)	0.12754(7)	0.47037(6)	0.4861(1)	0.0250(2)
C(3)	0.15392(8)	0.53630(7)	0.5622(1)	0.0292(3)
C(4)	0.11996(8)	0.60274(7)	0.5089(1)	0.0317(3)

Table 2.34 continued

C(5)	0.06012(7)	0.60348(7)	0.3791(1)	0.0282(3)
C(6)	0.03312(7)	0.53410(6)	0.3146(1)	0.0225(2)
C(7)	0.02795(8)	0.67216(7)	0.3129(2)	0.0373(3)
C(8)	0.0	0.16794(8)	0.25	0.0223(3)
C(9)	0.00352(7)	0.12082(6)	0.1109(1)	0.0262(2)
C(10)	0.09927(7)	0.11430(6)	0.0923(1)	0.0249(2)
C(11)	0.13802(7)	0.18241(6)	0.1757(1)	0.0237(2)
C(12)	0.21966(7)	0.21381(7)	0.1819(1)	0.0278(3)
C(13)	0.24344(7)	0.27437(7)	0.2720(1)	0.0280(3)
C(14)	0.18561(7)	0.30574(6)	0.3534(1)	0.0253(2)
C(15)	0.10363(7)	0.27561(6)	0.3468(1)	0.0239(2)
C(16)	0.08223(6)	0.21287(6)	0.2606(1)	0.0223(2)
C(17)	0.10807(9)	0.11521(7)	-0.0691(1)	0.0331(3)
C(18)	0.14150(8)	0.04240(7)	0.1607(1)	0.0309(3)

parameters ($Å^2$) with standard uncertainties in parentheses.

* U_{eq} is defined as one third of the trace of the orthogonalized U^{ij} tensor.

Table 2.35 Bond lengths (Å) with standard uncertainties in parentheses of **2**

O(1) -C(14)	1.374(1)	C(8) -C(16)	1.515(1)
O(1) -C(1)	1.437(2)	C(8) -C(9)	1.556(1)
N(1) -C(2)	1.332(1)	C(9) -C(10)	1.552(2)
N(1) -C(6)	1.355(1)	C(10) -C(11)	1.520(2)
C(1) -C(2)	1.504(2)	C(10) -C(17)	1.534(2)
C(2) -C(3)	1.406(2)	C(10) -C(18)	1.540(2)
C(3) -C(4)	1.365(2)	C(11) -C(16)	1.389(2)
C(4) -C(5)	1.407(2)	C(11) -C(12)	1.397(2)
C(5) -C(6)	1.416(2)	C(12) -C(13)	1.386(2)
C(5) -C(7)	1.432(2)	C(13) -C(14)	1.396(2)
C(6) -C(6')	1.459(2)	C(14) -C(15)	1.392(2)
C(7) -C(7')	1.346(3)	C(15) -C(16)	1.391(2)

Symmetry operators for primed atoms: ' $-x, y, \frac{1}{2}-z$

Table 2.36 Bond angles (°) with standard uncertainties in parentheses of **2**

C(14) -O(1) -C(1)	119.63(9)	C(10) -C(9) -C(8)	107.62(8)
C(2) -N(1) -C(6)	117.78(9)	C(11) -C(10) -C(17)	113.56(9)
O(1) -C(1) -C(2)	110.69(9)	C(11) -C(10) -C(18)	110.49(9)
N(1) -C(2) -C(3)	123.5(1)	C(17) -C(10) -C(18)	108.21(9)
N(1) -C(2) -C(1)	117.1(1)	C(11) -C(10) -C(9)	101.46(9)
C(3) -C(2) -C(1)	119.4(1)	C(17) -C(10) -C(9)	110.83(9)
C(4) -C(3) -C(2)	118.9(1)	C(18) -C(10) -C(9)	112.26(9)
C(3) -C(4) -C(5)	119.3(1)	C(16) -C(11) -C(12)	118.9(1)
C(4) -C(5) -C(6)	118.0(1)	C(16) -C(11) -C(10)	111.62(9)
C(4) -C(5) -C(7)	121.3(1)	C(12) -C(11) -C(10)	129.4(1)
C(6) -C(5) -C(7)	120.7(1)	C(13) -C(12) -C(11)	119.7(1)
N(1) -C(6) -C(5)	122.3(1)	C(12) -C(13) -C(14)	120.6(1)

Table 2.36 continued

N(1) -C(6) -C(6')	119.33(6)	O(1) -C(14) -C(15)	125.3(1)
C(5) -C(6) -C(6')	118.38(7)	O(1) -C(14) -C(13)	114.5(1)
C(7') -C(7) -C(5)	120.69(7)	C(15) -C(14) -C(13)	120.3(1)
C(16')-C(8) -C(16)	115.8(1)	C(16) -C(15) -C(14)	118.3(1)
C(16) -C(8) -C(9')	112.40(6)	C(11) -C(16) -C(15)	122.1(1)
C(16) -C(8) -C(9)	101.28(6)	C(11) -C(16) -C(8)	111.65(9)
C(9') -C(8) -C(9)	114.3(1)	C(15) -C(16) -C(8)	126.23(9)

Symmetry operators for primed atoms: ' $-x, y, \frac{1}{2}-z$

Table 2.37 Torsion angles (°) with standard uncertainties in parentheses of **2**

C(14) -O(1) -C(1) -C(2)	-107.9(1)	C(9) -C(10) -C(11) -C(16)	13.6(1)
C(6) -N(1) -C(2) -C(3)	3.8(2)	C(17) -C(10) -C(11) -C(12)	-50.7(2)
C(6) -N(1) -C(2) -C(1)	-176.3(1)	C(18) -C(10) -C(11) -C(12)	71.1(1)
O(1) -C(1) -C(2) -N(1)	65.2(1)	C(9) -C(10) -C(11) -C(12)	-169.7(1)
O(1) -C(1) -C(2) -C(3)	-114.9(1)	C(16) -C(11) -C(12) -C(13)	0.0(2)
N(1) -C(2) -C(3) -C(4)	-3.9(2)	C(10) -C(11) -C(12) -C(13)	-176.5(1)
C(1) -C(2) -C(3) -C(4)	176.2(1)	C(11) -C(12) -C(13) -C(14)	-1.9(2)
C(2) -C(3) -C(4) -C(5)	-0.4(2)	C(1) -O(1) -C(14) -C(15)	10.8(2)
C(3) -C(4) -C(5) -C(6)	4.4(2)	C(1) -O(1) -C(14) -C(13)	-170.52(9)
C(3) -C(4) -C(5) -C(7)	-175.0(1)	C(12) -C(13) -C(14) -O(1)	-177.7(1)
C(2) -N(1) -C(6) -C(5)	0.6(2)	C(12) -C(13) -C(14) -C(15)	1.1(2)
C(2) -N(1) -C(6) -C(6')	179.9(1)	O(1) -C(14) -C(15) -C(16)	-179.7(1)
C(4) -C(5) -C(6) -N(1)	-4.6(2)	C(13) -C(14) -C(15) -C(16)	1.7(2)
C(7) -C(5) -C(6) -N(1)	174.8(1)	C(12) -C(11) -C(16) -C(15)	2.9(2)
C(4) -C(5) -C(6) -C(6')	176.0(1)	C(10) -C(11) -C(16) -C(15)	-179.99(9)
C(7) -C(5) -C(6) -C(6')	-4.6(2)	C(12) -C(11) -C(16) -C(8)	-175.11(9)
C(4) -C(5) -C(7) -C(7')	178.6(2)	C(10) -C(11) -C(16) -C(8)	2.0(1)
C(6) -C(5) -C(7) -C(7')	-0.7(2)	C(14) -C(15) -C(16) -C(11)	-3.7(2)
C(16')-C(8) -C(9) -C(10)	148.91(9)	C(14) -C(15) -C(16) -C(8)	174.00(9)
C(16) -C(8) -C(9) -C(10)	24.7(1)	C(16')-C(8) -C(16) -C(11)	-138.43(9)
C(9') -C(8) -C(9) -C(10)	-96.39(8)	C(9') -C(8) -C(16) -C(11)	105.8(1)
C(8) -C(9) -C(10) -C(11)	-23.6(1)	C(9) -C(8) -C(16) -C(11)	-16.6(1)
C(8) -C(9) -C(10) -C(17)	-144.5(1)	C(16')-C(8) -C(16) -C(15)	43.64(9)
C(8) -C(9) -C(10) -C(18)	94.3(1)	C(9') -C(8) -C(16) -C(15)	-72.1(1)
C(17) -C(10) -C(11) -C(16)	132.6(1)	C(9) -C(8) -C(16) -C(15)	165.5(1)
C(18) –C(10) –C(11) –C(16)	-105.7(1)		

Table 2.38 Crystallographic Data of **80**

Crystallized from		MeCN / Et_2O
Empirical formula		$C_{42}H_{45}AgF_3N_3O_6S$
Formula weight [g mol^{-1}]		884.75
Crystal color, habit		colorless, prism
Crystal dimensions [mm]		0.18 × 0.20 × 0.25
Temperature [K]		160 (1)
Crystal system		triclinic
Space group		*P*1 (#1)
Z		2
Reflections for cell determination		98796
2θ range for cell determination [°]		4–55
Unit cell parameters	*a* [Å]	11.0040 (1)
	b [Å]	13.6737 (1)
	c [Å]	14.2536 (1)
	α [°]	80.1155 (4)
	β [°]	87.2178 (4)
	γ [°]	66.8566 (4)
	V [$Å^3$]	1942.38 (3)
F(000)		912
D_x [g cm^{-3}]		1.513
μ(Mo *K*α) [mm^{-1}]		0.638
Scan type		ϕ and ω
$2\theta_{(max)}$ [°]		55
Transmission factors (min; max)		0.818; 0.897
Total reflections measured		59044
Symmetry independent reflections		17085
R_{int}		0.050
Reflections with $I > 2\sigma(I)$		13782
Reflections used in refinement		17084
Parameters refined; restraints		1077; 477
Final *R(F)* [$I>2\sigma(I)$ reflections]		0.0605
wR(F^2) (all data)		0.1778
Weights:	$w = [\sigma^2(F_o^2) + (0.1316P)^2]^{-1}$ where $P = (F_o^2 + 2F_c^2)/3$	
Goodness of fit		1.029
Secondary extinction coefficient		0.022 (2)
Final Δ_{max}/σ		0.001
$\Delta\rho$ (max; min) [e $Å^{-3}$]		2.01; -0.81
$\sigma(d_{(C-C)})$ [Å]		0.006-0.002

Table 2.39 Fractional atomic coordinates and equivalent isotropic displacement of **80**

ATOM	x	y	z	U_{eq}*
Ag(1)	0.4211(1)	0.56543(9)	0.85756(7)	0.0569(1)
O(1)	0.0188(4)	0.6250(4)	0.7727(3)	0.0533(9)
O(2)	0.7364(4)	0.4502(3)	0.7672(3)	0.0579(9)
N(1)	0.2921(5)	0.4662(4)	0.9044(3)	0.054(1)
N(2)	0.5649(6)	0.3907(4)	0.9121(3)	0.059(1)
N(3)	0.3781(5)	0.7337(4)	0.8505(4)	0.057(1)

Table 2.39 continued

C(1)	0.0848(7)	0.6168(6)	0.8610(4)	0.061(2)
C(2)	0.1612(7)	0.5024(6)	0.9028(4)	0.058(2)
C(3)	0.089(1)	0.4407(8)	0.9388(5)	0.086(2)
C(4)	0.163(1)	0.3293(7)	0.9750(5)	0.085(2)
C(5)	0.300(1)	0.2890(8)	0.9770(5)	0.083(3)
C(6)	0.382(1)	0.1774(7)	1.0142(5)	0.090(3)
C(7)	0.511(1)	0.1433(6)	1.0186(4)	0.083(2)
C(8)	0.581(1)	0.2106(6)	0.9826(4)	0.078(2)
C(9)	0.719(1)	0.1782(6)	0.9854(6)	0.089(3)
C(10)	0.7758(9)	0.2492(7)	0.9491(5)	0.078(2)
C(11)	0.6947(7)	0.3577(6)	0.9125(5)	0.065(2)
C(12)	0.5047(8)	0.3230(5)	0.9452(4)	0.057(2)
C(13)	0.3643(8)	0.3593(5)	0.9426(4)	0.063(2)
C(14)	0.7508(8)	0.4359(6)	0.8683(6)	0.074(2)
C(15)	0.6542(5)	0.5510(4)	0.7207(4)	0.048(1)
C(16)	0.6819(5)	0.6408(4)	0.7221(4)	0.048(1)
C(17)	0.6016(5)	0.7402(4)	0.6672(4)	0.052(1)
C(18)	0.4995(5)	0.7468(4)	0.6116(4)	0.046(1)
C(19)	0.4084(5)	0.8407(4)	0.5409(4)	0.046(1)
C(20)	0.3024(5)	0.8023(4)	0.5181(4)	0.047(1)
C(21)	0.3598(4)	0.6758(4)	0.5426(3)	0.0366(8)
C(22)	0.4716(5)	0.6542(4)	0.6113(4)	0.038(1)
C(23)	0.5506(5)	0.5563(4)	0.6660(3)	0.0407(9)
C(24)	0.4074(5)	0.6150(4)	0.4566(3)	0.044(1)
C(25)	0.2937(5)	0.5845(4)	0.4278(3)	0.042(1)
C(26)	0.2177(4)	0.5859(3)	0.5188(3)	0.0356(8)
C(27)	0.1159(4)	0.5489(4)	0.5409(3)	0.0405(9)
C(28)	0.0559(4)	0.5594(4)	0.6299(4)	0.0411(9)
C(29)	0.0938(4)	0.6088(4)	0.6928(3)	0.0395(9)
C(30)	0.1921(4)	0.6474(3)	0.6707(3)	0.0353(8)
C(31)	0.2541(4)	0.6350(3)	0.5835(3)	0.0307(8)
C(32)	0.3473(7)	0.9438(5)	0.5850(4)	0.059(1)
C(33)	0.4854(6)	0.8619(4)	0.4531(4)	0.054(1)
C(34)	0.2047(6)	0.6706(5)	0.3482(4)	0.057(1)
C(35)	0.3477(6)	0.4759(4)	0.3946(4)	0.053(1)
C(36)	0.3682(7)	0.8163(5)	0.8561(4)	0.062(1)
C(37)	0.355(1)	0.9285(6)	0.8630(7)	0.098(3)
Ag(2)	0.5048(1)	0.21357(9)	0.21782(7)	0.0653(2)
O(41)	0.7815(4)	0.3153(3)	0.2767(3)	0.0557(9)
O(42)	0.3117(5)	0.1503(4)	0.3242(3)	0.062(1)
N(41)	0.5169(6)	0.3798(4)	0.1644(3)	0.057(1)
N(42)	0.2924(6)	0.3409(5)	0.2062(3)	0.063(1)
N(43)	0.6572(8)	0.0494(6)	0.2389(4)	0.077(2)
C(41)	0.7539(8)	0.3088(7)	0.1805(5)	0.070(2)
C(42)	0.6248(8)	0.3970(6)	0.1492(4)	0.064(2)
C(43)	0.625(1)	0.5010(7)	0.1063(5)	0.074(2)
C(44)	0.502(1)	0.5841(6)	0.0808(5)	0.078(2)
C(45)	0.3879(9)	0.5649(6)	0.0984(4)	0.066(2)
C(46)	0.2571(9)	0.6511(6)	0.0783(4)	0.076(2)
C(47)	0.1483(9)	0.6311(7)	0.0986(4)	0.073(2)

Table 2.39 continued

C(48)	0.1553(9)	0.5290(7)	0.1447(4)	0.071(2)
C(49)	0.0409(8)	0.5083(8)	0.1716(5)	0.086(2)
C(50)	0.0535(8)	0.4102(8)	0.2167(5)	0.082(2)
C(51)	0.1777(8)	0.3262(7)	0.2322(4)	0.069(2)
C(52)	0.2792(6)	0.4412(5)	0.1626(3)	0.054(1)
C(53)	0.3974(8)	0.4631(6)	0.1411(4)	0.059(2)
C(54)	0.1918(8)	0.2156(7)	0.2753(4)	0.074(2)
C(55)	0.3326(5)	0.1793(4)	0.4109(3)	0.045(1)
C(56)	0.2343(5)	0.2423(4)	0.4643(4)	0.047(1)
C(57)	0.2689(5)	0.2611(4)	0.5499(3)	0.0419(9)
C(58)	0.3996(4)	0.2212(3)	0.5785(3)	0.0318(7)
C(59)	0.4603(4)	0.2320(3)	0.6670(3)	0.0346(8)
C(60)	0.6060(5)	0.2033(4)	0.6386(4)	0.040(1)
C(61)	0.6341(4)	0.1266(4)	0.5627(3)	0.0401(9)
C(62)	0.4966(4)	0.1608(3)	0.5220(3)	0.0318(8)
C(63)	0.4627(6)	0.1382(4)	0.4383(4)	0.042(1)
C(64)	0.6997(5)	0.0058(4)	0.6030(4)	0.050(1)
C(65)	0.8435(6)	-0.0384(5)	0.5712(5)	0.057(1)
C(66)	0.8425(5)	0.0473(4)	0.4861(4)	0.048(1)
C(67)	0.9338(5)	0.0415(5)	0.4153(5)	0.058(1)
C(68)	0.9130(5)	0.1283(5)	0.3446(4)	0.056(1)
C(69)	0.8006(5)	0.2242(4)	0.3443(4)	0.047(1)
C(70)	0.7059(5)	0.2311(4)	0.4147(3)	0.0422(9)
C(71)	0.7280(5)	0.1409(4)	0.4840(4)	0.040(1)
C(72)	0.3979(5)	0.3445(4)	0.6943(3)	0.044(1)
C(73)	0.4503(5)	0.1493(4)	0.7513(3)	0.045(1)
C(74)	0.9368(6)	-0.0444(6)	0.6510(5)	0.073(2)
C(75)	0.8841(6)	-0.1510(5)	0.5446(6)	0.072(2)
C(76)	0.748(1)	-0.0329(7)	0.2469(5)	0.084(2)
C(77)	0.858(1)	-0.1337(9)	0.2529(9)	0.128(4)
C(81a)†	0.7551(8)	0.8495(5)	0.9073(5)	0.091(3)
F(1a)†	0.691(1)	0.9420(4)	0.9349(8)	0.126(4)
F(2a)†	0.702(2)	0.8404(9)	0.8318(5)	0.114(4)
F(3a)†	0.8805(9)	0.8291(8)	0.8974(8)	0.129(4)
S(1a)†	0.7421(6)	0.7421(4)	1.0073(3)	0.055(1)
O(81a)†	0.800(1)	0.6448(4)	0.9749(6)	0.084(3)
O(82a)†	0.6089(7)	0.7696(9)	1.0238(9)	0.115(5)
O(83a)†	0.809(1)	0.7460(9)	1.0851(5)	0.125(4)
C(81b)•	0.7648(9)	0.8598(6)	0.8982(5)	0.099(3)
F(1b)•	0.673(1)	0.9567(5)	0.8888(8)	0.111(4)
F(2b)•	0.766(2)	0.8120(8)	0.8269(5)	0.108(5)
F(3b)•	0.881(1)	0.859(1)	0.9155(9)	0.130(5)
S(1b)•	0.7225(6)	0.7788(6)	1.0081(4)	0.065(1)
O(81b)•	0.805(1)	0.6724(6)	1.0089(8)	0.107(4)
O(82b)•	0.5905(7)	0.797(1)	0.9975(8)	0.083(3)
O(83b)•	0.745(1)	0.818(1)	1.0857(5)	0.132(5)
C(82a)‡	0.2243(9)	-0.0541(6)	0.1570(8)	0.068(4)
F(4a)‡	0.228(2)	-0.1462(5)	0.141(2)	0.174(7)
F(5a)‡	0.201(1)	-0.044(2)	0.2461(6)	0.166(5)
F(6a)‡	0.3287(7)	-0.037(1)	0.127(1)	0.132(5)

Table 2.39 continued

S(2a)‡	0.0778(8)	0.0550(6)	0.0850(5)	0.062(2)
O(84a)‡	0.057(1)	0.1505(5)	0.1165(8)	0.062(3)
O(85a)‡	-0.029(1)	0.025(1)	0.105(1)	0.209(8)
O(86a)‡	0.111(2)	0.058(1)	-0.0093(5)	0.189(8)
C(82b)§	0.2446(9)	-0.0569(7)	0.1857(8)	0.117(8)
F(4b)§	0.292(2)	-0.1557(5)	0.170(1)	0.163(6)
F(5b)§	0.188(1)	-0.049(1)	0.2681(6)	0.158(5)
F(6b)§	0.3315(8)	-0.014(1)	0.174(1)	0.106(4)
S(2b)§	0.1085(8)	0.0243(8)	0.0920(6)	0.072(2)
O(84b)§	0.075(1)	0.1316(7)	0.098(1)	0.110(4)
O(85b)§	0.005(1)	-0.008(1)	0.117(1)	0.184(7)
O(86b)§	0.160(2)	-0.001(2)	0.0054(7)	0.194(8)

parameters (Å^2) with standard uncertainties in parentheses.

* U_{eq} is defined as one third of the trace of the orthogonalized U^{ij} tensor.

† Disordered atom with site occupation factor of 0.53(1).

• Disordered atom with site occupation factor of 0.47(1).

‡ Disordered atom with site occupation factor of 0.48(2).

§ Disordered atom with site occupation factor of 0.52(2).

Table 2.40 Bond Lengths (Å) with Standard Uncertainties and Parentheses of **80**

Ag(1) -N(3)	2.144(5)	C(43) -C(44)	1.39(1)
Ag(1) -N(2)	2.308(5)	C(44) -C(45)	1.39(1)
Ag(1) -N(1)	2.326(4)	C(45) -C(53)	1.39(1)
O(1) -C(29)	1.371(6)	C(45) -C(46)	1.46(1)
O(1) -C(1)	1.449(7)	C(46) -C(47)	1.34(1)
O(2) -C(15)	1.386(6)	C(47) -C(48)	1.41(1)
O(2) -C(14)	1.429(9)	C(48) -C(52)	1.42(1)
N(1) -C(2)	1.327(9)	C(48) -C(49)	1.42(1)
N(1) -C(13)	1.386(8)	C(49) -C(50)	1.34(1)
N(2) -C(11)	1.318(9)	C(50) -C(51)	1.39(1)
N(2) -C(12)	1.349(8)	C(51) -C(54)	1.48(1)
N(3) -C(36)	1.108(8)	C(52) -C(53)	1.453(9)
C(1) -C(2)	1.48(1)	C(55) -C(63)	1.366(8)
C(2) -C(3)	1.394(9)	C(55) -C(56)	1.380(8)
C(3) -C(4)	1.43(1)	C(56) -C(57)	1.389(7)
C(4) -C(5)	1.40(2)	C(57) -C(58)	1.377(6)
C(5) -C(13)	1.41(1)	C(58) -C(62)	1.386(6)
C(5) -C(6)	1.45(1)	C(58) -C(59)	1.511(6)
C(6) -C(7)	1.30(1)	C(59) -C(72)	1.528(6)
C(7) -C(8)	1.44(1)	C(59) -C(73)	1.534(6)
C(8) -C(9)	1.41(2)	C(59) -C(60)	1.545(6)
C(8) -C(12)	1.45(1)	C(60) -C(61)	1.571(7)
C(9) -C(10)	1.37(1)	C(61) -C(62)	1.510(6)
C(10) -C(11)	1.42(1)	C(61) -C(71)	1.529(6)
C(11) -C(14)	1.47(1)	C(61) -C(64)	1.534(6)
C(12) -C(13)	1.43(1)	C(62) -C(63)	1.385(6)
C(15) -C(16)	1.380(7)	C(64) -C(65)	1.533(8)

Table 2.40 continued

C(15) -C(23)	1.383(7)	C(65) -C(66)	1.532(8)
C(16) -C(17)	1.413(8)	C(65) -C(75)	1.535(9)
C(17) -C(18)	1.371(8)	C(65) -C(74)	1.540(9)
C(18) -C(22)	1.417(7)	C(66) -C(67)	1.379(8)
C(18) -C(19)	1.521(7)	C(66) -C(71)	1.396(7)
C(19) -C(20)	1.523(7)	C(67) -C(68)	1.370(9)
C(19) -C(33)	1.528(7)	C(68) -C(69)	1.405(8)
C(19) -C(32)	1.533(7)	C(69) -C(70)	1.398(7)
C(20) -C(21)	1.570(6)	C(70) -C(71)	1.388(7)
C(21) -C(22)	1.514(7)	C(76) -C(77)	1.43(1)
C(21) -C(31)	1.528(6)	C(81a)-F(2a)	1.299(3)
C(21) -C(24)	1.553(6)	C(81a)-F(3a)	1.301(3)
C(22) -C(23)	1.396(7)	C(81a)-F(1a)	1.302(3)
C(24) -C(25)	1.558(7)	C(81a)-S(1a)	1.907(5)
C(25) -C(26)	1.508(6)	S(1a) -O(81a)	1.381(3)
C(25) -C(35)	1.518(7)	S(1a) -O(82a)	1.382(3)
C(25) -C(34)	1.541(7)	S(1a) -O(83a)	1.383(3)
C(26) -C(31)	1.385(6)	C(81b)-F(2b)	1.297(3)
C(26) -C(27)	1.403(6)	C(81b)-F(3b)	1.302(3)
C(27) -C(28)	1.405(7)	C(81b)-F(1b)	1.302(3)
C(28) -C(29)	1.379(7)	C(81b)-S(1b)	1.907(5)
C(29) -C(30)	1.381(6)	S(1b) -O(81b)	1.377(3)
C(30) -C(31)	1.393(6)	S(1b) -O(83b)	1.382(3)
C(36) -C(37)	1.503(9)	S(1b) -O(82b)	1.386(3)
Ag(2) -N(43)	2.191(7)	C(82a)-F(6a)	1.297(3)
Ag(2) -N(42)	2.293(6)	C(82a)-F(5a)	1.303(3)
Ag(2) -N(41)	2.323(5)	C(82a)-F(4a)	1.305(3)
Ag(2) -O(42)	2.870(4)	C(82a)-S(2a)	1.903(5)
O(41) -C(69)	1.388(7)	S(2a) -O(86a)	1.373(3)
O(41) -C(41)	1.444(8)	S(2a) -O(84a)	1.385(3)
O(42) -C(54)	1.405(9)	S(2a) -O(85a)	1.390(3)
O(42) -C(55)	1.416(6)	C(82b)-F(6b)	1.298(3)
N(41) -C(42)	1.301(9)	C(82b)-F(4b)	1.300(3)
N(41) -C(53)	1.368(9)	C(82b)-F(5b)	1.304(3)
N(42) -C(52)	1.359(8)	C(82b)-S(2b)	1.908(5)
N(42) -C(51)	1.378(9)	S(2b) -O(86b)	1.375(3)
N(43) -C(76)	1.17(1)	S(2b) -O(84b)	1.381(3)
C(41) -C(42)	1.48(1)	S(2b) -O(85b)	1.388(3)
C(42) -C(43)	1.45(1)		

Table 2.41 Bond Angles (°) with Standard Uncertainties in Parentheses of **80**

N(3) -Ag(1) -N(2)	146.5(2)	C(46) -C(47) -C(48)	121.7(8)
N(3) -Ag(1) -N(1)	131.0(2)	C(47) -C(48) -C(52)	120.4(7)
N(2) -Ag(1) -N(1)	73.3(2)	C(47) -C(48) -C(49)	122.4(8)
C(29) -O(1) -C(1)	117.7(4)	C(52) -C(48) -C(49)	117.2(7)
C(15) -O(2) -C(14)	117.6(5)	C(50) -C(49) -C(48)	119.8(8)
C(2) -N(1) -C(13)	118.8(5)	C(49) -C(50) -C(51)	120.8(7)
C(2) -N(1) -Ag(1)	127.2(4)	N(42) -C(51) -C(50)	122.1(7)

Table 2.41 continued

C(13) -N(1) -Ag(1)	113.9(4)	N(42) -C(51) -C(54)	116.9(7)
C(11) -N(2) -C(12)	121.7(6)	C(50) -C(51) -C(54)	121.1(7)
C(11) -N(2) -Ag(1)	124.2(4)	N(42) -C(52) -C(48)	123.2(6)
C(12) -N(2) -Ag(1)	114.1(5)	N(42) -C(52) -C(53)	118.9(6)
C(36) -N(3) -Ag(1)	170.7(6)	C(48) -C(52) -C(53)	117.6(6)
O(1) -C(1) -C(2)	111.1(5)	N(41) -C(53) -C(45)	121.9(7)
N(1) -C(2) -C(3)	124.5(7)	N(41) -C(53) -C(52)	117.5(6)
N(1) -C(2) -C(1)	118.4(5)	C(45) -C(53) -C(52)	120.6(7)
C(3) -C(2) -C(1)	117.1(7)	O(42) -C(54) -C(51)	116.0(5)
C(2) -C(3) -C(4)	117.2(9)	C(63) -C(55) -C(56)	121.9(4)
C(5) -C(4) -C(3)	119.4(6)	C(63) -C(55) -O(42)	113.1(5)
C(4) -C(5) -C(13)	119.2(8)	C(56) -C(55) -O(42)	125.1(5)
C(4) -C(5) -C(6)	123.0(8)	C(55) -C(56) -C(57)	118.8(4)
C(13) -C(5) -C(6)	117.8(9)	C(58) -C(57) -C(56)	120.3(4)
C(7) -C(6) -C(5)	121.6(8)	C(57) -C(58) -C(62)	119.6(4)
C(6) -C(7) -C(8)	122.9(8)	C(57) -C(58) -C(59)	129.7(4)
C(9) -C(8) -C(7)	125.5(8)	C(62) -C(58) -C(59)	110.7(4)
C(9) -C(8) -C(12)	116.3(7)	C(58) -C(59) -C(72)	113.9(3)
C(7) -C(8) -C(12)	118.1(9)	C(58) -C(59) -C(73)	109.9(3)
C(10) -C(9) -C(8)	120.5(7)	C(72) -C(59) -C(73)	108.9(4)
C(9) -C(10) -C(11)	119.9(9)	C(58) -C(59) -C(60)	101.9(3)
N(2) -C(11) -C(10)	120.6(7)	C(72) -C(59) -C(60)	111.8(4)
N(2) -C(11) -C(14)	117.4(6)	C(73) -C(59) -C(60)	110.3(4)
C(10) -C(11) -C(14)	121.9(7)	C(59) -C(60) -C(61)	106.6(4)
N(2) -C(12) -C(13)	121.1(6)	C(62) -C(61) -C(71)	110.4(4)
N(2) -C(12) -C(8)	120.9(7)	C(62) -C(61) -C(64)	113.8(4)
C(13) -C(12) -C(8)	118.0(6)	C(71) -C(61) -C(64)	102.6(4)
N(1) -C(13) -C(5)	120.8(8)	C(62) -C(61) -C(60)	100.6(3)
N(1) -C(13) -C(12)	117.7(5)	C(71) -C(61) -C(60)	115.1(4)
C(5) -C(13) -C(12)	121.5(7)	C(64) -C(61) -C(60)	114.8(4)
O(2) -C(14) -C(11)	108.7(5)	C(63) -C(62) -C(58)	120.5(4)
C(16) -C(15) -C(23)	121.3(5)	C(63) -C(62) -C(61)	127.1(4)
C(16) -C(15) -O(2)	121.1(5)	C(58) -C(62) -C(61)	112.4(4)
C(23) -C(15) -O(2)	117.3(5)	C(55) -C(63) -C(62)	118.9(5)
C(15) -C(16) -C(17)	119.0(5)	C(65) -C(64) -C(61)	109.3(4)
C(18) -C(17) -C(16)	120.5(5)	C(66) -C(65) -C(64)	102.2(4)
C(17) -C(18) -C(22)	119.8(5)	C(66) -C(65) -C(75)	113.0(5)
C(17) -C(18) -C(19)	130.1(4)	C(64) -C(65) -C(75)	111.6(5)
C(22) -C(18) -C(19)	110.0(4)	C(66) -C(65) -C(74)	110.6(5)
C(18) -C(19) -C(20)	103.3(4)	C(64) -C(65) -C(74)	110.2(5)
C(18) -C(19) -C(33)	109.9(4)	C(75) -C(65) -C(74)	109.1(5)
C(20) -C(19) -C(33)	112.4(4)	C(67) -C(66) -C(71)	119.8(5)
C(18) -C(19) -C(32)	111.4(5)	C(67) -C(66) -C(65)	129.2(5)
C(20) -C(19) -C(32)	110.8(4)	C(71) -C(66) -C(65)	111.0(4)
C(33) -C(19) -C(32)	108.9(4)	C(68) -C(67) -C(66)	119.7(5)
C(19) -C(20) -C(21)	108.5(4)	C(67) -C(68) -C(69)	120.7(5)
C(22) -C(21) -C(31)	114.9(4)	O(41) -C(69) -C(70)	118.0(5)
C(22) -C(21) -C(24)	112.4(4)	O(41) -C(69) -C(68)	121.7(4)
C(31) -C(21) -C(24)	101.6(4)	C(70) -C(69) -C(68)	120.3(5)
C(22) -C(21) -C(20)	101.2(4)	C(71) -C(70) -C(69)	117.7(5)

Table 2.41 continued

C(31) -C(21) -C(20)	111.5(4)	C(70) -C(71) -C(66)	121.7(4)
C(24) -C(21) -C(20)	115.8(4)	C(70) -C(71) -C(61)	126.9(4)
C(23) -C(22) -C(18)	119.5(5)	C(66) -C(71) -C(61)	111.3(4)
C(23) -C(22) -C(21)	128.1(4)	N(43) -C(76) -C(77)	177.8(8)
C(18) -C(22) -C(21)	112.2(4)	F(2a) -C(81a)-F(3a)	112.4(3)
C(15) -C(23) -C(22)	119.7(4)	F(2a) -C(81a)-F(1a)	112.2(3)
C(21) -C(24) -C(25)	107.5(4)	F(3a) -C(81a)-F(1a)	112.1(3)
C(26) -C(25) -C(35)	113.8(4)	F(2a) -C(81a)-S(1a)	106.7(3)
C(26) -C(25) -C(34)	109.7(4)	F(3a) -C(81a)-S(1a)	106.5(3)
C(35) -C(25) -C(34)	109.0(4)	F(1a) -C(81a)-S(1a)	106.4(3)
C(26) -C(25) -C(24)	101.7(4)	O(81a)-S(1a) -O(82a)	112.4(3)
C(35) -C(25) -C(24)	111.3(4)	O(81a)-S(1a) -O(83a)	112.2(3)
C(34) -C(25) -C(24)	111.2(4)	O(82a)-S(1a) -O(83a)	112.2(3)
C(31) -C(26) -C(27)	119.7(4)	O(81a)-S(1a) -C(81a)	106.6(2)
C(31) -C(26) -C(25)	112.4(4)	O(82a)-S(1a) -C(81a)	106.5(3)
C(27) -C(26) -C(25)	127.8(4)	O(83a)-S(1a) -C(81a)	106.4(3)
C(26) -C(27) -C(28)	118.9(4)	F(2b) -C(81b)-F(3b)	112.5(3)
C(29) -C(28) -C(27)	120.2(4)	F(2b) -C(81b)-F(1b)	112.2(3)
O(1) -C(29) -C(28)	114.9(4)	F(3b) -C(81b)-F(1b)	112.1(3)
O(1) -C(29) -C(30)	123.6(4)	F(2b) -C(81b)-S(1b)	106.7(3)
C(28) -C(29) -C(30)	121.1(4)	F(3b) -C(81b)-S(1b)	106.4(3)
C(29) -C(30) -C(31)	118.9(4)	F(1b) -C(81b)-S(1b)	106.4(3)
C(26) -C(31) -C(30)	121.1(4)	O(81b)-S(1b) -O(83b)	112.5(3)
C(26) -C(31) -C(21)	111.1(4)	O(81b)-S(1b) -O(82b)	112.4(3)
C(30) -C(31) -C(21)	127.7(4)	O(83b)-S(1b) -O(82b)	112.0(3)
N(3) -C(36) -C(37)	179.6(7)	O(81b)-S(1b) -C(81b)	106.7(3)
N(43) -Ag(2) -N(42)	155.2(2)	O(83b)-S(1b) -C(81b)	106.4(3)
N(43) -Ag(2) -N(41)	131.5(2)	O(82b)-S(1b) -C(81b)	106.3(3)
N(42) -Ag(2) -N(41)	72.9(2)	F(6a) -C(82a)-F(5a)	112.4(3)
N(43) -Ag(2) -O(42)	93.6(2)	F(6a) -C(82a)-F(4a)	112.3(3)
N(42) -Ag(2) -O(42)	64.2(2)	F(5a) -C(82a)-F(4a)	111.7(3)
N(41) -Ag(2) -O(42)	133.1(2)	F(6a) -C(82a)-S(2a)	106.9(3)
C(69) -O(41) -C(41)	116.1(5)	F(5a) -C(82a)-S(2a)	106.6(3)
C(54) -O(42) -C(55)	116.3(5)	F(4a) -C(82a)-S(2a)	106.5(3)
C(54) -O(42) -Ag(2)	104.2(3)	O(86a)-S(2a) -O(84a)	112.7(3)
C(55) -O(42) -Ag(2)	96.3(3)	O(86a)-S(2a) -O(85a)	112.2(3)
C(42) -N(41) -C(53)	119.3(6)	O(84a)-S(2a) -O(85a)	111.4(3)
C(42) -N(41) -Ag(2)	125.9(5)	O(86a)-S(2a) -C(82a)	107.2(3)
C(53) -N(41) -Ag(2)	114.6(4)	O(84a)-S(2a) -C(82a)	106.6(2)
C(52) -N(42) -C(51)	116.9(6)	O(85a)-S(2a) -C(82a)	106.3(3)
C(52) -N(42) -Ag(2)	115.0(4)	F(6b) -C(82b)-F(4b)	112.5(3)
C(51) -N(42) -Ag(2)	127.9(5)	F(6b) -C(82b)-F(5b)	112.3(3)
C(76) -N(43) -Ag(2)	172.8(7)	F(4b) -C(82b)-F(5b)	112.0(3)
O(41) -C(41) -C(42)	108.1(5)	F(6b) -C(82b)-S(2b)	106.6(3)
N(41) -C(42) -C(43)	122.8(7)	F(4b) -C(82b)-S(2b)	106.5(3)
N(41) -C(42) -C(41)	119.4(6)	F(5b) -C(82b)-S(2b)	106.3(3)
C(43) -C(42) -C(41)	117.8(7)	O(86b)-S(2b) -O(84b)	112.7(3)
C(44) -C(43) -C(42)	117.0(7)	O(86b)-S(2b) -O(85b)	112.3(3)
C(45) -C(44) -C(43)	119.7(7)	O(84b)-S(2b) -O(85b)	111.9(3)
C(53) -C(45) -C(44)	119.3(7)	O(86b)-S(2b) -C(82b)	106.8(3)

Table 2.41 continued

C(53) -C(45) -C(46)	119.0(7)	O(84b)-S(2b) -C(82b)	106.5(3)
C(44) -C(45) -C(46)	121.5(7)	O(85b)-S(2b) -C(82b)	106.1(3)
C(47) -C(46) -C(45)	120.3(7)		

Table 2.42 Torsion angles (°) with standard uncertainties in parentheses of **80**

N(3) -Ag(1) -N(1) -C(2)	25.3(5)	N(41) -C(42) -C(43) -C(44)	0(1)
N(2) -Ag(1) -N(1) -C(2)	178.4(4)	C(41) -C(42) -C(43) -C(44)	-177.5(6)
N(3) -Ag(1) -N(1) -C(13)	-150.8(3)	C(42) -C(43) -C(44) -C(45)	1(1)
N(2) -Ag(1) -N(1) -C(13)	2.3(3)	C(43) -C(44) -C(45) -C(53)	0.0(9)
N(3) -Ag(1) -N(2) -C(11)	-39.8(6)	C(43) -C(44) -C(45) -C(46)	176.2(6)
N(1) -Ag(1) -N(2) -C(11)	178.4(5)	C(53) -C(45) -C(46) -C(47)	-1.8(9)
N(3) -Ag(1) -N(2) -C(12)	139.7(4)	C(44) -C(45) -C(46) -C(47)	-178.0(6)
N(1) -Ag(1) -N(2) -C(12)	-2.1(3)	C(45) -C(46) -C(47) -C(48)	4(1)
C(29) -O(1) -C(1) -C(2)	-76.8(6)	C(46) -C(47) -C(48) -C(52)	-6(1)
C(13) -N(1) -C(2) -C(3)	1.3(8)	C(46) -C(47) -C(48) -C(49)	176.2(6)
Ag(1) -N(1) -C(2) -C(3)	-174.7(5)	C(47) -C(48) -C(49) -C(50)	-178.9(7)
C(13) -N(1) -C(2) -C(1)	-179.5(4)	C(52) -C(48) -C(49) -C(50)	4(1)
Ag(1) -N(1) -C(2) -C(1)	4.5(7)	C(48) -C(49) -C(50) -C(51)	-4(1)
O(1) -C(1) -C(2) -N(1)	111.5(5)	C(52) -N(42) -C(51) -C(50)	-1.3(9)
O(1) -C(1) -C(2) -C(3)	-69.2(7)	Ag(2) -N(42) -C(51) -C(50)	-176.7(5)
N(1) -C(2) -C(3) -C(4)	-4(1)	C(52) -N(42) -C(51) -C(54)	177.0(5)
C(1) -C(2) -C(3) -C(4)	177.2(6)	Ag(2) -N(42) -C(51) -C(54)	1.6(8)
C(2) -C(3) -C(4) -C(5)	3(1)	C(49) -C(50) -C(51) -N(42)	3(1)
C(3) -C(4) -C(5) -C(13)	0(1)	C(49) -C(50) -C(51) -C(54)	-175.2(7)
C(3) -C(4) -C(5) -C(6)	178.8(7)	C(51) -N(42) -C(52) -C(48)	0.8(8)
C(4) -C(5) -C(6) -C(7)	-177.2(7)	Ag(2) -N(42) -C(52) -C(48)	176.8(4)
C(13) -C(5) -C(6) -C(7)	2(1)	C(51) -N(42) -C(52) -C(53)	174.8(5)
C(5) -C(6) -C(7) -C(8)	-4(1)	Ag(2) -N(42) -C(52) -C(53)	-9.2(6)
C(6) -C(7) -C(8) -C(9)	179.9(7)	C(47) -C(48) -C(52) -N(42)	-179.6(5)
C(6) -C(7) -C(8) -C(12)	4(1)	C(49) -C(48) -C(52) -N(42)	-1.9(9)
C(7) -C(8) -C(9) -C(10)	-179.8(7)	C(47) -C(48) -C(52) -C(53)	6.3(8)
C(12) -C(8) -C(9) -C(10)	-4(1)	C(49) -C(48) -C(52) -C(53)	-176.0(5)
C(8) -C(9) -C(10) -C(11)	3(1)	C(42) -N(41) -C(53) -C(45)	2.5(8)
C(12) -N(2) -C(11) -C(10)	-0.7(9)	Ag(2) -N(41) -C(53) -C(45)	-172.8(4)
Ag(1) -N(2) -C(11) -C(10)	178.7(5)	C(42) -N(41) -C(53) -C(52)	-177.7(5)
C(12) -N(2) -C(11) -C(14)	175.6(6)	Ag(2) -N(41) -C(53) -C(52)	6.9(6)
Ag(1) -N(2) -C(11) -C(14)	-5.0(8)	C(44) -C(45) -C(53) -N(41)	-1.8(8)
C(9) -C(10) -C(11) -N(2)	-1(1)	C(46) -C(45) -C(53) -N(41)	-178.0(5)
C(9) -C(10) -C(11) -C(14)	-176.9(7)	C(44) -C(45) -C(53) -C(52)	178.5(5)
C(11) -N(2) -C(12) -C(13)	-178.8(5)	C(46) -C(45) -C(53) -C(52)	2.2(8)
Ag(1) -N(2) -C(12) -C(13)	1.8(6)	N(42) -C(52) -C(53) -N(41)	1.4(7)
C(11) -N(2) -C(12) -C(8)	-0.2(8)	C(48) -C(52) -C(53) -N(41)	175.8(5)
Ag(1) -N(2) -C(12) -C(8)	-179.6(4)	N(42) -C(52) -C(53) -C(45)	-178.8(5)
C(9) -C(8) -C(12) -N(2)	2.3(8)	C(48) -C(52) -C(53) -C(45)	-4.4(7)
C(7) -C(8) -C(12) -N(2)	178.7(5)	C(55) -O(42) -C(54) -C(51)	69.7(8)
C(9) -C(8) -C(12) -C(13)	-179.0(6)	Ag(2) -O(42) -C(54) -C(51)	-34.8(7)
C(7) -C(8) -C(12) -C(13)	-2.6(8)	N(42) -C(51) -C(54) -O(42)	27.9(9)
C(2) -N(1) -C(13) -C(5)	1.7(7)	C(50) -C(51) -C(54) -O(42)	-153.8(6)

Table 2.42 continued

Ag(1) -N(1) -C(13) -C(5)	178.2(4)	C(54) -O(42) -C(55) -C(63)	-159.6(5)
C(2) -N(1) -C(13) -C(12)	-178.8(5)	Ag(2) -O(42) -C(55) -C(63)	-50.4(4)
Ag(1) -N(1) -C(13) -C(12)	-2.3(5)	C(54) -O(42) -C(55) -C(56)	20.5(7)
C(4) -C(5) -C(13) -N(1)	-2.1(9)	Ag(2) -O(42) -C(55) -C(56)	129.7(4)
C(6) -C(5) -C(13) -N(1)	178.7(5)	C(63) -C(55) -C(56) -C(57)	-2.2(7)
C(4) -C(5) -C(13) -C(12)	178.4(6)	O(42) -C(55) -C(56) -C(57)	177.7(4)
C(6) -C(5) -C(13) -C(12)	-0.8(9)	C(55) -C(56) -C(57) -C(58)	2.7(7)
N(2) -C(12) -C(13) -N(1)	0.4(7)	C(56) -C(57) -C(58) -C(62)	-0.8(7)
C(8) -C(12) -C(13) -N(1)	-178.3(5)	C(56) -C(57) -C(58) -C(59)	179.4(4)
N(2) -C(12) -C(13) -C(5)	179.9(5)	C(57) -C(58) -C(59) -C(72)	-41.4(6)
C(8) -C(12) -C(13) -C(5)	1.2(8)	C(62) -C(58) -C(59) -C(72)	138.8(4)
C(15) -O(2) -C(14) -C(11)	114.9(6)	C(57) -C(58) -C(59) -C(73)	81.2(5)
N(2) -C(11) -C(14) -O(2)	-73.4(8)	C(62) -C(58) -C(59) -C(73)	-98.6(4)
C(10) -C(11) -C(14) -O(2)	102.8(7)	C(57) -C(58) -C(59) -C(60)	-161.9(4)
C(14) -O(2) -C(15) -C(16)	62.7(7)	C(62) -C(58) -C(59) -C(60)	18.3(4)
C(14) -O(2) -C(15) -C(23)	-122.9(6)	C(58) -C(59) -C(60) -C(61)	-27.1(4)
C(23) -C(15) -C(16) -C(17)	0.6(8)	C(72) -C(59) -C(60) -C(61)	-149.2(4)
O(2) -C(15) -C(16) -C(17)	174.8(5)	C(73) -C(59) -C(60) -C(61)	89.5(4)
C(15) -C(16) -C(17) -C(18)	-1.5(8)	C(59) -C(60) -C(61) -C(62)	25.8(4)
C(16) -C(17) -C(18) -C(22)	1.9(8)	C(59) -C(60) -C(61) -C(71)	144.5(4)
C(16) -C(17) -C(18) -C(19)	-174.1(5)	C(59) -C(60) -C(61) -C(64)	-96.8(4)
C(17) -C(18) -C(19) -C(20)	-169.8(5)	C(57) -C(58) -C(62) -C(63)	-1.6(6)
C(22) -C(18) -C(19) -C(20)	13.9(5)	C(59) -C(58) -C(62) -C(63)	178.2(4)
C(17) -C(18) -C(19) -C(33)	70.1(7)	C(57) -C(58) -C(62) -C(61)	178.2(4)
C(22) -C(18) -C(19) -C(33)	-106.3(5)	C(59) -C(58) -C(62) -C(61)	-1.9(5)
C(17) -C(18) -C(19) -C(32)	-50.8(7)	C(71) -C(61) -C(62) -C(63)	42.8(6)
C(22) -C(18) -C(19) -C(32)	132.8(4)	C(64) -C(61) -C(62) -C(63)	-71.8(6)
C(18) -C(19) -C(20) -C(21)	-21.5(5)	C(60) -C(61) -C(62) -C(63)	164.9(4)
C(33) -C(19) -C(20) -C(21)	96.9(5)	C(71) -C(61) -C(62) -C(58)	-137.0(4)
C(32) -C(19) -C(20) -C(21)	-141.0(4)	C(64) -C(61) -C(62) -C(58)	108.3(4)
C(19) -C(20) -C(21) -C(22)	20.8(5)	C(60) -C(61) -C(62) -C(58)	-15.0(4)
C(19) -C(20) -C(21) -C(31)	143.5(4)	C(56) -C(55) -C(63) -C(62)	-0.3(7)
C(19) -C(20) -C(21) -C(24)	-101.1(5)	O(42) -C(55) -C(63) -C(62)	179.8(4)
C(17) -C(18) -C(22) -C(23)	-1.6(7)	C(58) -C(62) -C(63) -C(55)	2.2(6)
C(19) -C(18) -C(22) -C(23)	175.2(4)	C(61) -C(62) -C(63) -C(55)	-177.7(4)
C(17) -C(18) -C(22) -C(21)	-177.5(4)	C(62) -C(61) -C(64) -C(65)	136.2(5)
C(19) -C(18) -C(22) -C(21)	-0.7(5)	C(71) -C(61) -C(64) -C(65)	17.0(6)
C(31) -C(21) -C(22) -C(23)	52.0(6)	C(60) -C(61) -C(64) -C(65)	-108.6(5)
C(24) -C(21) -C(22) -C(23)	-63.5(6)	C(61) -C(64) -C(65) -C(66)	-19.2(6)
C(20) -C(21) -C(22) -C(23)	172.2(5)	C(61) -C(64) -C(65) -C(75)	-140.2(5)
C(31) -C(21) -C(22) -C(18)	-132.5(4)	C(61) -C(64) -C(65) -C(74)	98.5(6)
C(24) -C(21) -C(22) -C(18)	112.0(5)	C(64) -C(65) -C(66) -C(67)	-164.0(6)
C(20) -C(21) -C(22) -C(18)	-12.3(5)	C(75) -C(65) -C(66) -C(67)	-43.9(8)
C(16) -C(15) -C(23) -C(22)	-0.3(8)	C(74) -C(65) -C(66) -C(67)	78.7(8)
O(2) -C(15) -C(23) -C(22)	-174.6(4)	C(64) -C(65) -C(66) -C(71)	14.3(6)
C(18) -C(22) -C(23) -C(15)	0.7(7)	C(75) -C(65) -C(66) -C(71)	134.4(5)
C(21) -C(22) -C(23) -C(15)	175.9(4)	C(74) -C(65) -C(66) -C(71)	-103.0(6)
C(22) -C(21) -C(24) -C(25)	146.7(4)	C(71) -C(66) -C(67) -C(68)	1.4(9)
C(31) -C(21) -C(24) -C(25)	23.4(5)	C(65) -C(66) -C(67) -C(68)	179.6(6)
C(20) -C(21) -C(24) -C(25)	-97.6(5)	C(66) -C(67) -C(68) -C(69)	1.2(9)

Table 2.42 continued

C(21)	-C(24)	-C(25)	-C(26)	-22.8(5)	C(41)	-O(41)	-C(69)	-C(70)	-112.4(6)
C(21)	-C(24)	-C(25)	-C(35)	-144.3(4)	C(41)	-O(41)	-C(69)	-C(68)	69.4(7)
C(21)	-C(24)	-C(25)	-C(34)	93.9(5)	C(67)	-C(68)	-C(69)	-O(41)	176.1(5)
C(35)	-C(25)	-C(26)	-C(31)	133.3(5)	C(67)	-C(68)	-C(69)	-C(70)	-2.1(8)
C(34)	-C(25)	-C(26)	-C(31)	-104.2(5)	O(41)	-C(69)	-C(70)	-C(71)	-177.8(4)
C(24)	-C(25)	-C(26)	-C(31)	13.6(5)	C(68)	-C(69)	-C(70)	-C(71)	0.4(7)
C(35)	-C(25)	-C(26)	-C(27)	-49.7(7)	C(69)	-C(70)	-C(71)	-C(66)	2.2(7)
C(34)	-C(25)	-C(26)	-C(27)	72.7(6)	C(69)	-C(70)	-C(71)	-C(61)	-174.8(5)
C(24)	-C(25)	-C(26)	-C(27)	-169.4(4)	C(67)	-C(66)	-C(71)	-C(70)	-3.1(8)
C(31)	-C(26)	-C(27)	-C(28)	-2.1(6)	C(65)	-C(66)	-C(71)	-C(70)	178.4(5)
C(25)	-C(26)	-C(27)	-C(28)	-178.8(4)	C(67)	-C(66)	-C(71)	-C(61)	174.3(5)
C(26)	-C(27)	-C(28)	-C(29)	2.3(6)	C(65)	-C(66)	-C(71)	-C(61)	-4.2(6)
C(1)	-O(1)	-C(29)	-C(28)	145.7(5)	C(62)	-C(61)	-C(71)	-C(70)	47.8(7)
C(1)	-O(1)	-C(29)	-C(30)	-40.4(7)	C(64)	-C(61)	-C(71)	-C(70)	169.4(5)
C(27)	-C(28)	-C(29)	-O(1)	173.1(4)	C(60)	-C(61)	-C(71)	-C(70)	-65.3(7)
C(27)	-C(28)	-C(29)	-C(30)	-0.9(7)	C(62)	-C(61)	-C(71)	-C(66)	-129.5(4)
O(1)	-C(29)	-C(30)	-C(31)	-174.1(4)	C(64)	-C(61)	-C(71)	-C(66)	-7.9(6)
C(28)	-C(29)	-C(30)	-C(31)	-0.6(6)	C(60)	-C(61)	-C(71)	-C(66)	117.5(5)
C(27)	-C(26)	-C(31)	-C(30)	0.6(6)	F(2a)	-C(81a)	-S(1a)	-O(81a)	55.0(7)
C(25)	-C(26)	-C(31)	-C(30)	177.8(4)	F(3a)	-C(81a)	-S(1a)	-O(81a)	-65.3(7)
C(27)	-C(26)	-C(31)	-C(21)	-176.1(4)	F(1a)	-C(81a)	-S(1a)	-O(81a)	175.0(7)
C(25)	-C(26)	-C(31)	-C(21)	1.1(5)	F(2a)	-C(81a)	-S(1a)	-O(82a)	-65.2(7)
C(29)	-C(30)	-C(31)	-C(26)	0.8(6)	F(3a)	-C(81a)	-S(1a)	-O(82a)	174.6(7)
C(29)	-C(30)	-C(31)	-C(21)	176.9(4)	F(1a)	-C(81a)	-S(1a)	-O(82a)	54.8(7)
C(22)	-C(21)	-C(31)	-C(26)	-137.0(4)	F(2a)	-C(81a)	-S(1a)	-O(83a)	174.9(7)
C(24)	-C(21)	-C(31)	-C(26)	-15.3(5)	F(3a)	-C(81a)	-S(1a)	-O(83a)	54.7(7)
C(20)	-C(21)	-C(31)	-C(26)	108.6(4)	F(1a)	-C(81a)	-S(1a)	-O(83a)	-65.1(7)
C(22)	-C(21)	-C(31)	-C(30)	46.6(6)	F(2b)	-C(81b)	-S(1b)	-O(81b)	49.4(8)
C(24)	-C(21)	-C(31)	-C(30)	168.2(4)	F(3b)	-C(81b)	-S(1b)	-O(81b)	-70.9(8)
C(20)	-C(21)	-C(31)	-C(30)	-67.8(6)	F(1b)	-C(81b)	-S(1b)	-O(81b)	169.4(7)
N(43)	-Ag(2)	-O(42)	-C(54)	-143.3(4)	F(2b)	-C(81b)	-S(1b)	-O(83b)	169.7(7)
N(42)	-Ag(2)	-O(42)	-C(54)	25.3(4)	F(3b)	-C(81b)	-S(1b)	-O(83b)	49.4(8)
N(41)	-Ag(2)	-O(42)	-C(54)	51.0(4)	F(1b)	-C(81b)	-S(1b)	-O(83b)	-70.2(7)
N(43)	-Ag(2)	-O(42)	-C(55)	97.6(3)	F(2b)	-C(81b)	-S(1b)	-O(82b)	-70.8(7)
N(42)	-Ag(2)	-O(42)	-C(55)	-93.9(3)	F(3b)	-C(81b)	-S(1b)	-O(82b)	168.9(7)
N(41)	-Ag(2)	-O(42)	-C(55)	-68.1(4)	F(1b)	-C(81b)	-S(1b)	-O(82b)	49.2(7)
N(43)	-Ag(2)	-N(41)	-C(42)	-8.3(5)	F(6a)	-C(82a)	-S(2a)	-O(86a)	49(1)
N(42)	-Ag(2)	-N(41)	-C(42)	176.6(4)	F(5a)	-C(82a)	-S(2a)	-O(86a)	170(1)
O(42)	-Ag(2)	-N(41)	-C(42)	152.4(4)	F(4a)	-C(82a)	-S(2a)	-O(86a)	-71(1)
N(43)	-Ag(2)	-N(41)	-C(53)	166.7(3)	F(6a)	-C(82a)	-S(2a)	-O(84a)	-72(1)
N(42)	-Ag(2)	-N(41)	-C(53)	-8.5(3)	F(5a)	-C(82a)	-S(2a)	-O(84a)	49(1)
O(42)	-Ag(2)	-N(41)	-C(53)	-32.6(4)	F(4a)	-C(82a)	-S(2a)	-O(84a)	168(1)
N(43)	-Ag(2)	-N(42)	-C(52)	-162.1(4)	F(6a)	-C(82a)	-S(2a)	-O(85a)	169(1)
N(41)	-Ag(2)	-N(42)	-C(52)	9.2(3)	F(5a)	-C(82a)	-S(2a)	-O(85a)	-70(1)
O(42)	-Ag(2)	-N(42)	-C(52)	169.8(4)	F(4a)	-C(82a)	-S(2a)	-O(85a)	49(1)
N(43)	-Ag(2)	-N(42)	-C(51)	13.4(7)	F(6b)	-C(82b)	-S(2b)	-O(86b)	72(1)
N(41)	-Ag(2)	-N(42)	-C(51)	-175.3(5)	F(4b)	-C(82b)	-S(2b)	-O(86b)	-49(1)
O(42)	-Ag(2)	-N(42)	-C(51)	-14.8(4)	F(5b)	-C(82b)	-S(2b)	-O(86b)	-168(1)
C(69)	-O(41)	-C(41)	-C(42)	122.0(6)	F(6b)	-C(82b)	-S(2b)	-O(84b)	-49(1)
C(53)	-N(41)	-C(42)	-C(43)	-1.4(8)	F(4b)	-C(82b)	-S(2b)	-O(84b)	-169(1)

Table 2.42 continued

Ag(2) -N(41) -C(42) -C(43)	173.3(5)	F(5b) -C(82b)-S(2b) -O(84b)	71(1)
C(53) -N(41) -C(42) -C(41)	175.8(5)	F(6b) -C(82b)-S(2b) -O(85b)	-168(1)
Ag(2) -N(41) -C(42) -C(41)	-9.5(7)	F(4b) -C(82b)-S(2b) -O(85b)	71(1)
O(41) -C(41) -C(42) -N(41)	-89.9(7)	F(5b) -C(82b)-S(2b) -O(85b)	-48(1)
O(41) –C(41) –C(42) –C(43)	87.4(7)		

Table 2.43 Crystallographic Data of **81**

Crystallized from		MeCN / Et_2O
Empirical formula		$C_{40}H_{41.5}CuF_6N_{3.5}O_{2.5}P$
Formula weight [g mol^{-1}]		819.79
Crystal color, habit		yellow, prism
Crystal dimensions [mm]		0.15 × 0.23 × 0.30
Temperature [K]		160 (1)
Crystal system		monoclinic
Space group		*C*2 (#5)
Z		4
Reflections for cell determination		38895
2θ range for cell determination [°]		4–50
Unit cell parameters	*a* [Å]	24.2009 (7)
	b [Å]	11.3769 (4)
	c [Å]	14.4656 (5)
	α [°]	90
	β [°]	95.645 (1)
	γ [°]	90
	V [$Å^3$]	3963.5 (2)
F(000)		1696
D_x [g cm^{-3}]		1.374
μ(Mo *K*α) [mm^{-1}]		0.659
Scan type		ϕ and ω
$2\theta_{(max)}$ [°]		50
Transmission factors (min; max)		0.845; 0.930
Total reflections measured		27239
Symmetry independent reflections		6936
R_{int}		0.059
Reflections with $I > 2\sigma(I)$		5806
Reflections used in refinement		6935
Parameters refined; restraints		486; 1
Final *R(F)* [$I>2\sigma(I)$ reflections]		0.0446
wR(F^2) (all data)		0.1169
Weights:		$w = [\sigma^2(F_o^2) + (0.0772P)^2]^{-1}$ where $P = (F_o^2 + 2F_c^2)/3$
Goodness of fit		1.000
Secondary extinction coefficient		0.0019 (3)
Final Δ_{max}/σ		0.001
$\Delta\rho$ (max; min) [e $Å^{-3}$]		0.37; -0.36
$\sigma(d_{(C-C)})$ [Å]		0.005—0.007

Table 2.44 Fractional atomic coordinates and equivalent isotropic displacement of **81**

ATOM	x	y	z	U_{eq}^*
Cu	0.58409(2)	0.77632(4)	0.65816(3)	0.0464(2)
O(1)	0.5295(1)	1.0486(3)	0.7521(2)	0.0596(7)
O(2)	0.6264(1)	0.4366(2)	0.7831(2)	0.0490(6)
N(1)	0.5063(1)	0.8407(3)	0.6239(2)	0.0438(7)
N(2)	0.5436(1)	0.6203(3)	0.6454(2)	0.0417(7)
N(3)	0.6551(1)	0.8378(3)	0.6690(2)	0.0483(7)

Table 2.44 continued

C(1)	0.5298(2)	1.0452(4)	0.6537(3)	0.062(1)
C(2)	0.4877(2)	0.9534(4)	0.6175(3)	0.051(1)
C(3)	0.4332(2)	0.9803(4)	0.5850(3)	0.063(1)
C(4)	0.3964(2)	0.8918(4)	0.5610(3)	0.059(1)
C(5)	0.4133(1)	0.7738(5)	0.5701(2)	0.0496(8)
C(6)	0.3771(2)	0.6750(5)	0.5497(3)	0.054(1)
C(7)	0.3951(2)	0.5638(5)	0.5621(3)	0.057(1)
C(8)	0.4514(2)	0.5416(4)	0.5959(3)	0.050(1)
C(9)	0.4734(2)	0.4268(4)	0.6123(3)	0.058(1)
C(10)	0.5281(2)	0.4130(4)	0.6451(3)	0.054(1)
C(11)	0.5625(2)	0.5118(4)	0.6602(2)	0.0459(9)
C(12)	0.4893(2)	0.6359(4)	0.6133(2)	0.0413(9)
C(13)	0.4692(1)	0.7534(3)	0.6015(2)	0.0408(9)
C(14)	0.6217(2)	0.4950(4)	0.6939(3)	0.0478(9)
C(15)	0.6129(1)	0.5029(3)	0.8586(2)	0.0400(8)
C(16)	0.5853(1)	0.4419(3)	0.9238(2)	0.0418(8)
C(17)	0.5747(1)	0.4946(3)	1.0059(2)	0.0431(8)
C(18)	0.5918(1)	0.6110(3)	1.0227(2)	0.0374(8)
C(19)	0.5884(1)	0.6832(3)	1.1101(2)	0.0404(8)
C(20)	0.5998(1)	0.8089(3)	1.0734(2)	0.0427(8)
C(21)	0.6352(1)	0.7940(4)	0.9889(2)	0.0401(8)
C(22)	0.6180(1)	0.6725(3)	0.9562(2)	0.0342(7)
C(23)	0.6290(1)	0.6192(3)	0.8739(2)	0.0370(8)
C(24)	0.6998(1)	0.8006(4)	1.0149(3)	0.052(1)
C(25)	0.7193(2)	0.9223(4)	0.9894(3)	0.059(1)
C(26)	0.6735(2)	0.9631(4)	0.9183(3)	0.0503(9)
C(27)	0.6723(2)	1.0618(4)	0.8620(3)	0.063(1)
C(28)	0.6250(2)	1.0892(4)	0.8030(3)	0.063(1)
C(29)	0.5784(2)	1.0175(4)	0.8049(3)	0.0508(9)
C(30)	0.5786(2)	0.9206(3)	0.8619(3)	0.0441(8)
C(31)	0.6265(1)	0.8925(3)	0.9200(3)	0.0411(8)
C(32)	0.5313(1)	0.6768(4)	1.1464(3)	0.0501(9)
C(33)	0.6324(2)	0.6447(4)	1.1872(2)	0.0507(9)
C(34)	0.7759(2)	0.9174(6)	0.9512(4)	0.084(2)
C(35)	0.7231(2)	1.0043(5)	1.0751(4)	0.082(2)
C(36)	0.6984(2)	0.8795(4)	0.6733(3)	0.054(1)
C(37)	0.7532(2)	0.9336(5)	0.6770(3)	0.064(1)
P(1)	0.81657(5)	0.7241(1)	0.46769(9)	0.0560(3)
F(1)	0.7595(1)	0.7049(4)	0.5067(3)	0.125(1)
F(2)	0.7894(2)	0.7271(3)	0.3650(2)	0.131(2)
F(3)	0.8754(2)	0.7470(3)	0.4333(3)	0.130(2)
F(4)	0.8459(1)	0.7234(3)	0.5703(2)	0.096(1)
F(5)	0.8273(2)	0.5878(3)	0.4606(3)	0.105(1)
F(6)	0.8067(1)	0.8620(2)	0.4726(2)	0.0780(8)
N(4)†	0.7573(4)	0.6858(9)	0.7584(6)	0.082(3)
C(38)†	0.7680(4)	0.597(1)	0.7232(7)	0.068(3)
C(39)†	0.7831(5)	0.492(1)	0.6817(7)	0.089(4)

* U_{eq} is defined as one third of the trace of the orthogonalized U^{ij} tensor.

† Atom with site occupation factor of 0.491(9).

Table 2.45 Bond lengths (Å) with standard uncertainties in parentheses of **81**

Cu	-N(3)	1.848(3)	C(18)	-C(22)	1.392(5)
Cu	-N(2)	2.027(3)	C(18)	-C(19)	1.518(5)
Cu	-N(1)	2.035(3)	C(19)	-C(32)	1.526(4)
O(1)	-C(29)	1.389(5)	C(19)	-C(33)	1.528(5)
O(1)	-C(1)	1.425(5)	C(19)	-C(20)	1.560(5)
O(2)	-C(15)	1.393(4)	C(20)	-C(21)	1.569(5)
O(2)	-C(14)	1.446(5)	C(21)	-C(31)	1.500(5)
N(1)	-C(13)	1.358(5)	C(21)	-C(22)	1.506(5)
N(1)	-C(2)	1.359(5)	C(21)	-C(24)	1.574(4)
N(2)	-C(11)	1.327(5)	C(22)	-C(23)	1.385(5)
N(2)	-C(12)	1.363(5)	C(24)	-C(25)	1.520(6)
N(3)	-C(36)	1.146(5)	C(25)	-C(26)	1.509(6)
C(1)	-C(2)	1.515(6)	C(25)	-C(34)	1.529(6)
C(2)	-C(3)	1.391(6)	C(25)	-C(35)	1.547(7)
C(3)	-C(4)	1.367(7)	C(26)	-C(27)	1.385(6)
C(4)	-C(5)	1.406(7)	C(26)	-C(31)	1.395(5)
C(5)	-C(13)	1.403(5)	C(27)	-C(28)	1.394(6)
C(5)	-C(6)	1.437(7)	C(28)	-C(29)	1.395(6)
C(6)	-C(7)	1.345(7)	C(29)	-C(30)	1.377(5)
C(7)	-C(8)	1.423(6)	C(30)	-C(31)	1.400(5)
C(8)	-C(12)	1.417(6)	C(36)	-C(37)	1.459(5)
C(8)	-C(9)	1.422(6)	P(1)	-F(1)	1.558(3)
C(9)	-C(10)	1.371(6)	P(1)	-F(2)	1.565(3)
C(10)	-C(11)	1.403(6)	P(1)	-F(3)	1.575(3)
C(11)	-C(14)	1.480(5)	P(1)	-F(5)	1.577(3)
C(12)	-C(13)	1.428(6)	P(1)	-F(4)	1.581(3)
C(15)	-C(23)	1.391(5)	P(1)	-F(6)	1.589(3)
C(15)	-C(16)	1.393(5)	N(4)	-C(38)	1.17(1)
C(16)	-C(17)	1.377(5)	C(38)	-C(39)	1.40(2)
C(17)	-C(18)	1.401(5)			

Table 2.46 Bond angles (°) with standard uncertainties in parentheses of **81**

N(3)	-Cu	-N(2)	140.9(1)	C(32)	-C(19)	-C(20)	111.0(3)
N(3)	-Cu	-N(1)	135.6(1)	C(33)	-C(19)	-C(20)	112.1(3)
N(2)	-Cu	-N(1)	82.3(1)	C(19)	-C(20)	-C(21)	107.1(3)
C(29)	-O(1)	-C(1)	117.1(3)	C(31)	-C(21)	-C(22)	117.4(3)
C(15)	-O(2)	-C(14)	116.6(3)	C(31)	-C(21)	-C(20)	112.6(3)
C(13)	-N(1)	-C(2)	117.8(3)	C(22)	-C(21)	-C(20)	100.9(3)
C(13)	-N(1)	-Cu	111.7(2)	C(31)	-C(21)	-C(24)	101.2(3)
C(2)	-N(1)	-Cu	130.4(3)	C(22)	-C(21)	-C(24)	110.9(3)
C(11)	-N(2)	-C(12)	118.7(3)	C(20)	-C(21)	-C(24)	114.4(3)
C(11)	-N(2)	-Cu	130.2(2)	C(23)	-C(22)	-C(18)	120.8(3)
C(12)	-N(2)	-Cu	111.0(3)	C(23)	-C(22)	-C(21)	127.0(3)
C(36)	-N(3)	-Cu	177.2(3)	C(18)	-C(22)	-C(21)	112.0(3)
O(1)	-C(1)	-C(2)	107.1(3)	C(22)	-C(23)	-C(15)	118.6(3)
N(1)	-C(2)	-C(3)	121.8(4)	C(25)	-C(24)	-C(21)	108.1(3)
N(1)	-C(2)	-C(1)	114.8(4)	C(26)	-C(25)	-C(24)	102.8(3)

Table 2.46 continued

C(3) -C(2) -C(1)	123.2(4)	C(26) -C(25) -C(34)	112.9(4)
C(4) -C(3) -C(2)	119.8(4)	C(24) -C(25) -C(34)	111.4(4)
C(3) -C(4) -C(5)	120.2(4)	C(26) -C(25) -C(35)	110.1(4)
C(13) -C(5) -C(4)	116.7(4)	C(24) -C(25) -C(35)	110.5(4)
C(13) -C(5) -C(6)	119.1(4)	C(34) -C(25) -C(35)	109.0(4)
C(4) -C(5) -C(6)	124.2(4)	C(27) -C(26) -C(31)	120.5(4)
C(7) -C(6) -C(5)	121.7(4)	C(27) -C(26) -C(25)	128.5(3)
C(6) -C(7) -C(8)	120.0(4)	C(31) -C(26) -C(25)	110.8(4)
C(12) -C(8) -C(9)	116.1(3)	C(26) -C(27) -C(28)	120.7(4)
C(12) -C(8) -C(7)	120.5(4)	C(27) -C(28) -C(29)	118.3(4)
C(9) -C(8) -C(7)	123.4(4)	C(30) -C(29) -O(1)	119.1(3)
C(10) -C(9) -C(8)	119.8(4)	C(30) -C(29) -C(28)	121.6(4)
C(9) -C(10) -C(11)	120.0(4)	O(1) -C(29) -C(28)	119.2(4)
N(2) -C(11) -C(10)	122.1(3)	C(29) -C(30) -C(31)	119.8(3)
N(2) -C(11) -C(14)	118.7(3)	C(26) -C(31) -C(30)	119.1(4)
C(10) -C(11) -C(14)	119.2(4)	C(26) -C(31) -C(21)	112.4(3)
N(2) -C(12) -C(8)	123.3(4)	C(30) -C(31) -C(21)	128.5(3)
N(2) -C(12) -C(13)	117.9(3)	N(3) -C(36) -C(37)	179.0(5)
C(8) -C(12) -C(13)	118.7(3)	F(1) -P(1) -F(2)	92.5(3)
N(1) -C(13) -C(5)	123.5(4)	F(1) -P(1) -F(3)	176.9(3)
N(1) -C(13) -C(12)	116.5(3)	F(2) -P(1) -F(3)	90.2(3)
C(5) -C(13) -C(12)	120.0(4)	F(1) -P(1) -F(5)	92.5(2)
O(2) -C(14) -C(11)	110.0(3)	F(2) -P(1) -F(5)	91.0(2)
C(23) -C(15) -O(2)	123.7(3)	F(3) -P(1) -F(5)	89.0(2)
C(23) -C(15) -C(16)	120.8(3)	F(1) -P(1) -F(4)	89.5(2)
O(2) -C(15) -C(16)	115.3(3)	F(2) -P(1) -F(4)	177.9(3)
C(17) -C(16) -C(15)	120.6(3)	F(3) -P(1) -F(4)	87.8(2)
C(16) -C(17) -C(18)	118.9(3)	F(5) -P(1) -F(4)	89.7(2)
C(22) -C(18) -C(17)	120.2(3)	F(1) -P(1) -F(6)	88.9(2)
C(22) -C(18) -C(19)	111.7(3)	F(2) -P(1) -F(6)	88.3(2)
C(17) -C(18) -C(19)	128.1(3)	F(3) -P(1) -F(6)	89.7(2)
C(18) -C(19) -C(32)	112.7(3)	F(5) -P(1) -F(6)	178.5(2)
C(18) -C(19) -C(33)	111.2(3)	F(4) -P(1) -F(6)	91.1(2)
C(32) -C(19) -C(33)	108.9(3)	N(4) -C(38) -C(39)	178(1)
C(18) -C(19) -C(20)	100.8(3)		

Table 2.47 Torsion angles (°) with standard uncertainties in parentheses of **81**

N(3) -Cu -N(1) -C(13)	163.1(2)	C(16) -C(17) -C(18) -C(22)	1.3(5)
N(2) -Cu -N(1) -C(13)	-6.0(2)	C(16) -C(17) -C(18) -C(19)	-175.2(3)
N(3) -Cu -N(1) -C(2)	-14.5(4)	C(22) -C(18) -C(19) -C(32)	135.2(3)
N(2) -Cu -N(1) -C(2)	176.5(3)	C(17) -C(18) -C(19) -C(32)	-48.1(5)
N(3) -Cu -N(2) -C(11)	15.4(4)	C(22) -C(18) -C(19) -C(33)	-102.2(4)
N(1) -Cu -N(2) -C(11)	-176.8(3)	C(17) -C(18) -C(19) -C(33)	74.5(4)
N(3) -Cu -N(2) -C(12)	-162.0(2)	C(22) -C(18) -C(19) -C(20)	16.9(3)
N(1) -Cu -N(2) -C(12)	5.8(2)	C(17) -C(18) -C(19) -C(20)	-166.4(3)
C(29) -O(1) -C(1) -C(2)	117.1(4)	C(18) -C(19) -C(20) -C(21)	-26.3(3)
C(13) -N(1) -C(2) -C(3)	-3.1(5)	C(32) -C(19) -C(20) -C(21)	-145.9(3)
Cu -N(1) -C(2) -C(3)	174.4(3)	C(33) -C(19) -C(20) -C(21)	92.1(3)

Table 2.47 continued

C(13)	-N(1)	-C(2)	-C(1)	173.5(3)	C(19)	-C(20)	-C(21)	-C(31)	152.1(3)
Cu	-N(1)	-C(2)	-C(1)	-9.1(5)	C(19)	-C(20)	-C(21)	-C(22)	26.0(3)
O(1)	-C(1)	-C(2)	-N(1)	-81.3(4)	C(19)	-C(20)	-C(21)	-C(24)	-93.1(4)
O(1)	-C(1)	-C(2)	-C(3)	95.2(4)	C(17)	-C(18)	-C(22)	-C(23)	-1.8(5)
N(1)	-C(2)	-C(3)	-C(4)	1.9(6)	C(19)	-C(18)	-C(22)	-C(23)	175.2(3)
C(1)	-C(2)	-C(3)	-C(4)	-174.3(4)	C(17)	-C(18)	-C(22)	-C(21)	-177.6(3)
C(2)	-C(3)	-C(4)	-C(5)	0.8(6)	C(19)	-C(18)	-C(22)	-C(21)	-0.6(4)
C(3)	-C(4)	-C(5)	-C(13)	-2.0(5)	C(31)	-C(21)	-C(22)	-C(23)	45.8(4)
C(3)	-C(4)	-C(5)	-C(6)	177.7(4)	C(20)	-C(21)	-C(22)	-C(23)	168.6(3)
C(13)	-C(5)	-C(6)	-C(7)	1.6(5)	C(24)	-C(21)	-C(22)	-C(23)	-69.8(4)
C(4)	-C(5)	-C(6)	-C(7)	-178.2(4)	C(31)	-C(21)	-C(22)	-C(18)	-138.7(3)
C(5)	-C(6)	-C(7)	-C(8)	-0.1(6)	C(20)	-C(21)	-C(22)	-C(18)	-15.9(3)
C(6)	-C(7)	-C(8)	-C(12)	-2.5(6)	C(24)	-C(21)	-C(22)	-C(18)	105.7(3)
C(6)	-C(7)	-C(8)	-C(9)	178.9(4)	C(18)	-C(22)	-C(23)	-C(15)	0.6(4)
C(12)	-C(8)	-C(9)	-C(10)	1.5(6)	C(21)	-C(22)	-C(23)	-C(15)	175.7(3)
C(7)	-C(8)	-C(9)	-C(10)	-179.9(4)	O(2)	-C(15)	-C(23)	-C(22)	-173.6(3)
C(8)	-C(9)	-C(10)	-C(11)	-1.6(6)	C(16)	-C(15)	-C(23)	-C(22)	1.2(5)
C(12)	-N(2)	-C(11)	-C(10)	-1.0(5)	C(31)	-C(21)	-C(24)	-C(25)	20.1(4)
Cu	-N(2)	-C(11)	-C(10)	-178.2(3)	C(22)	-C(21)	-C(24)	-C(25)	145.5(3)
C(12)	-N(2)	-C(11)	-C(14)	179.2(3)	C(20)	-C(21)	-C(24)	-C(25)	-101.2(4)
Cu	-N(2)	-C(11)	-C(14)	1.9(5)	C(21)	-C(24)	-C(25)	-C(26)	-21.5(4)
C(9)	-C(10)	-C(11)	-N(2)	1.4(6)	C(21)	-C(24)	-C(25)	-C(34)	-142.6(3)
C(9)	-C(10)	-C(11)	-C(14)	-178.8(3)	C(21)	-C(24)	-C(25)	-C(35)	96.0(4)
C(11)	-N(2)	-C(12)	-C(8)	0.9(5)	C(24)	-C(25)	-C(26)	-C(27)	-171.0(4)
Cu	-N(2)	-C(12)	-C(8)	178.7(3)	C(34)	-C(25)	-C(26)	-C(27)	-50.8(6)
C(11)	-N(2)	-C(12)	-C(13)	177.4(3)	C(35)	-C(25)	-C(26)	-C(27)	71.3(6)
Cu	-N(2)	-C(12)	-C(13)	-4.9(4)	C(24)	-C(25)	-C(26)	-C(31)	14.9(5)
C(9)	-C(8)	-C(12)	-N(2)	-1.2(5)	C(34)	-C(25)	-C(26)	-C(31)	135.0(4)
C(7)	-C(8)	-C(12)	-N(2)	-179.8(3)	C(35)	-C(25)	-C(26)	-C(31)	-102.9(4)
C(9)	-C(8)	-C(12)	-C(13)	-177.6(3)	C(31)	-C(26)	-C(27)	-C(28)	-3.1(7)
C(7)	-C(8)	-C(12)	-C(13)	3.7(5)	C(25)	-C(26)	-C(27)	-C(28)	-176.8(4)
C(2)	-N(1)	-C(13)	-C(5)	1.7(5)	C(26)	-C(27)	-C(28)	-C(29)	2.7(7)
Cu	-N(1)	-C(13)	-C(5)	-176.2(2)	C(1)	-O(1)	-C(29)	-C(30)	-117.1(4)
C(2)	-N(1)	-C(13)	-C(12)	-177.0(3)	C(1)	-O(1)	-C(29)	-C(28)	66.6(5)
Cu	-N(1)	-C(13)	-C(12)	5.1(4)	C(27)	-C(28)	-C(29)	-C(30)	-1.2(6)
C(4)	-C(5)	-C(13)	-N(1)	0.8(5)	C(27)	-C(28)	-C(29)	-O(1)	174.9(4)
C(6)	-C(5)	-C(13)	-N(1)	-179.0(3)	O(1)	-C(29)	-C(30)	-C(31)	-175.9(3)
C(4)	-C(5)	-C(13)	-C(12)	179.5(3)	C(28)	-C(29)	-C(30)	-C(31)	0.2(6)
C(6)	-C(5)	-C(13)	-C(12)	-0.3(5)	C(27)	-C(26)	-C(31)	-C(30)	2.0(6)
N(2)	-C(12)	-C(13)	-N(1)	-0.2(4)	C(25)	-C(26)	-C(31)	-C(30)	176.8(3)
C(8)	-C(12)	-C(13)	-N(1)	176.5(3)	C(27)	-C(26)	-C(31)	-C(21)	-176.9(4)
N(2)	-C(12)	-C(13)	-C(5)	-178.9(3)	C(25)	-C(26)	-C(31)	-C(21)	-2.2(5)
C(8)	-C(12)	-C(13)	-C(5)	-2.3(5)	C(29)	-C(30)	-C(31)	-C(26)	-0.6(5)
C(15)	-O(2)	-C(14)	-C(11)	-72.1(4)	C(29)	-C(30)	-C(31)	-C(21)	178.1(4)
N(2)	-C(11)	-C(14)	-O(2)	119.3(3)	C(22)	-C(21)	-C(31)	-C(26)	-131.9(3)
C(10)	-C(11)	-C(14)	-O(2)	-60.6(4)	C(20)	-C(21)	-C(31)	-C(26)	111.5(3)
C(14)	-O(2)	-C(15)	-C(23)	-42.5(4)	C(24)	-C(21)	-C(31)	-C(26)	-11.1(4)
C(14)	-O(2)	-C(15)	-C(16)	142.5(3)	C(22)	-C(21)	-C(31)	-C(30)	49.4(5)
C(23)	-C(15)	-C(16)	-C(17)	-1.7(5)	C(20)	-C(21)	-C(31)	-C(30)	-67.2(5)
O(2)	-C(15)	-C(16)	-C(17)	173.5(3)	C(24)	-C(21)	-C(31)	-C(30)	170.2(4)

Table 2.47 continued

C(15) -C(16) -C(17) -C(18)	0.4(5)

Table 2.48 Crystallographic Data of **82**

Crystallized from		CH_2Cl_2 / hexanes
Empirical formula		$C_{35}H_{32}HgI_2N_2O_2$
Formula weight [g mol^{-1}]		966.96
Crystal color, habit		yellow, prism
Crystal dimensions [mm]		0.10 × 0.20 × 0.22
Temperature [K]		160 (1)
Crystal system		triclinic
Space group		$P\bar{1}$ (#2)
Z		2
Reflections for cell determination		41892
2θ range for cell determination [°]		4–55
Unit cell parameters	a [Å]	9.1738 (2)
	b [Å]	10.4862 (2)
	c [Å]	17.4758 (4)
	α [°]	89.3421 (7)
	β [°]	84.2641 (7)
	γ [°]	75.538 (1)
	V [Å^3]	1619.57 (6)
F(000)		916
D_x [g cm^{-3}]		1.983
μ(Mo $K\alpha$) [mm^{-1}]		6.703
Scan type		ϕ and ω
2$\theta_{(max)}$ [°]		55
Transmission factors (min; max)		0.330; 0.522
Total reflections measured		36884
Symmetry independent reflections		7425
R_{int}		0.086
Reflections with $I > 2\sigma(I)$		6222
Reflections used in refinement		7425
Parameters refined		384
Final $R(F)$ [I>2$\sigma(I)$ reflections]		0.0447
$wR(F^2)$ (all data)		0.1158
Weights:	$w = [\sigma^2(F_o^2) + (0.0456P)^2 + 7.7356P]^{-1}$ where $P = (F_o^2 + 2F_c^2)/3$	
Goodness of fit		1.107
Secondary extinction coefficient		0.0034 (3)
Final Δ_{max}/σ		0.001
$\Delta\rho$ (max; min) [e Å^{-3}]		1.13; -3.24
$\sigma(d_{(C-C)})$ [Å]		0.008—0.01

Table 2.49 Fractional atomic coordinates and equivalent isotropic displacement of **82**

ATOM	x	y	z	U_{eq}*
Hg	0.25773(3)	0.37961(3)	0.18951(1)	0.0349(1)
I(1)	0.32673(6)	0.42992(5)	0.32576(3)	0.0401(1)
I(2)	0.06203(6)	0.51974(5)	0.09798(3)	0.0440(2)
O(1)	0.1674(5)	-0.0059(4)	0.3145(3)	0.031(1)
O(2)	0.7443(5)	0.2746(4)	0.1243(2)	0.0283(9)
N(1)	0.2358(6)	0.1619(5)	0.1507(3)	0.024(1)

Table 2.49 continued

N(2)	0.4455(6)	0.2811(5)	0.0758(3)	0.026(1)
C(1)	0.1183(7)	0.1136(6)	0.2747(4)	0.028(1)
C(2)	0.1533(7)	0.0909(6)	0.1889(4)	0.028(1)
C(3)	0.1008(8)	-0.0058(7)	0.1525(4)	0.033(1)
C(4)	0.1308(8)	-0.0244(7)	0.0750(4)	0.034(2)
C(5)	0.2211(8)	0.0497(7)	0.0324(4)	0.032(1)
C(6)	0.2622(8)	0.0312(7)	-0.0486(4)	0.037(2)
C(7)	0.3516(8)	0.1009(7)	-0.0866(4)	0.035(2)
C(8)	0.4168(7)	0.1879(7)	-0.0464(4)	0.030(1)
C(9)	0.5235(8)	0.2496(7)	-0.0817(4)	0.033(1)
C(10)	0.5944(8)	0.3192(7)	-0.0380(4)	0.031(1)
C(11)	0.5532(7)	0.3312(6)	0.0413(3)	0.027(1)
C(12)	0.3799(7)	0.2071(6)	0.0338(4)	0.026(1)
C(13)	0.2729(7)	0.1400(6)	0.0732(4)	0.026(1)
C(14)	0.6446(8)	0.3863(6)	0.0933(4)	0.031(1)
C(15)	0.7387(7)	0.2688(6)	0.2036(3)	0.024(1)
C(16)	0.7697(7)	0.3686(6)	0.2462(4)	0.027(1)
C(17)	0.7638(7)	0.3587(6)	0.3259(3)	0.024(1)
C(18)	0.7329(6)	0.2485(5)	0.3625(3)	0.021(1)
C(19)	0.7214(7)	0.2182(6)	0.4475(3)	0.026(1)
C(20)	0.6471(8)	0.1002(6)	0.4486(3)	0.028(1)
C(21)	0.6847(7)	0.0327(6)	0.3683(3)	0.022(1)
C(22)	0.7062(6)	0.1468(6)	0.3180(3)	0.021(1)
C(23)	0.7083(6)	0.1568(6)	0.2387(3)	0.022(1)
C(24)	0.8324(7)	-0.0830(6)	0.3590(4)	0.033(1)
C(25)	0.7855(7)	-0.2140(6)	0.3537(4)	0.029(1)
C(26)	0.6241(7)	-0.1692(6)	0.3353(3)	0.024(1)
C(27)	0.5300(8)	-0.2461(6)	0.3140(4)	0.029(1)
C(28)	0.3797(7)	-0.1886(6)	0.3050(4)	0.029(1)
C(29)	0.3232(7)	-0.0540(7)	0.3173(4)	0.029(1)
C(30)	0.4154(7)	0.0254(6)	0.3365(4)	0.026(1)
C(31)	0.5668(7)	-0.0350(6)	0.3454(3)	0.022(1)
C(32)	0.6237(9)	0.3349(7)	0.4943(4)	0.037(2)
C(33)	0.8802(8)	0.1808(7)	0.4756(4)	0.035(2)
C(34)	0.7926(9)	-0.2860(7)	0.4315(4)	0.039(2)
C(35)	0.8871(9)	-0.3027(8)	0.2913(5)	0.044(2)

parameters ($Å^2$) with standard uncertainties in parentheses.

* U_{eq} is defined as one third of the trace of the orthogonalized U^{ij} tensor.

Table 2.50 Bond lengths (Å) with standard uncertainties in parentheses of **82**

Hg	-N(1)	2.451(5)	
Hg	-N(2)	2.541(5)	
Hg	-I(1)	2.6163(5)	
Hg	-I(2)	2.6728(6)	
O(1)	-C(29)	1.397(8)	
O(1)	-C(1)	1.421(8)	
O(2)	-C(15)	1.382(7)	
O(2)	-C(14)	1.433(8)	
C(12)	-C(13)	1.460(9)	
C(15)	-C(16)	1.393(8)	
C(15)	-C(23)	1.395(8)	
C(16)	-C(17)	1.393(8)	
C(17)	-C(18)	1.390(8)	
C(18)	-C(22)	1.410(8)	
C(18)	-C(19)	1.515(8)	
C(19)	-C(32)	1.516(9)	

Table 2.50 continued

N(1)	-C(2)	1.320(8)	
N(1)	-C(13)	1.371(8)	
N(2)	-C(11)	1.322(8)	
N(2)	-C(12)	1.356(8)	
C(1)	-C(2)	1.511(9)	
C(2)	-C(3)	1.408(9)	
C(3)	-C(4)	1.36(1)	
C(4)	-C(5)	1.43(1)	
C(5)	-C(13)	1.393(9)	
C(5)	-C(6)	1.43(1)	
C(6)	-C(7)	1.35(1)	
C(7)	-C(8)	1.435(9)	
C(8)	-C(9)	1.39(1)	
C(8)	-C(12)	1.413(9)	
C(9)	-C(10)	1.374(9)	
C(10)	-C(11)	1.398(9)	
C(11)	-C(14)	1.507(9)	
C(19)	-C(33)	1.540(9)	
C(19)	-C(20)	1.553(9)	
C(20)	-C(21)	1.548(8)	
C(21)	-C(22)	1.516(8)	
C(21)	-C(31)	1.520(8)	
C(21)	-C(24)	1.573(9)	
C(22)	-C(23)	1.387(8)	
C(24)	-C(25)	1.545(8)	
C(25)	-C(26)	1.504(9)	
C(25)	-C(35)	1.52(1)	
C(25)	-C(34)	1.55(1)	
C(26)	-C(31)	1.380(8)	
C(26)	-C(27)	1.397(8)	
C(27)	-C(28)	1.384(9)	
C(28)	-C(29)	1.388(9)	
C(29)	-C(30)	1.392(9)	
C(30)	-C(31)	1.398(8)	

Table 2.51 Bond angles (°) with standard uncertainties in parentheses of **82**

N(1)	-Hg	-N(2)	67.2(2)	C(16) -C(15) -C(23)	121.4(5)
N(1)	-Hg	-I(1)	123.0(1)	C(17) -C(16) -C(15)	119.1(5)
N(2)	-Hg	-I(1)	125.7(1)	C(18) -C(17) -C(16)	120.6(5)
N(1)	-Hg	-I(2)	96.8(1)	C(17) -C(18) -C(22)	119.4(5)
N(2)	-Hg	-I(2)	92.3(1)	C(17) -C(18) -C(19)	129.1(5)
I(1)	-Hg	-I(2)	131.92(2)	C(22) -C(18) -C(19)	111.6(5)
C(29)	-O(1)	-C(1)	117.1(5)	C(18) -C(19) -C(32)	111.3(5)
C(15)	-O(2)	-C(14)	116.4(5)	C(18) -C(19) -C(33)	110.0(5)
C(2)	-N(1)	-C(13)	119.0(5)	C(32) -C(19) -C(33)	109.3(5)
C(2)	-N(1)	-Hg	125.8(4)	C(18) -C(19) -C(20)	101.2(5)
C(13)	-N(1)	-Hg	111.6(4)	C(32) -C(19) -C(20)	112.1(6)
C(11)	-N(2)	-C(12)	118.8(5)	C(33) -C(19) -C(20)	112.6(5)
C(11)	-N(2)	-Hg	127.1(4)	C(21) -C(20) -C(19)	108.0(5)
C(12)	-N(2)	-Hg	108.0(4)	C(22) -C(21) -C(31)	115.2(5)
O(1)	-C(1)	-C(2)	110.6(5)	C(22) -C(21) -C(20)	101.1(5)
N(1)	-C(2)	-C(3)	122.2(6)	C(31) -C(21) -C(20)	114.4(5)
N(1)	-C(2)	-C(1)	118.0(5)	C(22) -C(21) -C(24)	109.8(5)
C(3)	-C(2)	-C(1)	119.8(6)	C(31) -C(21) -C(24)	101.6(5)
C(4)	-C(3)	-C(2)	119.5(6)	C(20) -C(21) -C(24)	115.1(5)
C(3)	-C(4)	-C(5)	119.5(6)	C(23) -C(22) -C(18)	120.6(5)
C(13)	-C(5)	-C(4)	117.2(6)	C(23) -C(22) -C(21)	128.4(5)
C(13)	-C(5)	-C(6)	120.3(6)	C(18) -C(22) -C(21)	110.9(5)
C(4)	-C(5)	-C(6)	122.5(6)	C(22) -C(23) -C(15)	118.8(5)
C(7)	-C(6)	-C(5)	120.6(6)	C(25) -C(24) -C(21)	108.3(5)
C(6)	-C(7)	-C(8)	121.2(6)	C(26) -C(25) -C(35)	112.8(6)
C(9)	-C(8)	-C(12)	117.4(6)	C(26) -C(25) -C(24)	102.7(5)
C(9)	-C(8)	-C(7)	123.1(6)	C(35) -C(25) -C(24)	110.3(6)
C(12)	-C(8)	-C(7)	119.4(6)	C(26) -C(25) -C(34)	110.0(6)
C(10)	-C(9)	-C(8)	119.9(6)	C(35) -C(25) -C(34)	109.8(6)

Table 2.51 continued

C(9) -C(10) -C(11)	118.9(6)	C(24) -C(25) -C(34)	111.1(6)
N(2) -C(11) -C(10)	122.6(6)	C(31) -C(26) -C(27)	119.4(6)
N(2) -C(11) -C(14)	116.1(5)	C(31) -C(26) -C(25)	112.3(5)
C(10) -C(11) -C(14)	120.8(6)	C(27) -C(26) -C(25)	128.2(6)
N(2) -C(12) -C(8)	122.2(6)	C(28) -C(27) -C(26)	120.2(6)
N(2) -C(12) -C(13)	119.0(5)	C(27) -C(28) -C(29)	119.5(6)
C(8) -C(12) -C(13)	118.8(5)	C(28) -C(29) -C(30)	121.4(6)
N(1) -C(13) -C(5)	122.5(6)	C(28) -C(29) -O(1)	115.9(5)
N(1) -C(13) -C(12)	118.1(5)	C(30) -C(29) -O(1)	122.6(6)
C(5) -C(13) -C(12)	119.3(6)	C(29) -C(30) -C(31)	118.0(6)
O(2) -C(14) -C(11)	105.8(5)	C(26) -C(31) -C(30)	121.4(5)
O(2) -C(15) -C(16)	120.8(5)	C(26) -C(31) -C(21)	112.2(5)
O(2) -C(15) -C(23)	117.7(5)	C(30) -C(31) -C(21)	126.4(5)

Table 2.52 Torsion angles (°) with standard uncertainties in parentheses of **82**

N(2) -Hg -N(1) -C(2)	170.7(5)	C(23) -C(15) -C(16) -C(17)	-3(1)
I(1) -Hg -N(1) -C(2)	51.9(5)	C(15) -C(16) -C(17) -C(18)	2(1)
I(2) -Hg -N(1) -C(2)	-99.7(5)	C(16) -C(17) -C(18) -C(22)	-0.5(9)
N(2) -Hg -N(1) -C(13)	-31.2(4)	C(16) -C(17) -C(18) -C(19)	180.0(6)
I(1) -Hg -N(1) -C(13)	-150.0(3)	C(17) -C(18) -C(19) -C(32)	47.4(9)
I(2) -Hg -N(1) -C(13)	58.4(4)	C(22) -C(18) -C(19) -C(32)	-132.1(6)
N(1) -Hg -N(2) -C(11)	-175.8(6)	C(17) -C(18) -C(19) -C(33)	-74.0(8)
I(1) -Hg -N(2) -C(11)	-60.6(5)	C(22) -C(18) -C(19) -C(33)	106.5(6)
I(2) -Hg -N(2) -C(11)	87.8(5)	C(17) -C(18) -C(19) -C(20)	166.7(6)
N(1) -Hg -N(2) -C(12)	32.5(4)	C(22) -C(18) -C(19) -C(20)	-12.8(6)
I(1) -Hg -N(2) -C(12)	147.7(3)	C(18) -C(19) -C(20) -C(21)	24.6(6)
I(2) -Hg -N(2) -C(12)	-63.9(4)	C(32) -C(19) -C(20) -C(21)	143.3(5)
C(29) -O(1) -C(1) -C(2)	73.0(7)	C(33) -C(19) -C(20) -C(21)	-92.9(6)
C(13) -N(1) -C(2) -C(3)	-0.6(9)	C(19) -C(20) -C(21) -C(22)	-26.7(6)
Hg -N(1) -C(2) -C(3)	156.0(5)	C(19) -C(20) -C(21) -C(31)	-151.2(5)
C(13) -N(1) -C(2) -C(1)	177.9(5)	C(19) -C(20) -C(21) -C(24)	91.6(6)
Hg -N(1) -C(2) -C(1)	-25.5(8)	C(17) -C(18) -C(22) -C(23)	-1.0(9)
O(1) -C(1) -C(2) -N(1)	-123.8(6)	C(19) -C(18) -C(22) -C(23)	178.6(5)
O(1) -C(1) -C(2) -C(3)	54.8(7)	C(17) -C(18) -C(22) -C(21)	176.5(5)
N(1) -C(2) -C(3) -C(4)	-2(1)	C(19) -C(18) -C(22) -C(21)	-4.0(7)
C(1) -C(2) -C(3) -C(4)	179.0(6)	C(31) -C(21) -C(22) -C(23)	-40.0(8)
C(2) -C(3) -C(4) -C(5)	3(1)	C(20) -C(21) -C(22) -C(23)	-164.0(6)
C(3) -C(4) -C(5) -C(13)	-1(1)	C(24) -C(21) -C(22) -C(23)	73.9(7)
C(3) -C(4) -C(5) -C(6)	177.3(7)	C(31) -C(21) -C(22) -C(18)	142.8(5)
C(13) -C(5) -C(6) -C(7)	0(1)	C(20) -C(21) -C(22) -C(18)	18.9(6)
C(4) -C(5) -C(6) -C(7)	-178.1(7)	C(24) -C(21) -C(22) -C(18)	-103.2(6)
C(5) -C(6) -C(7) -C(8)	5(1)	C(18) -C(22) -C(23) -C(15)	0.6(9)
C(6) -C(7) -C(8) -C(9)	172.2(7)	C(21) -C(22) -C(23) -C(15)	-176.3(5)
C(6) -C(7) -C(8) -C(12)	-4(1)	O(2) -C(15) -C(23) -C(22)	178.2(5)
C(12) -C(8) -C(9) -C(10)	4(1)	C(16) -C(15) -C(23) -C(22)	1.3(9)
C(7) -C(8) -C(9) -C(10)	-172.3(7)	C(22) -C(21) -C(24) -C(25)	-137.6(5)
C(8) -C(9) -C(10) -C(11)	-3(1)	C(31) -C(21) -C(24) -C(25)	-15.1(7)
C(12) -N(2) -C(11) -C(10)	4.9(9)	C(20) -C(21) -C(24) -C(25)	109.1(6)

Table 2.52 continued

Hg	-N(2)	-C(11)	-C(10)	-144.1(5)	C(21)	-C(24)	-C(25)	-C(26)	16.9(7)
C(12)	-N(2)	-C(11)	-C(14)	-167.0(6)	C(21)	-C(24)	-C(25)	-C(35)	137.3(6)
Hg	-N(2)	-C(11)	-C(14)	44.0(8)	C(21)	-C(24)	-C(25)	-C(34)	-100.7(6)
C(9)	-C(10)	-C(11)	-N(2)	-2(1)	C(35)	-C(25)	-C(26)	-C(31)	-131.2(6)
C(9)	-C(10)	-C(11)	-C(14)	169.7(6)	C(24)	-C(25)	-C(26)	-C(31)	-12.5(7)
C(11)	-N(2)	-C(12)	-C(8)	-3.6(9)	C(34)	-C(25)	-C(26)	-C(31)	105.8(6)
Hg	-N(2)	-C(12)	-C(8)	150.8(5)	C(35)	-C(25)	-C(26)	-C(27)	52.1(9)
C(11)	-N(2)	-C(12)	-C(13)	173.5(6)	C(24)	-C(25)	-C(26)	-C(27)	170.8(6)
Hg	-N(2)	-C(12)	-C(13)	-32.1(7)	C(34)	-C(25)	-C(26)	-C(27)	-70.8(8)
C(9)	-C(8)	-C(12)	-N(2)	-1(1)	C(31)	-C(26)	-C(27)	-C(28)	-1.5(9)
C(7)	-C(8)	-C(12)	-N(2)	175.5(6)	C(25)	-C(26)	-C(27)	-C(28)	174.9(6)
C(9)	-C(8)	-C(12)	-C(13)	-177.7(6)	C(26)	-C(27)	-C(28)	-C(29)	-0.1(9)
C(7)	-C(8)	-C(12)	-C(13)	-1.5(9)	C(27)	-C(28)	-C(29)	-C(30)	1.8(9)
C(2)	-N(1)	-C(13)	-C(5)	3.0(9)	C(27)	-C(28)	-C(29)	-O(1)	-173.8(6)
Hg	-N(1)	-C(13)	-C(5)	-156.7(5)	C(1)	-O(1)	-C(29)	-C(28)	-137.1(6)
C(2)	-N(1)	-C(13)	-C(12)	-172.3(6)	C(1)	-O(1)	-C(29)	-C(30)	47.2(8)
Hg	-N(1)	-C(13)	-C(12)	28.0(7)	C(28)	-C(29)	-C(30)	-C(31)	-1.9(9)
C(4)	-C(5)	-C(13)	-N(1)	-2(1)	O(1)	-C(29)	-C(30)	-C(31)	173.5(5)
C(6)	-C(5)	-C(13)	-N(1)	179.5(6)	C(27)	-C(26)	-C(31)	-C(30)	1.4(9)
C(4)	-C(5)	-C(13)	-C(12)	173.0(6)	C(25)	-C(26)	-C(31)	-C(30)	-175.5(6)
C(6)	-C(5)	-C(13)	-C(12)	-5(1)	C(27)	-C(26)	-C(31)	-C(21)	-179.9(5)
N(2)	-C(12)	-C(13)	-N(1)	4.3(9)	C(25)	-C(26)	-C(31)	-C(21)	3.1(7)
C(8)	-C(12)	-C(13)	-N(1)	-178.6(6)	C(29)	-C(30)	-C(31)	-C(26)	0.2(9)
N(2)	-C(12)	-C(13)	-C(5)	-171.2(6)	C(29)	-C(30)	-C(31)	-C(21)	-178.2(6)
C(8)	-C(12)	-C(13)	-C(5)	5.9(9)	C(22)	-C(21)	-C(31)	-C(26)	126.3(5)
C(15)	-O(2)	-C(14)	-C(11)	-124.9(5)	C(20)	-C(21)	-C(31)	-C(26)	-117.1(6)
N(2)	-C(11)	-C(14)	-O(2)	74.9(7)	C(24)	-C(21)	-C(31)	-C(26)	7.6(6)
C(10)	-C(11)	-C(14)	-O(2)	-97.1(7)	C(22)	-C(21)	-C(31)	-C(30)	-55.2(8)
C(14)	-O(2)	-C(15)	-C(16)	-59.4(8)	C(20)	-C(21)	-C(31)	-C(30)	61.4(8)
C(14)	-O(2)	-C(15)	-C(23)	123.7(6)	C(24)	-C(21)	-C(31)	-C(30)	-173.8(6)
O(2)	-C(15)	-C(16)	-C(17)	-179.6(6)					

Table 2.53 Crystallographic Data of **86**

Crystallized from		CH_2Cl_2 / benzene
Empirical formula		$C_{82}H_{76}CuF_6N_4O_4P$
Formula weight [g mol^{-1}]		1390.03
Crystal color, habit		orange, plate
Crystal dimensions [mm]		0.02 × 0.15 × 0.25
Temperature [K]		160 (1)
Crystal system		orthorhombic
Space group		$P2_12_12_1$ (#19)
Z		4
Reflections for cell determination		279347
2θ range for cell determination [°]		4–50
Unit cell parameters	a [Å]	14.1496 (2)
	b [Å]	17.9544 (3)
	c [Å]	27.6580 (5)
	α [°]	90
	β [°]	90
	γ [°]	90
	V [$Å^3$]	7026.4 (2)
F(000)		2904
D_x [g cm^{-3}]		1.314
μ(Mo $K\alpha$) [mm^{-1}]		0.404
Scan type		ϕ and ω
$2\theta_{(max)}$ [°]		50
Transmission factors (min; max)		0.865; 0.993
Total reflections measured		65106
Symmetry independent reflections		12335
R_{int}		0.077
Reflections with $I > 2\sigma(I)$		8741
Reflections used in refinement		12335
Parameters refined; restraints		1009; 510
Final $R(F)$ [$I>2\sigma(I)$ reflections]		0.0480
$wR(F^2)$ (all data)		0.1008
Weights:	$w = [\sigma^2(F_o^2) + (0.0416P)^2 + 1.8171P]^{-1}$ where $P = (F_o^2 + 2F_c^2)/3$	
Goodness of fit		1.028
Secondary extinction coefficient		0.0006 (1)
Final Δ_{max}/σ		0.001
$\Delta\rho$ (max; min) [e $Å^{-3}$]		0.32; -0.34
$\sigma(d_{(C-C)})$ [Å]		0.005

Table 2.54 Fractional atomic coordinates and equivalent isotropic displacement of **86**

ATOM	x	y	z	U_{eq}*
Cu	0.97901(3)	0.29877(2)	0.82983(2)	0.0346(1)
O(1)	0.9496(2)	0.4809(1)	0.85665(8)	0.0389(6)
O(2)	0.9535(2)	0.0691(1)	0.75524(8)	0.0442(7)
O(3)	1.0001(2)	0.4342(1)	0.67957(8)	0.0401(6)
O(4)	0.9031(2)	0.2006(2)	0.98269(9)	0.0484(7)
N(1)	1.0969(2)	0.3609(2)	0.8404(1)	0.0322(7)

Table 2.54 continued

N(2)	1.0792(2)	0.2231(2)	0.8035(1)	0.0329(7)
N(3)	0.8817(2)	0.3402(2)	0.7795(1)	0.0323(7)
N(4)	0.8594(2)	0.2580(2)	0.8604(1)	0.0343(7)
C(1)	1.0229(2)	0.4558(2)	0.8882(1)	0.0367(8)
C(2)	1.1052(2)	0.4286(2)	0.8594(1)	0.0337(9)
C(3)	1.1879(2)	0.4706(2)	0.8550(1)	0.041(1)
C(4)	1.2653(2)	0.4410(2)	0.8326(1)	0.0433(9)
C(5)	1.2612(2)	0.3688(2)	0.8144(1)	0.0390(9)
C(6)	1.3401(3)	0.3323(3)	0.7921(1)	0.050(1)
C(7)	1.3313(3)	0.2625(3)	0.7750(2)	0.054(1)
C(8)	1.2444(3)	0.2223(2)	0.7777(1)	0.041(1)
C(9)	1.2306(3)	0.1509(2)	0.7585(1)	0.050(1)
C(10)	1.1443(3)	0.1177(2)	0.7629(1)	0.047(1)
C(11)	1.0704(3)	0.1539(2)	0.7867(1)	0.0349(9)
C(12)	1.1655(2)	0.2572(2)	0.7992(1)	0.0345(9)
C(13)	1.1745(2)	0.3306(2)	0.8181(1)	0.0331(9)
C(14)	0.9793(3)	0.1144(2)	0.7955(1)	0.0400(9)
C(15)	0.8958(3)	0.1055(2)	0.7220(1)	0.0383(9)
C(16)	0.8003(3)	0.1137(2)	0.7330(1)	0.043(1)
C(17)	0.7411(3)	0.1462(2)	0.6994(2)	0.046(1)
C(18)	0.7768(2)	0.1695(2)	0.6553(1)	0.0352(9)
C(19)	0.7225(2)	0.2025(2)	0.6139(1)	0.0406(9)
C(20)	0.7977(2)	0.2091(2)	0.5740(1)	0.0439(9)
C(21)	0.8979(2)	0.1975(2)	0.5971(1)	0.0358(8)
C(22)	0.8728(2)	0.1623(2)	0.6452(1)	0.0328(8)
C(23)	0.9336(2)	0.1301(2)	0.6789(1)	0.0352(9)
C(24)	0.9664(3)	0.1568(2)	0.5633(1)	0.044(1)
C(25)	1.0140(3)	0.2174(2)	0.5312(1)	0.046(1)
C(26)	1.0098(2)	0.2838(2)	0.5649(1)	0.0368(9)
C(27)	1.0579(3)	0.3504(2)	0.5631(1)	0.045(1)
C(28)	1.0514(3)	0.4015(2)	0.6014(1)	0.041(1)
C(29)	0.9979(2)	0.3835(2)	0.6415(1)	0.0359(9)
C(30)	0.9451(2)	0.3184(2)	0.6428(1)	0.0347(9)
C(31)	0.9506(2)	0.2704(2)	0.6035(1)	0.0348(9)
C(32)	0.9915(2)	0.4037(2)	0.7273(1)	0.0343(9)
C(33)	0.8918(2)	0.3871(2)	0.7424(1)	0.0337(9)
C(34)	0.8141(3)	0.4162(2)	0.7179(1)	0.0386(9)
C(35)	0.7251(3)	0.3939(2)	0.7288(1)	0.043(1)
C(36)	0.7120(2)	0.3409(2)	0.7654(1)	0.0381(9)
C(37)	0.6222(2)	0.3084(2)	0.7769(1)	0.048(1)
C(38)	0.6142(3)	0.2565(2)	0.8113(2)	0.051(1)
C(39)	0.6935(3)	0.2357(2)	0.8403(1)	0.042(1)
C(40)	0.6889(3)	0.1837(2)	0.8784(2)	0.052(1)
C(41)	0.7659(3)	0.1723(2)	0.9069(2)	0.049(1)
C(42)	0.8497(3)	0.2127(2)	0.8986(1)	0.0391(9)
C(43)	0.7820(2)	0.2688(2)	0.8316(1)	0.0333(8)
C(44)	0.7920(2)	0.3186(2)	0.7916(1)	0.0326(9)
C(45)	0.9308(2)	0.2101(2)	0.9335(1)	0.0419(9)
C(46)	0.8636(3)	0.2624(2)	1.0060(1)	0.042(1)
C(47)	0.8801(3)	0.2676(2)	1.0555(1)	0.053(1)

Table 2.54 continued

C(48)	0.8459(3)	0.3268(2)	1.0817(1)	0.049(1)
C(49)	0.7929(2)	0.3817(2)	1.0582(1)	0.0400(9)
C(50)	0.7508(3)	0.4531(2)	1.0787(1)	0.0407(9)
C(51)	0.7297(3)	0.4970(2)	1.0318(1)	0.042(1)
C(52)	0.7164(2)	0.4396(2)	0.9903(1)	0.0360(9)
C(53)	0.7751(2)	0.3752(2)	1.0098(1)	0.0357(9)
C(54)	0.8103(3)	0.3161(2)	0.9827(1)	0.0397(9)
C(55)	0.6113(2)	0.4173(2)	0.9796(1)	0.041(1)
C(56)	0.5802(2)	0.4613(2)	0.9341(1)	0.043(1)
C(57)	0.6751(2)	0.4729(2)	0.9085(1)	0.0335(9)
C(58)	0.6928(3)	0.4884(2)	0.8606(1)	0.0392(9)
C(59)	0.7854(2)	0.4922(2)	0.8448(1)	0.0386(9)
C(60)	0.8590(2)	0.4819(2)	0.8769(1)	0.0338(9)
C(61)	0.8428(2)	0.4705(2)	0.9255(1)	0.0359(9)
C(62)	0.7489(2)	0.4640(2)	0.9407(1)	0.0341(9)
C(63)	0.6816(3)	0.2786(2)	0.6273(2)	0.060(1)
C(64)	0.6423(3)	0.1503(2)	0.5988(2)	0.055(1)
C(65)	0.9583(3)	0.2315(2)	0.4844(1)	0.060(1)
C(66)	1.1158(3)	0.1957(3)	0.5188(2)	0.063(1)
C(67)	0.8176(3)	0.4967(2)	1.1113(1)	0.056(1)
C(68)	0.6606(3)	0.4352(2)	1.1070(1)	0.051(1)
C(69)	0.5383(3)	0.5373(2)	0.9476(2)	0.060(1)
C(70)	0.5097(3)	0.4176(2)	0.9035(2)	0.059(1)
C(71a)†	0.3338(5)	0.3712(4)	0.6667(3)	0.085(2)
C(72a)†	0.4058(3)	0.3229(5)	0.6530(3)	0.086(2)
C(73a)†	0.3848(5)	0.2495(5)	0.6411(3)	0.092(2)
C(74a)†	0.2920(6)	0.2244(4)	0.6429(3)	0.088(2)
C(75a)†	0.2201(4)	0.2727(5)	0.6567(4)	0.084(2)
C(76a)†	0.2410(4)	0.3460(4)	0.6686(3)	0.083(2)
C(71b)•	0.3576(9)	0.3374(7)	0.6581(5)	0.091(2)
C(72b)•	0.4070(5)	0.2713(9)	0.6517(5)	0.091(3)
C(73b)•	0.3583(8)	0.2054(7)	0.6430(5)	0.086(3)
C(74b)•	0.2602(8)	0.2056(7)	0.6408(5)	0.086(3)
C(75b)•	0.2107(5)	0.2718(8)	0.6472(6)	0.087(3)
C(76b)•	0.2594(9)	0.3377(7)	0.6558(6)	0.086(3)
C(77a)‡	0.1834(9)	0.3813(8)	0.9739(4)	0.111(3)
C(78a)‡	0.1001(9)	0.3688(7)	0.9992(5)	0.114(3)
C(79a)‡	0.0639(8)	0.4238(9)	1.0294(5)	0.116(3)
C(80a)‡	0.111(1)	0.4913(8)	1.0341(5)	0.118(3)
C(81a)‡	0.1943(9)	0.5039(7)	1.0087(6)	0.115(3)
C(82a)‡	0.2305(7)	0.4489(9)	0.9786(5)	0.107(3)
C(77b)§	0.2141(6)	0.4272(6)	0.9779(3)	0.109(3)
C(78b)§	0.1286(7)	0.3929(5)	0.9889(4)	0.118(3)
C(79b)§	0.0701(5)	0.4230(6)	1.0242(4)	0.111(2)
C(80b)§	0.0970(6)	0.4874(6)	1.0485(3)	0.120(3)
C(81b)§	0.1824(6)	0.5217(5)	1.0375(4)	0.114(3)
C(82b)§	0.2409(5)	0.4916(6)	1.0022(4)	0.106(3)
P(1)	0.49783(7)	0.54722(7)	0.73321(4)	0.0575(3)
F(1a)¶	0.497(2)	0.461(2)	0.715(1)	0.096(9)
F(2a)¶	0.483(3)	0.620(1)	0.754(1)	0.074(9)

Table 2.54 continued

F(3a)¶	0.602(2)	0.542(2)	0.734(1)	0.060(7)
F(4a)¶	0.474(3)	0.517(3)	0.786(2)	0.12(1)
F(5a)¶	0.495(2)	0.569(2)	0.6803(8)	0.130(9)
F(6a)¶	0.384(2)	0.530(2)	0.7303(9)	0.078(6)
F(1b)¢	0.5099(6)	0.4792(5)	0.6965(3)	0.070(2)
F(2b)¢	0.4930(8)	0.6194(6)	0.7687(4)	0.085(3)
F(3b)¢	0.6036(7)	0.5344(6)	0.7536(3)	0.064(2)
F(4b)¢	0.4613(8)	0.4955(6)	0.7743(4)	0.105(3)
F(5b)¢	0.5410(5)	0.6017(3)	0.6926(2)	0.077(2)
F(6b)¢	0.3954(4)	0.5647(5)	0.7137(3)	0.089(2)

parameters ($Å^2$) with standard uncertainties in parentheses.

* U_{eq} is defined as one third of the trace of the orthogonalized U^{ij} tensor.

† Disordered atom with site occupation factor of 0.617(10).

• Disordered atom with site occupation factor of 0.383(10).

‡ Disordered atom with site occupation factor of 0.412(10).

§ Disordered atom with site occupation factor of 0.588(10).

¶ Disordered atom with site occupation factor of 0.22(2).

¢ Disordered atom with site occupation factor of 0.78(2).

Table 2.55 Bond lengths (Å) with standard uncertainties in parentheses of **86**

Cu	-N(1)	2.028(3)	C(39)	-C(43)	1.405(5)
Cu	-N(4)	2.029(3)	C(39)	-C(40)	1.410(5)
Cu	-N(2)	2.095(3)	C(40)	-C(41)	1.360(5)
Cu	-N(3)	2.095(3)	C(41)	-C(42)	1.410(5)
O(1)	-C(60)	1.399(4)	C(42)	-C(45)	1.500(5)
O(1)	-C(1)	1.429(4)	C(43)	-C(44)	1.429(5)
O(2)	-C(15)	1.393(4)	C(46)	-C(54)	1.385(5)
O(2)	-C(14)	1.427(4)	C(46)	-C(47)	1.392(5)
O(3)	-C(29)	1.392(4)	C(47)	-C(48)	1.374(5)
O(3)	-C(32)	1.435(4)	C(48)	-C(49)	1.400(5)
O(4)	-C(46)	1.399(4)	C(49)	-C(53)	1.369(5)
O(4)	-C(45)	1.426(4)	C(49)	-C(50)	1.523(5)
N(1)	-C(2)	1.330(4)	C(50)	-C(67)	1.522(5)
N(1)	-C(13)	1.371(4)	C(50)	-C(68)	1.532(5)
N(2)	-C(11)	1.332(4)	C(50)	-C(51)	1.545(5)
N(2)	-C(12)	1.371(4)	C(51)	-C(52)	1.555(5)
N(3)	-C(33)	1.335(4)	C(52)	-C(62)	1.511(5)
N(3)	-C(44)	1.369(4)	C(52)	-C(53)	1.522(5)
N(4)	-C(42)	1.342(4)	C(52)	-C(55)	1.568(5)
N(4)	-C(43)	1.367(4)	C(53)	-C(54)	1.392(5)
C(1)	-C(2)	1.493(5)	C(55)	-C(56)	1.551(5)
C(2)	-C(3)	1.399(5)	C(56)	-C(70)	1.524(5)
C(3)	-C(4)	1.366(5)	C(56)	-C(57)	1.532(5)
C(4)	-C(5)	1.392(5)	C(56)	-C(69)	1.534(5)
C(5)	-C(13)	1.409(5)	C(57)	-C(58)	1.378(5)
C(5)	-C(6)	1.433(5)	C(57)	-C(62)	1.383(5)

Table 2.55 continued

C(6) -C(7)	1.344(5)	C(58) -C(59)	1.383(5)
C(7) -C(8)	1.428(5)	C(59) -C(60)	1.381(5)
C(8) -C(9)	1.401(5)	C(60) -C(61)	1.379(5)
C(8) -C(12)	1.411(5)	C(61) -C(62)	1.398(5)
C(9) -C(10)	1.364(5)	C(71a)-C(72a)	1.390
C(10) -C(11)	1.396(5)	C(71a)-C(76a)	1.390
C(11) -C(14)	1.491(5)	C(72a)-C(73a)	1.390
C(12) -C(13)	1.425(5)	C(73a)-C(74a)	1.390
C(15) -C(23)	1.380(5)	C(74a)-C(75a)	1.390
C(15) -C(16)	1.392(5)	C(75a)-C(76a)	1.390
C(16) -C(17)	1.381(5)	C(71b)-C(72b)	1.390
C(17) -C(18)	1.386(5)	C(71b)-C(76b)	1.390
C(18) -C(22)	1.392(5)	C(72b)-C(73b)	1.390
C(18) -C(19)	1.499(5)	C(73b)-C(74b)	1.390
C(19) -C(63)	1.529(5)	C(74b)-C(75b)	1.390
C(19) -C(64)	1.531(5)	C(75b)-C(76b)	1.390
C(19) -C(20)	1.538(5)	C(77a)-C(78a)	1.390
C(20) -C(21)	1.570(5)	C(77a)-C(82a)	1.390
C(21) -C(22)	1.516(5)	C(78a)-C(79a)	1.390
C(21) -C(31)	1.516(5)	C(79a)-C(80a)	1.390
C(21) -C(24)	1.532(5)	C(80a)-C(81a)	1.390
C(22) -C(23)	1.393(5)	C(81a)-C(82a)	1.390
C(24) -C(25)	1.558(5)	C(77b)-C(78b)	1.390
C(25) -C(26)	1.515(5)	C(77b)-C(82b)	1.390
C(25) -C(66)	1.532(5)	C(78b)-C(79b)	1.390
C(25) -C(65)	1.535(5)	C(79b)-C(80b)	1.390
C(26) -C(27)	1.377(5)	C(80b)-C(81b)	1.390
C(26) -C(31)	1.378(5)	C(81b)-C(82b)	1.390
C(27) -C(28)	1.405(5)	P(1) -F(1a)	1.63(3)
C(28) -C(29)	1.380(5)	P(1) -F(2a)	1.45(3)
C(29) -C(30)	1.387(5)	P(1) -F(3a)	1.48(3)
C(30) -C(31)	1.388(5)	P(1) -F(4a)	1.58(5)
C(32) -C(33)	1.501(5)	P(1) -F(5a)	1.52(2)
C(33) -C(34)	1.393(5)	P(1) -F(6a)	1.64(2)
C(34) -C(35)	1.356(5)	P(1) -F(1b)	1.596(7)
C(35) -C(36)	1.402(5)	P(1) -F(2b)	1.63(1)
C(36) -C(44)	1.403(5)	P(1) -F(3b)	1.62(1)
C(36) -C(37)	1.433(5)	P(1) -F(4b)	1.56(1)
C(37) -C(38)	1.336(5)	P(1) -F(5b)	1.610(4)
C(38) -C(39)	1.430(5)	P(1) -F(6b)	1.578(6)

Table 2.56 Bond angles (°) with standard uncertainties in parentheses of **86**

N(1) -Cu -N(4)	145.6(1)	N(4) -C(42) -C(41)	121.7(3)
N(1) -Cu -N(2)	81.4(1)	N(4) -C(42) -C(45)	116.7(3)
N(4) -Cu -N(2)	118.4(1)	C(41) -C(42) -C(45)	121.6(3)
N(1) -Cu -N(3)	116.2(1)	N(4) -C(43) -C(39)	123.7(3)
N(4) -Cu -N(3)	81.7(1)	N(4) -C(43) -C(44)	117.3(3)
N(2) -Cu -N(3)	116.4(1)	C(39) -C(43) -C(44)	119.0(3)

Table 2.56 continued

C(60) -O(1) -C(1)	115.1(3)	N(3) -C(44) -C(36)	122.6(3)
C(15) -O(2) -C(14)	113.4(3)	N(3) -C(44) -C(43)	117.3(3)
C(29) -O(3) -C(32)	116.5(2)	C(36) -C(44) -C(43)	120.0(3)
C(46) -O(4) -C(45)	117.0(3)	O(4) -C(45) -C(42)	114.0(3)
C(2) -N(1) -C(13)	118.0(3)	C(54) -C(46) -C(47)	120.2(3)
C(2) -N(1) -Cu	129.2(2)	C(54) -C(46) -O(4)	123.7(3)
C(13) -N(1) -Cu	112.1(2)	C(47) -C(46) -O(4)	116.1(3)
C(11) -N(2) -C(12)	118.0(3)	C(48) -C(47) -C(46)	120.8(4)
C(11) -N(2) -Cu	131.5(2)	C(47) -C(48) -C(49)	119.3(3)
C(12) -N(2) -Cu	110.1(2)	C(53) -C(49) -C(48)	119.6(3)
C(33) -N(3) -C(44)	117.8(3)	C(53) -C(49) -C(50)	111.3(3)
C(33) -N(3) -Cu	131.6(2)	C(48) -C(49) -C(50)	129.1(3)
C(44) -N(3) -Cu	110.2(2)	C(67) -C(50) -C(49)	114.2(3)
C(42) -N(4) -C(43)	117.6(3)	C(67) -C(50) -C(68)	108.8(3)
C(42) -N(4) -Cu	129.2(2)	C(49) -C(50) -C(68)	109.8(3)
C(43) -N(4) -Cu	112.1(2)	C(67) -C(50) -C(51)	110.8(3)
O(1) -C(1) -C(2)	110.1(3)	C(49) -C(50) -C(51)	101.1(3)
N(1) -C(2) -C(3)	122.1(3)	C(68) -C(50) -C(51)	112.0(3)
N(1) -C(2) -C(1)	116.2(3)	C(50) -C(51) -C(52)	107.8(3)
C(3) -C(2) -C(1)	121.5(3)	C(62) -C(52) -C(53)	112.0(3)
C(4) -C(3) -C(2)	120.1(4)	C(62) -C(52) -C(51)	116.2(3)
C(3) -C(4) -C(5)	119.6(3)	C(53) -C(52) -C(51)	100.1(3)
C(4) -C(5) -C(13)	117.5(3)	C(62) -C(52) -C(55)	101.0(3)
C(4) -C(5) -C(6)	123.3(3)	C(53) -C(52) -C(55)	113.0(3)
C(13) -C(5) -C(6)	119.1(3)	C(51) -C(52) -C(55)	115.1(3)
C(7) -C(6) -C(5)	120.3(4)	C(49) -C(53) -C(54)	121.8(3)
C(6) -C(7) -C(8)	122.2(4)	C(49) -C(53) -C(52)	112.5(3)
C(9) -C(8) -C(12)	117.1(4)	C(54) -C(53) -C(52)	125.7(3)
C(9) -C(8) -C(7)	124.3(4)	C(46) -C(54) -C(53)	118.4(3)
C(12) -C(8) -C(7)	118.6(4)	C(56) -C(55) -C(52)	107.0(3)
C(10) -C(9) -C(8)	119.4(4)	C(70) -C(56) -C(57)	112.8(3)
C(9) -C(10) -C(11)	120.6(4)	C(70) -C(56) -C(69)	109.9(3)
N(2) -C(11) -C(10)	121.9(4)	C(57) -C(56) -C(69)	109.3(3)
N(2) -C(11) -C(14)	117.8(3)	C(70) -C(56) -C(55)	111.9(3)
C(10) -C(11) -C(14)	120.2(3)	C(57) -C(56) -C(55)	101.2(3)
N(2) -C(12) -C(8)	122.9(3)	C(69) -C(56) -C(55)	111.4(3)
N(2) -C(12) -C(13)	117.4(3)	C(58) -C(57) -C(62)	120.4(3)
C(8) -C(12) -C(13)	119.7(3)	C(58) -C(57) -C(56)	129.2(3)
N(1) -C(13) -C(5)	122.5(3)	C(62) -C(57) -C(56)	110.4(3)
N(1) -C(13) -C(12)	117.4(3)	C(57) -C(58) -C(59)	119.1(3)
C(5) -C(13) -C(12)	120.0(3)	C(60) -C(59) -C(58)	120.3(3)
O(2) -C(14) -C(11)	111.4(3)	C(61) -C(60) -C(59)	121.5(3)
C(23) -C(15) -C(16)	122.1(3)	C(61) -C(60) -O(1)	122.8(3)
C(23) -C(15) -O(2)	119.6(3)	C(59) -C(60) -O(1)	115.7(3)
C(16) -C(15) -O(2)	118.3(3)	C(60) -C(61) -C(62)	117.6(3)
C(17) -C(16) -C(15)	119.1(4)	C(57) -C(62) -C(61)	121.0(3)
C(16) -C(17) -C(18)	119.9(3)	C(57) -C(62) -C(52)	112.9(3)
C(17) -C(18) -C(22)	120.2(3)	C(61) -C(62) -C(52)	125.9(3)
C(17) -C(18) -C(19)	127.1(3)	C(72a)-C(71a)-C(76a)	120.0
C(22) -C(18) -C(19)	112.6(3)	C(71a)-C(72a)-C(73a)	120.0

Table 2.56 continued

C(18) -C(19) -C(63)	111.3(3)	C(72a)-C(73a)-C(74a)	120.0
C(18) -C(19) -C(64)	110.2(3)	C(75a)-C(74a)-C(73a)	120.0
C(63) -C(19) -C(64)	109.4(3)	C(74a)-C(75a)-C(76a)	120.0
C(18) -C(19) -C(20)	102.9(3)	C(75a)-C(76a)-C(71a)	120.0
C(63) -C(19) -C(20)	111.5(3)	C(72b)-C(71b)-C(76b)	120.0
C(64) -C(19) -C(20)	111.3(3)	C(71b)-C(72b)-C(73b)	120.0
C(19) -C(20) -C(21)	108.8(3)	C(74b)-C(73b)-C(72b)	120.0
C(22) -C(21) -C(31)	111.9(3)	C(75b)-C(74b)-C(73b)	120.0
C(22) -C(21) -C(24)	118.9(3)	C(76b)-C(75b)-C(74b)	120.0
C(31) -C(21) -C(24)	100.0(3)	C(75b)-C(76b)-C(71b)	120.0
C(22) -C(21) -C(20)	101.6(3)	C(78a)-C(77a)-C(82a)	120.0
C(31) -C(21) -C(20)	112.2(3)	C(79a)-C(78a)-C(77a)	120.0
C(24) -C(21) -C(20)	112.8(3)	C(80a)-C(79a)-C(78a)	120.0
C(18) -C(22) -C(23)	120.5(3)	C(79a)-C(80a)-C(81a)	120.0
C(18) -C(22) -C(21)	111.4(3)	C(82a)-C(81a)-C(80a)	120.0
C(23) -C(22) -C(21)	128.0(3)	C(81a)-C(82a)-C(77a)	120.0
C(15) -C(23) -C(22)	118.1(3)	C(78b)-C(77b)-C(82b)	120.0
C(21) -C(24) -C(25)	106.7(3)	C(79b)-C(78b)-C(77b)	120.0
C(26) -C(25) -C(66)	112.0(3)	C(78b)-C(79b)-C(80b)	120.0
C(26) -C(25) -C(65)	111.7(3)	C(81b)-C((77b)	120.0
C(66) -C(25) -C(24)	110.9(3)	F(2a) -P(1) -F(3a)	101(2)
C(65) -C(25) -C(24)	112.0(3)	F(2a) -P(1) -F(80b)-C(79b)	120.0
C(66) -C(25) -C(65)	109.6(3)	C(82b)-C(81b)-C(80b)	120.0
C(26) -C(25) -C(24)	100.5(3)	C(81b)-C(82b)-C 5a)	98(2)
C(27) -C(26) -C(31)	118.7(3)	F(3a) -P(1) -F(5a)	94(1)
C(27) -C(26) -C(25)	129.9(3)	F(2a) -P(1) -F(4a)	85(2)
C(31) -C(26) -C(25)	111.3(3)	F(3a) -P(1) -F(4a)	100(2)
C(26) -C(27) -C(28)	120.5(3)	F(5a) -P(1) -F(4a)	165(2)
C(29) -C(28) -C(27)	119.2(3)	F(4b) -P(1) -F(6b)	93.7(6)
C(28) -C(29) -C(30)	120.9(3)	F(4b) -P(1) -F(1b)	92.5(5)
C(28) -C(29) -O(3)	116.2(3)	F(6b) -P(1) -F(1b)	91.9(4)
C(30) -C(29) -O(3)	122.9(3)	F(4b) -P(1) -F(5b)	176.7(5)
C(29) -C(30) -C(31)	118.2(3)	F(6b) -P(1) -F(5b)	89.3(3)
C(26) -C(31) -C(30)	122.1(3)	F(1b) -P(1) -F(5b)	88.9(3)
C(26) -C(31) -C(21)	111.0(3)	F(4b) -P(1) -F(3b)	88.1(6)
C(30) -C(31) -C(21)	126.9(3)	F(6b) -P(1) -F(3b)	176.7(5)
O(3) -C(32) -C(33)	114.3(3)	F(1b) -P(1) -F(3b)	90.8(5)
N(3) -C(33) -C(34)	121.8(3)	F(5b) -P(1) -F(3b)	88.8(3)
N(3) -C(33) -C(32)	116.1(3)	F(4b) -P(1) -F(2b)	91.2(5)
C(34) -C(33) -C(32)	122.1(3)	F(6b) -P(1) -F(2b)	90.6(4)
C(35) -C(34) -C(33)	120.9(4)	F(1b) -P(1) -F(2b)	175.5(5)
C(34) -C(35) -C(36)	118.9(3)	F(5b) -P(1) -F(2b)	87.4(4)
C(35) -C(36) -C(44)	117.5(3)	F(3b) -P(1) -F(2b)	86.7(6)
C(35) -C(36) -C(37)	123.6(3)	F(2a) -P(1) -F(1a)	169(2)
C(44) -C(36) -C(37)	118.9(3)	F(3a) -P(1) -F(1a)	87(2)
C(38) -C(37) -C(36)	121.2(4)	F(5a) -P(1) -F(1a)	87(1)
C(37) -C(38) -C(39)	121.0(4)	F(4a) -P(1) -F(1a)	88(2)
C(43) -C(39) -C(40)	116.6(4)	F(2a) -P(1) -F(6a)	93(2)
C(43) -C(39) -C(38)	119.5(3)	F(3a) -P(1) -F(6a)	165(2)
C(40) -C(39) -C(38)	123.8(4)	F(5a) -P(1) -F(6a)	89(1)

Table 2.56 continued

C(41) -C(40) -C(39)	119.7(4)	F(4a) -P(1) -F(6a)	77(2)
C(40) -C(41) -C(42)	120.2(4)	F(1a) -P(1) -F(6a)	78(2)

Table 2.57 Torsion angles (°) with standard uncertainties in parentheses of **86**

N(4) -Cu -N(1) -C(2)	-49.7(4)	C(27) -C(26) -C(31) -C(30)	-6.5(5)
N(2) -Cu -N(1) -C(2)	-178.8(3)	C(25) -C(26) -C(31) -C(30)	170.8(3)
N(3) -Cu -N(1) -C(2)	66.0(3)	C(27) -C(26) -C(31) -C(21)	175.2(3)
N(4) -Cu -N(1) -C(13)	140.1(2)	C(25) -C(26) -C(31) -C(21)	-7.4(4)
N(2) -Cu -N(1) -C(13)	11.1(2)	C(29) -C(30) -C(31) -C(26)	3.2(5)
N(3) -Cu -N(1) -C(13)	-104.1(2)	C(29) -C(30) -C(31) -C(21)	-178.8(3)
N(1) -Cu -N(2) -C(11)	177.6(3)	C(22) -C(21) -C(31) -C(26)	151.6(3)
N(4) -Cu -N(2) -C(11)	27.5(3)	C(24) -C(21) -C(31) -C(26)	24.7(4)
N(3) -Cu -N(2) -C(11)	-67.4(3)	C(20) -C(21) -C(31) -C(26)	-95.0(3)
N(1) -Cu -N(2) -C(12)	-10.1(2)	C(22) -C(21) -C(31) -C(30)	-26.6(5)
N(4) -Cu -N(2) -C(12)	-160.2(2)	C(24) -C(21) -C(31) -C(30)	-153.5(3)
N(3) -Cu -N(2) -C(12)	104.9(2)	C(20) -C(21) -C(31) -C(30)	86.8(4)
N(1) -Cu -N(3) -C(33)	23.0(3)	C(29) -O(3) -C(32) -C(33)	-81.2(4)
N(4) -Cu -N(3) -C(33)	172.1(3)	C(44) -N(3) -C(33) -C(34)	3.0(5)
N(2) -Cu -N(3) -C(33)	-70.2(3)	Cu -N(3) -C(33) -C(34)	-169.9(2)
N(1) -Cu -N(3) -C(44)	-150.2(2)	C(44) -N(3) -C(33) -C(32)	-174.5(3)
N(4) -Cu -N(3) -C(44)	-1.2(2)	Cu -N(3) -C(33) -C(32)	12.7(5)
N(2) -Cu -N(3) -C(44)	116.5(2)	O(3) -C(32) -C(33) -N(3)	161.5(3)
N(1) -Cu -N(4) -C(42)	-60.1(4)	O(3) -C(32) -C(33) -C(34)	-15.9(5)
N(2) -Cu -N(4) -C(42)	59.1(3)	N(3) -C(33) -C(34) -C(35)	-4.6(5)
N(3) -Cu -N(4) -C(42)	174.7(3)	C(32) -C(33) -C(34) -C(35)	172.7(3)
N(1) -Cu -N(4) -C(43)	132.7(2)	C(33) -C(34) -C(35) -C(36)	0.2(5)
N(2) -Cu -N(4) -C(43)	-108.1(2)	C(34) -C(35) -C(36) -C(44)	5.3(5)
N(3) -Cu -N(4) -C(43)	7.5(2)	C(34) -C(35) -C(36) -C(37)	-174.1(3)
C(60) -O(1) -C(1) -C(2)	157.7(3)	C(35) -C(36) -C(37) -C(38)	178.0(4)
C(13) -N(1) -C(2) -C(3)	3.6(5)	C(44) -C(36) -C(37) -C(38)	-1.4(6)
Cu -N(1) -C(2) -C(3)	-166.1(3)	C(36) -C(37) -C(38) -C(39)	4.9(6)
C(13) -N(1) -C(2) -C(1)	-173.1(3)	C(37) -C(38) -C(39) -C(43)	-1.9(6)
Cu -N(1) -C(2) -C(1)	17.2(4)	C(37) -C(38) -C(39) -C(40)	177.2(4)
O(1) -C(1) -C(2) -N(1)	-78.4(4)	C(43) -C(39) -C(40) -C(41)	5.1(5)
O(1) -C(1) -C(2) -C(3)	104.9(4)	C(38) -C(39) -C(40) -C(41)	-174.1(4)
N(1) -C(2) -C(3) -C(4)	-3.2(5)	C(39) -C(40) -C(41) -C(42)	0.6(6)
C(1) -C(2) -C(3) -C(4)	173.3(3)	C(43) -N(4) -C(42) -C(41)	5.5(5)
C(2) -C(3) -C(4) -C(5)	-0.2(6)	Cu -N(4) -C(42) -C(41)	-161.1(3)
C(3) -C(4) -C(5) -C(13)	2.8(5)	C(43) -N(4) -C(42) -C(45)	-171.6(3)
C(3) -C(4) -C(5) -C(6)	-177.4(4)	Cu -N(4) -C(42) -C(45)	21.8(5)
C(4) -C(5) -C(6) -C(7)	-179.7(4)	C(40) -C(41) -C(42) -N(4)	-6.2(6)
C(13) -C(5) -C(6) -C(7)	0.1(6)	C(40) -C(41) -C(42) -C(45)	170.8(4)
C(5) -C(6) -C(7) -C(8)	0.7(6)	C(42) -N(4) -C(43) -C(39)	0.6(5)
C(6) -C(7) -C(8) -C(9)	177.1(4)	Cu -N(4) -C(43) -C(39)	169.4(3)
C(6) -C(7) -C(8) -C(12)	-0.4(6)	C(42) -N(4) -C(43) -C(44)	178.4(3)
C(12) -C(8) -C(9) -C(10)	-2.2(5)	Cu -N(4) -C(43) -C(44)	-12.8(4)
C(7) -C(8) -C(9) -C(10)	-179.7(4)	C(40) -C(39) -C(43) -N(4)	-5.9(5)
C(8) -C(9) -C(10) -C(11)	-0.7(6)	C(38) -C(39) -C(43) -N(4)	173.3(3)

Table 2.57 continued

C(12)	-N(2)	-C(11)	-C(10)	-3.4(5)	C(40)	-C(39)	-C(43)	-C(44)	176.4(3)
Cu	-N(2)	-C(11)	-C(10)	168.5(3)	C(38)	-C(39)	-C(43)	-C(44)	-4.4(5)
C(12)	-N(2)	-C(11)	-C(14)	174.4(3)	C(33)	-N(3)	-C(44)	-C(36)	2.9(5)
Cu	-N(2)	-C(11)	-C(14)	-13.8(5)	Cu	-N(3)	-C(44)	-C(36)	177.2(3)
C(9)	-C(10)	-C(11)	-N(2)	3.6(5)	C(33)	-N(3)	-C(44)	-C(43)	-179.6(3)
C(9)	-C(10)	-C(11)	-C(14)	-174.1(3)	Cu	-N(3)	-C(44)	-C(43)	-5.3(3)
C(11)	-N(2)	-C(12)	-C(8)	0.3(5)	C(35)	-C(36)	-C(44)	-N(3)	-7.1(5)
Cu	-N(2)	-C(12)	-C(8)	-173.2(3)	C(37)	-C(36)	-C(44)	-N(3)	172.3(3)
C(11)	-N(2)	-C(12)	-C(13)	-178.9(3)	C(35)	-C(36)	-C(44)	-C(43)	175.6(3)
Cu	-N(2)	-C(12)	-C(13)	7.6(4)	C(37)	-C(36)	-C(44)	-C(43)	-5.0(5)
C(9)	-C(8)	-C(12)	-N(2)	2.4(5)	N(4)	-C(43)	-C(44)	-N(3)	12.4(4)
C(7)	-C(8)	-C(12)	-N(2)	-179.9(3)	C(39)	-C(43)	-C(44)	-N(3)	-169.7(3)
C(9)	-C(8)	-C(12)	-C(13)	-178.3(3)	N(4)	-C(43)	-C(44)	-C(36)	-170.1(3)
C(7)	-C(8)	-C(12)	-C(13)	-0.7(5)	C(39)	-C(43)	-C(44)	-C(36)	7.8(5)
C(2)	-N(1)	-C(13)	-C(5)	-0.8(5)	C(46)	-O(4)	-C(45)	-C(42)	-74.4(4)
Cu	-N(1)	-C(13)	-C(5)	170.6(3)	N(4)	-C(42)	-C(45)	-O(4)	145.2(3)
C(2)	-N(1)	-C(13)	-C(12)	178.1(3)	C(41)	-C(42)	-C(45)	-O(4)	-31.9(5)
Cu	-N(1)	-C(13)	-C(12)	-10.5(4)	C(45)	-O(4)	-C(46)	-C(54)	31.7(5)
C(4)	-C(5)	-C(13)	-N(1)	-2.4(5)	C(45)	-O(4)	-C(46)	-C(47)	-148.8(3)
C(6)	-C(5)	-C(13)	-N(1)	177.8(3)	C(54)	-C(46)	-C(47)	-C(48)	-1.5(6)
C(4)	-C(5)	-C(13)	-C(12)	178.7(3)	O(4)	-C(46)	-C(47)	-C(48)	179.0(4)
C(6)	-C(5)	-C(13)	-C(12)	-1.1(5)	C(46)	-C(47)	-C(48)	-C(49)	0.7(6)
N(2)	-C(12)	-C(13)	-N(1)	1.7(4)	C(47)	-C(48)	-C(49)	-C(53)	0.9(6)
C(8)	-C(12)	-C(13)	-N(1)	-177.5(3)	C(47)	-C(48)	-C(49)	-C(50)	-177.6(4)
N(2)	-C(12)	-C(13)	-C(5)	-179.3(3)	C(53)	-C(49)	-C(50)	-C(67)	-133.9(3)
C(8)	-C(12)	-C(13)	-C(5)	1.4(5)	C(48)	-C(49)	-C(50)	-C(67)	44.7(5)
C(15)	-O(2)	-C(14)	-C(11)	-92.0(3)	C(53)	-C(49)	-C(50)	-C(68)	103.6(4)
N(2)	-C(11)	-C(14)	-O(2)	143.1(3)	C(48)	-C(49)	-C(50)	-C(68)	-77.9(5)
C(10)	-C(11)	-C(14)	-O(2)	-39.1(4)	C(53)	-C(49)	-C(50)	-C(51)	-14.9(4)
C(14)	-O(2)	-C(15)	-C(23)	104.3(4)	C(48)	-C(49)	-C(50)	-C(51)	163.7(4)
C(14)	-O(2)	-C(15)	-C(16)	-77.8(4)	C(67)	-C(50)	-C(51)	-C(52)	146.8(3)
C(23)	-C(15)	-C(16)	-C(17)	1.3(6)	C(49)	-C(50)	-C(51)	-C(52)	25.4(4)
O(2)	-C(15)	-C(16)	-C(17)	-176.6(3)	C(68)	-C(50)	-C(51)	-C(52)	-91.5(3)
C(15)	-C(16)	-C(17)	-C(18)	0.5(5)	C(50)	-C(51)	-C(52)	-C(62)	-146.8(3)
C(16)	-C(17)	-C(18)	-C(22)	-1.7(5)	C(50)	-C(51)	-C(52)	-C(53)	-26.0(4)
C(16)	-C(17)	-C(18)	-C(19)	177.1(4)	C(50)	-C(51)	-C(52)	-C(55)	95.4(4)
C(17)	-C(18)	-C(19)	-C(63)	66.2(5)	C(48)	-C(49)	-C(53)	-C(54)	-1.6(6)
C(22)	-C(18)	-C(19)	-C(63)	-114.9(4)	C(50)	-C(49)	-C(53)	-C(54)	177.1(3)
C(17)	-C(18)	-C(19)	-C(64)	-55.4(5)	C(48)	-C(49)	-C(53)	-C(52)	179.7(3)
C(22)	-C(18)	-C(19)	-C(64)	123.5(3)	C(50)	-C(49)	-C(53)	-C(52)	-1.5(4)
C(17)	-C(18)	-C(19)	-C(20)	-174.2(3)	C(62)	-C(52)	-C(53)	-C(49)	140.9(3)
C(22)	-C(18)	-C(19)	-C(20)	4.7(4)	C(51)	-C(52)	-C(53)	-C(49)	17.1(4)
C(18)	-C(19)	-C(20)	-C(21)	-13.3(4)	C(55)	-C(52)	-C(53)	-C(49)	-105.8(4)
C(63)	-C(19)	-C(20)	-C(21)	106.1(4)	C(62)	-C(52)	-C(53)	-C(54)	-37.7(5)
C(64)	-C(19)	-C(20)	-C(21)	-131.4(3)	C(51)	-C(52)	-C(53)	-C(54)	-161.5(3)
C(19)	-C(20)	-C(21)	-C(22)	16.5(4)	C(55)	-C(52)	-C(53)	-C(54)	75.6(4)
C(19)	-C(20)	-C(21)	-C(31)	-103.2(4)	C(47)	-C(46)	-C(54)	-C(53)	0.8(6)
C(19)	-C(20)	-C(21)	-C(24)	144.9(3)	O(4)	-C(46)	-C(54)	-C(53)	-179.7(3)
C(17)	-C(18)	-C(22)	-C(23)	1.3(5)	C(49)	-C(53)	-C(54)	-C(46)	0.8(6)
C(19)	-C(18)	-C(22)	-C(23)	-177.7(3)	C(52)	-C(53)	-C(54)	-C(46)	179.3(3)

Table 2.57 continued

C(17) -C(18) -C(22) -C(21)	-174.8(3)	C(62) -C(52) -C(55) -C(56)	-24.6(4)
C(19) -C(18) -C(22) -C(21)	6.2(4)	C(53) -C(52) -C(55) -C(56)	-144.4(3)
C(31) -C(21) -C(22) -C(18)	106.0(3)	C(51) -C(52) -C(55) -C(56)	101.5(4)
C(24) -C(21) -C(22) -C(18)	-138.2(3)	C(52) -C(55) -C(56) -C(70)	147.4(3)
C(20) -C(21) -C(22) -C(18)	-13.8(4)	C(52) -C(55) -C(56) -C(57)	27.0(4)
C(31) -C(21) -C(22) -C(23)	-69.7(4)	C(52) -C(55) -C(56) -C(69)	-89.1(4)
C(24) -C(21) -C(22) -C(23)	46.1(5)	C(70) -C(56) -C(57) -C(58)	39.1(5)
C(20) -C(21) -C(22) -C(23)	170.5(3)	C(69) -C(56) -C(57) -C(58)	-83.5(5)
C(16) -C(15) -C(23) -C(22)	-1.7(5)	C(55) -C(56) -C(57) -C(58)	158.9(4)
O(2) -C(15) -C(23) -C(22)	176.1(3)	C(70) -C(56) -C(57) -C(62)	-139.4(3)
C(18) -C(22) -C(23) -C(15)	0.4(5)	C(69) -C(56) -C(57) -C(62)	98.0(4)
C(21) -C(22) -C(23) -C(15)	175.8(3)	C(55) -C(56) -C(57) -C(62)	-19.7(4)
C(22) -C(21) -C(24) -C(25)	-154.2(3)	C(62) -C(57) -C(58) -C(59)	2.4(5)
C(31) -C(21) -C(24) -C(25)	-32.3(3)	C(56) -C(57) -C(58) -C(59)	-176.0(3)
C(20) -C(21) -C(24) -C(25)	87.1(4)	C(57) -C(58) -C(59) -C(60)	-1.3(5)
C(21) -C(24) -C(25) -C(26)	28.5(4)	C(58) -C(59) -C(60) -C(61)	-2.4(5)
C(21) -C(24) -C(25) -C(66)	147.0(3)	C(58) -C(59) -C(60) -O(1)	175.1(3)
C(21) -C(24) -C(25) -C(65)	-90.2(4)	C(1) -O(1) -C(60) -C(61)	9.3(4)
C(66) -C(25) -C(26) -C(27)	46.1(5)	C(1) -O(1) -C(60) -C(59)	-168.2(3)
C(65) -C(25) -C(26) -C(27)	-77.3(5)	C(59) -C(60) -C(61) -C(62)	4.8(5)
C(24) -C(25) -C(26) -C(27)	163.9(4)	O(1) -C(60) -C(61) -C(62)	-172.5(3)
C(66) -C(25) -C(26) -C(31)	-130.8(3)	C(58) -C(57) -C(62) -C(61)	0.1(5)
C(65) -C(25) -C(26) -C(31)	105.8(4)	C(56) -C(57) -C(62) -C(61)	178.8(3)
C(24) -C(25) -C(26) -C(31)	-13.1(4)	C(58) -C(57) -C(62) -C(52)	-174.2(3)
C(31) -C(26) -C(27) -C(28)	4.1(5)	C(56) -C(57) -C(62) -C(52)	4.5(4)
C(25) -C(26) -C(27) -C(28)	-172.7(4)	C(60) -C(61) -C(62) -C(57)	-3.6(5)
C(26) -C(27) -C(28) -C(29)	1.5(6)	C(60) -C(61) -C(62) -C(52)	169.8(3)
C(27) -C(28) -C(29) -C(30)	-4.9(5)	C(53) -C(52) -C(62) -C(57)	133.1(3)
C(27) -C(28) -C(29) -O(3)	175.4(3)	C(51) -C(52) -C(62) -C(57)	-112.7(3)
C(32) -O(3) -C(29) -C(28)	-147.6(3)	C(55) -C(52) -C(62) -C(57)	12.6(4)
C(32) -O(3) -C(29) -C(30)	32.7(4)	C(53) -C(52) -C(62) -C(61)	-40.8(5)
C(28) -C(29) -C(30) -C(31)	2.6(5)	C(51) -C(52) -C(62) -C(61)	73.4(4)
O(3) -C(29) -C(30) -C(31)	-177.7(3)	C(55) -C(52) -C(62) -C(61)	-161.3(3)

2.6 Calculations of Dihedral Angles of [Cu(I)2]PF_6 (86)

Table 2.58 Calculations of Dihedral Angles of [Cu(I)**2**]PF_6(**86**)

		Comp1	Comp2	Cu(I)**2**	Comp3	Comp4	Comp5	Comp6
α	**1A-Cu-1B**	82.4	81.7	81.4	82.7	82.7	81.3	80.6
β	**1A-Cu-2A**	124.3	127.9	145.6	122.3	133.7	126.9	133.5
γ	**1A-Cu-2B**	122.9	121.5	116.2	123.8	109.9	114.9	121.2
ρ	**1B-Cu-2A**	114.7	117.4	118.4	119.3	121.3	127	115.4
σ	**1B-Cu-2B**	135.2	134.1	116.4	131.2	133.3	130.8	133.5
ω	**2A-Cu-2B**	82.9	81	81.7	83.2	82.7	81.7	80.6
	n1	-0.65216	-0.71024	-0.85785	-0.68186	-0.80619	-0.7923	-0.73249
	l1	-0.11057	-0.11779	-0.26797	-0.03403	-0.12969	0.001071	-0.20054
	m1	0.749973	0.694036	0.438493	0.730686	0.577261	0.610136	0.650572
	SUM	1	1	1	1	1	1	1
	n2	-0.83248	-0.80538	-0.58442	-0.80925	-0.68351	-0.70809	-0.7909
	l2	0.126309	0.132563	0.002399	0.077494	0.261436	0.178363	0.131672
	m2	-0.53946	-0.57775	-0.81145	-0.58233	-0.68152	-0.68323	-0.59762
	SUM	1	1	1	1	1	1	1
		Cos(Theta)	Cos(Theta)	Cos(Theta)	Cos(Theta)	Cos(Theta)	Cos(Theta)	Cos(Theta)
	Theta X	0.140381	0.076496	-0.24647	0.098961	-0.06955	-0.04831	0.034705
	Theta Y	0.010497	0.00972	-0.1755	0.02899	0.08788	0.118607	-0.04514
	Theta Z	-0.17578	-0.19134	-0.16036	-0.081	-0.30173	-0.14205	-0.25856
		ARCcos	ARCcos	ARCcos	ARCcos	ARCcos	ARCcos	ARCcos
	Theta X	81.93012	85.61284	104.2685	84.32067	93.98798	92.76925	88.01117
	Theta Y	89.39854	89.44308	100.108	88.33874	84.95836	83.18827	92.58703
	Theta Z	100.1243	101.031	99.22778	94.64629	107.5616	98.16627	104.9848

(From MS Excel Sheet)

CHAPTER 3. ASYMMETRIC CATALYSIS

3.1 Introduction

3.1.1 Cyclophanes as Asymmetric Catalysts

Chiral organometallic catalysts in asymmetric transformation reactions have been widely used to produce enantiomerically pure compounds.[28.29] With the development of supramolecular chemistry, it is possible to synthesize not only chiral ligands that bind metals, but many cavity-containing host molecules that can selectively bind and recognize right substrates.[60] In spite of great potential in using the chiral host molecules with metal centers as asymmetric catalysts, the field has not been exploited until the mid-1990's.[247.248] Several noteworthy reports of using metal-complexed chiral macrocycles, especially chiral cyclophanes and cyclic ethers, as enantioselective catalysts are discussed in the section.

Sunjic[249] and coworkers have used copper(I) complexes of chiral cyclophanes **95a--d**, with built-in bisoxazoline unit, as catalysts for asymmetric cyclopropanation (Figure 3.1). Their report indicates that the best catalysts were smallest macrocycles, **95b** and **95c**, with the rigid structure. These catalysts showed 77 % cumulative (dia and enantio-)selectivity and one of the highest diastereoselectivity (86 % de, favoring *trans*) in the cyclopropanation of styrene with ethyl diazoacetate. The average yield of reactions is over 55 %, and (1*S*,2*R*)-*cis* and (1*S*,2*S*)-*trans* products were favored.

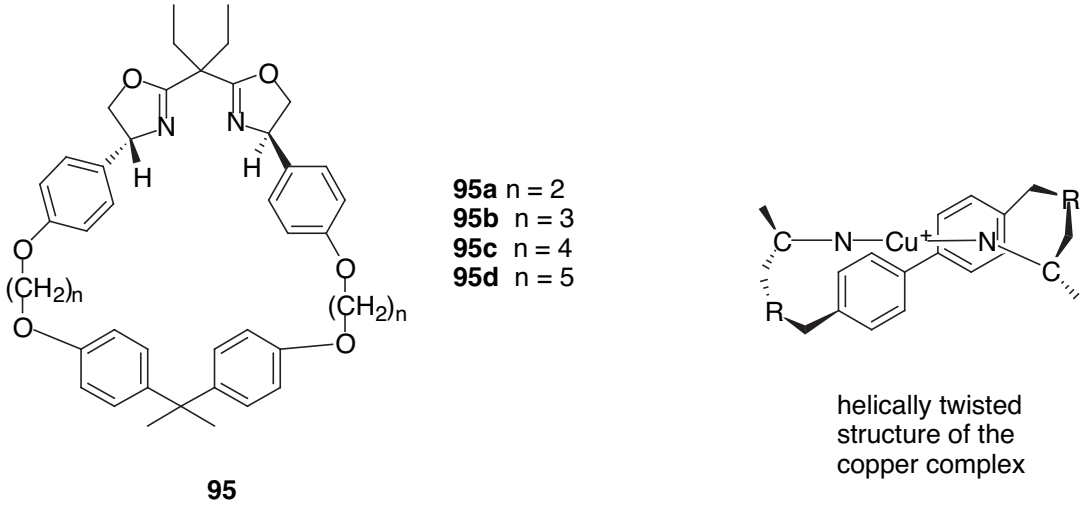

Figure 3.1 (a) General structure of C_2-symmetric supramolecular Cu(I) catalyst **95**. (b) Helicity of the macrocycle containing stereogenic centers of the bisoxazoline unit.

Braddock[250] used planar chiral organocatalyst PHANOL[251] **96a**—4,12-dihydroxy[2.2]-paracyclophane—and its dinitro-derivative, 4,12-dihydroxy-7,15-dinitro[2.2]paracyclophane **96b**, as catalysts to activate α,β-unsaturated aldehydes and ketones for the Diels-Alder reaction. In the reaction between neat cyclopentadiene and crotonaldehyde, the addition of **96a** and **96b** resulted in 17 % and 37 % conversion to the desired cycloadduct, respectively. Without the catalyst, the same reaction proceeds to <1 % during the same reaction time. The double hydrogen-bonding to the carbonyl group of the dienophile by the catalyst is thought to activate the reaction. The enantiopure (*R*)-**96a** was used as an asymmetric catalyst for the same reaction; however, the enantioselection was found to be minimal (< 5%). It was suggested that the low chiral induction was due to the lack of expression of the planar chirality associated with the paracyclophane backbone around the olefin of the dienophile.

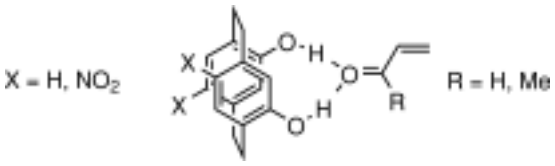

96a-b

Figure 3.2 Braddock's PHANOL **96a** and its dinitro derivative **96b**.

Hydroxy[2.2]paracyclophane ketimine ligands have been used to catalyze the asymmetric 1,2-addition reaction of zinc reagents,[252] containing alkyl-,[253-255] alkenyl,[256] aryl,[257] and alkynylzinc reagents[258] to aldehydes. In particular, Bräse's group converted *ortho*-acylated hydroxy[2.2]paracyclophane, such as **97**, into asymmetric ketimine ligands, like **98** and **99**, after condensation with chiral primary amines. In general the S_pS-configured ligand was more selective and reactive than its enantiomeric counterpart. For example, when benzaldehyde was reacted with the S_pS-configured ligand, **99** and diethyl zinc, the secondary alcohol had an enantiomeric excess of 90 % ee (*R*). The R_pS-configured ligand **98** produced the chiral alcohol in 79 % ee (*S*). It was possible to tune the ligand and substrate to achieve an enantiomeric excess of up to 95 % ee when 2-napthaldehyde was used as substrate and the R_pS-configured ligand**98** was used as chiral auxiliary.

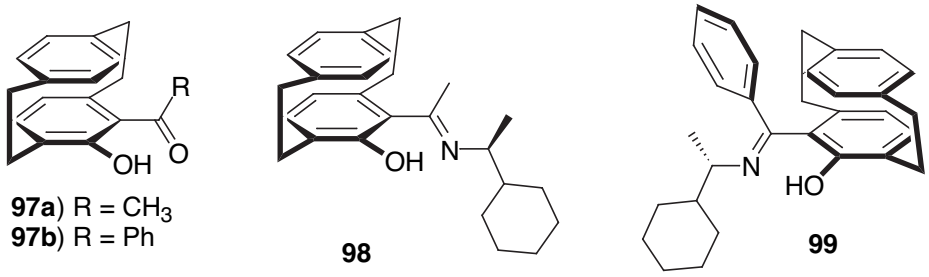

Figure 3.3 Bräse's catalysts **97**—**99**.

Potassium coordinated complexes of Cram's chiral hosts **100**--**102**[259] are known to catalyze Michael additions of carbon acids to a α,β-unsaturated esters and ketones efficiently. The butyllithium complexed to chiral ethelendiamine **102**[260-262] reduced benzaldehyde with high asymmetric induction (upto 92 % ee) and catalyzed the polymerization of methacrylate esters to produce helical polymers.

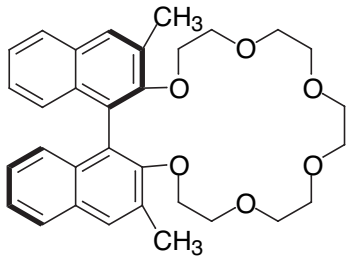

100

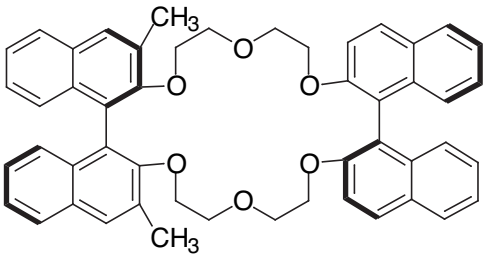

101

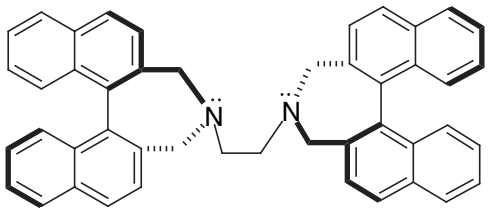

102

Figure 3.4 Cram's cyclic ethers **100**--**102**.

Benaglia and coworkers[143] have synthesized a novel class of macrocycles using widely known chiral templates, such as BINOL and diphenyl derivatives, with metal-binding ligands, such as phen and bpy analogues. [NOTE: syntheses of these macrocycles were discussed in Ch. 1]. Cyclopropanation of styrene with ethyldiazoacetate was chosen as the model system to study copper(I) complexes of these ligands for the development of asymmetric catalysts. The best ligand was **71**, which afforded products in 53 % yield with diastereoselectivity of 56 %, favoring the

trans isomer with 67 % ee. The ligand **72**, with different spacer unit, reversed the diastereoselectivity of the ligand to favor the *cis* isomer (91:9) and 46 % product yield with 63 % ee for the *cis* product. Varying reaction conditions, such as changing reagent ratios or lowering temperature, did not improve the stereoselectivity of the process.

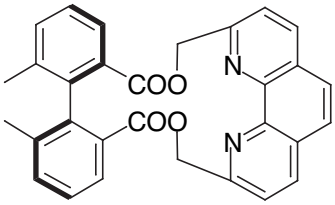

71

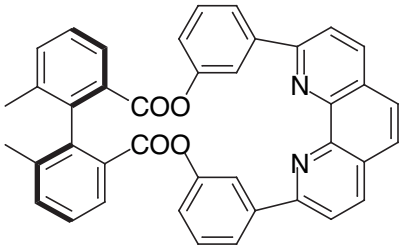

72

Figure 3.5 Macrocycles **71** and **72**.

3.1.2 Allylic Oxidation

The allylic oxidation of olefins with peresters in the presence of copper catalyst to form allylic esters is known as the Kharash-Sosnovsky reaction.[263-265] In their seminal work reported in the late 1950s, Kharash and coworkers produced allylic benzoates **103** in good yields (~80 %) using cyclohexene and *tert*-butyl perester as the oxidant in the presence of a copper or cobalt salt (Scheme 3.1). In most cases, copper catalysts worked better.[266.267] The reaction takes advantage of the special nature of allylic CH bond and proceeds in regioselective manner. For instance, in an acyclic terminal olefin, secondary ester is the major product even though some primary ester is formed in the reaction. Allylic esters can be converted into allylic alcohols after saponification or reduction. Asymmetric version of the Kharash reaction can be viewed as an alternative scheme to produce chiral allylic alcohols, which are useful building blocks in organic synthesis.[268.269]

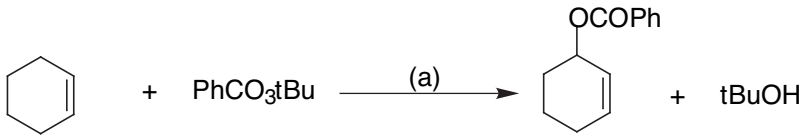

rac-**103**

Scheme 3.1 The Karasch-Sosnovsky reaction. a) cupric 2-ethylhexanoate or CuBr, 80 °C, benzene

The Kharash reaction was very useful in the key step of the synthesis of leukotriene B_4, which is an important inflammation mediator. Wallace and co-workers[270] succeeded in converting (*S*)-cyclohexenyl benzoate into key intermediate, aldehyde-methyl ester, in a single step using Schreiber's selective ozonolysis work-up

method.[271] Prior to the report, the most efficient method used 6 steps and the least efficient step used 11 steps to obtain the same intermediate.

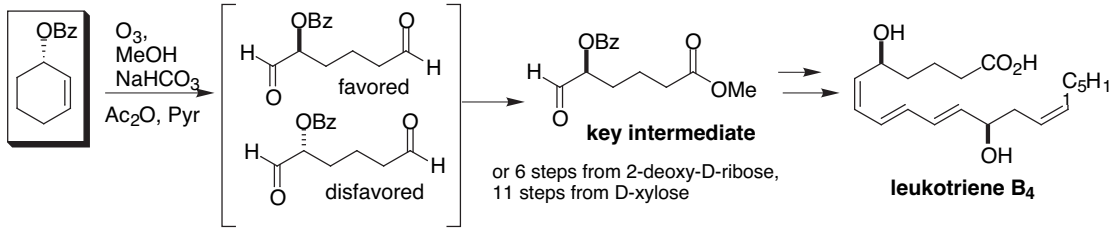

Figure 3.6 Conversion of cyclohexenyl benzoate to leukotriene B_4 using selective ozonolysis.

Mechanisms of the Kharash reaction are generally understood to involve radical chemistry with a transient copper(III)-intermediate structure. The initiation step begins with the homolysis of the perester oxygen-oxygen bond by the copper(I) catalyst to produce *t*-butoxy radical and copper(II)benzoate[272] as shown in (Scheme 3.2). The abstraction of allylic hydrogen atom from cyclohexene by the *t*-butoxy radical forms *t*-butanol and an allylic radical.[273.274] Copper(II)benzoate subsequently adds to the allylic radical to generate the Cu(III) intermediate with an η^1 allylic group.[275] In the case of acylic internal alkenes, the structure of the olefin is retained due to a high rotation barrier of the allylic radical (~20 kcal/mol). In the last step, the 16 e Cu(III)benzoate rearranges in a concerted manner to yield the desired allylic benzoate, and the Cu(I) catalyst gets regenerated. The one-to-one copper-ligand chelate arrangement is modeled after the established X-ray structures for Diels-Alder, aldol, ene, and Michael intermediates reported by Evans.[276-279] Mechanistic studies reveal that copper is intimately involved in the formation of the C-O bond; therefore, it

suggests that the reaction might be rendered enantioselective if a suitable chiral ligand is coordinated to the copper ion.

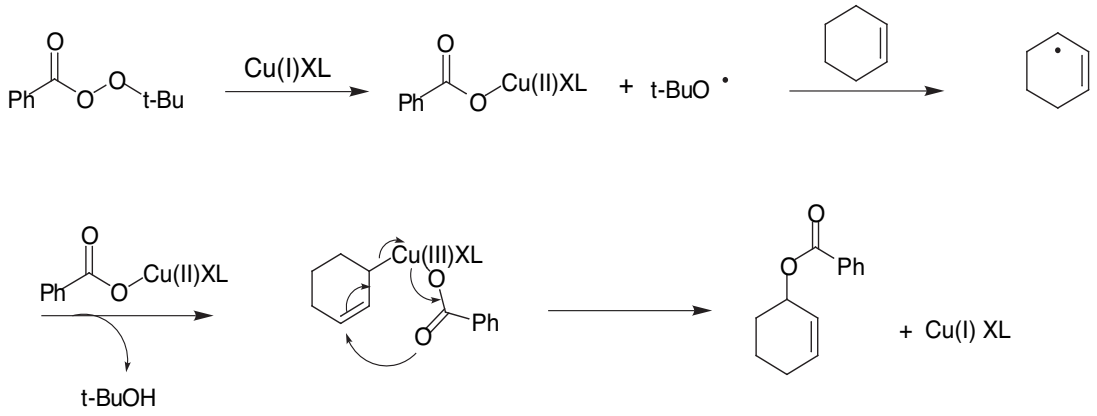

Scheme 3.2 Mechanisms of the Kharasch-Sosnovsky reaction

In spite of the potential synthetic utility of the reaction, only a few attempts in asymmetric versions of the reaction were reported with little success. These early attempts included reactions using copper complexes of (+)-α-ethyl camphorate[280], chiral Schiff bases[279.281], and optically active amino acids[279.281], which provided enantiomeric excess around 5-17 %. Starting in the middle of 1990s, groups of Pfaltz[282], Andrus[283], and Katsuki[284] began to report independently of synthetically useful asymmetric catalysts using chiral nitrogen-containing ligands, such as bisoxazolines and trisoxazolines. Chiral bpy and phen were also used as auxiliaries in the reaction by Kocovsky[285.286] and Chelucci[287.288] with some success. However, most of these reactions suffered from low reactivity, requiring several days to sometimes close to a month for completion.[289] Also, bigger cyclic olefins, such as cyclooctene had poor optical and chemical yields.

Both Pfaltz[282] and Andrus[283] used the same series of enantiomerically pure C_2-symmetric bisoxazoline ligands, **104a-e**, coordinated to copper(I) triflate for the asymmetric allylic oxidation of cyclic olefins **105a-c** as shown in (Scheme 3.3). Enantioselectivity was generally good (77 % ee to 84 % ee) with the product yields ranging from 44 % to 64 %. All products favored the *S*-configuration at the newly formed allylic stereocenter. The steric bulk at the R^2 group had a major impact on the outcome of the stereocontrol. For example, changing from **104b** to **104d** reduced the enantioselectivity of the product, dropping from 70 % ee to 42 % ee in the synthesis of (*S*)-**106**. Smaller cyclic olefins, such as **105a-c** worked well with the group of catalysts, but only a small enantioselectivity was obtained with larger rings, such as cyclooctene, and acylic olefins, such as allylbenzene and 1-octene.

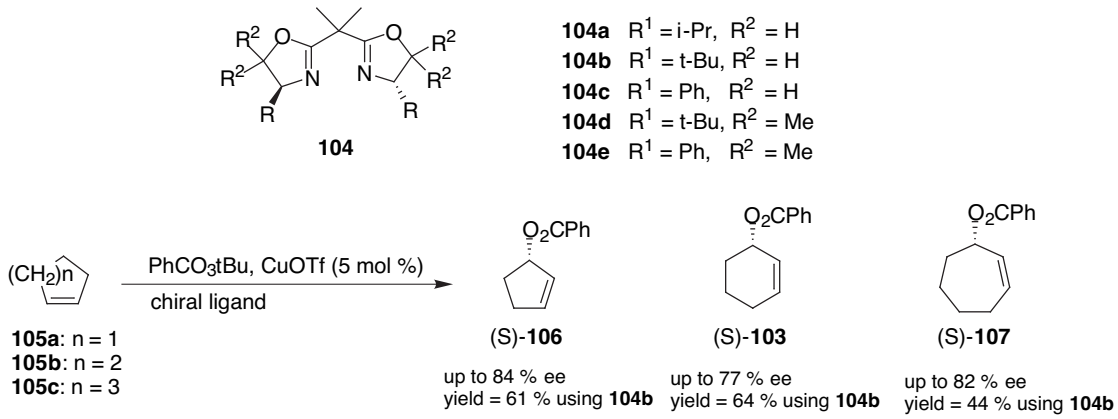

Scheme 3.3 Asymmetric allylic oxidation of cyclic olefins using C_2-symmetric bioxazoline ligands **104a--e**.

Andrus[290] also synthesized bi-*o*-tolylbisoxazoline ligands as listed in (Figure 3.7) and used their copper(I) triflate complexes as catalysts for the asymmetric Kharash reaction. After seeing Hayashi[291] and Ikeda[292]'s successes with related binaphthyl and biphenyl bisoxazoline ligands with other reactions, the group reasoned

that a wider bite angle between the two nitrogen atoms in **108** and **109** and copper would lead to a better enantioselectivity. A widening of the catalyst would bring the reacting allyl and benzoate groups closer together, which would increase the energy difference between diastereomeric transition states. The ligand **108** turned out to the ligand of choice. High enantioselectivity and product yield (73 % ee, 78 % yield) were obtained with the *p*-nitro-*tert*-butyl perbenzoate, **108a** and cyclohexene. For cycloheptene, **108c** provided the product with 72 % ee and 63 % yield.

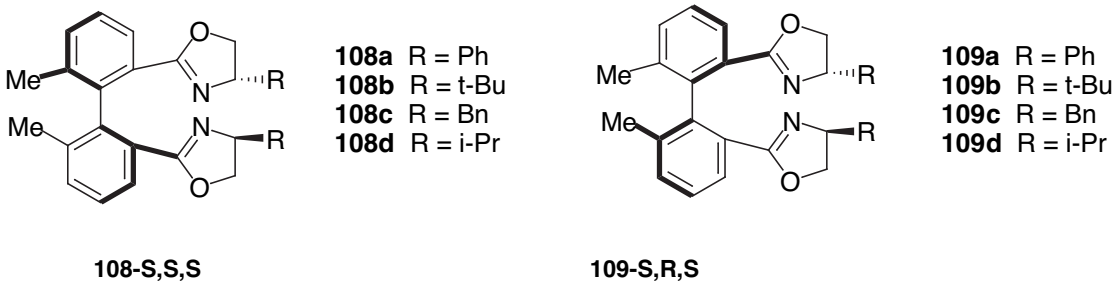

Figure 3.7 Andrus' bi-*o*-tolylbisoxazoline ligands **108** and **109**.

In 2002, Andrus[293] and co-workers reported much improved chiral ligands, **110a-h**. When these ligands are coordinated to Cu(I)PF_6, they could catalyze allylic oxidation of cyclic olefins at –20 °C with < 96 % ee and product yields around 40 % (Scheme 3.4). The *S,S*-biox ligand **110b**, with gem di-*tert*-butyl substituents at the R^1 group worked especially well for two smaller cyclic olefins, cyclopentene and cyclohexene. The enantioselectivity remained very good for bigger cycloheptene (99 % ee); however, the reactivity was reduced to a mere 14 %, which indicates only one turnover of the catalyst. Competitive enantioselectivity (94 % ee) was obtained for the oxidation of cyclooctadiene with the gem-dimethyl di-*tert*-butyl copper catalyst **110e**, but the product yield remained at 13 %. There was no single universal ligand that

worked well for all reactions. All newly formed chiral centers favored the *S*-configuration, as was in the case in earlier works.[290.294] In spite of the high enantioselectivity, the reaction still suffers from low reactivity since average reaction takes a week or more to be completed.

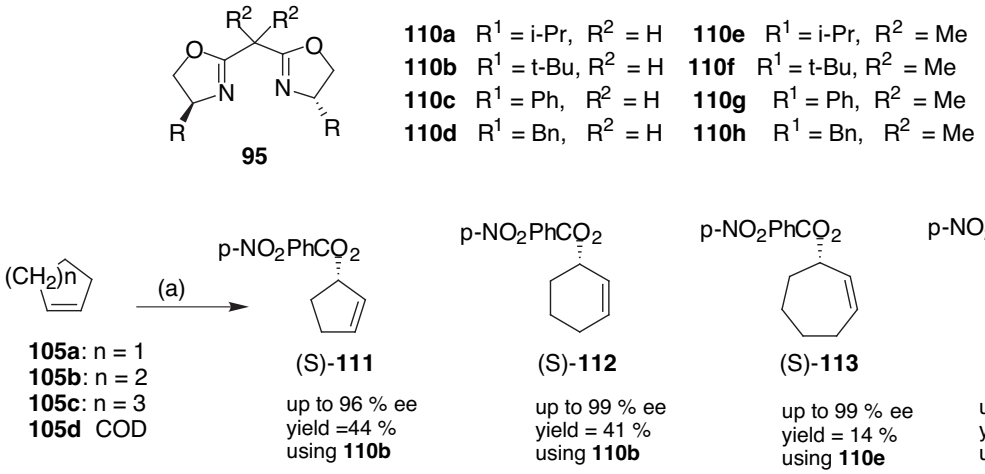

Scheme 3.4 Enantioselective allylic oxidation of cyclic olefins using bioxazoline ligands **110a-h** with *tert*-butyl *p*-nitroperbenzoate. (a) *p*-NO_2PhCO_3tBu, $CuPF_6$, CH_3CN, -20 °C

Katsuki developed C_3-symmetric ligands, such as **115** and **116a--d**. The ligand **115** turned out to be an effective catalyst for stereoselective oxidation of cyclopentene, which produced 83 % of the desired allylic ester with 76 % ee.[295] In this work, Katsuki found out that the enantiomeric excess decreased as the reaction time got longer. They fixed the problem by simply adding 4 Å molecular sieves to the acetone reaction mixture. Reducing the temperature could improve the enantioselectivity (up to 93 % ee); however, the product yield suffered as a result.

In later work,[296] Katsuki and coworkers developed another series of C_3-symmetric tris(oxazoline) ligands, **116a-d** (Scheme 3.5). The ligand **116b** turned out to an efficient chiral auxiliary for asymmetric oxidation of allylic cyclic olefins.

Regardless of the ring size of the substrate, the enantioselectivity surpassed 80 % ee when the reaction was run at room temperature. Lowering the temperature could improve the enantioselection (upto 92 % ee for cycloheptene), but the product yield was reduced. Ligands, **116a-b** favored the formation of allylic esters with (*R*)-configuration, but the other two auxiliaries, **116c-d** favored the (*S*)-configuration instead.

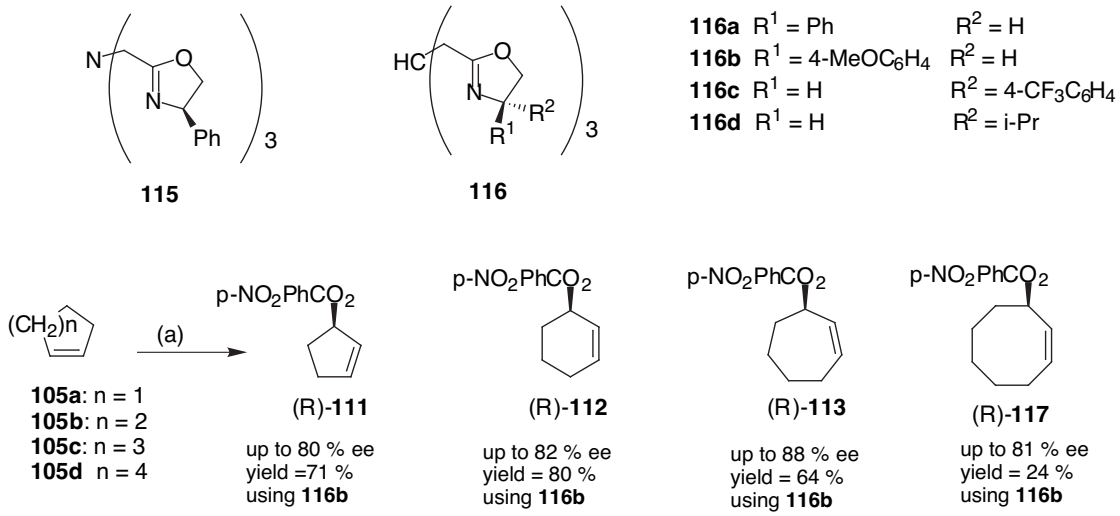

Scheme 3.5 Asymmetric allylic oxidation of cycloalkenes using Katsuki's C_3-symmetric ligands, **115** and **116a--d**. (a) $PhCO_3t$-Bu, $Cu(OTf)_2$, **116**, dichloroethane, r.t.

Kocovsky[286] and coworkers have reported that C_2-symmetric chiral bipyridine ligands, **118 – 126**, were effective auxiliaries for asymmetric allylic oxidation when complexed to Cu^I ion. In the reaction scheme, Cu(II)-ion from $Cu(OTf)_2$ was initially coordinated to chiral ligands, then they were reduced in situ by phenylhydrazine to the desired Cu^I species.[285.297] Ligands (+)-**118** (PINDY), synthesized from β-pinene, and the carene-derived bipyridine ligand (-)-**121** (CANDY) provided the best

enantioselectivity (up to 82 % ee) with the cycloalkenes when reactions were run at –20 °C (Scheme 3.6).

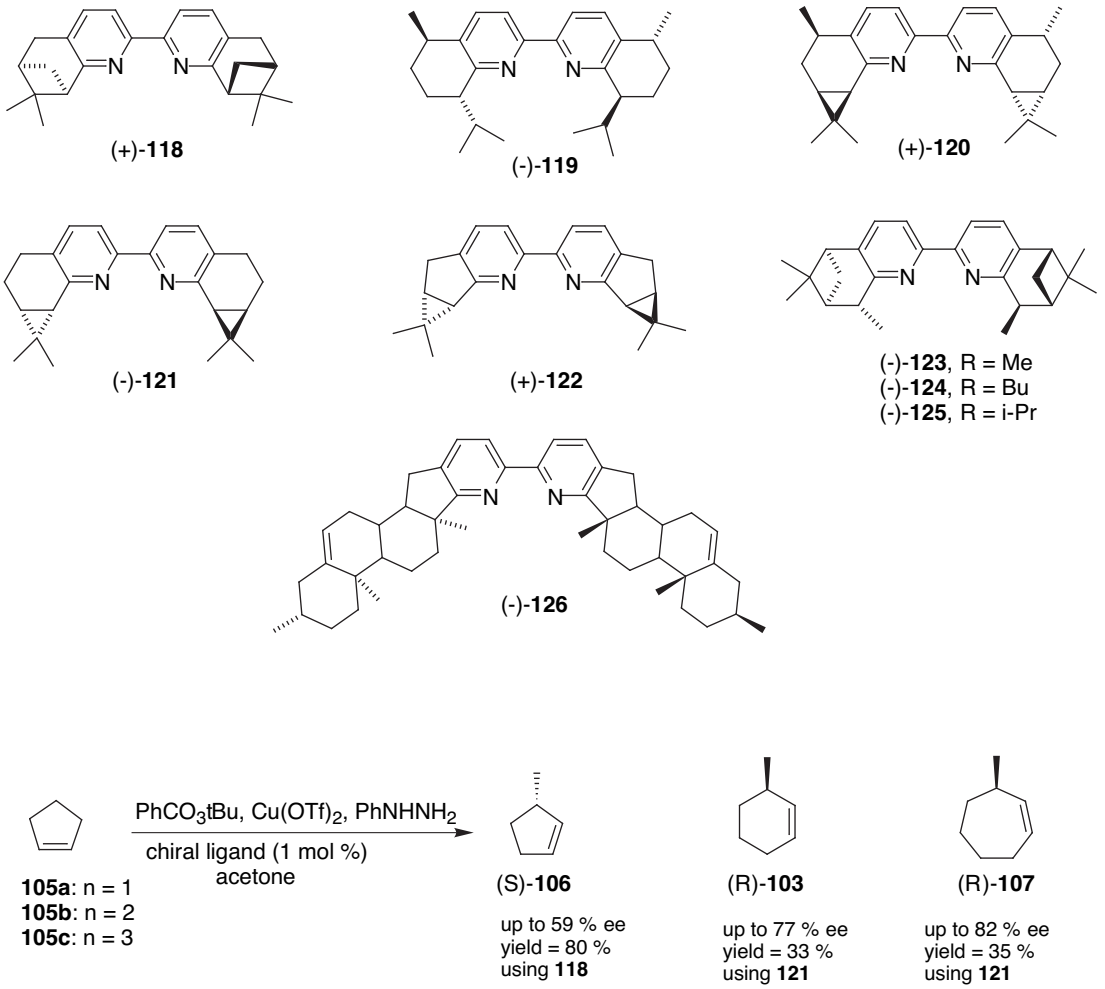

Scheme 3.6 Enantioselective allylic oxidation of cyclic olefins using Kocovsky's chiral bipyridine ligands, **118** – **126**.

Different reaction conditions were tried to improve the product outcome, and results reveal that when reactions were run at room temperature, enantioselection decreased, but reactivity improved drastically. For instance, (+)-**118** catalyzed allylic oxidation of cyclohexene was completed in only 30 min with 96 % yield and 49 % ee. This is a significant improvement from other reported works using structurally similar

catalysts.[289] *Iso*-PINDY type of ligands, **123** – **125**, had high reactivity with the average <80 % yield, but gave racemic products. The steroid ligand, **126**, gave products with low enantioselectivity of 6-18 % ee. The increase in reactivity is attributed to the stabilization of the copper geometry by chiral bipyridine ligands--halfway between square planar, which is favored by Cu^{II}, and tetrahedral coordination, which is favored by Cu^{I}. Albeit similar catalytic effectiveness, Cu^{I} complexes, which were obtained from Cu^{II} ion source after in situ reduction with phenylhydrazine, were more robust than those formed directly from a Cu^{I} ion. Addition of molecular sieves caused dramatic decrease in reactivity while the enantioselectivity remained the same.

In the meantime, Chelucci[287] reported similar results as the Kocovsky's group using phenanthroline analogue of PINDY **127** shown in (Figure 3.8). Even though both bpy and phen ligands were used in asymmetric catalysis,[298.299] they showed different catalytic activity and stereoselectivity due to the inherently different conformational mobility of each ligand.[300-302] Chelucci and coworkers postulated that the more rigid phenanthroline would be locked into a single conformation when coordinated to Cu ion; whereas, bipyridine would have more degree of freedom due to the its more flexible backbone. Chelucci used the same reaction condition as Kocovsky's group, reducing Cu^{II} complex in situ with phenylhydrazine and using *tert*-butylperbenzoate as the oxidant. Similar to Kocovsky's catalysts, Chelucci's ligands accelerated reactions to completion in 30 min at room temperature with three small cycloalkenes, cyclopentene to cycloheptene. Cyclooctene, however, was unreactive to the catalyst in the given reaction condition. Modest enantioselectivity was obtained

with cyclopentene and cyclohexene (47 – 57 % ee) and higher stereoselectivity was afforded with cycloheptene (63 - 71 % ee).

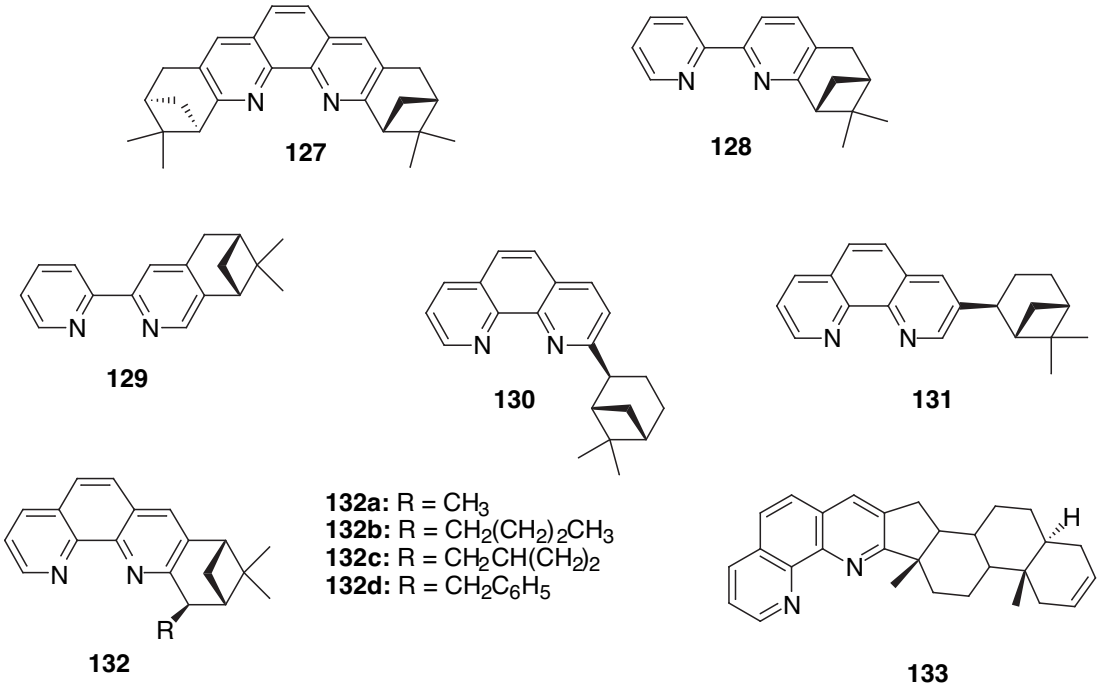

Figure 3.8 Chelucci's chiral phen ligands **127**--**133**.

In his more recent work,[288] Chelucci reported that the chiral auxiliaries do not need to be C_2-symmetric in order to afford effective catalysts upon complexation with copper ion. For example, the Cu(I) complex from the C_1-symmetric analogue of PINDY, **128**, provided an effective catalyst, but its isomer, **129**, showed no catalytic activity. Results indicate that the most important feature in the ligand is to have the chiral substituent as close to the reactive site of the catalyst, or to the heterocyclic nitrogen. To test if the trend applies to phenanthroline, Chelucci synthesized a series of C_1-symmetric phenanthroline ligands, such as **130** – **133**. As expected, the 2-substituted phenanthroline ligand **130** afforded a chiral cyclohexene carboxylate in 20

% ee, but the 3-substituted phenanthroline ligand **131** showed no catalytic activity. Among other ligands that were synthesized, **132a** and **132b** with smaller substituents provided modest enantiomeric excess (19-21 % ee). Bulkier substituents in **132c** and **132d** reduced the stereoselectivity to less than 10 % ee. The ligand **133** had a steroidal moiety incorporated to the phenanthroline backbone. It afforded the best enantioselectivity among C_1-symmetric ligands with 36 % ee.

3.1.3 Cyclopropanation

The first application of soluble chiral transition-metal catalyst in enantioselective transformation was with the reaction between a diazoester and an alkene to form cyclopropanes in 1966.[303] In the study, Nozaki and coworkers used a Schiff base-Cu^{II} complex **134** whose chiral auxiliary was derived from α-phenethylamine. This Cu^{II} catalyst was used in the cyclopropanation of ethyl diazoacetate with styrene[304] to give *cis* and *trans*-2-phenylcyclopropanecarboxylate in < 10 % enantiomeric excess as shown in (Scheme 3.7).

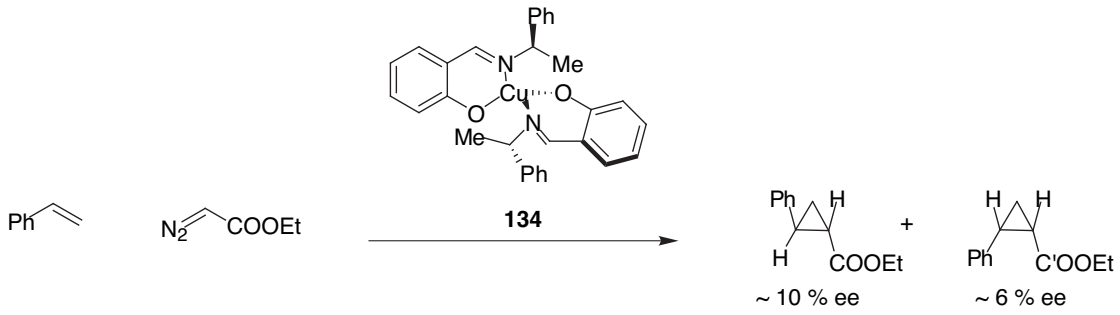

Scheme 3.7 Nozaki's cyclopropanation of styrene and ethyldiazoacetate using Schiff base-Cu(II) complex

Cyclopropanation reactions fall under the class of C-C bond formation transformations caused by metal carbenes reacting with diazo compounds. Transition-metal compounds that can act as Lewis acids are potentially effective catalysts for metal carbene transformation. Many different metals, such as Ru, Co, Fe, Os, Pd, Pt, and Cr have been used to form metal carbenes that catalyze the diazo reagent decomposition. Metal carbenes derived from Rh, Ru, Co, and Cu have a tendency to react faster with electron-rich alkenes, and Pd metal carbenes are better with electron-

deficient alkenes.[305] The most attention has been received by transition-metal catalysts derived from Cu and Rh.[306-308]

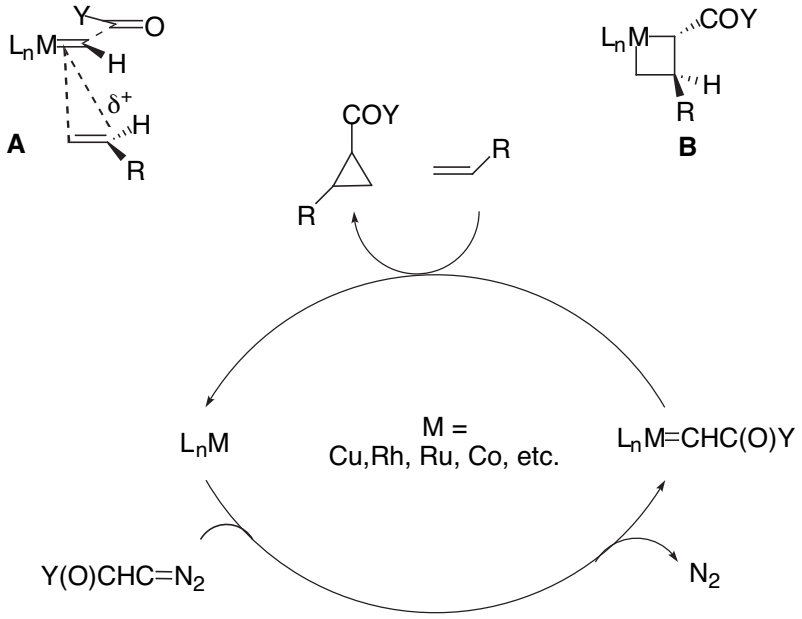

Scheme 3.8 Catalytic Cycle for the Cyclopropanation.

Generally accepted mechanisms for cyclopropanation with metal carbenes formed from Rh, Co, and Cu, involve the initial decomposition of diazocarbonyl compound, followed by transient formation of a metal carbene[309] complex **A** or metallocyclobutane intermediate **B** (Scheme 3.8). X-ray structure of Cu carbene has never been studied. However, a recent study of the solution-state NMR of **135**[310] shows a striking similarity to the mechanistic picture **136** proposed by Pfaltz and co-workers[311] (Figure 3.9). Calculations,[209] isotope effect and Hammett studies[312] on the copper(I)-catalyzed cyclopropanation of propene with diazo compounds were carried out. Results support the rapid formation of the metallocarbene **A** at the earlier transition state to the substrate alkene with cationic character on one of the carbons of

the alkene. No transient metallocyclobutane **B** formation was detected from these studies

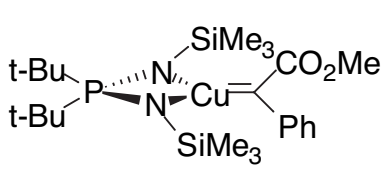

135

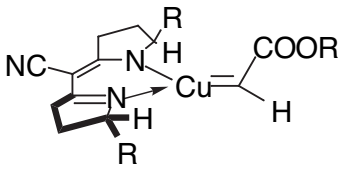

136

Figure 3.9 Mechanistic pictures of the Cu(I) carbene proposed by **135** and **136**.

In the copper-catalyzed cyclopropanation, it has been shown that the Cu(I)-catalyst is the reactive species in the reaction even if Cu(II)-salt was used as a precursor[313]. Bis-oxazoline, semicorrin, and the Aratani catalyst are all active only when Cu is reduced to its +1 oxidation state. The reactive Cu(I) complex can be produced by reduction of the Cu(II) complex with phenylhydrazine prior to use or ligand replacement by Cu(I) OTf or Cu(I) *tert*-butoxide. Recently, Salvatella and Garcia successfully made stereochemical prediction of the bis(oxazoline)copper-(I) catalyzed cyclopropanation using theoretical studies (DFT)[209]. Their calculated relative energies closely correlate to enantiomeric excess and diastereomeric selectivity found in experimental results.

More effective chiral Schiff base-Cu(II) complexes were developed by several groups following Nozaki's report. For example, Aratani[314-316] and coworkers successfully designed another Schiff base-Cu(II) complexes, **137**, which led to a very efficient enantioselective cyclopropanation reaction to produce (*S*)-2,2-dimethylcyclopropane-carboxylic acid in 92 % ee (Figure 3.10). This asymmetric step was the key point in the Sumotomo-Merck synthesis of cilastatin, which is an

excellent in vivo stabilizer of antibiotic imipenem. Aratani found that the steric bulk of the ligand R and the size of the alkyl substituent derived from the amino alcohol could influence the stereoselection of the catalyst. Also, when bulkier substituent was used for diazo ester, more *trans* product was formed with improved enantiomeric excess.

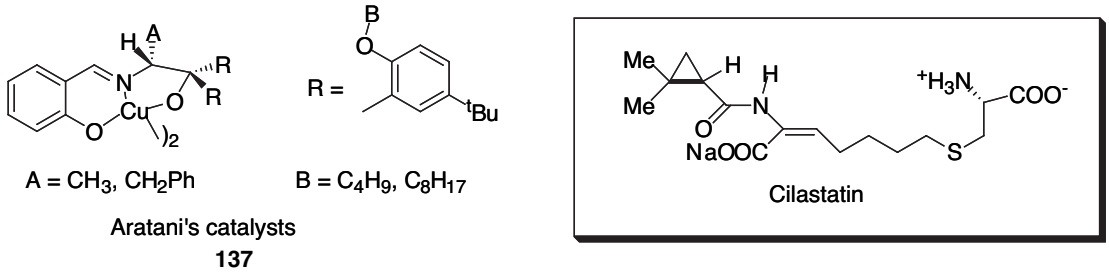

Figure 3.10 Aratani's Schiff base-Cu(II) catalysts **137a-b** and cilastatin.

Besides the chiral salicylaldemine-Cu catalysts described above, other C_2-symmetric ligands, such as chiral semicorrin[27] and bis-oxazoline Cu catalysts, have been widely used in asymmetric cyclopropanation reactions. Pfaltz and co-workers produced the first series of semicorrin Cu(II) complexes[317]— **138a--c** and its aza analogue[318], **139a--c** (Figure 3.11). Of all the catalysts that were initially made,[319] the first series of compound **138** showed the highest enantioselectivity[311] upto 90 % ee. Similar to the Aratani's catalyst, the efficiency of the catalyst was related to the steric bulk of the diazo ester. *Trans* products produced better enantiomeric excess than the *cis* isomer. Also, the absolute configuration of the chiral diazo ester influenced the handedness of products. Over all, these semicorrin-based Cu(II) complexes produced higher enantioselectivity in the cyclopropanation of mono-

substituted alkenes than the Aratani's catalyst, but the reverse was true for 1,2-di and tri-substituted alkene substrates.

138a R = CMe_2OH
138b R = $CH_2OSiMe_2{}^tBu$
138c R = COOMe

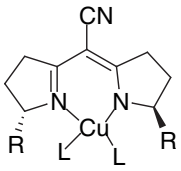

138

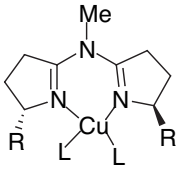

139

139a R = $CH_2OSiMe_2{}^tBu$
139b R = CMe_2OSiMe_3
139c R = $CMe_2OSiMe_2{}^tBu$

Figure 3.11 Pfaltz's semicorrin ligands **138** and **139**.

Masamuni and co-workers first reported Cu-complexes of chiral bis-oxazoline ligands[320] **140a--i**. These complexes garnered an instant interest because they showed such an efficient stereocontrol (upto 99 % ee) as catalysts in asymmetric cyclopropane reactions. Other analogous ligands—**141**[321]**a--b**, **142a--b**, and **143**[322.323]**a--c**--were soon developed and studied. Pfaltz, who studied a series of ligands similar to **143a--c**, concluded that C_2-symmetric bis-oxazoline copper complexes worked just as well as copper complexes from semicorrin ligands in catalyzing asymmetric intramolecular cyclopropanation. As expected, increasing the size of the R-group on the ligand increased its enantioselection, but the R-substituent played a minor role in product diastereoselection. Evans[321] on the other hand, used the bulky BHT ester to increase the *trans*:*cis* ratio upto 94:6, with 99 % enantiomeric excess for the *trans* product. His group also optimized the reaction condition[321] so that in 0.25 mol reaction scale, only 0.1 mol % of catalyst was necessary to obtain a 91 % yield of the (*S*)-cyclopropane enantiomer with 99 % enantiomeric excess.

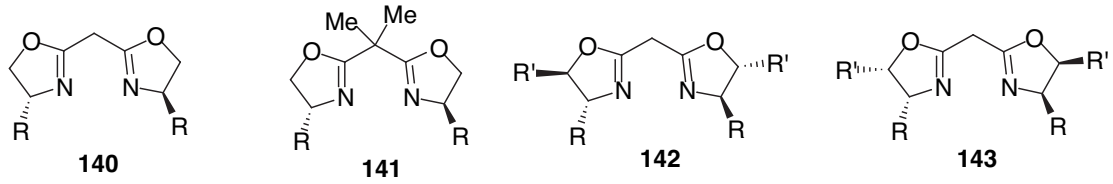

140

a R = Ph
b R = Me_2CH
c R = (S)--EtCH(Me)
d R = Et
e R = $PhCH_2$
f R = ^tBu
g R = CH_2OH
h R = $Me_2C(OH)$
i R = $CH_2OSiMe_2{}^tBu$

141

a R = ^iPr
b R = ^tBu

142

a R = Me, R' = Ph
b R = CH_2OH, R' = Ph

143

a R = Me, R' = Ph
b R = Et, R' = ^tBu
c R = R' = Ph

Figure 3.12 Chiral bisoxazoline ligands **140** – **143**.

Another type of chiral bidentate nitrogen-containing ligands, bpy, was synthesized by Katsuki[232.324.325] and coworkers for asymmetric cyclopropanation reaction (Figure 3.13). Even with small substituents, such as methyl groups at the stereogenic centers in **144**, *cis* and *trans* products were synthesized with enantioselectivity around 75 % ee for both of them. Diastereoselectivity was around 5:2-favoring *trans* isomer. Increasing the bulkiness at the same C8(8')-positions with TMS-groups in ligand **145** reversed the diastereoselectivity. *Cis*-selectivity[326.327] was manifested (1:99-*trans*:*cis*), and the resulting *cis*-isomer had high enantioselectivity (>99 % ee). However, when even bulkier groups were used, as in **146**, the *trans*-selectivity (2:1-*trans*:*cis*) returned with diminished enantioselectivity (74 % ee).

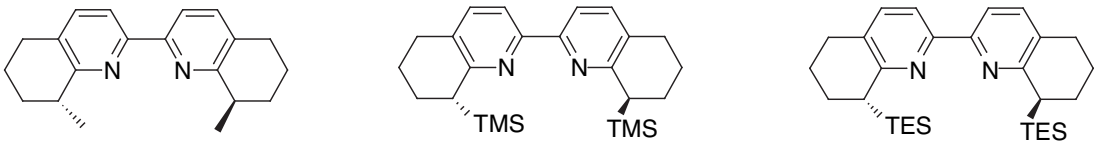

144 **145** **146**

Figure 3.13 Katsuki's chiral bipyridine ligands, **144**– **146**.

Kocovsky[286] and coworkers tried the same series of ligands, **118** – **126** used in allylic oxidation catalysis, for the asymmetric cyclopropanation of styrene with esters of diazoacetic acids (Scheme 3.6). The reaction was carried out in dichloromethane with Cu(I) ion, which was reduced in situ from Cu(II) with phenylhydrazine. These ligands afforded products with yields around 90 %, and their effectiveness as a chiral catalyst differed from what was found in asymmetric allylic oxidation reaction. For instance, MINDY, **119**, outperformed PINDY, **118** (70 % ee vs. 15 % ee) in stereoselectivity. Both ethyl and bulkier *tert*-butyl diazoacetate showed essentially the same enantioselectivity, but the latter showed better diastereoselectivity, favoring slightly more *trans* isomer formation. The highest enantioselectivity was obtained from *n*-Bu-*iso*-PINDY, **124**, with upto 78 % ee for the *cis* isomer.

3.2 Results and Discussion

3.2.1 Introduction

Classical chiral transfer reactions, such as optical resolution of racemates and transformation of chiral compounds, are both stoichiometric processes in terms of chirality. They require one equivalent of a chiral source in order to create a new stereocenter. Recently, some metal complexes of chiral organic ligands have shown to perform catalytically and amplify chirality.[328] Chiral cyclophanes **1** – **5** and their metal complexes have a potential to become catalysts for asymmetric reactions for several reasons: 1) macrocyclic hosts are helically chiral; 2) molecules are sterically congested and rigid; 3) they can selectively bind small cationic metal ions; and 4) the C_2-symmetric construction of the cyclophane reduces the number of possible conformations of diastereomeric transition states.

A screening of several enantioselective reactions using a copper(I) complex of **1** as a catalyst was attempted. Final results indicate that asymmetric allylic oxidation of cyclohexene using *tert*-butylperoxybenzoate and cyclopropanation of styrene with ethyldiazoacetate have shown some promises.

3.2.2 Allylic Oxidation

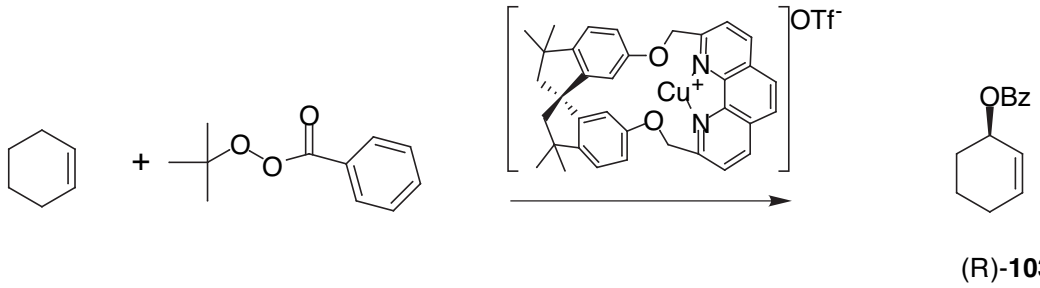

Scheme 3.9 Asymmetric allylic oxidation of cyclohexene with *t*-butylperoxybenzoate and Cu-complexed (*R*)-**1** catalyst.

The chiral ligand **(*R*)-1** effectively increased the reaction rate of the allylic oxidation of cyclohexene and catalyzed the reaction in enantioselective fashion. Catalytic asymmetric allylic oxidation[263] of cyclohexene with 5 mol % of either copper(I) or copper(II)-complexed (*R*)-**1** and *tert*-butylperoxybenzoate as an oxidant favored the formation of the product **103** with (*R*)-configuration. The chiral cyclophane (*R*)-**1** can transfer stereoselective information with both copper(II) ion, derived from readily available $Cu(OTf)_2$, and copper(I) ion, reduced from $Cu(OTf)_2$ in situ with phenylhydrazine.[329] Results from both reactions are very similar (<80 % yield and 16 % ee) and took about a day at room temperature for completion, which is moderately faster than some previously reported works.[267.289] At lower temperature, the rate of the reaction decelerated and took 9 days to be completed with slightly better enantiomeric excess. The product yield was unaffected by the lowering of temperature.

Table 3.1 Effects of the copper-complexed ligand **1**, phenylhydrazine, and reaction temperature on catalytic enantioselective allylic oxidation of cyclohexene and cyclopentene.

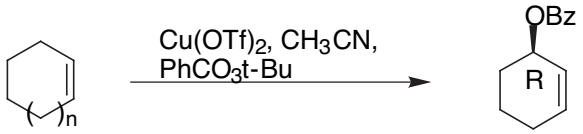

Entry	(*R*)-1	*n*	$PhNHNH_2$	Time	°C	% Yield	% ee
1	No	1	No	4 d	23	88	----
2	No	1	Yes	3 d	23	15	----
3	Yes	1	No	23 h	23	94	16
4	Yes	1	Yes	26 h	23	80	16
5	Yes	1	Yes	9 d	0	95	19
6	Yes	0	Yes	3 d	23	81	6

Chelucci[288] had reported that copper(I) complex of neither phen nor bpy produced any catalytic activity; however, 2,9-dimethyl-1,10-phenathroline, dmp, was shown to increase the reaction rate as much as the chiral catalyst **1** when coordinated to a Cu(I) metal center. Even only in the presence of a copper ion, the reaction could take upto 4 days to be completed at room temperature in acetonitrile (Table 3.1, entry 1 and 2). In order to prevent the background reaction to compete against the catalytic pathway, a slight excess of the cyclophane **1** was used in the reaction condition. Lastly, cyclopentene is another suitable substrate for the given reaction condition. The reaction rate was slower, taking 3 days to be completed with 81 % yield, and the enantioselectivity (only 6 % ee) was also inferior to the products formed from cyclohexene (Table 3.1, entry 6).

Table 3.2 Effects of solvent on catalytic enantioselective allylic oxidation of cyclohexene with either Cu(I) or Cu(II) complex.

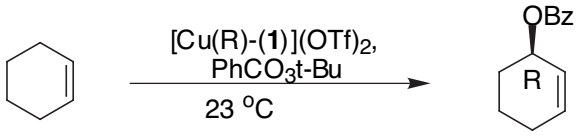

Entry	$PhNHNH_2$	Solvent	Time	% Yield	% ee
1	Yes	CH_3CN	42 h	100	15
2	Yes	CH_2Cl_2	23 h	95	18
3	Yes	Acetone		NR	
4	No	CH_3CN	18 h	73	17
5	No	CH_2Cl_2	5 d	98	18
6	No	Acetone		NR	

In most reported studies, either acetone or acetonitrile was used as the solvent of choice. In our study though, non-coordinating, polar solvent, dichloromethane, provided the best condition for the catalysis. Phenylhydrazine definitely increased the reaction rate in dichloromethane with higher enantioselectivity than the reactions run in acetonitrile. Both copper(II) and copper(I) catalysts worked equally well in catalyzing the reaction.

Table 3.3 Effects of different copper ions and molecular sieves on catalytic enantioselective allylic oxidation of cyclohexene.

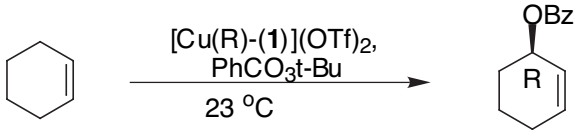

Entry	Metal	$PhNHNH_2$	4 Å	Solvent	Time	% Yield	% ee
1	$Cu(OTf)_2$	Yes	No	CH_3CN	42 h	100	15
2	$Cu(OTf)_2$	Yes	Yes	CH_3CN	24 h	98	12
3	$Cu(OTf)_2$	No	Yes	CH_3CN	16 h	98	20
4	CuI	No	No	CH_3CN	6 d	NR	
5	$Cu(I)PF_6$	No	No	CH_3CN	16 h	98	17
6	$Cu(I)PF_6$	No	No	CH_2Cl_2	16 h	91	21

Different copper ions and molecular sieves,[289] which had shown to improve enantioselectivity, were used to optimize the product outcome. Singh reported that their chiral pyridine-bis(oxazoline) complex of CuI catalyzed allylic oxidation of cyclohexene in acetonitrile with low selectivity (37 % yield, 9 % ee).[289] However, the Cu(I) complex of cyclophane **1,** made from CuI, exhibited no catalytic activity even after stirring the reaction mixture for 6 days. Between $Cu(OTf)_2$ and $[Cu(CH_3CN)_4](PF_6)$, the latter afforded products with slightly better enantioselectivity. The best reaction condition was run in dichloromethane, with $[Cu(CH_3CN)_4](PF_6)$ as copper ion source, which catalyzed the allylic oxidation in 16 h with < 90 % yield, and 21 % ee.

In the same study, Singh also reported the addition of molecular sieves improved the enantioselectivity. It was thought that the removal of the last trace of water with molecular sieves would enhance the catalytic effect of the copper complex. However, there are other contrary reports where the addition of molecular sieves either reduced the reaction rate without affecting enantioselectivity[286] or improved the rate and enantioselectivity.[295] In our study, the addition of molecular sieves reduced the enantioselectivity of the reaction in copper(I) condition with phenylhydrazine (Table 3.3, entry 2), and improved the enantioselectivity in the case of copper(II) condition (Table 3.3, entry 3).

It should be noted that the reaction with the catalyst from copper(II) ion (entry **3**) proceeded faster than the copper(I) catalyst formed from the in situ reduction of copper(II) ion with phenylhydrazine (entry **1** and **2**). This result was contrary to what

was found in the work by Kocovsky[286]. In his report, the copper(I) complex, which was reduced in situ from $Cu(OTf)_2$ with phenylhydrazine, was found to be more robust. This brings one to question the accepted mechanism, which needs copper(I) ion to initiate the radical mechanism. Both Singh[289] and Muzart[330] questioned the mechanisms. In Singh's study, he observed that the allylic oxidation also proceeded, albeit with lower rate and enantioselectivity, with Cu(II) ion. Additionally, Muzart showed through visible spectroscopic studies that Cu(II) complex of (*S*)-proline remained largely unmodified during allylic benzoyloxylation of cyclohexene. Singh suggested an alternative Cu(II) intermediate structure **147** instead of the generally accepted Cu(III)-complex in (Figure 3.14). The proposed structure implies that the copper complexes of the chiral cyclophane also may undergo a more complex reaction pathway.

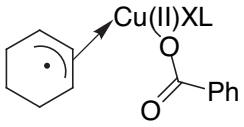

147

Figure 3.14 Singh's alternate Cu(II)-intermediate complex **147**.

3.2.3 Cyclopropanation

Catalytic asymmetric cyclopropanation[210.331] of styrene with ethyldiazoacetate by copper(II) complexed (*R*)-**1** favored the formation of the product (*trans)*-(1*S*,2*S*)-2-phenylcyclopropanecarboxylate and (*cis*)-(1*S*,2*R*)-2-phenylcyclopropanecarboxylate with the enantiomeric excess of the *trans* isomer at ~20 % ee. The product yields ranged from 61 % to 87 %, and the diastereoselectivity was around 2:1, with *trans* isomer being the dominant product.

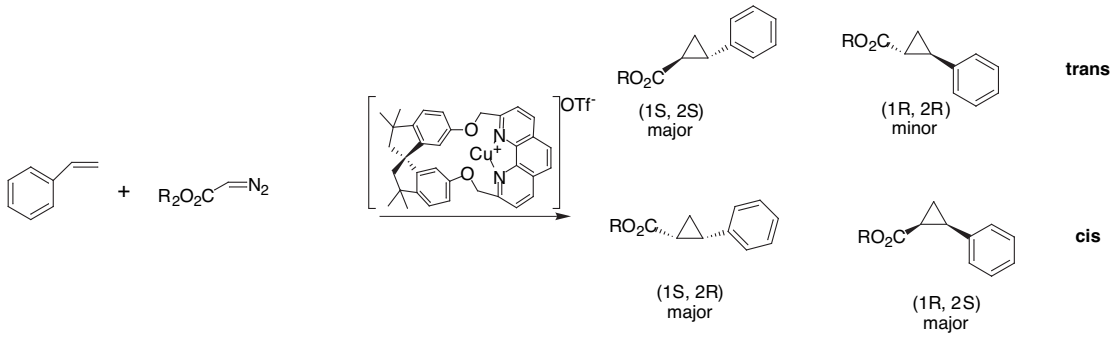

Scheme 3.10 Cyclopropanation of styrene with ethyldiazoacetate by copper complex of *(R)*-**1.**

Table 3.4 Effects of the ligand and temperature on asymmetric cyclopropanation of styrene.

Entry	Ligand	Time	°C	Cis/Trans	% Yield	% ee[(a)]
1	Neocuproine	3 d	23 °C	38:62	74 %	---------
2	(*R*)-**1**	16 h	23 °C	36:64	83 %	21
3[(b)]	(*R*)-**1**	21h	0°C	36:64	87 %	21

[a)] *trans* isomer [b)] 4 Å molecular sieves were added.

The copper complex of the chiral cyclophane (*R*)-**1** catalyzed the cyclopropanation reaction enantioselectively and improved the reaction rate. The same reaction took 3 d to be completed with copper(II) complexed dmp; however, the copper(II) complexed (*R*)-**1** not only reduced the reaction time to 16 h at room

temperature, but also increased the product yield by 9 % (Table 3.4 entry 1 vs. 2). Decreasing the temperature had no effect on improving the stereoselectivity as the enantiomeric excess remained at 21 %. The product yield was greater despite the slightly longer reaction time.

Table 3.5 Effects of different diazoacetate addition times and metal ions on enantioselective cyclopropanation of styrene.

Entry	Metal	Time	Cis/Trans	% Yield	% ee [(c)]
1[(a)]	$Cu(OTf)_2$	16 h	36:64	83 %	21
2[(a)]	$Cu(CH_3CN)_4PF_6$	17h	43:57	64 %	18
3[(b)]	$Cu(OTf)_2$	6h	37:63	76 %	28
4[(b)]	$Cu(CH_3CN)_4PF_6$	6 h	37:63	61 %	4
5[(b)]	$(Cu(OTf)_2)_2$toluene	9h	37:63	67 %	6

[a)] Diazoacetate was added in 7 h. [b)] Diazoacetate was added in 3 h and 4 Å molecular sieves were added. [c)] *trans* isomer

Cu^I complex is generally accepted as the catalytic species in the cyclopropanation reaction. The Cu^{II} triflate used in the reaction is actually reduced to +1 oxidation state by the diazo compound under the reaction condition.[332] Therefore, the oxidation state of the precatalyst does not affect the reaction as long as the copper can assume its +1 oxidation state[311.316]. Copper(II) triflate consistently outperformed Cu(I) ions in its enantioselectivity and product yield. It is no surprise since Kochi had reported that Cu(OTf)[333] is one of the most effective catalysts for cyclopropanation reaction. The commercially available copper(I) ion, such as $(Cu(OTf)_2)_2$toluene, did not work as well as the copper(II) triflate. The addition of molecular sieves and reduction of the addition time for diazo ester decreased the product yield, but they

improved the enantioselectivity for copper(II) triflate. For $[Cu(CH_3CN)_4](PF_6)$, the above reaction condition reduced both the product yield and enantioselectivity.

Table 3.6 Effects of different diazoesters and solvent on stereoselective cyclopropanation of styrene.

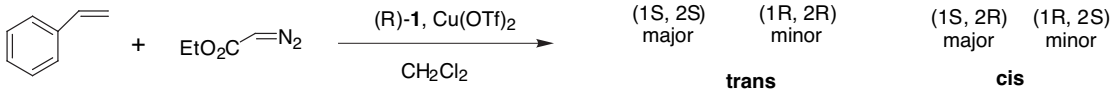

Entry	R	Solvent	Time	Cis/Trans	% Yield	% ee [b]
1 [a]	ethyl	CH_2Cl_2	6h	37:63	76%	28%
2 [a]	ethyl	CH_3CN	5d	37:63	10%	2%
3	*tert*-butyl	CH_2Cl_2	16 h	22:78	23%	29%

[a] Diazoacetate was added in 3 h and 4 Å molecular sieves were added. [b] *trans* isomer

Effects of solvent and different diazoesters showed that dichloromethane was the solvent of choice. More coordinating solvent such as acetonitrile decreased the enantiomeric excess of the product to a mere 2 % from ~20 %. It is expected since the X-ray crystal structure of the Cu(I) complex of **1** showed the nitrogen from acetonitrile coordinated to the metal center. The longer addition time of ethyldiazoacetate seemed to increase the product yield because it decreased the by-product formation. The diastereoselectivity favored the formation of *trans* isomer-- *trans*/*cis* ratio of products remained about 2:1--which is about what to expect in the presence of just neocuproine. With a bulkier R-group, such as *tert*-butyl, the diastereoselectivity improved to 4:1, favoring the *trans* isomer. The enantioselectivity from the reaction, however, did not show much improvement.

In understanding the role of chiral ligands, both Pfaltz[311] and Fraile[209] suggested that the stereoselectivity stems from the steric interaction between one of the substituents of the chiral catalyst and the ester group. Diastereoselectivity in the product, however, was not influenced by the chiral ligand, which is generally a

problem in metal-catalyzed cyclopropanation reactions.[334-336] The only major factor in the *cis*/*trans* selectivity was the steric interaction between the diazo compound and the olefinic substrate, irrespective of the catalyst structure.

The X-ray crystal structure of [Cu(**1**)](PF$_6$) **81** provides a good visual model of what the cyclophane **1** may look like when it is coordinated to a copper(I) ion (Figure 2.16). The cyclophane is puckered up in order to accommodate the trigonal planar coordination of copper(I) metal center with two nitrogen molecules from phenanthroline and nitrogen from acetonitrile. The metal-carbene intermediate, which is coordinated to the cyclophane, may look like the structure proposed in (Scheme 3.11). There are two possible pathways that the double bond from styrene can attach to the carbenoid center (path **A** or path **B**). Two pathways explain why a certain enantiomer is favored. However, it is important to note that **81** is very flexible in solution at room temperature. In the NMR time scale, the metal complex retains its C_2-symmetry. Therefore, the copper(I)-carbenoid can be formed not only above the spirobiindanol of the cyclophane, but also below it as well.

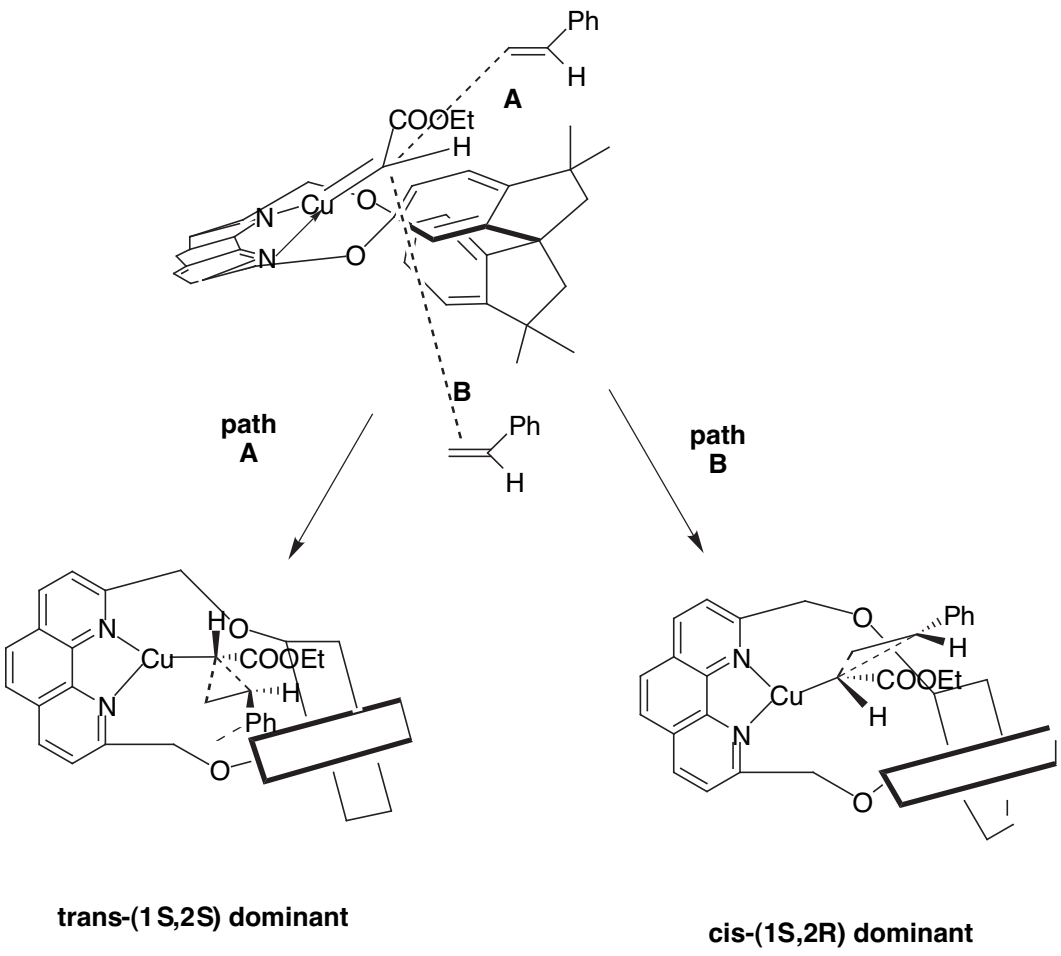

Scheme 3.11 Proposed mechanistic pathways **A** and **B**.

Almost all the successful chiral auxiliaries, notably chiral bisoxazoline groups, have the chiral substituents closer to the copper ion. The chiral cyclophane **1**, however, derives its chirality not directly from the phenanthroline ligand, but from the spirobiindanol, which is placed farther away from the metal source. The crystal structure of **81** shows longer Cu--N bonds than the calculated Cu--N distances for Fraile's bisoxazoline (2.02 Å vs. 1.95 A). It means **1** creates a slightly bigger chiral environment for its substrates, becoming less effective at transferring stereochemical

information; thus, it explains why the enantiomeric excess of final products remained below 20 %.

3.3 Conclusion

Copper complexes of chiral cyclophane **1** have shown to catalyze two asymmetric organic transformation reactions--allylic oxidation of cyclic olefin and cyclopropanation of styrene with alkyldiazoacetate. Their efficiency in chiral induction was low, but they effectively increased the reaction rates for both reactions. For allylic oxidation reactions, the enantiomeric excess of the final product was ~16 % ee with 80 % yield, and the cyclopropanation reaction produced *trans*-2-phenylcyclopropane carboxylate in ~ 20 % ee with upto 87 % yield.

Further assessment of metal complexes of the cyclophane as possible enantioselective catalysts may be accomplished through optimizing reaction conditions and screening more substrates in the future.

3.4 Experimental

General Data. Varian Mercury 300 MHz and 400 MHz Model L 600 Pulsed Gradient Driver spectrometer were used for ^{1}H and ^{13}C NMR. Chemical shifts (δ) are reported in parts per million (ppm). Multiplicities are given as follows: s (singlet), d (doublet), t (triplet), q (quartet), dd (doublet of doublets), and m (mutiplet). ^{1}H NMR spectra were referenced to tetramethylsilane (TMS) at 0.00 ppm. ^{13}C NMR spectra were referenced to deuterated chloroform, $CDCl_3$, at 77.0 ppm was used to monitor the reaction progress. Optical rotations were determined at the sodium D line on a Jasco P-1010 polarimeter in Professor Emmanuel Theodorakis lab, at the University of California, San Diego. The progress of the reaction was monitored by ThermoFinnigan GC-MS in Professor Seth Cohen lab at UCSD and high-pressure liquid chromatographic (HPLC) analyses were carried out on a Hewlett-Packard Series 1100 HPLC system equipped with a diode array UV detector in Professor Nathaniel Finney's lab. UV detection was performed at 250 nm, and Chiracel OD column was used for the measurement of enantiomeric excess. The enantiomeric excess (ee) was measure by the chiral HPLC and comparing the optical rotation of the product with known values. The diastereomeric excess (de) was measure by integration of ^{1}H NMR peaks, HPLC, and GC/MS.

Chromatography. Silica gel (230-425 mesh) for flash column chromatography was purchased from Aldrich/Fisher Scientific Company. Radial Chromatography, using

Harrison Chromatotron was used with silica plate. Thin layer chromatography (TLC) was performed on alumina backed silica gel 60 F_{254} plates from Aldrich.

Materials. Cyclohexene (99 %), *t*-butylperoxybenzoate (98 %), ethyldiazoacetate (90% in CH_2Cl_2) and phenylhydrazine (97 %) were all purchased from Sigma-Aldrich and were stored in a freezer and used without further purification. Styrene was purified by fractional distillation and stored with Lindlar type 5 Å molecular sieves in a freezer. $Cu(OTf)_2$ was stored in a dry box. Stirring and distilling over CaH2 dried methylene chloride, acetonitrile, and acetone. All glassware was flame dried and kept in an oven. Dry needles, Hamilton syringes, and cannula were used to transfer liquid reagents.

General Procedures for Catalytic Enantioselective Allylic Oxidation. Into a round-bottomed flask equipped with a Teflon-coated stirring bar and rubber septum, (*R*)**-1** cyclophane (6 mg, 0.03 mmol) was added under argon. Cu(II) triflate (9 mg, 0.025 mmol) was added, then distilled CH_3CN (2 mL) was injected. The resulting green solution was stirred and degassed with argon at room temperature for 5 min. Phenylhydrazine (3μL, 0.03 mmol) was injected, and the orange solution was stirred for additional 5 min under Ar. Cyclohexene (2.5 mL, 5 mmol) was added, then *t*-butyl peroxybenzoate (95 μL, 0.5 mmol) was injected dropwise. The reaction was stirred at room temperature under argon overnight and was quenched with saturated $NaHCO_2$ solution. Excess cyclohexene was evaporated under reduced pressure. The organic

phase was taken up in CH_2Cl_2, washed with sat. $NaHCO_3$, water, and brine. The combined organic phase was dried over Na_2SO_3, filtered, and concentrated under reduced pressure. The residue was purified by flash column chromatography on silica (petroleum ether:EtOAc=20:1). (94-100% yield, clear liquid). The formation of the (*R*)-cyclohex-2-en-1yl-benzoate (*R*)-**103** is favored. Cyclohex-2-en-1-yl-benzoate **103** (analytical data is same as the reference)[337] ^{1}H-NMR ($CDCl_3$, 300 MHz) δ 1.6-2.2 (3 *m*, no baseline sep., $H_2C(4)$, $H_2C(5)$, $H_2C(6)$; 5.51-5.53 (*m*, HC(2)); 5.81-5.87, 5.98-6.03 (2 *m*, HC(1), HC(3)); 7.40-7.57 (2 *m*, Ph); 8.05-8.08 (*m*, Ph). ^{13}C-NMR ($CDCl_3$, 75 MHz) δ 18.9, 25.0, 28.4, 68.5, 125.5, 128.1, 129.4, 130.6, 132.6, 132.7, 166.0. HPLC: Chiracel OD, hexane:*i*-PrOH=1000:1, elution rate: 0.5 mL/min, t_R= (*S*)-**103** 19.3 min, (*R*)-**103** 20.2 min. Polarimeter: +18.5 ° (c. 0.067 $CHCl_3$) (*R*)-carboxylate

General Procedure for Catalytic Enantioselective Cyclopropanation. Into an oven-dried 5-mL glass vial equipped with magnetic stirbar and rubber septum, **(*R*)-1** (17 mg, 0.03 mmol) and $Cu(OTf)_2$ (11 mg, 0.03 mmol) were charged under argon. Freshly distilled CH_2Cl_2 (4 mL) was injected, and the resulting green solution was stirred for 5 min at room temperature. Distilled styrene (937 mg, 9 mmol) was added via syringe and a needle. Ethyldiazoacetate in 10 %-CH_2Cl_2 solution (404 mg, 3 mmol) [CAREFUL! It explodes when heated] was dissolved in 3 mL of CH_2Cl_2 and was slowly added into the stirring Cu(II) solution over 3 h, using a syringe pump[in order to minimize the formation of diethyl fumarate and maleate). The stirring reaction slowly turned red and remained so throughout the reaction. The reaction

mixture was stirred at room temperature for 12 h and the reaction progress was monitored by TLC and ^{1}H NMR. The crude product was concentrated under reduced pressure and put through a short plug of silica gel with 15:1-hexanes:ethyl acetate to remove the catalyst. Radial chromatography with silica plate and 15:1-hexanes-ethyal acetate solvent system was used for purification of the product. *Trans* product is eluted first, which in its pure state solidifies at room temperature. All physical characteristic values correspond to the reference values[304.338.339]. Absolute configuration was determined by comparing specific rotation of products with the literature value[304].

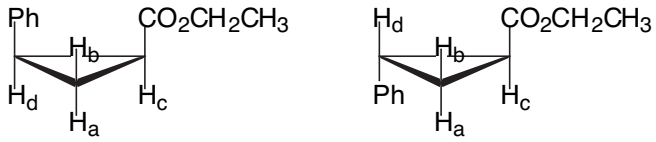

(*cis*)-(+)-(1*S*)-ethyl-(2*R*)-phenylcyclopropanecarboxylate ***cis***: ^{1}H-NMR (CD_3Cl, 400 MHz) δ 0.97 (*t*, CH_3, *J* = 6.8 Hz), 1.33 (*m*, H_a), 1.72 (*m*, H_b), 2.09 (*m*, CH_c), 2.59 (*q*, H_d, *J* = 8.8 Hz), 3.87 (*q*, CH_2, *J* = 6.8 Hz), 7.18-7.21 (*m*, 1H from Ph), 7.27 (*d*, 4H from Ph, *J* = 4.0 Hz); $[\alpha]^{25}_D$ = +1.8 ° (c = 0.05 in $CHCl_3$).

(*trans*)-(+)-(1*S*)-ethyl-(2*S*)-phenylcyclopropanecarboxylate ***trans***: ^{1}H-NMR (CD_3Cl, 400 MHz) δ 1.29 (*t*, CH_3, *J* = 7.2 Hz), 1.31 (*m*, H_a), 1.60 (*m*, H_b), 1.90 (*m*, CH_c), 2.52 (*m*, H_d), 4.17 (*q*, CH_2, *J* = 6.8 Hz), 7.19-7.23 (*m*, 1H from Ph), 7.10 (*d*, 2H from Ph, *J* = 7.2 Hz), 7.27 (*d*, 2H from Ph, *J* = 8.0 Hz); $[\alpha]^{25}_D$ = +30 ° (c = 0.07 in $CHCl_3$). HPLC: Chiracel OD, hexane:*i*-PrOH=95:5, elution rate: 1 mL/min, t_R= (*trans*)-

(1*R*,2*R*)-carboxylate 12 min, (*trans*)-(1*S*,2*S*)-carboxylate 26 min. It was not possible to determine the enantiomeric excess of *cis* isomer with the HPLC.

REFERENCES

1. Nishimura, J.; Okada, Y.; Inokuma, S.; Nakamura, Y.; Gao, S. R. *Synlett* **1994**, 884-894.

2. Cram, D. J.; Cram, J. M. *Accounts of Chemical Research* **1971**, *4*, 204-213.

3. Vogtle, F., ed. *Cyclophanes II*. Topics in Current Chemistry. Vol. 115. **1983**, Springer: Berlin.

4. Vogtle, F., *Cyclophane Chemistry*. **1993**, Chichester: Wiley-VCH.

5. Vogtle, F., ed. *Cyclophanes I*. Topics in Current Chemistry. Vol. 113. **1983**, Springer: Berlin.

6. Diederich, F., *Cyclophanes*. **1991**, Cambridge: Royal Society of Chemistry.

7. MacNico, D. D.; Toda, F.; Bishop, R., eds. *Comprehensive Supramolecular Chemistry*. Vol. 6. **1996**, Pergamon: Oxford.

8. Sritana-Anant, Y.; Seiders, T. J.; Siegel, J. S. *Topics in Current Chemistry* **1998**, *196*, 1-43.

9. Lehn, J.-M. *Angew. Chem. Int. Ed. Engl.* **1988**, *27*, 89-112.

10. Cram, D. J. *Angew. Chem. Int. Ed. Engl.* **1988**, *27*, 1009-1020.

11. Weber, E., *Synthesis of Macrocycles, the Design of Selective Complexing Agents*, in *Progress in Macrocyclic Chemistry*, Christensen, J. J., Editor. **1989**, John Wiley & Sons: New York. p. 337-.

12. Koga, K.; Odashima, K. J. *J. Incl. Phenon* **1989**, *7*, 53-60.

13. Diederich, F. *Angew. Chem. Int. Ed. Engl.* **1988**, *27*, 362-386.

14. Reinhoudt, D. N.; Herman, J. J.; Den, H. *Bull. Soc. Chim. Belg.* **1988**, *97*, 645-653.

15. Hou, X.-L.; You, S. L.; Tu, T.; Deng, W. P.; Wu, X. W.; Li, M.; Yuan, K.; Zhang, T. Z.; Dai, L.-X. *Topics in Catalysis* **2005**, *35*, 87-103.

16. Brown, C. J.; Farthing, A. C. *Nature* **1953**, *164*, 915.

17. Cram, D. J.; Steinberg, H. *Journal of the American Chemical Society* **1951**, *73*, 5691-5704.

18. Jenneskens, L. W.; de Kanter, F. J. J.; Kraakman, P. A.; Turkenberg, L. A. M.; Koolhaas, W. E.; de Wolf, W. H.; Bickelhaupt, F. *J. Am. Chem. Soc.* **1985**, *107*, 3716-3717.

19. Kostermans, G. B. M.; Bobeldijk, M.; de Wolf, W. H.; Bickelhaupt, F. *J. Am. Chem. Soc.* **1987**, *109*, 2471-2475.

20. Dewhirst, K. C.; Cram, D. J. *Journal of the American Chemical Society* **1958**, *80*, 3115-3125.

21. Cram, D. J.; Dewhirst, K. C. *Journal of the American Chemical Society* **1959**, *81*, 5963-5971.

22. Hubert, A. J. *J. Chem. Soc. C.* **1967**, 13-14.

23. Psiorz, M.; Hopf, H. *Angew. Chem. Int. Ed. Engl.* **1982**, *21*, 623-624.

24. Judice, J. K.; Keipert, S. J.; Cram, D. J. *Journal of the Chemical Society, Chemical Communications* **1993**, 1323-1325.

25. Fanta, P. E. *Synthesis* **1974**, 9-21.

26. Pirkle, W. H.; Liu, Y.; Welch, C. J. *Enantiomer* **1998**, *3*, 477-483.

27. Pfaltz, A. *Acc. Chem. Rev.* **1993**, *26*, 339-345.

28. Jacobsen, E. N.; Pfalz, A.; Yamamoto, H., *Comprehensive Asymmetric Catalysis*, ed. Yamamoto, H. **1999**, Berlin: Springer.

29. Noyori, R., *Asymmetric Catalysis in Organic Synthesis*. **1994**, New York: J. Wiley & Sons.

30. Suzuki, R.; Ootsuji, A.; Urakami, T.; Sugimoto, K.; Takuma, K., *Polyesters containing spirobiindanol derivatives with excellent transparency and heat resistance and low birefringence and optical materials therefrom*, in *Jpn. Kokai Tokkyo Koho*. **1999**, (Mitsui Chemicals Inc., Japan). Jp. p. 16 pp.

31. Shiomura, T.; Sonobe, Y.; Yamaguchi, T.; Iimuro, S., *Melt-moldable liquid crystal polyesters*, in *Jpn. Kokai Tokkyo Koho*. **1988**, (Mitsui Toatsu Chemicals, Inc., Japan). Jp. p. 5 pp.

32. Gordon, J. L.; Stewart, K. R., *Polycarbonates derived from spirobiindanols and dihydroxy aromatic compounds*, in *U.S.* **2001**, (Molecular Optoelectronics Corporation, USA). Us. p. 7 pp., Cont. of U.S. Ser. No. 799,798, abandoned.

33. Suzuki, R.; Ohtsuji, A.; Urakami, T.; Takuma, K., *Transparent copolyesters with excellent heat stability and their application to optical instruments*, in *Jpn. Kokai Tokkyo Koho*. **1999**, (Mitsui Chemicals Inc., Japan). Jp. p. 26 pp.

34. Ootsuji, A.; Suzuki, R.; Urakami, T.; Takuma, K., *Spirobiindanol monoethers for manufacture of polymers with good optical properties and heat resistance*, in *Jpn. Kokai Tokkyo Koho*. **1999**, (Mitsui Chemicals Inc., Japan). Jp. p. 15 pp.

35. Ishihara, H.; Karasawa, A.; Motojima, T.; Takuma, H.; Yamaguchi, K., *Spirobiindanol-based novolak resins, their manufacture, and their use as photo-sensitive material*, in *Jpn. Kokai Tokkyo Koho*. **1997**, (Mitsui Toatsu Chemicals, Japan). Jp. p. 18 pp.

36. Prusikova, M.; Pospisil, J. *Collection of Czechoslovak Chemical Communications* **1975**, *40*, 1367-1373.

37. Pospisil, J.; Kotulak, L.; Taimr, L. *Eur. Polym. J.* **1971**, *7*, 255-261.

38. Braun, v. *Annalen* **1929**, *472*, 65.

39. Curtis, R. F. *J. Chem. Soc.* **1962**, 415-418.

40. Curtis, R. F.; Lewis, K. O. *J. Chem. Soc.* **1962**, 418-421.

41. Hoffmann, J. *J. Am. Chem. Soc.* **1929**, *57*, 2542-2247.

42. Barnes, R. A.; Beitchman, B. D. *J. Am. Chem. Soc.* **1954**, *76*, 5430-5433.

43. Silvis, H. C.; Morgan, T. A., *Spirobiindanols*, in *U.S.* **1986**, (Dow Chemical Co., USA). Us. p. 3 pp.

44. Faler, G. R.; Lynch, J. C., *Method for preparing spirobiindanols*, in *U.S.* **1987**, (General Electric Co., USA). Us. p. 4 pp.

45. Faler, G. R.; Lynch, J. C., *Preparation of spirobiindanediol polycarbonates with high glass temperature and low birefringence by interfacial polymerization*, in *Eur. Pat. Appl.* **1988**, (General Electric Co., USA). Ep. p. 13 pp.

46. Barclay, L. R. C.; Chapman, R. A. *Canadian Journal of Chemistry* **1964**, *42*, 25-35.

47. Cahn, R. S., Ingold, C., Prelog, V. *Experientia* **1956**, *12*, 81-94.

48. Cahn, R. S., Ingold, C., Prelog, V. *Angew. Chem. Int. Ed. Engl.* **1966**, *5*, 385-415.

49. Hagishita, S.; Kuriyama, K.; Hayashi, M.; Nakano, Y.; Shingu, K.; Nakagawa, M. *Bulletin of the Chemical Society of Japan* **1971**, *44*, 496-505.

50. Kazlauskas, R. J., *Method for preparing optically active binaphthol and spirobiindanol by asymmetric hydrolysis of diesters using cholesterol esterase*, in *U.S.* **1989**, (General Electric Co., USA). Us. p. 7 pp.

51. Kazlauskas, R. J. *Journal of the American Chemical Society* **1989**, *111*, 4953-4959.

52. Kazlauskas, R. J. *Biocatalysis* **1990**, 195-216.

53. Brockerhoff, H.; Jensen, R. G., in *Lipolytic Enzymes*. **1974**, Academics: New York. p. 176-193.

54. Rudd, E. A.; Brockman, H. L., *Lipase*, ed. Brockman, H. L. E. **1984**, Amsterdam: Elsevier. 185-204.

55. Baker, W.; Besly, D. M. *J. Chem. Soc.* **1939**, 1421.

56. Cairns, T. L. *J. Am. Chem. Soc.* **1941**, *63*, 871.

57. Consiglio, G. A.; Finocchiaro, P.; Failla, S.; Hardcastle, K. I.; Ross, C.; Caccamese, S.; Giudice, G. *European Journal of Organic Chemistry* **1999**, *1999*, 2799-2806.

58. Birman, V. B.; Rheingold, A. L.; Lam, K.-C. *Tetrahedron: Asymmetry* **1999**, *10*, 125-131.

59. Zhang, J.-H.; Liao, J.; Cui, X.; Yu, K.-B.; Zhu, J.; Deng, J.-G.; Zhu, S.-F.; Wang, L.-X.; Zhou, Q.-L.; Chung, L. W.; Ye, T. *Tetrahedron: Asymmetry* **2002**, *13*, 1363-1366.

60. Lehn, J. M., *Supramolecular Chemistry. Concepts and Perspectives*. **1995**, Weinheim: VHS.

61. Lehn, J.-M.; Rigault, A. *Angew. Chem. Int. Ed. Engl.* **1988**, *27*, 1095-1097.

62. Lehn, J.-M.; Rigault, A.; Siegel Jay, S.; Harrowfield, J.; Chevrie, B.; Moras, D. *Proc. Natl. Acad. Sci. USA* **1987**, *84*, 2565-2569.

63. Joshi, H., S.; jamshidi, R.; Tor, Y. *Angew. Chem. Int. Ed. Engl.* **1999**, *38*, 2722-2725.

64. Woods, C. R.; Benaglia, M.; Cozzi, F.; Siegel, J. S. *Angewandte Chemie, International Edition in English* **1996**, *35*, 1830-1833.

65. Philip, D.; Stoddart, J. F. *Angew. Chem. Int. Ed. Engl.* **1996**, *35*, 1154-1196.

66. Cheng, R. P.; Fisher, S. L.; Imperiali, B. *J. Am. Chem. Soc.* **1996**, *118*, 11349-11356.

67. Ghadiri, M. R.; Soares, C.; Choi, C. *J. Am. Chem. Soc.* **1992**, *114*, 825-831.

68. Sardesai, N.; Lin, S. C.; Zimmermann, K.; Barton, J. K. *Bioconjugate Chem.* **1995**, *6*, 302-312.

69. Harding, M. M.; Lehn, J.-M. *Australian Journal of Chemistry* **1996**, *49*, 1023-1027.

70. Lou, B.-Y.; Wang, R.-H.; Yuan, D.-Q.; Wu, B.-L.; Jiang, F.-L.; Hong, M.-C. *Inorganic Chemistry Communications* **2005**, *8*, 971-974.

71. Szemes, F.; Hesek, D.; Chen, Z.; Dent, S. W.; Drew, M. G. B.; Goulden, A. J.; Graydon, A. R.; Grieve, A.; Mortimer, R. J.; Wear, T.; Weightman, J. S.; Beer, P. D. *Inorganic Chemistry* **1996**, *35*, 5868-5879.

72. Torrado, A.; Imperiali, B. *J. Org. Chem.* **1996**, *61*, 8940-8948.

73. Ng, P.-L.; Lee, C.-S.; Kwong, H.-L.; Chan, A. S. C. *Inorganic Chemistry Communications* **2005**, *8*, 769-772.

74. Lamba, J. J. S.; Fraser, C. L. *J. Am. Chem. Soc.* **1997**, *119*, 1801-1802.

75. Matyjaszewski, K.; Patten, T. E.; Xia, J. *J. Am. Chem. Soc.* **1997**, *119*, 674-680.

76. Eisenbach, C. D.; Goldel, A.; Terskan-Reinold, M.; Schubert, U. S. *Macromolecular Chemistry and Physics* **1995**, *196*, 1077-1091.

77. Suh, J.; Lee, S. H. *J. Org. Chem.* **1998**, *63*, 1519-1526.

78. Gould, S.; Strouse, G. F.; Meryer, T. J.; Sullivan, B. P. *Inorganic Chemistry* **1991**, *30*, 2942-2949.

79. Summers, L. A. *Adv. Heterocycl. Chem.* **1978**, *22*, 1.

80. Michael, J. P.; Pattenden, G. *Angew. Chem. Int. Ed. Engl.* **1993**, *32*, 1-23.

81. Newkome, G. R.; Kiefer, G. E.; Puckett, W. E.; Vreeland, T. *J. Org. Chem.* **1983**, *48*, 5112-5114.

82. Chandler, C. J.; Deady, L. W.; Reiss, J. A. *Journal of Heterocyclic Chem.* **1981**, *18*, 599-604.

83. Vogtle, F.; Hochberg, R.; Kochendorfer, F.; Windscheif, P.-M.; Volkmann, M.; Jansen, M. *Chem. Ber.* **1990**, *123*, 2181-2185.

84. Toyota, S.; Woods, C. R.; Benaglia, M.; Siegel, J. S. *Tetrahedron Letters* **1998**, *39*, 2697-2700.

85. Benaglia, M.; Toyota, S.; Woods, C. R.; Siegel, J. S. *Tetrahedron Letters* **1997**, *38*, 4737-4740.

86. Sammes, P. G.; Yahioglu, G. *Chem. Soc. Rev.* **1994**, *23*, 327-329.

87. Sammes, P. G.; Yahioglu, G.; Yearwood, G. D. *J. Chem. Soc. Chem. Commun.* **1992**, 1282-1283.

88. Gabbay, E. J.; DeStefano, R.; Sanford, K. *Biochemical and Biophysical Research Communications* **1972**, *46*, 155-161.

89. Gabbay, E. J.; Scofield, R. E.; Baxter, C. S. *J. Am. Chem. Soc.* **1973**, *95*, 7850-7857.

90. Long, E. C.; Barton, J. K. *Acc. Chem. Rev.* **1990**, *23*, 271-273.

91. Rehman, J. P.; Barton, J. K. *Biochemistry* **1990**, *29*, 1701-1709.

92. Ottaviani, M. F.; Ghatlia, N. D.; Bossmann, S. H.; Barton, J. K.; Duerr, H.; Turro, N. J. *J. Am. Chem. Soc.* **1992**, *114*, 8946-8952.

93. Hemmila, I.; Dakubu, S.; Mukkala, V.-M.; Siitari, H.; Lovgren, T. *Analytical Biochemistry* **1984**, *137*, 335-343.

94. Case, F. H. *J. Am. Chem. Soc.* **1948**, *70*, 3994-3996.

95. Chandler, C. J.; Deady, L. W.; Reiss, J. A.; Tzimos, V. *Heterocycl. Chem.* **1982**, *19*, 1017-1018.

96. LeFave, G. M.; Scheurer, P. G. *J. Am. Chem. Soc.* **1950**, *72*, 2464-2465.

97. Brown, M. S.; Rapoport, H. *J. Org. Chem.* **1963**, *28*, 3261-3263.

98. Bishop, M. M.; Lewis, J.; O'Donoghue, T. D.; Raithby, P. R. *Chem. Commun.* **1978**, *11*, 476-478.

99. Dziomko, V. M.; Parusnikov, B. V. *Chem. Abstr.* **1975**, *83*, 178874q, 178875r, 178876s.

100. Dziomko, V. M.; Parusnikov, B. V. *Metody Poluch. Khim. Reakt. Prep.* **1974**, 122, 285, 289.

101. Seyhan, M.; Fernelius, W. C. *Chem. Ber.* **1958**, *91*, 469-470.

102. Mukkala, V. T.; Sund, C.; Kwiatkowski, M.; Pasanen, P.; Hogberg, M.; Kankare, J.; Takalo, H. *Helvetica Chimica Acta* **1992**, *75*, 1621-1632.

103. Bates, G. B.; Cole, E.; Parker, D.; Kataky, R. *J. Chem. Soc. Perkin Trans. 1* **1996**, *13*, 2693-2698.

104. Savage, S. A.; Smith, A. P.; Fraser, C. L. *J. Org. Chem.* **1998**, *63*, 10048-10051.

105. Parks, J. E.; Wagner, B. E.; Homes, R. H. *J. Organomet. Chem.* **1973**, *56*.

106. Parks, J. E., *Ph.D. Dissertation*. **1972**, University of Wisconsin.

107. Wagner, B. E., *Ph.D. Dissertation*. **1972**, Massachusetts Institute of Technology.

108. Sauer, J. D., *Ph.D. Dissertation*. **1976**, Louisiana State University.

109. Vogel, A. I., *Practical Organic Chemistry*. **1973**, London: Longmans. 189.

110. Bailey, T. D.

111. Rode, T.; Breitmaier, E. *Synthesis* **1987**, 574-575.

112. DeTar, D. R. *Org. React.* **1957**, *9*, 409.

113. Fabian, R. H.; Klassen, D. M.; Sonntag, R. W. *Inorg. Chem.* **1980**, *19*.

114. Kauffmann, T.; Konig, J.; woltermann, A. *Chem. Ber.* **1976**, *109*, 3864-3868.

115. Mathes, W.; Schuly, H. *Angew. Chem. Int. Ed. Engl.* **1963**, *2*, 144-149.

116. Kanno, H.; Kashiwabara, K.; Fujita, J. *Bull. Chem. Soc. Jpn.* **1979**, *52*, 1908.

117. Murase, I. *Nippon Kagaku Zasshi* **1956**, *77*, 682.

118. Cohen, T.; Deets, G. L. *J. Am. Chem. Soc.* **1967**, *89*, 3939-3940.

119. Weijnen, J. G. J.; Engbersen, J. F. J. *Recl. Trav. Chim. Pays-Bas* **1993**, *112*, 351-357.

120. Newkome, G. R.; Puckett, W. E.; Kiefer, G. E.; Gupta, V. D.; Xia, Y.; Coreil, M.; Hackney, M. A. *Journal of Organic Chemistry* **1982**, *47*, 4116-4120.

121. Offermann, W.; Voegtle, F. *J. Org. Chem.* **1979**, *44*, 710-713.

122. Eisenbach, C. D.; Goldel, A.; Terskan-Reinold, M.; Schubert, U. S., *Polymeric Materials Encyclopedia*, ed. Salamone, J. C. Vol. 10. **1996**, Boca Raton: CRC Press. 8162 ff.

123. Harding, M. M.; Koert, U.; Lehn, J.-M.; Marquis-Rigault, A.; Piguet, C.; Siegel, J. *Helv. Chim. Acta.* **1991**, *74*, 594-610.

124. Fraser, C. L.; Anastasi, N. R.; Lamba, J. J. *J. Org. Chem.* **1997**, *62*, 9314-9317.

125. Della Ciana, L.; Hamachi, I.; Meyer, T. J. *J. Org. Chem.* **1989**, *54*, 1731-1735.

126. Youinou, M. T.; Ziessel, R.; Lehn, J. M. *Inorganic Chemistry* **1991**, *30*, 2144-2148.

127. Meyer, M.; Albrecht-Gary, A.-M.; Dietrich-Buchecker, C. O.; Sauvage, J.-P. *Inorganic Chemistry* **1999**, *38*, 2279-2287.

128. Jimenez, M. C.; Dietrich-Buchecker, C.; Sauvage, J.-P.; De Cian, A. *Angewandte Chemie, International Edition* **2000**, *39*, 1295-1298.

129. Kramer, R.; Lehn, J.-M.; De Clan, A.; Fischer, J. *Angew. Chem. Int. Ed. Engl.* **1993**, *32*, 703-706.

130. Dietrich-Buchecker, C. O.; Hemmert, C.; Khemiss, A. K.; Sauvage, J. P. *Journal of the American Chemical Society* **1990**, *112*, 8002-8008.

131. Albrecht-Gary, A. M.; Saad, Z.; Dietrich-Buchecker, C. O.; Sauvage, J. P. *Journal of the American Chemical Society* **1985**, *107*, 3205-3209.

132. Dietrich-Buchecker, C. O.; Sauvage, J.-P.; De Cian, A.; Fischer, J. *Journal of the Chemical Society, Chemical Communications* **1994**, 2231-2232.

133. Carina, R. F.; Dietrich-Buchecker, C.; Sauvage, J. P. *J. Am. Chem. Soc.* **1996**, *118*, 9110-9116.

134. Baxter Paul, N. W.; Lehn, J.-M.; Fischer, J.; Youinou, M. T. *Angew. Chem. Int. Ed. Engl.* **1994**, *33*, 2284-2287.

135. Jimenez, M. C.; Dietrich-Buchecker, C.; Sauvage, J.-P. *Angewandte Chemie, International Edition* **2000**, *39*, 3284-3287.

136. Jimenez-Molero, M. C.; Dietrich-Buchecker, C.; Sauvage, J.-P. *Chemistry--A European Journal* **2002**, *8*, 1456-1466.

137. Dietrich-Buchecker, C.; Sauvage, J. P., in *Bioorganic Chemistry Frontiers*, Dugas, H., Editor. **1991**, Springer: Berlin. p. 195-248.

138. Bannwarth, W.; Pfleiderer, W.; Muller, F. *Helv. Chim. Acta*. **1991**, *74*, 1991-1999.

139. Loren, J. C.; Yoshizawa, M.; Haldimann, R.; Linden, A.; Siegel Jay, S. *Angew. Chem. Int. Ed. Engl*. **2003**, *42*.

140. Annunziata, R.; Benaglia, M.; Cinquini, M.; Cozzi, F.; Woods, C. R.; Siegel, J. S. *European Journal of Organic Chemistry* **2001**, 173-180.

141. Annunziata, R.; Benaglia, M.; Raimondi, L.; Famulari, A. *Magn. Res. Chem*. **2001**, *39*, 341-354.

142. Annunziata, R.; Benaglia, M.; Bologna, A. *Magn. Res. Chem*. **2002**, *40*, 461-466.

143. Puglisi, A.; Benaglia, M.; Annunziata, R.; Bologna, A. *Tet. Lett*. **2003**, *44*, 2947-2951.

144. Consiglio, G. A.; Failla, S.; Finocchiaro, P.; Marchetti, F. *Mendeleev Communications* **2000**, 214-216.

145. Consiglio, G. A.; Failla, S.; Finocchiaro, P.; Marchetti, F. *Journal of Supramolecular Chemistry* **2002**, *2*, 293-300.

146. Wehner, M.; Schrader, T.; Finnocchiaro, P.; Failla, S.; Consiglio, G. A. *Organic Letters* **2000**, *2*, 605-608.

147. Frank, N. L.; Clerac, R.; Sutter, J.-P.; Daro, N.; Kahn, O.; Coulon, C.; Green, M. T.; Golhen, S.; Ouahab, L. *J. Am. Chem. Soc*. **2000**, *122*, 2053-2061.

148. Woods, C. R.; Benaglia, M.; Blom, P.; Fuchicello, A.; Cozzi, F.; Siegel, J. S. *Polymer Preprints (American Chemical Society, Division of Polymer Chemistry)* **1996**, *37*, 204-205.

149. Fuchicello, A. **1992**, University of California, San Diego: La Jolla, CA.

150. Craig, L. *J. Am. Chem. Soc*. **1934**, *56*, 231-232.

151. Penalva, V.; Hassan, J.; Lavenot, L.; Gozzi, C.; M., L. *Tet. Lett*. **1998**, *39*, 2559-2560.

152. Loren, J. C.; Siegel, J. S. *Angewandte Chemie, International Edition* **2001**, *40*, 754-757.

153. Barnes, R. A.; Buckwalter, G. R. *Journal of the American Chemical Society* **1951**, *73*, 3858-3861.

154. Saigo, K.; Lin, R. J.; Kubo, M.; Youda, A.; Hasegawa, M. *J. Am. Chem. Soc.* **1986**, *108*, 1996-2000.

155. Newkome, G. R.; Nayak, A.; Fronczek, F.; Kawato, T.; Taylor, H. C. R.; Leade, L.; Mattice, W. *J. Am. Chem. Soc.* **1979**, *101*, 4472-4480.

156. Buhleier, E.; Wehner, W.; Vogtle, F. *Chem. Ber.* **1978**, *111*, 200.

157. Newkome, G. R.; Taylor, H. C. R.; Fronczek, F. R.; Delord, T. J.; Kohli, D. K.; Voegtle, F. *Journal of the American Chemical Society* **1981**, *103*, 7376-7378.

158. Kubas, G. J. *Inorg. Synth.* **1990**, *26*, 68.

159. Wang, Z.; Reibenspies, J.; Motekaitis, R. J.; Martell, A. E. *J. Chem. Soc. Dalton Trans.* **1995**, 1511-1518.

160. Constable, E. C., in *Comprehensive Supramolecular Chemistry*, Lehn, J.-M., Editor. **1996**, Pergamon: Oxford. p. 213-252.

161. Jaffe, H. H.; Orchin, M., *Theory and Applications of Ultraviolet Spectroscopy*. **1962**, New York: Wiley.

162. Crews, P.; Rodriguez, J.; Jaspars, M., *Organic Structure Analysis*. Topics in Organic Chemistry: A Series of Advanced Textbooks, ed. Loudon, G. M. **1998**, New York: Oxford University Press.

163. Werner, A. *Ber.* **1911**, 1887.

164. Cotton, A. *Compt. Rend.* **1885**, *120*, 1044.

165. Cotton, A. *Ann. Chim. Phys.* **1896**, *8*, 347.

166. Loudon, G. M., *Organic Chemistry*. 3rd ed. **1995**, Redwood City: The Benjamin/Cummings Publishing Company, Inc.

167. Emeis, C. A.; Oosterhoff, L. J.; de Vries, G. *Proc. R. Soc. A* **1967**, *297*, 54.

168. Kramers, H. A. *Atti Congr. Int. Fis.* **1927**, *2*, 545.

169. Kronig, R. L. *J. Opt. Soc. Am.* **1926**, *12*, 547.

170. Ziegler, M.; von Zelewsky, A. *Coordination Chemistry Reviews* **1998**, *177*, 257-300.

171. Bijvoet, J. M.; Peerdeman, A. F.; Van Bommel, A. J. *Nature* **1951**, 271.

172. Ripa, L.; Hallber, A.; Sandstrom, J. *J. Am. Chem. Soc.* **1997**, *119*.

173. Hawkins, C. J.; Larsen, E. *Acta Chemica Scandinavica* **1965**, *19*, 1969.

174. Richardson, F. S. *J. Chem. Phys.* **1971**, *54*, 2453-2468.

175. Martin, R. B.; Tsangaris, J. M.; Chang, J. W. *J. Am. Chem. Soc.* **1968**, *90*, 821-823.

176. Tsangaris, J. M.; Martin, R. B. *J. Am. Chem. Soc.* **1970**, *92*, 4255-4260.

177. Kuroda, R.; Saito, Y., in *Circular Dichroism. Principles and Applications*, Woody, R. W., Editor. **1994**, VCH: New York. p. 217.

178. Harada, N.; Nakanishi, K., *Circular Dichroic Spectroscopy: Exciton Coupling in Organic Stereochemistry*. **1983**, Mill Valley, CA: University Science Books.

179. Berova, N.; Nakanishi, K., *Ch.12 Exciton Chirality Method: Principles and Application*, in *Circular Dichroism: Principles and Applications*, Woody, R. W., Editor. **2000**, Wiley-VCH Inc.: New York. p. 337-382.

180. Jeffrey, G. A.; Sundaralingam, M., *Advances in Carbohydrate Chemistry and Biochemistry*, in *Advances in Carbohydrate Chemistry and Biochemistry*, Horton, D., Editor. **1985**, Academic Press: Orlando, FL. p. 204-272.

181. Harada, N.; Ono, H.; Nishiwaki, T.; Uda, H. *J. Chem. Soc., Chem. Commun.* **1991**, 1753-1755.

182. Bjork, J. A.; Brostrom, M. L.; Whitcomb, D. R. *Journal of Chemical Crystallography* **1997**, *27*, 223-230.

183. Hass, G.; Prelog, V. *Helv. Chim. Acta.* **1969**, *52*, 1202-1218.

184. Haas, G.; Hulbert, P. B.; Klyne, W.; Prelog, V.; Snatzke, G. *Helv. Chim. Acta.* **1971**, *54*, 491-509.

185. Harada, N.; Ono, H. *Enantiomer* **1996**, *1*, 115-118.

186. Ono, H.; Harada, N. *Enantiomer* **1998**, *3*, 245-250.

187. Hagishita, S.; Kuriyama, K.; Shingu, K.; Nakagawa, M. *Bulletin of the Chemical Society of Japan* **1971**, *44*, 2177-2181.

188. Hagishita, S.; Kuriyama, K. *Bulletin of the Chemical Society of Japan* **1971**, *44*, 617-623.

189. Clar, E., *The Aromatic Sextet*. **1972**, New York: John Wiley & Son Inc.

190. Melnik, M.; Macaskova, L.; Holloway, C. E. *Coordination Chemistry Reviews* **1993**, *126*.

191. Black, J. R.; Levason, W. *J. Chem. Soc., Dalt. Trans*. **1994**, 3225-3230.

192. Hill, A. E. *J. Am. Chem. Soc*. **1921**, *43*, 254-268.

193. Lindeman, S. V.; Rathore, R.; Kochi, J. K. *Inorganic Chemistry* **2000**, *39*, 5707-5716.

194. Elliott Eric, L.; Hernandez, G. A.; Linden, A.; Siegel Jay, S. *Org. Biomol. Chem*. **2005**, *3*, 407-413.

195. Cotton, F. A.; Wilkinson, G.; Murillo, C. A.; Bochmann, M., *Advanced Inorganic Chemistry*. Sixth ed. **1999**, New York: John Wiley & Sons, Inc.

196. Bell, N. A.; Johnson, E.; March, L. A.; Marsden, S. D.; Nowell, I. W.; Walker, Y. *Inorg Chim Acta* **1989**, *156*, 205-211.

197. Airoldi, C.; De Oliveira, S. F.; Ruggioero, S. G.; Lechat, J. R. *Inorg Chim. Acta* **1990**, *174*, 103-108.

198. Alcock, N. W.; Benniston, A. C.; Moor, P.; Pike, G. A.; Rawle, S. C. *Journal of the Chemical Society, Chemical Communications* **1991**, 706-708.

199. Sessler, J. L.; Murai, T.; Lynch, V. *Inorganic Chemistry* **1989**, *28*, 1333-1341.

200. Hergold-Brundi, A.; Kaitner, B.; Kamenar, B.; Leovac, V. M.; Ivege, E. Z.; Jurani, N. *Inorg. Chim. Acta* **1991**, *188*, 151-158.

201. Fujita, M.; Kwon, Y. J.; Miyazawa, M.; Ogura, K. *Journal of the Chemical Society, Chemical Communications* **1994**, *17*, 1977-1978.

202. Johnson, C. K., *ORTEPII*. **1976**, Oak Ridge National Laboratory, Oak Ridge: Tennessee.

203. Fanizzi, F. P.; Maresca, L.; Natile, G.; Lanfranchi, M.; Tiripiccchio, A.; Pacchioni, G. *J. Chem. Soc., Chem. Commun*. **1992**, 333-335.

204. Cattalini, L.; Gasparrini, F.; Maresca, L.; Natile, G. *J. Chem. Soc., Chem. Commun*. **1973**, 369-370.

205. Yip, H.-K.; Chen, L.-K.; Cheung, K.-K.; Che, C.-M. *J. Chem. Soc. Dalton Trans.* **1993**, 2933-2938.

206. Constable, E. C.; Hannon, M. J.; Martin, A.; Raithby, P. R.; Tocher, D. A. *Polyhedron* **1992**, *11*, 2967-2971.

207. Constable, E. C.; Elder, S. M.; Hannon, M. J.; Martin, A.; Raithby, P. R.; Tocher, D. A. *J. Chem. Soc., Dlalton Trans.* **1996**, *12*, 2423-2433.

208. Baum, G.; Constable, E. C.; Fenske, D.; Kulke, T. *Chem Commun (Camb) FIELD Publication Date:2001 Sep 21* **1997**, 2043-2044.

209. Fraile, J. M.; Garcia, J. I.; Martinez-Merino, V.; Mayoral, J. A.; Salvatella, L. *J. Am. Chem. Soc.* **2001**, *123*, 7616-7625.

210. Lotscher, D.; Rupprecht, S.; Stoeckli-Evans, H.; von Zelewsky, H. *Tetrahedron: Asymmetry* **2000**, *11*, 4341-4357.

211. Kasselouri, S.; Garoufis, A.; Paschalidou, S.; Perlepes, S. P.; Butler, I. S.; hadjiliadis, N. *Inorg. Chim. Acta* **1994**, *227*, 129-136.

212. Battaglia, L. P.; Corradi, A. B.; Cramarossa, M. R.; Vezzosi, I. M.; Giusti, J. G. *Polyhedron* **1993**, *12*, 2235-2239.

213. Williams, R. J. *Eur. J. Biochem.* **1995**, *234*, 363-381.

214. Dietrich-Buchecker, C.; Sauvage, J. P.; Kern, J. M. *J. Am. Chem. Soc.* **1989**, *111*, 7791-7800.

215. Armaroli, N. *Chem. Soc. Rev.* **2001**, *30*, 113-124.

216. Scaltrito, D. V.; Thompson, D. W.; O'Callaghan, J. A.; Meyer, G. J. *Coord. Chem. Rev.* **2000**, *208*, 243-266.

217. McMillin, D. R.; Buckner, M. T.; Ahn, B. T. *Inorganic Chemistry* **1977**, *16*, 943-945.

218. Ruthkosky, M.; Castellano, F. N.; Meyer, G. J. *Inorganic Chemistry* **1996**, *35*, 6406-6412.

219. Stacy, E. M.; McMillin, D. R. *Inorganic Chemistry* **1990**, *29*, 393-396.

220. Cunningham, C. T.; Moore, J. J.; Cunningham, K. L. H.; Fanwick, P. E.; McMillin, D. R. *Inorg. Chem.* **2000**, *39*, 3638-3644.

221. Burke, P. J.; Hendrick, K.; McMillin, D. R. *Inorg. Chem.* **1982**, *21*, 1881-1886.

222. Bardwell, D. A.; Jeffery, J. C.; Otter, C. A.; Ward, M. D. *Polyhedron* **1996**, *15*, 191-194.

223. Dobson, J. F.; Green, B. E.; Healy, P. C.; Kennard, C. H. L.; Pakawatchai, C.; White, A. H. *Australian Journal of Chemistry* **1984**, *37*, 649-659.

224. Klemens, F. K.; Fanwick, P. E.; Bibler, J. K.; McMillin, D. R. *Inorg. Chem.* **1989**, *28*, 3076-3079.

225. Eggleston, M. K.; Fanwick, P. E.; Pallenberg, A. J.; McMillin, D. R. *Inorganic Chemistry* **1997**, *36*, 4007-4010.

226. Cesario, M.; Dietrich-Buchecker, C.; Guilhem, J.; Pascard, C.; Sauvage, J. P. *J. Chem. Soc. Chem. Commun.* **1985**, 244-247.

227. Hoffman, S. K.; Corvan, P. J.; Singh, P.; Sethulekshmi, C. N.; Metzger, R. M.; Hartfield, W. E. *J. Am. Chem. Soc.* **1983**, *105*, 4608-4617.

228. Kovalevsky, A. Y.; Gembicky, M.; Novozhilova, I. V.; Coppens, P. *Inorganic Chemistry* **2003**, *42*, 8794-8802.

229. Garret, T. M.; Koert, U.; Lehn, J. M.; Rigault, A.; Meyer, D.; Fischer, J. *J. Chem. Soc. Chem. Commun.* **1990**, 557-558.

230. Martell, A. E.; Smith, R. M., *Critical Stability Constants*. Vol. II. **1982**, New York: Plenum Press. 236.

231. Burke, P. J.; McMillin, D. R.; Robinson, W. R. *Inorganic Chemistry* **1980**, *19*, 1211-1214.

232. Katsuji, I.; Katsuki, T. *Tetrahedron Letters* **1993**, *34*, 2661-2664.

233. Otwinowski, Z.; Minor, W., *Methods in Enzymology*. Macromolecular Crystallography, Part A, ed. Sweet, R. M. **1997**, New York: Academic Press. 207-326.

234. Blessing, R. H. *Acta Crystallogr., Sect A* **1995**, *51*, 33-38.

235. Altomare, A.; Cascarano, G.; Giacovazzo, C.; Guagliardi, A.; Burla, M. C.; Polidori, G.; Camalli, M. *SIR92, J. Appl. Crystallogr.* **1994**, *27*, 435.

236. Flack, H. D.; Bernardinelli, G. *Acta Crystallogr., Sect A* **1999**, *55*, 908-915.

237. Flack, H. D.; Bernardinelli, G. *J. Appl. Crystallogr.* **2000**, *33*, 1143-1148.

238. Hooft, R., *KappaCCD Collect Software*. **1999**, Nonius BV: Delft, The Netherlands.

239. van der Sluis, P.; Spek, A. L. *Acta Crystallogr*. **1990**, *A46*, 194-201.

240. Spek, A. L., *PLATON, Program for the Analysis of Molecular Geometry*. **2002**, University of Utrecht: The Netherlands.

241. Maslen, E. N.; Fox, A. G.; O'Keefe, M. A., eds. *International Tables for Crystallography*. ed. Wilson, A. J. C. Vol. C. **1992**, Kluwer Academic Publishers: Dordrecht. Table 6.1.1.1, pp. 477-486.

242. Stewart, R. F.; Davidson, E. R.; Simpson, W. T. *J. Chem. Phys*. **1965**, *42*, 3175-3187.

243. Ibers, J. A.; Hamilton, W. C. *Acta Crystallogr., Sect A* **1964**, *17*, 781-782.

244. Creagh, D. C.; McAuley, W. J., eds. *International Tables for Crystallography*. ed. Wilson, A. J. C. Vol. C. **1992**, Kluwer Academic Publishers: Dordrecht. Table 4.2.6.8, pp. 219-222.

245. Creagh, D. C.; Hubbell, J. H., *International Tables for Crystallography*, ed. Wilson, A. J. C. Vol. C. **1992**, Dordrecht: Kluwer Academic Publishers. Table 4.2.4.3, pp. 200-206.

246. Sheldrick, G. M., *SHELXL97, Program for the Refinement of Crystal Structures*. **1997**, University of Göttingen: Germany.

247. Coolen, H. K. A. C.; Meeuwis, J. A. M.; van Leeuwen, P. W. M. N.; Nolte, R. J. M. *J. Am. Chem. Soc*. **1995**, *117*, 11906-11913.

248. Benson, D. R.; Valentekovich, R.; Diederich, F. *Angew. Chem. Int. Ed. Engl*. **1990**, *29*, 191-193.

249. Portada, T.; Roje, M.; Raza, Z.; Caplar, V.; Zinic, M.; Sunjic, V. *Chem. Commun*. **2000**, 1993-1994.

250. Braddock, D. C.; MacGilp, I. D.; Perry, B. G. *Synlett* **2003**, 1121-1124.

251. Braddock, D. C.; MacGilp, I. D.; Perry, B. G. *J. Org. Chem*. **2002**, *67*, 8679-8681.

252. Pu, L. *Tetrahedron* **2003**, *59*, 9873-9886.

253. Danilova, T. I.; Rozenberg, V. I.; Sergeeva, E. V.; Starikova, Z. A.; Brase, S. *Tetrahedron: Asymmetry* **2003**, *14*, 2013-2019.

254. Danilova, T. I.; Rozenberg, V. I.; Strikova, Z. A.; Brase, S. *Tetrahedron: Asymmetry* **2003**, *15*, 223-229.

255. Vorontsova, N.; Vorontsov, E.; Antonov, D.; Starikova, Z.; Butin, K.; Brase, S.; Hofener, S.; Rozenberg, V. *Advanced Synthesis & Catalysis* **2005**, *347*, 129-135.

256. Dahmen, S.; Brase, S. *Org. Lett.* **2001**, *3*, 4119-4122.

257. Hermanns, N.; Dahmen, S.; Bolm, C.; Brase, S. *Angew. Chem. Int. Ed. Engl.* **2002**, *41*, 3692-3694.

258. Dahmen, S. *Org. Lett.* **2004**, *6*, 2113-2116.

259. Cram, D. J.; Sogah, G. D. Y. *Journal of the Chemical Society, Chemical Communications* **1981**, 625-628.

260. Cram, D. J.; Sogah, D. Y. *Journal of the American Chemical Society* **1985**, *107*, 8301-8302.

261. Helgeson, R. C.; Mazaleyrat, J. P.; Cram, D. J. *Journal of the American Chemical Society* **1981**, *103*, 3929-3931.

262. Mazaleyrat, J. P.; Cram, D. J. *Journal of the American Chemical Society* **1981**, *103*, 4585-4586.

263. Kharasch, M. S.; Sosnovsky, G. *J. Am. Chem. Soc.* **1958**, *80*, 756.

264. Rawlinson, D. J.; Sosnovsky, G. *synthesis* **1972**, 1-28.

265. Kharasch, M. S.; Sosnovsky, G.; Yang, N. C. *J. Am. Chem. Soc.* **1959**, *81*, 5819-5824.

266. Katsuki, T., in *Asymmetric C-H Oxidation in Comprehensive Asymmetric Catalysis*, Yamamoto, H., Editor. **1999**, Springer: Berlin. p. 791-802.

267. Eames, J.; Watkinson, M. *Angew. Chem. Int. Ed. Engl.* **2001**, *40*, 3567-3571.

268. Johnson, R. A.; Sharpless, K. B., *Comprehensive Organic Synthesis*, Trost, B. M., Editor. **1991**, Pergamon Press: Oxford. p. 389.

269. Wipf, P., *Comprehensive Organic Synthesis*, Trost, B. M., Editor. **1991**, Pergamon Press: Oxford. p. 827.

270. Hayes, R.; Wallace, T. W. *Tetrahedron Letters* **1990**, *31*, 3555-3556.

271. Schreiber, S. L.; Clause, R. E.; Reagan, J. *Tetrahedron Letters* **1982**, *23*, 3867-3870.

272. Kochi, J. K. *J. Am. Chem. Soc.* **1962**, *84*, 774-784.

273. Walling, C.; Thaler, W. *J. Am. Chem. Soc.* **1961**, *83*, 3877-3884.

274. Walling, C.; Zavitsas, A. A. *J. Am. Chem. Soc.* **1963**, *85*, 2084-2090.

275. Bechwith, A. L. J.; Zavitsas, A. A. *J. Am. Chem. Soc.* **1986**, *108*, 8230-8234.

276. Evans, D. A.; Miller, S. J.; Lectka, T. *J. Am. Chem. Soc.* **1993**, *115*, 6460-6461.

277. Evans, D. A.; Murry, J. A.; von Matt, P.; Norcross, R. D.; Miller, S. J. *J. Angew. Chem. Int. Ed. Engl.* **1995**, *34*, 798-800.

278. Denmark, S. E.; Nakajima, N.; Nicaise, O. J.-C.; Faucher, A.-M.; Edwards, J. P. *J. Org. Chem.* **1995**, *60*, 4884-4892.

279. Araki, M.; Nagase, T., *Method for the Preparation of Optically Active Allylic Esters*, in *U.S.* **1976**, (Sumitomo Chemical Company, Limited, Osaka, Japan): U.S. p. 8.

280. Denney, D. B.; Napier, R.; Cammarata, A. *J. Org. Chem.* **1965**, *30*.

281. Araki, M.; Nagase, T. *Chem. Abstr.* **1977**, *86*, 120886r.

282. Gokhale, A. S.; Minidis, A. B. E.; Pfaltz, A. *Tet. Lett.* **1995**, *36*, 1831-1834.

283. Andrus, M. B.; Argade, A. B.; Chen, X.; Pamment, M. G. *Tetrahedron Letters* **1995**, *36*.

284. Kawasaki, K.; Tsumura, S.; Katsuki, T. *Synlett* **1995**, 1245-1246.

285. Malkov, A. V.; Baxendale, I. R.; Bella, M.; Langer, V.; Fawcett, J.; Russell, D. R.; Mansfield, D. J.; Valko, M.; Kocovsky, P. *Organometallics* **2001**, *20*, 673-690.

286. Malkov, A. V.; Pernazza, D.; Bell, M.; Bella, M.; Massa, A.; Teply, F.; Meghani, P.; Kocovsky, P. *J. Org. Chem.* **2003**, *68*, 4727-4742.

287. Chelucci, G.; Loriga, G.; Murineddu, G.; Pinna, G. A. *Tet. Lett.* **2002**, *43*, 3601-3604.

288. Chelucci, G.; Iuliano, A.; Muroni, D.; Saba, A. *Journal of Molecular Catalysis A: Chemical* **2003**, *191*, 29-33.

289. Sekar, G.; DattaGupta, A.; Singh, V. K. *J. Org. Chem.* **1998**, *63*, 2961-2967.

290. Andrus, M. B.; Asagari, D. *Tetrahedron* **2000**, *56*, 5775-5780.

291. Uozumi, Y.; Kyota, H.; Kishi, E.; Kitayama, K.; hayashi, T. *Tetrahedron: Asymmetry* **1996**, *7*, 1603-1619.

292. Imai, Y.; Zhang, W.; Kida, T.; Nakatsuji, Y.; Ikeda, I. *Tetrahedron Letters* **1997**, *38*, 2681-2684.

293. Andrus, M. B.; Zhou, Z. *J. Am. Chem. Soc.* **2002**, *124*, 8806-8807.

294. Andrus, M. B.; Chen, X. *Tetrahedron* **1997**, *53*, 16229-16240.

295. Kawasaki, K.-i.; Katsuki, T. *Tetrahedron* **1997**, *53*, 6337-6350.

296. Kohmura, Y.; Katsuki, T. *Tet. Lett.* **2000**, *41*, 3941-3945.

297. Malkov, A. V.; Bella, M.; Langer, V.; Kocovsky, P. *Org. Lett.* **2000**, *2*, 3047-3049.

298. Chelucci, G.; Pinna, G. A.; Saba, A. *Tetrahedron: Asymmetry* **1998**, *9*, 531-534.

299. Chelucci, G.; Caria, V.; Saba, A. *Journal of Molecular Catalysis A: Chemical* **1998**, *130*, 51-55.

300. Chelucci, G.; Medici, S.; Saba, A. *Tetrahedron: Asymmetry* **1999**, *10*, 543-550.

301. Chelucci, G.; Gladiali, S.; Sanna, M. G.; Brunner, H. *Tetrahedron: Asymmetry* **2000**, *11*, 3419-3426.

302. Chelucci, G.; Gladiali, S.; Saba, A. *Tetrahedron: Asymmetry* **1999**, *10*, 1393-1400.

303. Noyori, R. *Science* **1990**, *248*, 1194-1199.

304. Nozaki, H.; Moriuti, S.; Takaya, H.; Noyori, R. *Tet. Lett.* **1966**, *43*, 5239-5244.

305. Doyle, M. P., *Asymmetric Addition and Insertion Reactions of Catalytically-Generated Metal Carbenes*, in *Catalytic Asymmetric Synthesis*, Ojima, I., Editor. **2000**, A John Wiley & Sons, Inc., Publication: New York. p. 191-228.

306. Doyle, M. P.; McKervey, M. A.; Ye, T., *Modern Catalytic Methods for Organic Synthesis with Diazo Compounds: From Cyclopropanes to Ylides*. **1998**, New York: Wiley & Sons.

307. Ye, T.; McKervey, M. A. *Chem. Rev.* **1994**, *94*, 1091-1160.

308. Nefedov, O. M.; Shapiro, E. A.; Dyatkin, A. B., in *Supplement B: The Chemistry of Acid Derivatives*, Patai, S., Editor. **1992**, Wiley: New York. p. Ch. 25.

309. Pfaltz, A., in *Comprehensive Asymmetric Catalysis*, Yamamoto, H., Editor. **1999**, Springer-Verlag: Berlin. p. 513.

310. Straub, B. F.; Hofmann, P. *Angew. Chem. Int. Ed. Engl.* **2001**, *40*, 1288.

311. Fritschi, H.; Leutenegger, U.; Pfaltz, A. *Helvetica Chimica Acta* **1988**, *71*, 1553-1565.

312. Rasmussen, T.; Jensen, J. F.; Ostergaard, N.; Tanner, D.; Ziergler, T.; Norrby, P. O. *Chem. Eur. J.* **2002**, *8*, 177.

313. Moser, W. R. *J. Am. Chem. Soc.* **1968**, *91*, 1135.

314. Aratani, T.; Yoneyoshi, Y.; Nagase, T. *Tetrahedron Letters* **1975**, *16*, 1707-1710.

315. Aratani, T.; Yoneyoshi, Y.; Nagase, T. *Tetrahedron Letters* **1977**, *18*, 2599-2602.

316. Aratani, T. *Pure and Applied Chemistry* **1985**, *57*, 1839.

317. Fritschi, H.; Leutenegger, U.; Pfaltz, A. *Angew. Chem. Int. Ed. Engl.* **1986**, *25*, 1005.

318. Leutenegger, U.; Umbricht, G.; Fahrni, C.; von Matt, P.; Pfaltz, A. *Tetrahedron* **1992**, *48*, 2143.

319. Fritschi, H.; Leutenegger, U.; Siegmann, K.; Pfaltz, A.; Keller, W.; Kratky, C. *Helv. Chim. Acta.* **1988**, *71*, 1541.

320. Lowenthal, R. E.; Abiko, A.; Masamuni, S. *Tetrahedron Lett.* **1990**, *31*, 6005-6008.

321. Evans, D. A.; Woerpel, K. A.; Hinman, M. M. *J. Am. Chem. Soc.* **1991**, *113*, 726.

322. Lowenthal, R. E.; Masamuni, S. *Tetrahedron Letters* **1991**, *32*, 7171.

323. Muller, D.; Umbricht, G.; Weber, B.; Pfaltz, A. *Helv. Chim. Acta.* **1991**, *74*, 232.

324. Katsuji, I.; Seiichiro, T.; Katsuki, T. *Synlett* **1992**, 575-576.

325. Katsuji, I.; Katsuki, T. *Synlett* **1993**, 638-640.

326. O'Malley, S.; Kodadek, T. *Tetrahedron Letters* **1991**, *32*, 2445-2448.

327. Brunner, H.; Singh, U. P.; Boeck, T.; Altmann, S.; Scheck, T.; Wrackmeyer, B. *J. Organomet. Chem.* **1993**, *443*, C16-C18.

328. Noyori, R.; Kitamura, M., in *Modern Synthetic Methods*, Scheffold, R., Editor. **1989**, Springer-Verlag: Berlin. p. 115-198.

329. Kosower, E. M. *Accounts of Chemical Research* **1971**, *4*, 193-198.

330. Levina, A.; Henin, F.; Muzart, J. *Journal of Organometallic Chemistry* **1995**, *494*, 165-168.

331. Evans, D. A.; Woerpel, K. A.; Scott, M. J. *Angew. Chem. Int. Ed. Engl* **1992**, *31*, 430-432.

332. Salomon, R. G.; Kochi, J. K. *J. Am. Chem. Soc.* **1973**, *95*, 3300-3310.

333. Salomon, R. G.; Kochi, J. k. *J. Am. Chem. Soc.* **1969**, *95*, 3300.

334. Doyle, M. P. *Chem. Rev.* **1986**, *86*, 919-939.

335. Doyle, M. P. *Accounts of Chemical Research* **1986**, *19*, 348-356.

336. Brookhart, M. *Chem. Rev.* **1987**, *87*, 411-432.

337. Fahrni, C. J. *Tetrahedron* **1998**, *54*, 5465-5470.

338. Nakamura, A.; Konish, A.; Tatsuno, Y.; Otsuka, S. *J. Am. Chem. Soc.* **1978**, *100*, 3443-3448.

339. Nakamura, A.; Konish, A.; Tsujitani, R.; Kudo, M.-a.; Otsuka, S. *J. Am. Chem. Soc.* **1978**, *100*, 3449-3461.